Doctoral Thesis

Oxidative stress in higher plants studied by novel experimental approaches

By

Aditya Kumar, M.Sc.

Department of Biophysics
Faculty of Science
Palacký University Olomouc, Czech Republic

Supervisor: Doc. RNDr. Pavel Pospíšil, Ph.D.

Olomouc 2020

Bibliographical identification

Name of the author: Aditya Kumar

Title of thesis: Oxidative stress in higher plants studied by novel experimental approaches

Type of thesis: Ph.D. thesis

Department: Department of Biophysics

Duration of doctoral study: 2014-2020

Supervisor: Doc. RNDr. Pavel Pospíšil, Ph.D.

Year of defense: 2020

Abstract: Proteins are the major target for reactive oxygen species as a result of their abundance in biological systems. Stress conditions induce the upsurge in the level of reactive oxygen species causing protein oxidation recognized by the formation of protein radicals, fragments, aggregates, and subsequent degradation. In the current study, we used the immuno-spin trapping technique for the detection of protein radicals *in vivo* and *in vitro*. We performed western blotting for the characterization of proteins involved in the formation of protein radicals, fragments, and aggregates. We observed that light stress triggered the upsurge in the level of hydroxyl radical and singlet oxygen. Hydroxyl radical and singlet oxygen induced protein oxidation, which is recognized by the formation of reactive carbon-centered (alkyl) and oxygen-centered (peroxyl and alkoxyl) protein radicals. Generation and kinetic behavior of reactive oxygen species and molecular oxygen in spinach leaves have been studied under abiotic stress. We used electrochemical biosensor techniques for the real-time monitoring of superoxide anion radical and hydrogen peroxide formation and two-dimensional imaging of light-induced oxygen evolution. Immuno-spin trapping technique for the detection and characterization of protein radical formation is imperative for better understating of the mechanism of oxidative modification in PSII proteins under high light stress and electrochemical biosensor techniques can offer precise information on the qualitative determination of superoxide anion radical, hydrogen peroxide and molecular oxygen.

Keywords: biosensor, electrochemical techniques, light, oxidative stress, photosynthesis, photosystem II, protein oxidation, reactive oxygen species

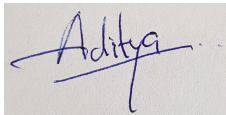**Number of pages including references:** 67
Number of appendices: 6
Language: English

Declaration

I hereby declare that the work presented in this Ph.D. thesis is completely my original work and this thesis has been composed solely by myself using the literature listed in the section "References" and it has not been submitted, in whole or in part, in any previous application for the degree of Doctor of Philosophy (Ph.D.).

15/06/2020

In Olomouc

Aditya Kumar

Contents

List of Publications

This thesis is based on the following six research papers. These research papers are referred to in the text by the bold and sky-blue letters and are enclosed at the end of the thesis.

1. **Kumar, A.**, Prasad, A., Sedlářová, M., Pospíšil, P. (2019). Organic radical imaging in plants: focus on protein radicals. *Free Radical Biology and Medicine*, 130, 568–575. (Kumar, A. contributed to the conception and design of the study, measured, analyzed the data on immunoblots, interpreted the data, and wrote the paper).

2. **Kumar, A.**, Prasad, A., Sedlářová, M., Pospíšil, P. (2018). Data on detection of singlet oxygen, hydroxyl radical and organic radical in *Arabidopsis thaliana*. *Data in Brief*, 21, 2246–2252. (Kumar, A. designed the experiments, performed EPR measurement and wrote the paper).

3. **Kumar, A.**, Prasad, A., Sedlářová, M., Pospíšil, P. (2019). Characterization of Protein Radicals in Arabidopsis. *Frontiers in Physiology*, 10, 958.
(Kumar, A. contributed to the conception and design of the study, measured, analyzed the data on immunoblots, interpreted the data, and wrote the paper).

4. Prasad, A., **Kumar, A.**, Matsuoka, R., Takahashi, A., Fujii, R., Sugiura, Y., Kikuchi, H., Aoyagi, S., Aikawa, T., Kondo, T., Yuasa, M., Pospíšil, P., Kasai, S. (2017). Real-time monitoring of superoxide anion radical generation in response to wounding: electrochemical study. *PeerJ*, 5, e3050.
(Kumar, A. performed the measurements and participated in paper writing).

5. Prasad, A., **Kumar, A.**, Suzuki, M., Kikuchi, H., Sugai, T., Kobayashi, M., Pospíšil, P., Tada, M., Kasai, S. (2015). Detection of hydrogen peroxide in Photosystem II (PSII) using a catalytic amperometric biosensor. *Frontiers in Plant Science*, 6, 862.
(Kumar, A. performed the measurements and participated in paper writing).

6. Kasai, S., Sugiura, Y., Prasad, A., Inoue, K., Sato, T., Honmo, T., **Kumar, A.**, Pospíšil, P., Ino, K., Hashi, Y., Furubayashi, Y., Matsudaira, M., Suda, A., Kunikata, R., Matsue, T. (2019). Real-time imaging of photosynthetic oxygen evolution from spinach using LSI-based biosensor. *Scientific Reports*, 9, 12234.
(Kumar, A. participated in data interpretation).

Abbreviations

Bio-LSI	-	bio-Large scale integration
^{1}Chl*	-	singlet excited state of chlorophyll
^{3}Chl*	-	triplet excited state of chlorophyll
CMOS	-	complementary metal-oxide-semiconductor
DHE	-	dihydroethidium
DMPO	-	5,5-dimethyl-1-pyrroline N-oxide
DNPH	-	2,4-dinitrophenylhydrazine
EMPO	-	5-ethoxycarbonyl-5-methyl-1-pyrroline N-oxide
EPR	-	electron paramagnetic resonance
EtOH	-	ethanol
FITC	-	fluorescein isothiocyanate
GSH	-	reduced glutathione
GSSG	-	oxidized glutathione
4HNE	-	4-hydroxy-2-nonenal
H_2O_2	-	hydrogen peroxide
HPF	-	3'-p-(hydroxyphenyl) fluorescein
HPLC	-	high performance liquid chromatography
HRP	-	horseradish peroxidase
ISC	-	intersystem crossing
LHC	-	light harvesting comples
MDA	-	malondialdehyde
^{1}P680*	-	singlet excited state of primary electron donor of PSII
^{3}P680*	-	triplet excited state of primary electron donor of PSII
POBN	-	α-(4-pyridyl N-oxide)-N-(tert-butylnitrone)
PSI	-	photosystem I
PSII	-	photosystem II
ROS	-	reactive oxygen species
SDS-PAGE	-	sodium dodecyl sulfate- polyacrylamide gel electrophoresis
SOSG	-	singlet oxygen sensor green
TMPD	-	2, 2, 6, 6-tetramethyl-4-piperidone

Curriculum Vitae

Personal profile:

Name: Aditya Kumar
Email: sunnyaditya.16@gmail.com
ORCID iD: 0000-0002-7337-7090
Date of birth: 17.05.1983
Languages known English & Hindi
Nationality: Indian
Current address: Jirovcova 544/11, Brno, 62300, Czech Republic
Permanent address: Salkhan, 231205, Sonbhadra, U.P. India,

Educational Qualifications:

2006-2008   Master of Science (M. Sc.)
                  J.C. Bose Institute of Life Sciences, Bundelkhand University
                  Jhansi, Uttar Pradesh, India
                  Subject: Biotechnology

2002-2005   Bachelor of Science (B. Sc.)
                  D.S.N.P.G. College, C.S.J.M. University
                  Kanpur, Uttar Pradesh, India
                  Subjects: Chemistry, Zoology & Botany

Awards and national level competitive examination qualified:

Awarded "Director's award for excellence in scientific publication" in 2020 by Centre of the Region Haná for Biotechnological and Agricultural Research, Šlechtitelů 11, Olomouc, Czech Republic.

Awarded "Junio Research Fellowship" in 2010 by Council of Scientific & Industrial Research, New Delhi, India

Awarded "Lectureship" in 2013 by Council of Scientific & Industrial Research University Grant Commission, New Delhi, India

Research experiences at other institutions:

February 2014 to present, Ph.D. Study
Department of Biophysics
Centre of the region haná for biotechnological and agricultural research, Palacký University
Olomouc, 78371, Czech Republic
Supervisor: Doc. RNDr. Pavel Pospíšil, Ph.D.
Project: Oxidative stress in higher plants studied by novel experimental approaches.

September 2014 to November 2014, Ph.D. Research Stay
Biomedical Engineering Research Center,
Department of Electronics and Intelligent System, Tohoku Institute of Technology,
35-1 Yagiyama Kasumicho, Taihakuku, Sendai, Japan.
Supervisor: Prof. Masaki Kobayashi
Project: Development of electrochemical methods and its application in photosynthesis.

October 2011 to December 2013, Council of Scientific & Industrial Research-Junior Research Fellow
Stem cell differentiation lab, National Centre for Cell Science
NCCS Complex, Savitribai Phule Pune University Campus, Pune – 411007, Maharashtra, India
Supervisor: Nibedita Lenka
Project: Temporal proteomic profiling of mouse embryonic stem cells during neural differentiation to pave the path for dopaminergic neuron development to treat Parkinson's disease.

March 2010 to April 2011: Project-Junior Research Fellow
Biophysical Chemistry Lab. School of Life Science
Jawaharlal Nehru University, New Delhi, 110067, India
Project: Determination of the enzyme kinetics of the enzyme, N-Acetyl-D-glucosaminyl phosphatidyl inositol de-N-acetylase from *Entamoeba histolytica*.
Supervisor: Prof. Sneha Sudha Komath

December 2008 to February 2010: Teacher
Teaching Life Science
Prabudh IAS Academy
Aliganj, Lucknow, Uttar Pradesh, India

Conference presentations:
- **Aditya Kumar**, Ankush Prasad, and Pavel Pospíšil, Poster presentation on "Heat-induced formation of singlet oxygen in PSII of *Arabidopsis thaliana*: contribution of non-heme iron" in G4G conference held in 2015 and organized by CRH, Palacky University, Olomouc, Czech Republic.

Publications:

Published:

1. **Kumar, A.**, Prasad, A., Sedlářová, M., Pospíšil, P. (2019). Organic radical imaging in plants: focus on protein radicals. Free Radical Biology and Medicine, 130, 568–575.
2. **Kumar, A.**, Prasad, A., Sedlářová, M., Pospíšil, P. (2018). Data on detection of singlet oxygen, hydroxyl radical and organic radical in Arabidopsis thaliana. Data in Brief, 21, 2246–2252.
3. **Kumar, A.**, Prasad, A., Sedlářová, M., Pospíšil, P. (2019). Characterization of Protein Radicals in Arabidopsis. Frontiers in Physiology, 10, 958.
4. Prasad, A., **Kumar, A.**, Matsuoka, R., Takahashi, A., Fujii, R., Sugiura, Y., Kikuchi, H., Aoyagi, S., Aikawa, T., Kondo, T., Yuasa, M., Pospíšil, P., Kasai, S. (2017). Real-time monitoring of superoxide anion radical generation in response to wounding: electrochemical study. PeerJ, 5, e3050.
5. Prasad, A., **Kumar, A.**, Suzuki, M., Kikuchi, H., Sugai, T., Kobayashi, M., Pospíšil, P., Tada, M., Kasai, S. (2015). Detection of hydrogen peroxide in Photosystem II (PSII) using a catalytic amperometric biosensor. Frontiers in Plant Science, 6, 862.
6. Kasai, S., Sugiura, Y., Prasad, A., Inoue, K., Sato, T., Honmo, T., **Kumar, A.**, Pospíšil, P., Ino, K., Hashi, Y., Furubayashi, Y., Matsudaira, M., Suda, A., Kunikata, R., Matsue, T. (2019). Real-time imaging of photosynthetic oxygen evolution from spinach using LSI-based biosensor. Scientific Reports, 9, 12234.

Under revision:

• **Kumar, A.**, Prasad, A., Pospíšil, P. (2020). Formation of α-tocopherol hydroperoxide and α-tocopheroxyl radical – relevance for photooxidative stress in Arabidopsis. (manuscript submitted to **Scientific Reports**).
• **Kumar, A.**, Prasad, A., Sedlářová, M., Ksas, B., Havaux, M., Pospíšil, P. (2020). Interplay between antioxidants in response to photooxidative stress in Arabidopsis. (manuscript submitted to **Free Radical Biology and Medicine**).

Under preparation:

• **Kumar, A.**, Prasad, A., Sedlářová, M., Kale, R., Frankel, L. K., Bricker, T. M., & Pospíšil, P. (2020). Tocopherol controls D1 amino acid oxidation by oxygen radicals: relevance to tocopherol localization and regulation of electron transport in Photosystem II.

My deepest gratitude to my mom, my elder brother, and whole family members for always being there for me and providing me their unconditional love, support, and constant encouragement.

I cannot express my indebtedness to my lovely wife and best friend Dr. Shweta Saxena, Ph.D. for her immense love and unlimited patience. My dear wife, thanks a lot for being with me every moment and providing me constant support in scientific discussions and advice from qualifying national exams till finishing my Ph.D. in both ways academically and psychologically. You always reminded me of my strength and whenever I broke, you were there as my strength and inspiration. I would have not completed my Ph.D. without your love, support, and patience.

I bow down to almighty God who has blessed me with wisdom, strength, acceptability, and patience, without God's grace it was impossible to achieve this Ph.D. degree.

And last but not least, thank you dad for your belief in me! I am convinced that you are looking at me from heaven and feeling proud.

1. INTRODUCTION

The dissertation thesis is based on six publications and focuses on the use of novel methods to study protein oxidation, reactive oxygen species (ROS) formation, and two-dimensional imaging of photosynthetic oxygen evolution. In particular, the first half of the thesis deals with the study of protein oxidation in plant cells exposed to photooxidative stress and characterization of oxidized proteins by immuno-spin trapping in combination with SDS-PAGE and immunoblotting. The second half of the thesis deals with the development and application of electrochemical methods to detect ROS formation and photosynthetic oxygen evolution.

The release of molecular oxygen (O_2) as a by-product of the photosynthetic oxidation of water has permitted O_2 based respiration, a process indispensable for most of the higher life forms on the planet. At the same time, an O_2 rich environment triggered the formation of ROS, an unavoidable species which in excess can cause oxidative stress. The ROS induce protein oxidation, a very common metabolic process during oxidative stress which is characterized by several modifications in protein structure, for example, protein radical formation, protein fragmentation, protein aggregation, and ultimately degradation. In the last chapter, I summarize all the experimental approaches used during my research.

The thesis is written in the form of a mini-review briefing the current knowledge related to protein oxidation and the methods for the detection of protein oxidation, ROS formation, and photosynthetic O_2 evolution. The results of my research are published in **Kumar et al. (2018)**, **(2019a)**, **(2019b)**, **Prasad et al. (2015)**, **(2017)** and **Kasai et al. (2019)** are discussed in the context of up-to-date findings and are referred in the text by bold sky-blue letters. The publications are enclosed in the Appendix of the thesis.

1.1. Protein oxidation

Protein oxidation can be defined as the covalent modification of a protein brought either directly by ROS or indirectly by reaction with secondary by-products of oxidative stress (Shacter, 2000). Proteins are the common target for oxidants because of their richness in biological systems. A wide range of oxidants can be generated *in vivo*, as a result of various endogenous processes and exogenous processes (biotic and abiotic stresses). Photosystem I (PSI) and photosystem II (PSII) are the major sites of ROS formation (Asada, 2006). Reactive oxygen species, such as superoxide anion radical ($O_2^{\bullet-}$), hydrogen peroxide (H_2O_2), hydroxyl radical ($HO^\bullet$), and singlet oxygen ($^1O_2$), are potent oxidizing agents, thereby damaging the photosynthetic apparatus. The basic mechanisms of protein oxidation are derived from radiolytic studies (Stadtman, 1993). The most common mechanisms of protein oxidation are hydrogen abstraction from the α-carbon atom by $HO^\bullet$ and the addition of $^1O_2$ to deprotonated amino acids (Davies, 2016). Hydrogen abstraction by $HO^\bullet$ is a common mode of protein oxidation for aliphatic amino acids, whereas the addition of $HO^\bullet$ and $^1O_2$ is a common mechanism of protein oxidation for aromatic amino acids (Gracanin et al., 2009). Based on oxidant proteins can undergo direct or indirect oxidative modification. We describe direct modifications as (i) hydrogen abstraction, (ii) formation of organic radicals and the occurrence of chain reaction, (iii) hydroxylation, and (iv) oxygenation. Other redox-based direct modifications are done by different chemical modifications such as glycosylation, phosphorylation, acetylation, *s*-nitrosylation, disulfide bond formation, glutathionylation, and ubiquitination (Beltrán et al., 2000). Indirect modification of proteins occurs due to the interaction of proteins with the products of lipid peroxidation (Hadacek & Bachmann, 2015). For example, 4-hydroxy-2-nonenal (HNE), malondialdehyde (MDA), and acrolein formed as breakdown products of lipid peroxidation can bind covalently to lysine, histidine and cysteine residues, leading to the addition of aldehyde moieties to the protein (Levine et al., 1994). An increase in the ROS concentration due to stress leads to the site-specific modification of amino acids and increases vulnerability to proteolytic degradation (Moller et al., 2007). The amino acids differ in their vulnerability to the ROS attack. The amino acids, cysteine, methionine,

histidine, arginine, proline, lysine, and tryptophan contain side groups that can be easily oxidized by different ROS leading to stable covalent modifications, for example, cysteine and methionine are both prone to damage by the $HO^\bullet$ and $^1O_2$. Protein oxidation is associated with the formation of protein radicals involving carbon-centered (alkyl) and oxygen-centered (peroxyl and alkoxyl) radicals and as a consequence of protein oxidation, proteins can undergo cleavage and cross-linking processes to form fragments and aggregates, respectively.

1.1.1. Direct modifications

1.1.1.1. Hydrogen abstraction

It has been well established that hydrogen abstraction from free and peptide bound amino acids occurs predominantly by $HO^\bullet$ (Davies, 2016; Stadtman, 1993). However, apart from $HO^\bullet$ other ROS produced as an intermediate of protein or lipid oxidation such as alkyl, peroxyl, and alkoxyl radicals can also abstract hydrogen from free or bound amino acids. The hydrogen abstraction can be done from both amino acid side chains and the peptide backbone, causing the formation of different radical byproducts of proteins (Stadtman, 2006). Hydrogen abstraction by $HO^\bullet$ in oxidative modification of aliphatic amino acids has been considered as the first step with an ideal abstraction taking place at α- carbon or at the branch point, such as β-CH for valine, isoleucine, and γ-CH for leucine based on the stability of tertiary radical > secondary radical > primary radical (Davies, 2005; Nukuna et al., 2001; Xu & Chance, 2007). Hydrogen abstraction for proline takes place at δ-CH_2, γ-CH_2, and β-CH_2 in the ratio of 2.7:1.4:1 due to its cyclic structure (Nukuna et al., 2001). The inductive effect of the adjacent peptide bond makes δ-CH_2 highly reactive. Similarly, δ-CH_2 of arginine has a higher reaction rate toward $HO^\bullet$ mediated hydrogen abstraction due to higher electron density at δ-CH_2 (Xu & Chance, 2007). Hydrogen abstraction from the β-position of the side chain by $HO^\bullet$ has been reported for histidine oxidation. The histidine oxidation by $HO^\bullet$ occurs via addition at the ε^1-position of the side chain (Liu et al., 2019). Hydrogen abstraction from all of the

possible atoms on the side chains of aromatic amino acids occurs as a minor way of protein oxidation.

1.1.1.2. Formation of organic radicals and the occurrence of chain reactions

Oxidation of protein on the backbone and the side chains can result in the formation of protein radicals involving carbon-centered (alkyl) and oxygen-centered (peroxyl and alkoxyl) radicals. Formation of protein radicals might be initiated either by HO$^{\bullet}$ (Hawkins & Davies, 1998) or $^1O_2$ (Gracanin et al., 2009). Hydrogen abstraction from the α-carbon position creates alkyl radical on the peptide backbone. Formation of alkyl radical usually followed by a reaction with O_2 to generate peroxyl radical. In biological systems with high concentrations of C–H and S–H bonds, peroxyl radical can remove hydrogen either from the α-carbon site or at C–H and S–H bonds on the side chain and form hydroperoxides as major products (Davies, 2016). Hydroperoxides can also be formed from the reaction of amino acids (tryptophan, tyrosine, and histidine) side chains containing unsaturated bonds with $^1O_2$. In the presence of O_2, high yields of peroxyl radicals and hydroperoxides are formed because of the reaction between alkyl radical and O_2, the hydroperoxides represent up to 70% of the initial oxidant flux (Davies, 2016). One-electron reduction of hydroperoxides results in the formation of alkoxyl radical and subsequent chain reactions. Alkoxyl radical can either abstract hydrogen from another protein to form hydroxy products and alkyl radical or re-arrange the unpaired electron located on oxygen atom to the carbon atom of the carboxylic group which eventually results in cleavage/fragmentation of the protein, creating amide and carbonyl fragments as products (Fig. 1).
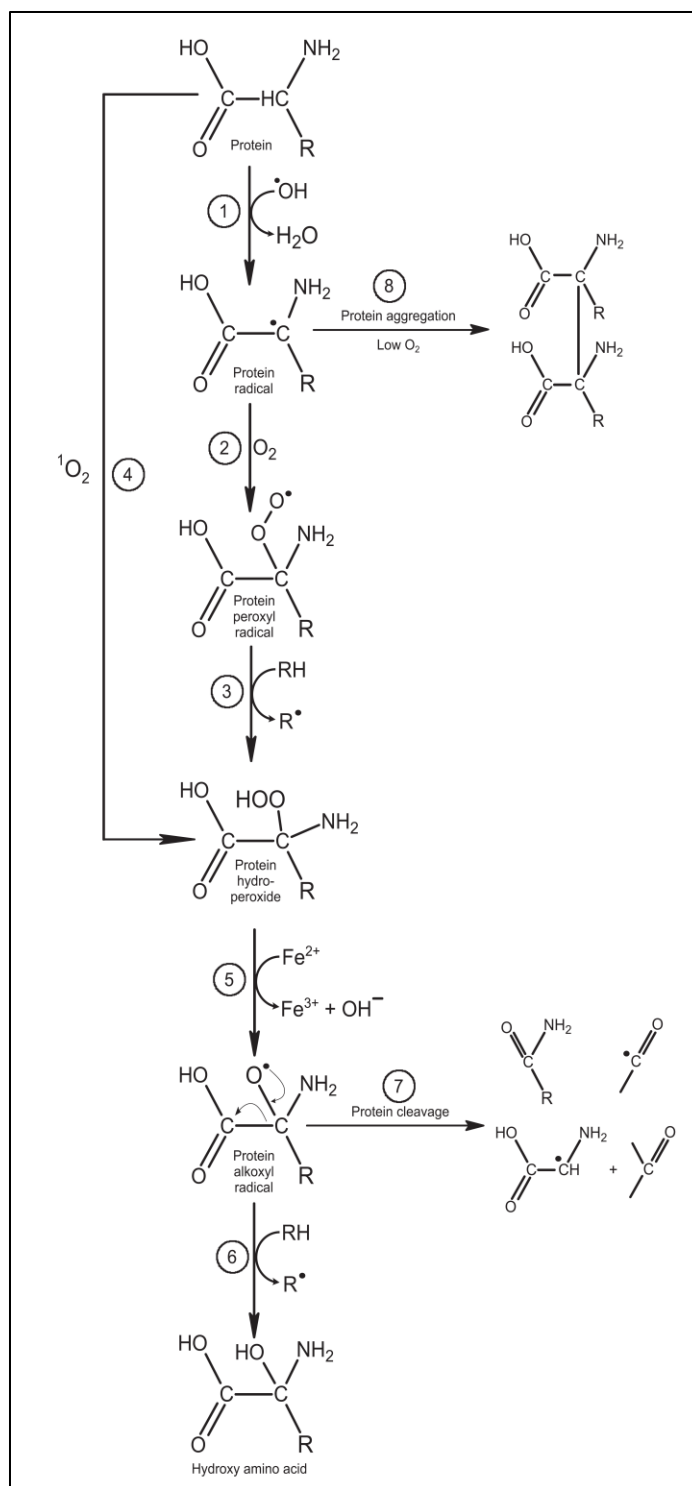
Fig. 1. Schematic representation of the formation of organic radicals and the occurrence of chain reactions. Hydrogen abstraction from protein by HO• generates alkyl radical (reaction 1). In the presence of O_2, the alkyl radical readily reacts with O_2 and forms peroxyl radical (reaction 2). Peroxyl radical abstracts another hydrogen from an adjacent protein, while hydroperoxide and another alkyl radical are formed (reaction 3). The

addition of $^1O_2$ to double bonds of aromatic amino acids forms hydroperoxide (reaction 4). Hydroperoxide is reduced to alkoxyl radical by ferrous iron (reaction 5). Hydrogen abstraction from an adjacent protein by alkoxyl radical forms hydroxy amino acids (reaction 6). Alkoxyl radical formed on the protein causes cleavage of the protein and creates alkyl radical and protein carbonyl (reaction 7). In the absence or low level of O_2, aggregation of alkyl radicals via covalent bond forms protein aggregates (reaction 8). Adapted from (**Kumar et al., 2019b**).

In our study (**Kumar et al., 2019b**), we observed that exposure of Arabidopsis to high light leads to the formation of HO$^\bullet$ and $^1O_2$ in the chloroplasts located at the periphery of the mesophyll cells. We monitored the damage caused by HO$^\bullet$ and $^1O_2$ by detecting the protein radicals formed as an intermediate during the protein oxidation process in Arabidopsis leaves, intact chloroplasts, and thylakoid membranes. To detect the protein radical formation many approaches have been developed. The most common approaches include direct spectroscopic methods such as UV/Vis, resonance Raman, conductivity, and electron paramagnetic resonance (EPR). Due to the short half-life of most radicals, only EPR is specific for radical detection using spin trap 5,5-dimethyl-1-pyrroline N-oxide (DMPO). There is no selective and sensitive technique available for the detection of protein radicals in plant cells.

In our study (**Kumar et al., 2019b**), based on the analogy with animal cells, we introduced the immuno-spin trapping technique to study the protein oxidation in plants. In this technique, short-lived protein radicals are trapped by spin trap DMPO to form more stable DMPO nitrone adducts, which can be recognized by the anti-DMPO antibody. We performed immuno-spin trapping to visualize/detect the formation of protein radicals in Arabidopsis leaves exposed to high light (Fig. 2) (**Kumar et al., 2019b**).
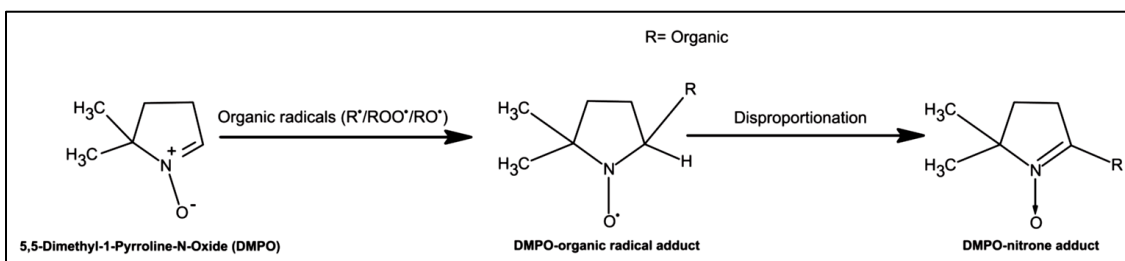
Fig. 2. Schematic representation of immuno-spin trapping of organic radicals. Organic radicals are trapped by DMPO to form DMPO-organic radical adducts. Unstable DMPO-organic radical adducts decay to stable DMPO nitrone adduct. The DMPO motif of DMPO nitrone adduct can be detected with anti-DMPO antibody and visualized either by using FITC conjugated antibody or conventional immunoblot techniques using HRP conjugated secondary antibody and luminol chemiluminescence. Adapted from (Kumar et al., 2019b).

1.1.1.3.   Hydroxylation

Hydroxylation has been considered as a major oxidative pathway of aromatic amino acids (phenylalanine, tyrosine, and tryptophan) by the attack of $HO^\bullet$. Hydroxylation of aromatic amino acids occurs by the addition reaction of $HO^\bullet$ onto the aromatic ring atoms. Although the attack of the $HO^\bullet$ on an aliphatic carbon atom is energetically favored, attack on the aromatic ring prevails due to the larger delocalization and concomitant stabilization. It has been evidenced by previous studies that hydroxylation of the aromatic ring is the first step in the oxidation of aromatic amino acids. Furthermore, the studies indicate that the hydroxylation of the aromatic ring can be favored in the concealed region of the proteins (Mujika et al., 2013).

1.1.1.4.   Oxygenation

The addition of $^1O_2$ to amino acids during photosensitization is known as oxygenation. The reactions of imidazole ring with $^1O_2$ are of special interest due to its plausible involvement in the photooxidative inactivation of certain proteins (histidine-containing). Oxygenation reaction leads to the formation of hydroperoxides as final products (Gracanin et al., 2009). Oxygenation reaction most commonly occurs at the C=C of aromatic amino acids. Oxygenation of tyrosine, tryptophan, and histidine have been studied in the past. Based on observation by Gracanin et al. and Plowman et al. it has been established that oxygenation of tryptophan leads to the formation of kynurenine-based products. Therefore, kynurenine-based products are likely to be good markers for $^1O_2$ mediated oxygenation (Gracanin et al., 2009; Plowman et al., 2013).

1.1.1.5.   Glycosylation

Glycosylation is the process by which a carbohydrate is covalently attached to proteins. Glycosylation is the most abundant post-translational modification (PTM) in plants and has extensive biological significance. The glycosylation can be either N-glycosylation occurring at aspartic acid residue, or O-glycosylation, which occurs on serine, threonine, or tyrosine residue (Williams, 2006). N-glycosylation occurs in the proteins of the secretory pathway in the endoplasmic reticulum (ER), which are later efficiently folded with the help of calreticulin (CRT), calnexin (CNX), and heat shock proteins (HSPs) (Williams, 2006). Under salt stress, the overexpression of HSPs in tomato facilitates the protein folding in the ER, thereby preventing cellular damage and increasing the stress tolerance of the plant.

1.1.1.6.   Phosphorylation

Phosphorylation is one of the most ubiquitous PTM, critical for almost all types of cellular processes such as cell cycle and signaling transduction (Hunter, 2009; Pawson & Scott, 2005). Phosphorylation might modify the structural and/or functional state of the protein by transferring a phosphate group from adenosine triphosphate (ATP) to the hydroxyl group of a residue, in most cases to serine, threonine, and tyrosine (Meyer et al., 2019). Phosphorylation is reversibly catalyzed by kinases and phosphatase and then contributed to the dynamic cellular signaling in organisms. In plants, phosphorylation plays a significant role in a variety of physiological processes (Gollan et al., 2015; Kangasjarvi et al., 2014). It has been established that reversible phosphorylation plays an important role in the regulation of D1 and D2 proteins of PSII in higher plants (Koivuniemi et al., 1995).

1.1.1.7.   Acetylation

Acetylation is the addition of an acetyl group into the side-chain amino group in the Lys residues of proteins. It is another well-known PTM which is involved in the regulation of gene expression. Acetylation taking place on histone/nonhistone proteins is

controlled by several factors like ROS, infectious diseases, and physiological stresses (Hashiguchi & Komatsu, 2016). Protein acetylation can be reversible, i.e., modification of amino group of lysine (K) by (K)-acetyl-transferases (KATs) and (K)-deacetylases (KDACs), or irreversible, i.e., N-terminal modification by N-terminal acetyltransferases (NATs) (Nallamilli et al., 2014). Reversible acetylation occurs on histone proteins. The abiotic stresses involving the regulation/association of histone acetyltransferase (HAT) activities with different protein partners regulate various specific genes leading to the biological response (Zhao et al., 2014).

1.1.1.8. *S*-Nitrosylation

S-Nitrosylation is a redox-based PTM that covalently links nitric oxide ($NO^\bullet$) to the reactive cysteine-thiol group (-SH) to form S-nitroso-thiol (-SNO). Nitrosylation is a very conserved posttranslational mechanism that plays crucial roles in diverse physiological and pathological processes by modulating protein activities. S-nitrosylation is a dynamic and reversible process, involving nitrosylation, de-nitrosylation, and transnitrosylation (Stomberski et al., 2019). *S*-Nitrosylation is mostly involved in the regulation of biotic and abiotic stress responses. The homeostasis of ROS is regulated by the *S*-nitrosylation of respiratory burst oxidase homolog D (RBOHD), peroxiredoxin II E (PrxII E) and ascorbate peroxidase1 (APX1), which modulates the biosynthesis or turnover of ROS (Romero-Puertas et al., 2007; Yang et al., 2015; Yun et al., 2011). Emerging evidence suggests that chlorophyll metabolism and photosynthesis are extensively regulated by the redox-based *S*-nitrosylation. S-nitrosylation has been found as an imperative modification to regulate the regulators (Gupta et al., 2020)

1.1.1.9. Disulfide bond formation

Disulfide bonds are usually formed during the PTM with the assistance of appropriate enzymes and co-factors. Cysteines, sulfhydryl-containing amino acids, which are located to an appropriate distance or next to one another within a polypeptide chain, can form a disulfide bond through their oxidizable thiol groups (Patil et al., 2015). Disulfide

bonds are universal structural motifs in many bioactive peptides and proteins including hormones, growth factors, enzyme inhibitors, and antimicrobial peptides (Góngora-Benítez et al., 2014; Marshall et al., 2011; Moroder et al., 2005). Disulfide bond plays a critical role in maintaining the overall fold of the peptides and proteins therefore important for the stability and function of proteins and peptides (Patil et al., 2015).

1.1.1.10.   Glutathionylation

Glutathionylation is a ubiquitous redox-sensitive and reversible covalent PTM that takes place by the addition of glutathione to the thiolate of cysteines in target proteins (Calderón et al., 2017). Glutathionylation is involved in the protection of protein cysteines from irreversible oxidation and considered a protective mechanism against overoxidation, it also controls protein activity and allows signaling (Calderón et al., 2017). Glutathione is a small tripeptide (γ-L-glutamyl-L-cysteinyl-glycine) that exists in the reduced form (GSH) or the oxidized form (GSSG) in which two glutathione molecules are linked via a disulfide bond (Gao et al., 2009). The tripeptide glutathione assists significant functions in plants as a reductant, quickly accruing under stress conditions as its oxidized disulfide form (GSSG). As well as forming disulfides with itself, GSH can also form mixed disulfides with proteinaceous cysteine (Dixon et al., 2005). In plants, glutathione is considered important in many other processes. The several functions of glutathione in photosynthetic organisms have been extensively reviewed recently (Foyer & Noctor, 2005; Meyer & Hell, 2005; Ogawa, 2005; Rouhier et al., 2008; Zaffagnini et al., 2012).

1.1.1.11.   Ubiquitination

Ubiquitination is the process by which ubiquitin is covalently attached to substrate proteins via their C-terminal carboxyl group, often on a lysine residue, thereby modifying the stability, localization, or function of the target protein. Ubiquitin is a small, highly conserved, ubiquitously expressed eukaryotic protein with immeasurably important and diverse regulatory functions. A well-studied function of ubiquitin is its role in selective proteolysis by the ubiquitin-proteasome system (UPS) (Stone, 2014, 2019).

Approximately 6% of Arabidopsis protein-coding genes are supposed to have functions related to ubiquitin modification. Therefore, it is not surprising to believe that ubiquitin plays significant roles in various aspects of plant biology, from growth and development to responses to biotic and abiotic stress (Bartel & Citovsky, 2012).

1.1.2. Indirect modifications

1.1.2.1. HNE-protein adduct

HNE is one of the most reactive electrophilic aldehydes which forms adducts with proteins (Anavi et al., 2015; Riahi et al., 2010; Łuczaj et al., 2017). The presence of carbonyl group at the C1 carbon, the double bond between the C2 and C3 carbons, and the hydroxyl group on the C4 carbon makes 4-HNE highly reactive and can generate both Schiff bases and Michael adducts with proteins (Gegotek & Skrzydlewska, 2019). The amino acid residues, cysteine, histidine, and lysine are known to form adducts with 4-HNE. The formation of 4-HNE adducts is linked with antioxidant enzymes, for instance, glutathione peroxidase, catalase, and thioredoxin reductase. HNE inhibits antioxidant action of the enzyme by binding to the cysteine residue at the active site of the enzyme (Bauer & Zarkovic, 2015; Fang & Holmgren, 2006). At higher concentrations, 4-HNE can modify protein expression at the deoxyribose nucleic acid (DNA) level by forming adducts with histones.

1.1.2.2. MDA-protein adducts

MDA is another reactive end product of lipid peroxidation which generally displays a high affinity to form adducts with DNA, but it can also form adducts with proteins at higher concentrations. The presence of a carbonyl group at the C2 and C4 carbon makes MDA reactive. MDA's electrophilicity makes it highly reactive toward nucleophiles, such as basic amino acid residues, lysine, histidine, or arginine. Initial reactions between MDA and free amino acids or protein generate Schiff-base adducts (Alche, 2019).

1.1.2.3. Acrolein – protein adducts

Acrolein is another highly reactive unsaturated aldehyde. Acrolein reacts with similar amino acid residues as 4-HNE to form acrolein-adducts. Acrolein is highly reactive because both the double bond and aldehydic moieties at C2 and C4 can participate in a variety of reactions. The reaction between acrolein and proteins may occur spontaneously or catalyze by an enzyme (Awasthi et al., 2004). The acrolein-protein adducts are capable to modify the expression of proteins at the biosynthesis level and can also regulate their degradation (Gegotek & Skrzydlewska, 2019).

The adducts formed by 4-HNE, MDA and acrolein with proteins have been used as immunogens to raise many highly valuable antibodies, which can be used in Western blotting, ELISA, immunocytochemistry/immunohistochemistry, immunoprecipitation, and other immunoassays, for the identification of oxidized lipid adducts with proteins (Alche, 2019).

It is well established that end-products of lipid peroxidation, such as MDA and HNE cause protein damage through reactions with lysine amino groups, cysteine sulfhydryl groups, and histidine imidazole groups (Refsgaard et al., 2000). Due to the amphiphilic nature of aldehydes, they can easily diffuse across membranes and can covalently modify any protein in the cytoplasm and nucleus, far from their site of origin. Aldehyde toxicity is mainly due to the alterations of several cell functions, caused by the formation of covalent adducts with cellular proteins (Pizzimenti et al., 2013). Even though it was established that MDA does not react with glycine and glutathione, and reacts slowly with cysteine under physiological conditions, cellular proteins are much more readily modified by MDA (Esterbauer et al., 1991). HNE is a highly electrophilic molecule that easily reacts with glutathione, proteins, and at higher concentration with DNA. HNE forms adducts with three different aminoacyl side chains, namely cysteine, histidine, and lysine residues, via Michael addition either to thiol (−SH) or to amino (−NH2) groups (Esterbauer et al., 1991). The formation of protein adducts with lipid peroxidation products can stimulate the antioxidant system, which may also possess proinflammatory or proapoptotic effects.

1.1.3. Consequences of protein oxidation

It is well-known that protein oxidation has a wide range of downstream consequences. Oxidative modifications of proteins can change their physical and chemical properties, including conformation, structure, solubility, susceptibility to proteolysis, and enzyme activities. ROS can cause oxidation in both amino acid side chains and backbones, resulting in protein cleavage (fragmentation) or protein-protein cross-linkages (aggregation) (Fig. 1) and protein degradation.

1.1.3.1.   Fragmentation and aggregation

Protein oxidation can result in major physical changes in protein structure ranging from cleavage of peptide bonds, cross-linking and aggregation. Direct cross-linking can occur via intermolecular radical–radical dimerization reactions (Fig. 1). As PSII is a well-known site of ROS formation (Pospíšil 2012), we (**Kumar et al., 2019a**) studied the oxidation of PSII proteins during high light stress and showed that PSII proteins are involved in the formation of fragments and aggregates as proposed in previous studies by different groups (Davies, 2016; Yamamoto et al., 2008). The formation and consequent accumulation of protein fragments and aggregates due to protein cleavage and protein-protein cross-linking respectively have been linked to photooxidative stress and hence there is considerable interest in the detection, characterization, and quantification of these protein modifications (Komenda et al., 2006; Lupínková & Komenda, 2004; Shipton & Barber, 1994; Wolff & Dean, 1986). Analysis of fragments and aggregates at the peptide level, typically involves proteolytic digestion and subsequent LC-MS^n analysis, but this is challenging as linear (non-cross-linked) peptides usually constitute the majority of the peptides, and the cross-linked peptides are easily missed (Hagglund et al., 2018). Several strategies have therefore been applied to separate or enrich fragments and aggregates at the protein or peptide level, to reduce the complication and simplify analysis.

In our study (**Kumar et al., 2019b**), we performed SDS-PAGE to separate the fragments and aggregates from parent proteins and immuno-spin trapping in combination with immunoblotting for the characterization of protein radicals to

investigate the effect of high light stress on PSII proteins (Fig. 3). The main target of high light stress is the D1 protein in the reaction center of PS II, which is competently replaced by a newly synthesized copy after its oxidative damage (Andersson & Aro, 2001). We observed a gradual loss of the 32 kDa band of D1 protein under light stress. The oxidation of D1 protein leads to fragmentation and cross-linking with other PSII proteins. Our results show the formation of protein radicals on two fragments at approximately 18 and 23 kDa and three aggregates at approximately 41, 55, and 68 kDa. Our results agree with earlier studies where authors have shown that origin of 18 kDa protein band is from the C-terminus of the D1 protein (Kale et al., 2017) or it may arise from the cleavage in the lumenal loop joining helices C and D of D1 protein (Aro et al., 1990; Lupínková & Komenda, 2004; Shipton & Barber, 1991).
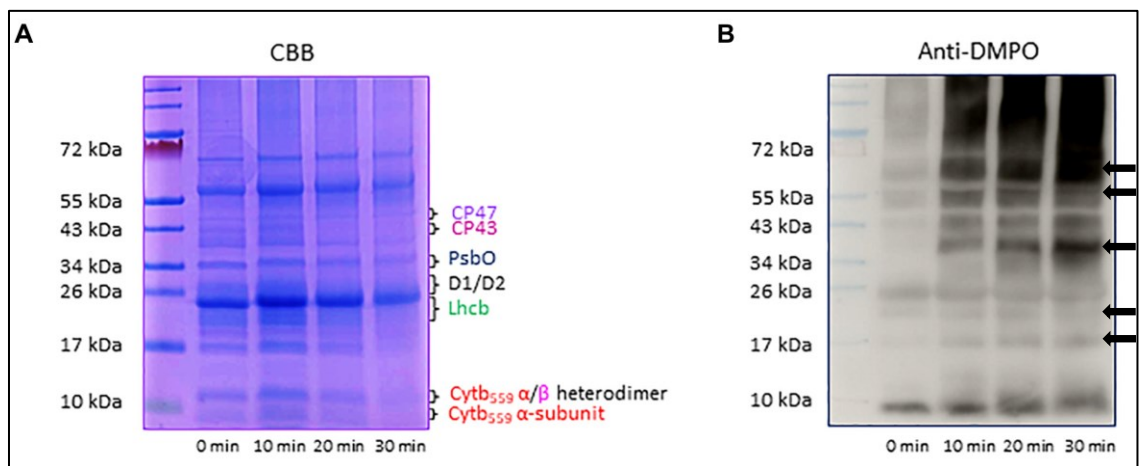
Fig. 3. (A) Separation of PSII proteins by SDS-PAGE and stained with CBB. Pre-stained standard protein ladder (lane 1), thylakoid membranes incubated in dark (0 min) (lane 2), thylakoid membranes incubated in high white light for 10, 20, and 30 min (lane 3, lane 4, and lane 5, respectively). The identity of the proteins is as per their mass. **(B) Detection of protein radical in thylakoid membranes using immuno-spin trapping technique.** Pre-stained standard protein ladder (lane 1), thylakoid membranes incubated in dark (0 min) in presence of DMPO (lane 2), thylakoid membranes exposed to high white light in the presence of DMPO for 10, 20 and 30 min (lane 3, lane 4, and lane 5, respectively). Analysis of DMPO-protein nitrone adducts in thylakoid membranes incubated with DMPO under high white light for different time points. Indicated by the arrow are the protein radicals formed on proteins, protein fragments, and protein aggregates. Adapted from (Kumar et al., 2019a).

The cross-linking of protein radicals with other protein radicals leads to the formation of protein aggregates. It has been shown by Komenda and his group that 41 kDa band is an aggregate formed by cross-linking between the oxidized His252 residue of the D1 polypeptide and the amino group of the N-terminal serine of the cyt b_{559} α-subunit. In our study (**Kumar et al., 2019a**), we observed that 41 kDa band cross-reacted with both the anti-D1 and anti-cyt b_{559} α-subunit antibody, confirming that this band is an aggregate formed by cross-linking between the D1 polypeptide and cyt b_{559} α-subunit. Our results of probing the anti-DMPO blot with anti-D1 antibody and anti-cyt b_{559} α-subunit antibody detected 41 kDa confirms that protein radical is formed on an aggregate of D1 protein and the anti-cyt b_{559} α-subunit which is in agreement with earlier studies (Barbato et al., 1992; Henmi et al., 2003; Lupínková & Komenda, 2004; Yamamoto, 2001; Yamashita et al., 2008). Probing the anti-DMPO blot with anti-D1, anti- C-terminal, anti-D-de loop and anti-Lhcb3 antibodies detected 55 kDa band suggest that protein radical may be formed on (i) the aggregates of 23 kDa fragment of D1 protein and D1 protein, (ii) the aggregates of three 18 kDa fragments of the D1 protein, (iii) the aggregates of Lhcb3 protein and C-terminal of D1 protein, (iv) the aggregates of two Lhcb3 proteins (**Kumar et al., 2019a**). Recent studies suggest that light-driven trimer to monomer transition is associated with the appearance of LHCII dimers (Janik et al., 2017; Janik et al., 2013). Probing the anti-DMPO blot with anti-cyt b_{559} α-subunit, anti-D-de loop and anti-D2 antibodies detected the appearance of the 68 kDa band suggests the involvement of these proteins or their peptides in aggregate formation (**Kumar et al., 2019a**).

A commonly used method to study protein oxidation is the detection of carbonyl formation, which occurs on lysine, arginine, serine, threonine, and proline residues (Dalle-Donne et al., 2003; Davies, 2016). Carbonyl groups react with 2,4-dinitrophenylhydrazine (DNPH) and other aldehyde reaction probes such as N'-amino-oxy-methyl-carbonyl-hydrazino-D-biotin, which offers the possibility for colorimetric detection or selective enrichment approaches. Anti-DNP antibodies form the basis of carbonyl-focused western blotting ("oxy-blotting") and ELISAs (Domingues et al., 2013; Shacter, 2000). Carbonyl assays are widespread because they offer the advantage over others because no special

or expensive equipment is required therefore, they can be performed in any normally equipped biochemistry laboratory. Carbonyl group makes a stable DNP adduct after interacting with DNPH which can be detected by various means. The DNP group itself absorbs ultra-violet light so total carbonyl content of a protein or mixture of proteins can be quantified by a spectrophotometric assay and after coupling it with protein fractionation by high-performance liquid chromatography (HPLC) followed by SDS-PAGE and western blotting it can provide greater sensitivity and specificity than measuring total carbonyls in a protein mixture (Levine et al., 1990; Levine et al., 1994).

In our study (Kumar et al., 2019b), we separated DNPH-derivatized proteins by SDS-PAGE and blotted the carbonylated proteins to an adsorbent porous nitrocellulose membrane. The identification of carbonylated proteins was done by anti-DNP antibodies that recognize the DNP portion of the hydrazone. We observed that the protein carbonyls are formed at 18, 23, 32, 34, 43, and 55 kDa proteins. Based on the apparent molecular weight of carbonylated proteins we propose that carbonyls formed on D1 protein, (32 kDa), D2 protein (34 kDa), and CP43 subunit protein (43 kDa). Observation of protein carbonyls at 18 kDa and 55 kDa suggests that carbonyls formed on the 18 kDa fragment and 55 kDa aggregate.

1.1.3.2.   Degradation

Several studies on a wide range of organisms show that protein degradation has a multitude of vital roles in physiology and development. One of the most important roles of protein degradation is in cellular housekeeping (Finley & Chau, 1991; Goldberg & Dice, 1974; Goldberg et al., 1974). Removal of oxidized proteins created by the ROS induced damage through their degradation would ultimately prevent their accumulation to toxic levels. In some circumstances, damaged proteins can be repaired or re-folded, with chaperonins helping to restore native conformations but in others, proteolytic degradation is the only solution (Deshaies et al., 1988; Rothman, 1989). High light stress results in loss of the photosynthetic capacity of higher plants due to the damage of PSII (Powles, 1984). The damage of PSII during high light stress involves photoinactivation of

PSII activity due to the specific degradation of the D1 protein (Aro et al., 1993). Selective degradation of photooxidized D1 protein followed by replacement with a functional counterpart is necessary to restore electron flow. In our study (Kumar et al., 2019a), we analyzed the loss of protein by visualizing the protein band intensity in the CBB stained gel and observed that intensity of protein bands of apparent molecular weight 47 kDa, 43 kDa, and 34 kDa decreased in high light stress (Fig. 3). We identified loss of CP47, CP43, and D1 proteins during high light stress. Our study agrees with previous studies (Mizusawa et al., 2003). It has been reported that D1 protein is normally shielded by the CP43 protein and removal of CP43 leads to exposure of D1 protein for selective degradation by the protease FtsH (Krynicka et al., 2015). In our study, we observed loss of both CP47 and CP43 proteins in high light stress suggesting that loss of these two proteins provides accessibility of FtsH to the D1 proteins for its selective degradation (Krynicka et al., 2015; Nixon et al., 2005).

To sum up, oxidation of PSII proteins leads to the protein radical formation followed by the formation of protein fragments and aggregates and subsequently formation of alkyl, alkoxyl and peroxyl radicals on these fragments and aggregates. Our results show the gradual loss of parent protein band (such as D1 protein band) and appearance of bands representing protein fragments (such as 18 and 23 kDa) and protein aggregate (such as 41, 55 and 68 kDa) (Kumar et al., 2019b). The findings of our study agree with other studies published in past (Aro et al., 1993; Edelman & Mattoo, 2008; Komenda et al., 2006; Lupínková & Komenda, 2004; Yamashita et al., 2008). However, as our understanding of the precise mechanism of PSII protein oxidations is still limited we propose that application of immuno-spin trapping technique unlocks new prospects to study the role of protein radicals in the overall understanding of plant behavior for its survival during the oxidative stress and opens new possibilities to characterize the oxidized proteins and study their role in several physiological processes.

1.2. ROS formation

In nature, plants have to survive under the exposure to various types of abiotic and biotic stress factors (Liebthal & Dietz, 2017; Noctor et al., 2015; Suzuki et al., 2012). These adverse conditions lead to the formation of ROS known to oxidize biomolecules (lipids, proteins, and nucleic acids) (Apel & Hirt, 2004; Asada, 2006; Farmer & Mueller, 2013; Foyer, 2018; Ledford & Niyogi, 2005; Pospíšil 2016). Photosynthesis is a well-established source of ROS in plants (Foyer & Shigeoka, 2011). Electron transport in chloroplasts and mitochondria are the major sites of ROS formation in the plant cell (Apel & Hirt, 2004). Reactive oxygen species are generally present in plant cells in normal conditions, mainly as by-products of photosynthetic metabolism (Tripathy & Oelmuller, 2012). Under various stress conditions, ROS increase to high levels resulting in the agitation of the homeostatic cellular redox state and ultimately leading to oxidative stress (Dumont & Rivoal, 2019).

Reactive oxygen species can be classified as radical ($O_2^{\bullet-}$, $HO^{\bullet}$) and non-radical (H_2O_2, $^1O_2$) species. Moreover, a family of reactive species containing nitrogen moieties associated with oxygen is classified as reactive nitrogen species (RNS) and reactive species containing carbonyl moieties is classified as reactive carbonyl species (RCS). The level of ROS is precisely regulated by enzymatic and non-enzymatic antioxidant defense systems. Accumulation of these ROS causes oxidative damage and finally resulting in cell death. Although the formation of ROS has been implicated with the damaging effect, lately, ROS have been also recognized as crucial players in the complex signaling network of plant stress responses (Baxter et al., 2014; You & Chan, 2015). It has been well established that cells need to regulate ROS production and removal to avoid excessive and irreversible oxidation, nowadays ROS are recognized for their positive roles as essential pro-life signals (Foyer et al., 2017; Noctor & Foyer, 2016).

Molecular oxygen is an important electron acceptor in photosynthesis. It has been known since long that the photoreduction of O_2 leads to the formation of H_2O_2 in PSI (Mehler, 1951). Reduction of O_2 offers an alternate electron sink and generates $O_2^{\bullet-}$, which dismutates to H_2O_2 either via spontaneous dismutation or via enzymatic

dismutation by copper/zinc superoxide dismutase (SOD) of the thylakoid. Free H_2O_2 converts to $HO^\bullet$ via Fenton reaction and bound H_2O_2 converts to $HO^\bullet$ via Fenton like reaction. Chloroplast ascorbate peroxidase (APX) and the peroxiredoxins (PRX) reduce H_2O_2 to water (Awad et al., 2015). In PSII, triplet excited state of chlorophyll transfer the excess energy to O_2 to generate $^1O_2$ (Dogra & Kim, 2019; Dogra et al., 2018; Pospíšil 2012). Besides the energy transfer, electron transport is also associated with the formation of ROS in PSII, such as reduction of plastoquinone, and the oxidation of water is linked to the formation of $O_2^{\bullet-}$, H_2O_2 and $HO^\bullet$ (Pospíšil 2012).

Based on the mechanism of their formation, ROS can be divided into two groups: (i) ROS formed by the electron transfer mechanism (type I mechanism), such as $O_2^{\bullet-}$, H_2O_2, and $HO^\bullet$, (ii) ROS formed by the energy transfer mechanism (type II mechanism), such as $^1O_2$. Detection of ROS in the biological system is always challenging due to their short life-span and high reactivity. Lately, different detection techniques and methodologies were used to detect, quantify and localize ROS and their reactive intermediates *in vitro* and *in vivo* systems (Ichiishi et al., 2015; Kohno et al., 2008; Mattila et al., 2015; Tada et al., 2009).

1.2.1. Superoxide anion radical

Superoxide anion radical is known to be produced in PSI and PSII. In PSI, $O_2^{\bullet-}$ is produced by the Mehler reaction (Asada, 1999). In PSII, $O_2^{\bullet-}$ is produced by the electron leakage to O_2 on the PSII acceptor side. The $O_2^{\bullet-}$ is moderately reactive with a short half-life of 2-4 µs and it does not cause extensive damage by itself, rather it transforms into more reactive and toxic $HO^\bullet$ and causes more damage (Halliwell, 2006). It has been proposed by several groups that under certain conditions (such as absence or full reduction of the PQ pool), O_2 is reduced to $O_2^{\bullet-}$ by the PSII electron acceptor species (Ananyev et al., 1994; Cleland & Grace, 1999). Although it has not been clear that which of the reduced acceptor, reduced Pheo ($Pheo^{\bullet-}$) or reduced primary quinone ($Q_A^{\bullet-}$) on the PSII acceptor side is the actual reductant of O_2 but from the thermodynamic point of view it can be understood that $Pheo^{\bullet-}$ and $Q_A^{\bullet-}$ are capable to reduce O_2 to $O_2^{\bullet-}$. The

reduction of O_2 on the electron acceptor side of PSII initiates a series of reactions leading to the generation of different ROS.

Various techniques including EPR spin-trapping spectroscopy (Vongonner et al., 1993; Zhang et al., 2003), epinephrine-adrenochrome acceptor method (Vylegzhanina et al., 2001), staining with dyes such as tetrazolium dye and nitro blue tetrazolium (NBT) (Wohlgemuth et al., 2002), probing with fluorescent/chemiluminescent probes such as dihydroethidium (DHE), Mito-SOX, lucigenin, luminol, luminol analog 8-amino-5-chloro-2,3-dihydro-7-phenylpyrido [3,4-d] pyridazine sodium salt (L-012), cytochrome c reduction and aconitase inactivation and fluorescent protein, such as circularly permuted green fluorescent protein (cpYFP) based methods have been used to detect the formation of $O_2^{\bullet-}$ in many cells and systems. EPR is the gold standard technique for the detection of free radicals. Among the many kinds of spin traps for the analysis of free radicals, the nitrone compound 5-ethoxycarbonyl-5-methyl-1-pyrroline N-oxide (EMPO) is the most popular one. The EMPO interacts with $O_2^{\bullet-}$ and forms EMPO-OOH adduct which could be monitored by the EPR spectrometer to generate specific spectra. Apart from these above-mentioned methods, electrochemical biosensor designed by alternating layers of cytochrome c and poly (aniline sulfonic acid) on a gold wire electrode has also been applied for the sensitive, selective, and stable quantification of $O_2^{\bullet-}$. The electrochemical method using different modified electrodes have been successfully applied and optimized for the detection of various ROS including $O_2^{\bullet-}$ during the recent past (Groenendaal et al., 2000; Yuasa et al., 2005).

In our study (Prasad et al., 2017), we have demonstrated that polymeric iron-porphyrin-based modified carbon electrode is a useful tool that provides a direct method for real-time monitoring and precise detection of $O_2^{\bullet-}$ with its kinetics in biological samples in-situ. We provided evidence that mechanical stress such as wounding causes the $O_2^{\bullet-}$ formation. We determine the concentration of $O_2^{\bullet-}$ generated in mechanically injured spinach leaves. The expected production was found to be about 40 nM and about 200 nM which is in agreement with studies in the past (Diaz et al., 2016; Diaz & Plummer,

2018). To confirm the production of $O_2^{\bullet-}$, we examined the effect of exogenous SOD, which causes the dismutation of $O_2^{\bullet-}$ to H_2O_2 on the oxidation current in a wounded spinach leaf. The exogenous addition of SOD suppressed the oxidation current of $O_2^{\bullet-}$ significantly. However, the complete suppression of the oxidation current was not observed. The oxidation current, which persisted can be attributed to rapid $O_2^{\bullet-}$ diffusion to the electrode before its conversion to H_2O_2 or the limited SOD activity at a fixed concentration.

Our study (**Prasad et al., 2017**), opens a new area of study which has always been difficult to explore using other available methods such as EPR spin-trapping spectroscopy, fluorescence microscopy, and other biochemical methods. Thus, polymeric iron-porphyrin-based modified carbon electrode has a strong potential for a wide application in plant research for the specific and sensitive detection of $O_2^{\bullet-}$ formation and the kinetic behavior in real. Additionally, the application of synthetic porphyrin has an additional advantage. Moreover, the use of synthetic porphyrin in our study has an additional advantage over $O_2^{\bullet-}$ sensors based on naturally derived enzymes such as SOD and cytochrome c oxidase (Di et al., 2004; Gobi & Mizutani, 2001). Though enzymes on the sensor are sensitive to denaturation, whereas the porphyrin-based sensor can be used without denaturation. Our porphyrin-based sensor is cost-effective although it has certain limitations such as light-sensitivity, which might hinder its photo-electrochemical applicability (Brett C.M.A., 1984). Representation of our experimental set up to measure $O_2^{\bullet-}$ shown in figure 4.
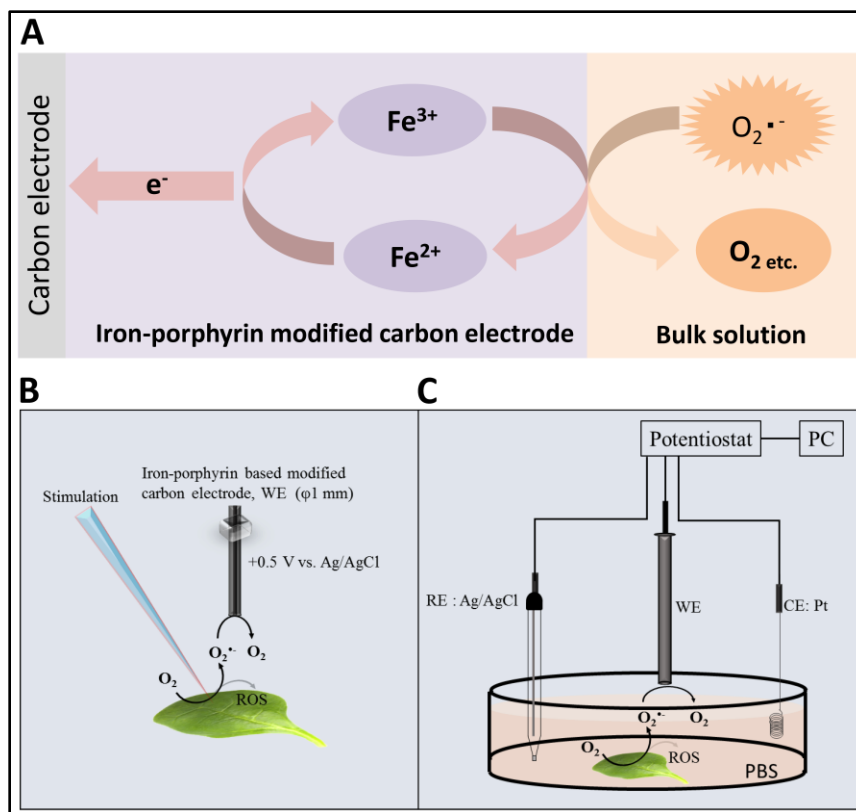
Fig. 4. Representation of our experimental set up to measure O$_2^{\bullet-}$ (A) Schematic diagram of the reaction mechanism for the amperometric detection of O$_2^{\bullet-}$ using the polymeric iron-porphyrin-based modified carbon electrode depicting the reduction-oxidation cycle leading to the generation of the oxidation current. **(B)** The stimulation was performed using a glass capillary, and the polymeric iron-porphyrin-based modified carbon electron was positioned at 1 mm using a motor-driven XYZ microscopic stage. **(C)** The *in vivo* generation of O$_2^{\bullet-}$ was measured using a polymeric iron-porphyrin-based modified carbon electron (working electrode, WE), platinum wire (counter electrode, CE), and silver (Ag)/ silver chloride (AgCl) (reference electrode, RE).

1.2.2. Hydrogen peroxide

Hydrogen peroxide is produced in PSI and PSII. Enzymatic or non-enzymatic one-electron reduction of O$_2^{\bullet-}$ leads to the formation of H$_2$O$_2$. Enzymatic reduction of O$_2^{\bullet-}$ by heme and non-heme iron forms free and bound peroxide, respectively. Non-enzymatic reduction of O$_2^{\bullet-}$ by plastoquinol forms free H$_2$O$_2$. In enzymatic dismutation, the ferrous heme iron of high potential form of cyt b_{559} catalyzes the one-electron reduction of HO$_2^{\bullet}$

to H_2O_2 (Pospíšil 2009, 2011). In spontaneous dismutation, $O_2^{\bullet-}$ provides an additional electron to another $O_2^{\bullet-}$, and with simultaneous protonation generates H_2O_2. The availability of protons favors spontaneous dismutation such as at the membrane edge, whereas, in the interior of the membrane, PSII metal centers are chosen to catalyze the dismutation reaction (Pospíšil 2012).

Many spectroscopic and chromatographic techniques have been used to detect H_2O_2 in living cells (Chen et al., 2009; Mills et al., 2007). Oxidation of thiobenzamide with lactoperoxidase has been used to measure the formation of light-induced H_2O_2 in PSII membranes (Arato et al., 2004; Pospíšil et al., 2004). Amplex Red fluorescence assays have been used to measure the formation of H_2O_2 in chloroplasts (Mubarakshina & Ivanov, 2010; Yadav & Pospíšil 2012). Probes to detect the H_2O_2 like 3,3 diaminobenzidine (DAB), amplex red (AR), amplex ultra red (AUR), and a europium-tetracycline complex (Eu3Tc) has been tested and compared for the sensitivity to light, toxicity, subcellular localization, sensitivity to H_2O_2 by infiltrating into tobacco leaves (Šnyrychová et al., 2009). The 3,3'-Diaminobenzidine (DAB) has been used to detect the H_2O_2 generation at the leaf level after 3-acetyl-4-hydroxyl-5-isopropylpyrroline-2-dione (3-AIPTA) or bentazon treatment (Chen et al., 2012). Moreover, a reporter system, based on HSP70A promoter-luciferase fusions and cyclic voltammetry have also been developed for the detection of H_2O_2 *in vivo* (Shao et al., 2007). Mediator and non-mediator-based electrodes have been used in the past as the electrochemical method for the detection of H_2O_2. Horseradish peroxidase (HRP) is the most commonly used material for the modification of the electrode among the mediator based modified electrodes (Liu et al., 2016; Rad et al., 2012).

In our study (Prasad et al., 2015), we developed and used a mediator (osmium) based modified carbon electrode for real-time detection of H_2O_2 generation at the level of sub-cellular organelles. We studied the effect of high light stress in leaf and PSII membranes reflected by H_2O_2 as the stress response formed via the dismutation of $O_2^{\bullet-}$. We observed that light stress caused a gradual increase in the reduction current which is directly proportional to the formation of H_2O_2. We also studied the effect of SOD on $O_2^{\bullet-}$ to find out the contribution of $O_2^{\bullet-}$ in H_2O_2 formation under light stress and observed that

when exogenous SOD was added to the light exposed PSII membrane, reduction current for H_2O_2 progressively increased leading to the conclusion that the H_2O_2 produced in the PSII membrane is formed via the dismutation of $O_2^{\bullet-}$. To confirm that the increase in the reduction current was due to the rise in H_2O_2 concentration, we subsequently examined the effect of catalase which converts H_2O_2 to water and O_2. We observed that the exogenous addition of catalase brings back the reduction current close to the value observed under the dark condition.

Our mediator based modified carbon electrode for the electrochemical detection of H_2O_2 by catalytic amperometry is an auspicious biosensor device for the detection of H_2O_2 in photosynthetic cells and subcellular structures including PSII or thylakoid membranes. Our biosensor can be used to deliver precise information on the qualitative determination of H_2O_2 and therefore it has wide application in photosynthetic research. Representation to shows the working principle of our biosensor shown in figure 5.
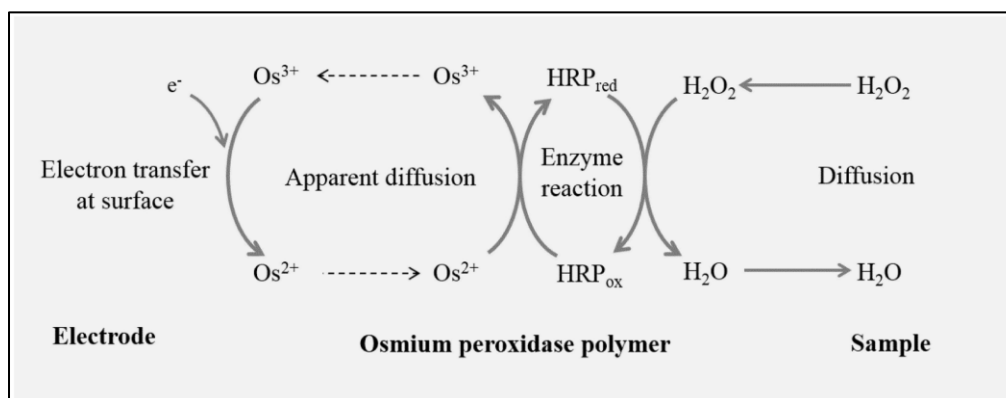
Fig. 5. Schematic drawing to demonstrate the working principle of osmium-HRP modified carbon electrode representing the oxidation-reduction cycle leading to the generation of reduction current for H_2O_2. Adapted from (**Prasad et al., 2015**).

1.2.3. Hydroxyl radical

Hydroxyl radical is the most potent yet short-lived radical, generated by the metal-catalyzed reduction of free H_2O_2, via a well-known phenomenon in inorganic chemistry called Fenton reaction (Liochev, 1999). Generation of $HO^\bullet$ from bound H_2O_2 occurs via Fenton like reaction in many biological systems. Reduction of H_2O_2 to the $HO^\bullet$ by several

low-valent metals such as Fe^{2+}, Mn^{2+}, or Cu^+ has been reported in biological systems. The Fe^{2+} is known to be the strongest reductant of H_2O_2 (Pospíšil, 2009). The chloroplast has long been recognized as an important site of $HO^\bullet$ formation through O_2 production at PSII. The Mn^{2+} and Fe^{2+} in PSII are implicated in $HO^\bullet$ generation that can lead to photoinhibition. PSII acceptor and donor sites are the major sites for the generation of $HO^\bullet$ (Pospíšil, 2009). The detection methods for $HO^\bullet$ are far more limited compared to other ROS. Among the many kinds of spin traps for the analysis of $HO^\bullet$ radical by EPR spectroscopy, the nitrone compound DMPO is the most popular and classic one. Interaction of DMPO with $HO^\bullet$ forms DMPO-OH adduct, which could be captured using the EPR spectrometer to generate specific spectra. One of the major drawbacks of using DMPO for the detection of $HO^\bullet$ is that DMPO-OH adduct spectra in EPR can be obtained from the decay of DMPO-OOH adduct.

In our studies (**Kumar et al., 2018, 2019a, 2019b**) we used the EPR spectroscopy with a promising spin trap α-(4-pyridyl N-oxide)-N-(tert-butylnitrone) POBN in combination with ethanol (EtOH) (POBN/EtOH system) for the detection of $HO^\bullet$ *in vitro* and fluorescent probe 3'-p-(hydroxyphenyl) fluorescein (HPF) for the qualitative detection of $HO^\bullet$ *in vivo* to examine the effect of high light on the formation of $HO^\bullet$. We observed that high light stress leads to the formation of $HO^\bullet$. Hydroxyl radical is composed of a hydrogen atom bonded to an oxygen atom which makes it highly reactive. It readily steals hydrogen atoms from other molecules to form water (Gligorovski et al., 2015). In our study, we observed that illumination of light increased the formation of protein radicals on PSII proteins. Based on our *in vitro* and *in vivo* results of $HO^\bullet$ formation and protein oxidation we propose that most of the protein oxidation might be caused by $HO^\bullet$ (**Kumar et al., 2018**).

1.2.4. Singlet oxygen

Singlet oxygen is produced in plant leaves in light via chlorophylls as photosensitizers. The production of $^1O_2$ is spatially resolved within thylakoid membranes and is enhanced under light stress conditions. The $^1O_2$ is produced by the energy transfer

from triplet excited chlorophyll (^{3}Chl*) to O_2 formed either by the intersystem crossing from singlet excited chlorophyll (^{1}Chl*) in the PSII antennae complex or the recombination of the charge-separated radical pair ^{3}[P680$^{\bullet+}$Pheo$^{\bullet-}$] in the PSII reaction center (Fig. 6). Apart from PSII, light-harvesting antenna complexes (LHCs) are also involved in the formation of $^1O_2$ (Fischer et al., 2013; Pospíšil 2012; Triantaphylides & Havaux, 2009).
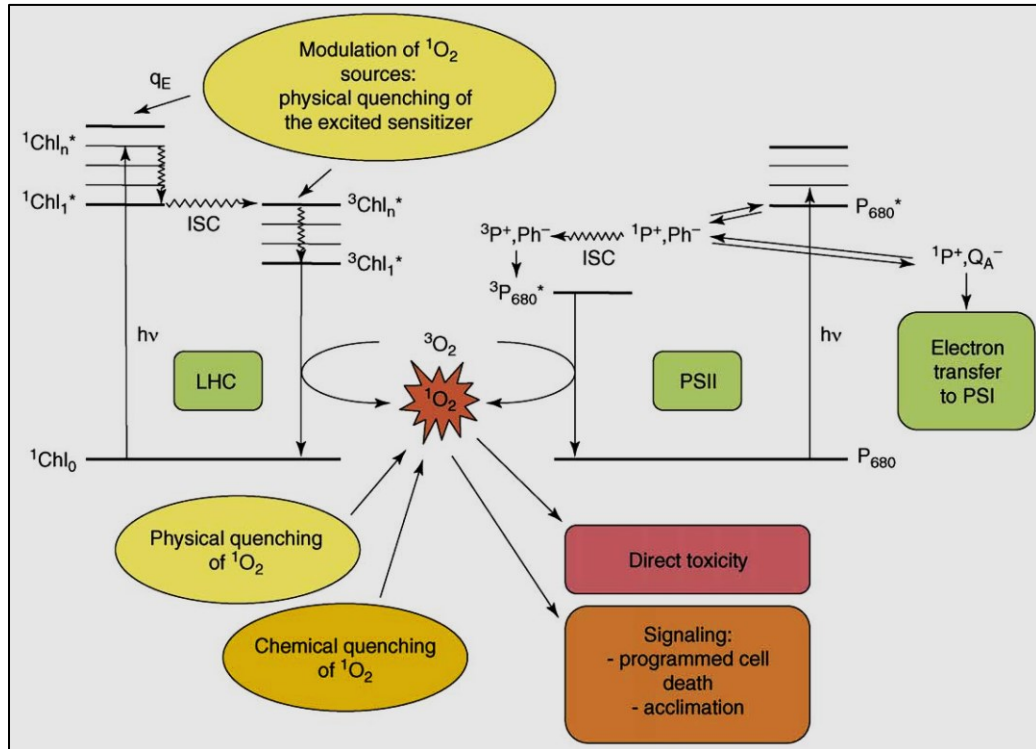
Fig. 6. Schematic presentation of the $^1O_2$ in photosynthetic. In LHCs, ^{3}Chl* formed by electron spin-flip [intersystem crossing (ISC)] from ^{1}Chl*. In the PSII reaction centers, charge separation between the singlet excited state of primary electron donor of PSII (^{1}P680*) and pheophytin (Pheo) is followed by electron transfer to the primary quinone electron acceptor of PSII (Q_A) and then to PSI. Reduction of Q_A promotes charge recombination reactions in PSII ultimately giving rise to the triplet state ^{3}P680*. Accumulation of triplet states in both LHCs and PSII centers leads to the activation of O_2 to produce $^1O_2$. Both of these reactions are favored in strong light. Adapted from (Triantaphylides & Havaux, 2009).

The study of $^1O_2$ in biological systems is challenging because of its instability and high reactivity towards biomolecules making it difficult to quantify accurately. Several methods have been developed to study the formation and detection of $^1O_2$, but most of

the studies so far have focused on those conditions that produce relatively large amounts of $^1O_2$. However, the need for more sensitive methods is required as one begins to explore the levels of $^1O_2$ required in signaling and regulatory processes. An indirect method to detect the $^1O_2$ has been performed by qRT-PCR of transcripts activated by $^1O_2$ and direct methods to detect $^1O_2$ include using probes that interact directly with $^1O_2$ (Koh & Fluhr, 2016; Prasad et al., 2018). In our studies (**Kumar et al., 2018, 2019a, 2019b**) we used the EPR spectroscopy with a $^1O_2$ specific spin probe 2, 2, 6, 6-tetramethyl-4-piperidone (TMPD) for the detection of $^1O_2$ *in vitro* and fluorescent probe singlet oxygen sensor green (SOSG) for the qualitative detection of $^1O_2$ *in vivo* and observed that light stress induces the formation of $^1O_2$.

Singlet oxygen is very reactive because of its high electrophilicity and excited-state energy. Above all, the singlet spin state of $^1O_2$ permits the spin-allowed reaction pathways, allowing a variety of oxygenation reactions (You, 2018). Singlet oxygen directly oxidizes proteins, unsaturated fatty acids, and nucleic acids (Wagner et al., 2004). It has been well established that $^1O_2$ is the most important ROS accountable for the loss of PSII under light stress (Krieger-Liszkay et al., 2008; Triantaphylides et al., 2008). Singlet oxygen can be quenched by β-carotene, α-tocopherol, plastoquinol (Ferretti et al., 2018; Krieger-Liszkay, 2005).

1.3. Photosynthetic oxygen evolution

Introduction of O_2 into our atmosphere by photosynthetic organisms during the evolution of aerobic life on the planet has brought us, ROS as an essential part of life. It has been established that excitation or reduction of O_2 leads to the formation of ROS (Pospíšil 2009; Tripathy & Oelmuller, 2012). Since the photosynthetic O_2 evolution has been considered as the source of ROS several techniques have been used to measure photosynthetic O_2 evolution in the last years. Due to the importance of O_2 in medical and industrial applications, its measurement has received much attention. Out of many techniques available, polarography is a predominant technique supported with extensive

documentation of its use in biological and medical research (Delieu & Walker, 1981; Schumpe et al., 1978; Stengel & Reckermann, 1978; Wei et al., 2019).

In photosynthesis research, the traditional Warburg manometry was replaced by polarography. Many types of electrochemical cells have been designed to measure O_2. For the routine measurements of photosynthetic O_2 evolution, commercially available equipment based on the Clark electrode is used frequently (Clark, 1956). The Clark electrode is a 'bipolar' electrochemical O_2 sensor. Teflon membrane used in Clark electrode is permeable to O_2 but impermeable to water and ions, therefore, used to separate the sample from the cathode (platinum) and anode (silver) and the connecting electrolyte solution. The cathode reduces O_2 to hydroxide ions (OH^-). At the anode, AgCl is formed initially, and later as OH^- accumulates AgOH also formed. The Clark electrode is essentially a closed system and can be used to measure O_2 in the gas phase as well as in solution (Delieu & Walker, 1981; Delieu & Walker, 1983). The measured current is simply proportional to the O_2 tension (partial pressure) in the sample and is easily calibrated by comparison to the signal in an air-saturated solution at the same temperature. Although Clark electrode is used frequently in photosynthesis research, conditions often arise where the unmodified Clark electrode is too unresponsive, too slow, or both.

Another technique, EPR oximetry has also been used extensively in the past to measure the O_2. This technique is based on the fact that O_2 is paramagnetic. The collision between paramagnetic O_2 and a properly chosen spin probe (Lithium phthalocyanine, CTPO, TRITYL) causes expansion of the EPR Line (Liu et al., 1993; Subczynski & Swartz, 2005). This technique is non-invasive, and it does not consume O_2 or produce harmful reaction products and does not require continuous stirring of the sample while stirring (in solution) of the sample in the Clark electrode method is very important to ensure that the O_2 concentration gradient is restricted to the membrane. EPR Oximetry can be used to measure the O_2 concentration in very small structures, like cells. A major drawback of EPR oximetry has been the fact that many spin probes/labels are toxic (Subczynski & Swartz, 2005). Another difficulty is that the broadening of the EPR line can be caused by many

other parameters than O_2, like the presence of paramagnetic ions, nitroxide concentration, viscosity, microwave power, pH, and temperature (Salikhov et al., 1971). Thus, it is essential to standardize the O_2 effect for each system and keep parameters like temperature, microwave power, and nitroxide concentration constant. Besides at high O_2 concentrations EPR oximetry is not very sensitive. So far there are only a few reports available on the use of EPR oximetry in photosynthesis (Tikhonov & Subczynski, 2019).

Photosynthetic O_2 evolution involves the rearrangement of nuclei to form one kind of molecule from another and this kind of rearrangement of nuclei can be studied by using traditional biochemical tools by tagging of the substrate by nuclear isotopes and measuring the isotope arrangement of the product. The importance of mass spectrometry in photosynthesis research was established by Hoch and Kok (Hoch & Kok, 1963). In addition to the above-mentioned techniques, there are few reports on the use of photoacoustic spectroscopy and galvanic sensors in photosynthesis (Mauzerall, 1990; Meyer et al., 1989). Quenching based O_2 sensors that are prepared by embedding the fluorophore in O_2 permeable polymer matrix [Polyvinyl chloride (PVC) or silicone] has an advantage as they are generally used in both liquid and gaseous phase (Tyystjarvi et al., 1998). As quenching-based O_2 sensors, ruthenium (Ru) (II) α-diimine complexes (15) and platinum (Pt) (II)/palladium (Pd) (II) porphyrin systems are among the most studied (Demas & DeGraff, 1997; Demas et al., 1999; Gouterman, 1997; Kneas et al., 1997).

Each method applied for the detection and estimation of O_2 has some strengths and limitations. The electrochemical technique has an advantage of direct detection of O_2 without labels and additional reagents. As an example, electrochemical O_2 analyzers based on the reduction of O_2 at a negatively polarized platinum electrode has been established. An ultra-microelectrode (diameter: 1.5 µm) was also introduced and inserted into a single cell to determine intercellular reduction current for O_2 (Matsue et al., 1992; Matsue et al., 1993).

In our study (Kasai et al., 2019), we used our recently developed LSI-based amperometric biosensor array system referred to as the Bio-LSI chip for two-dimensional imaging of light-induced O_2 evolution from spinach leaves (Inoue et al., 2012; Inoue et al.,

2015). The Bio-LSI contains a 10.4 mm × 10.4 mm complementary metal-oxide-semiconductor (CMOS) sensor chip with 20 × 20-unit cells, an external circuit box, a control unit for data acquisition, and a direct current (DC) power box. Each unit cell of the chip consists of an operational amplifier with a switched-capacitor type I–V converter for in-pixel signal amplification, which grasps a fast acquisition of electrochemical images with high sensitivity. To the best of our knowledge, this is the first study to describe real-time electrochemical imaging of light-induced O_2 release from a photosynthetic organism using LSI-based amperometric sensors.

2. AIM OF THE STUDY

There are several methods available to study the protein oxidation, ROS formation, and photosynthetic O_2 evolution in plants. However, to date, there is no selective and sensitive technique available for the detection of protein radicals in plant cells to study the protein oxidation. Neither there is any method available for the real-time measurement of ROS ($O_2^{\bullet-}$, H_2O_2) formation and to perform two-dimensional imaging of photosynthetic O_2 evolution to study their kinetics as a result of oxidative stress. All things considered; we have aimed our study as follows:

I. Introduction of immuno-spin trapping to detect protein radicals *in vitro* and *in vivo* to study the protein oxidation due to photooxidative stress in leaves.

II. Characterization of PSII proteins involved in protein radical formation by protein oxidation in thylakoid membranes.

III. Develop an amperometric based detection method to provide evidence of $O_2^{\bullet-}$ generation and its kinetics in the leaves subjected to wounding.

IV. Develop an amperometric based detection method for the real-time measurement of H_2O_2 generation and its kinetic study at the level of sub-cellular organelles.

V. Develop an amperometric based detection method for the two-dimensional imaging of light-induced O_2 evolution from leaves.

3. EXPERIMENTAL APPROACH

To accomplish our aims of the study we have used a broad range of materials and methods. This chapter briefly describes the materials and different methods used in my doctoral study.

3.1. Chemicals

The important chemicals used in the study are listed here. Different spin traps were used including EMPO from Alexis Biochemicals (Switzerland), DMPO from Dojindo, Munich, Germany, POBN, spin probe TMPD, and fluorescence probe hydroxyphenyl fluorescein (HPF) from Sigma Aldrich, Germany. The capillary tube used for EPR measurements was from Blaubrand intraMARK, Brand, Germany. Reagent SOSG was obtained by Molecular Probes Inc. (U.S.A.),

A brief list of other chemicals used in the study are as follows; sucrose ($C_{12}H_{22}O_{11}$), sodium chloride (NaCl), magnesium chloride ($MgCl_2$), calcium chloride ($CaCl_2$), sodium bicarbonate ($NaHCO_3$), 4-2-hydroxyethyl-1-piperazine ethane sulfonic acid (HEPES, $C_8H_{18}N_2O_4S$),sodium-ascorbate ($C_6H_7NaO_6$), bovine serum albumin (BSA), 2-N-morpholino-ethane sulfonic acid (MES, $C_6H_{13}NO_4S$), triton X-100 [$C_{14}H_{22}O(C_2H_4O)n$], horseradish peroxidase (HRP), 3-(3,4-dichlorophenyl)-1,1-dimethyl urea (DCMU, $C_9H_{10}Cl_2N_2O$), ethanol (C_2H_5OH), etc. from Sigma-Aldrich Chemie Gmbh (Munich, Germany). The carbon electrodes from BAS Inc., ALS Co., Ltd. (Tokyo, Japan). Superoxide dismutase (SOD), xanthine oxidase, and xanthine (X/XO) from Wako Pure Chemicals Industries, Ltd. (Osaka, Japan), Sigma-Aldrich Chemie Gmbh (Munich, Germany) or Sigma-Aldrich Japan K.K. (Tokyo, Japan). The anti-D1, anti-C-terminal, anti-D-*de* loop, anti-cyt b_{559} α-subunit, anti-D2, anti-CP43, anti-CP47, and anti-Lhcb3 antibodies from Agrisera, an anti-DMPO antibody from Abcam, Cambridge, UK and anti-DNP antibody from Molecular Probes Europe BV, Leiden, Netherlands. Sodium dodecyl sulfate (SDS), 2,4-dinitrophenylhydrazine (DNPH), hydrochloric acid (HCl), tris-aminomethane (TRIS) and glycerol from Sigma Aldrich, Missouri, United States. Mini-PROTEAN tetra vertical

electrophoresis cell from Bio-Rad, California, USA, nitrocellulose (NC) membrane, semi-dry blotter (Trans-Blot SD, Semi-dry transfer cell, Bio-Rad, USA.

3.2. Growing of *Arabidopsis thaliana* plants

Seeds of wild-type Arabidopsis (Arabidopsis thaliana, cv. Columbia-0; WT) purchased from the Nottingham Arabidopsis Stock Center (NASC), University of Nottingham (Loughborough, United Kingdom) were waterlogged in distilled water followed by potting in growing pots with a peat substrate (Klasmann, Potgrond H). Plants were kept in a growing chamber (Photon Systems Instruments, Drásov, Czechia) under regulated environmental conditions with a light intensity of 100 µmol photons $m^{-2} s^{-1}$, photoperiod of 8/16 hour and temperature of 25° C (unless specified otherwise) with a relative air humidity of 60%.

3.3. Spinach (*Spinacia oleracea*) leaves collection

For Spinach experiments, fresh leaves were purchased from the local market.

3.4. High-light treatment for photoinhibition

Arabidopsis plants (5 or 6 weeks old) were exposed to high light stress (1500 µmol photons $m^{-2} s^{-1}$) at 8° C for 13 hours using AlgaeTron AG 230 (Photon Systems Instruments, Drásov 470, Czechia). The Arabidopsis leaves (5-6 weeks) were collected for further experiments. For confocal experiments leaf pieces and intact chloroplasts were illuminated with high red light (1000 µmol photons $m^{-2} s^{-1}$) at 25° C for 30 min.

3.5. Intact chloroplast isolation from Arabidopsis

Intact chloroplasts were prepared from Arabidopsis leaves following the protocol of Seigneurin et al. (Seigneurin-Berny et al., 2008). In brief, prepare two 20 ml polypropylene tubes containing 10 ml discontinuous percoll gradients solution prepared by successively layering 2 ml of 80% and 8 ml of 40% percoll solutions for chloroplast purification. Collect and wash the Arabidopsis leaves, strain the leaves, and store them in the dark cold room

(4° C) overnight. Leaf material covered with enough grinding buffer (with BSA) to cover the leaves in the blender cup and homogenize the leaf material twice, each time 5 to 10 sec in a blender at low speed and a third time (2 to 10 sec) at high speed. Quickly filter the homogenate through 4 to 5 layers of muslin and one layer of nylon blutex and collect the filtered homogenate in a glass beaker. Equally, distribute the filtered suspension into two tubes for centrifugation and centrifuge them for 10 min at 1200 × g at 4° C. Cautiously remove the supernatant from each tube, retaining the pellets. Get rid of the remaining supernatant with a Pasteur pipet and keep the crude chloroplast fraction containing pellets on ice followed by washing of pellets with washing buffer twice and loading the crude chloroplast suspension on the top of the discontinuous percoll gradients by wall transfer to avoid mixing of suspension to upper percoll layer. Centrifuge the gradients for 20 min at 3000 × g at 4° C using the swinging rotor.

Intact chloroplasts are recovered at the bottom interface (80%/40% percoll) and broken chloroplasts + extra-chloroplastic membrane systems form a band at the upper interface (sample/40% percoll). Cautiously take away the upper part of the gradient holding the broken chloroplasts by aspirating with a Pasteur pipet, recover intact chloroplasts (at the interface 80%/40% Percoll) with 5 ml pipet and softly pool the intact chloroplasts in a 10 ml tubes. Dilute the chloroplast suspension 3 to 4-fold with washing medium and centrifuge the suspension for 5 min at 4000 × g at 4° C. Cautiously remove the supernatant and repeat the wash step, centrifuge for 5 min at 3000 × g at 4° C, remove the supernatant and save the pellet containing purified intact chloroplasts on ice and use it immediately for experiments.

3.6. Thylakoid membrane isolation from Arabidopsis

Five to-six-weeks old rosette leaves were harvested from plants. The harvested leaves (0.3–0.5 g) were floated on ice-cold water for 20–30 min in the dark at 4° C followed by blotting. All following steps were carried out at 4° C in the dark and all materials and buffers used were precooled. The leaves were rapidly homogenized using mortar and pestle in 2–3 ml of grinding buffer (GB) containing 0.4 M sorbitol, 5 mM EDTA,

5 mM EGTA, 5 mM MgCl$_2$, 10 mM NaHCO$_3$, 20 mM Tricine/NaOH (pH 8.4) and 0.5% (w/v) fatty acid-free BSA. The homogenate was filtered through 8 layers of cheesecloth, with a gentle hand pressure being applied to increase the final thylakoid yield. The suspension was centrifuged at 2600 g for 3 min at 4 ∘C, the supernatant carefully discarded and the pellet resuspended in 2–3 ml of resuspending buffer (RB) containing 0.3 M sorbitol, 2.5 mM EDTA, 5 mM MgCl$_2$, 10 mM NaHCO$_3$, 20 mM HEPES (pH 7.6) and 0.5% (w/v) fatty acid-free BSA. After centrifugation (2600 g for 3 min at 4 ∘C), the pellet was washed again in RB and then resuspended in 1 ml of hypotonic buffer (HB) containing 2.5 mM EDTA, 5 mM MgCl$_2$, 10 mM NaHCO$_3$, 20 mM HEPES (pH 7.6) and 0.5% (w/v) fatty acid-free BSA, and the final volume was adjusted to 5 ml with HB. The thylakoid membranes were collected by centrifugation (2600 g for 3 min at 4 ∘C). Finally, the pellet was resuspended in a small volume (0.5–1 ml) of RB and the suspension was stored in ice in the dark until use. The chlorophyll concentrations from thylakoid preparations and intact leaves were calculated from the absorbances at 645 and 663 nm of 80% (v/v) acetone extract, according to Arnon (1949).

NOTE: All solutions, glassware, centrifuge tubes, and equipment should be precooled to 0° C to 4° C and kept on ice throughout.

NOTE: All operations are carried out at 0° C to 5° C by keeping samples on ice in the darkroom.

3.7. PSII membrane isolation from Spinach

The PSII membranes were isolated from fresh spinach leaves following the protocol of Berthold et al. (Berthold et al., 1981) with few modifications described by Ford and Evans (Ford & Evans, 1983). Each step through the isolation process was performed at 4°C in green light using green LED strip (Photon Systems Instruments (PSI), Drásov, Czech Republic) or under dark condition using different buffers (A and B). The buffer A (pH 7.5) contain 400 mM sucrose, 15 mM NaCl, 5 mM MgCl2, 5 mM CaCl2, 40 mM HEPES (pH 7.5), 5 mM Na-ascorbate, and 2 g/l bovine serum albumin (BSA) whereas, buffer B contain 400 mM sucrose, 15 mM NaCl and 5 mM MgCl2, 40 mM MES (pH 6.5). Dark-adapted fresh

spinach leaves were rinsed twice with deionized water followed by grinding in buffer A with the addition of Na-ascorbate and BSA. After grinding the homogenate was filtered through 2 layers of nylon bolting cloth. The filtrate was removed into the chilled centrifugation tubes and centrifuged for 10 min at 9950 × g at 4°C. The supernatant was removed, and the pellet was resuspended in buffer B and again centrifuged at 9950 × g for 10 min at 4°C. Repeat this step and determine the concentration of chlorophyll following the protocol described by (Lichtenthaler, 1987). This step was followed by treating the suspension with 5% Triton X-100 on ice bath with nonstop stirring of the solution for 17 min, followed by centrifugation at 7000 × g for 7 min at 4°C. The supernatant was collected, centrifuged at 48,000 × g for 20 min at 4°C, again the pellet was collected and washed 3 times with buffer B. At the last step, chlorophyll concentration was determined again. PSII membranes were diluted to the desired final chlorophyll concentration and stored at −80° C until further use.

3.8. EPR spin-trapping spectroscopy

The detection of $O_2^{\bullet-}$, $HO^\bullet$ and $^1O_2$ was performed using EPR spectroscopy. For $O_2^{\bullet-}$, $HO^\bullet$ and $^1O_2$ detection, spin traps, EMPO, POBN/ethanol system, and spin probe TMPD were used, respectively. The detection of $O_2^{\bullet-}$ in the Xanthine/Xanthine Oxidase system was performed using 25 mM EMPO in phosphate buffer and for the detection of $O_2^{\bullet-}$ in PSII membranes 150 µg Chl ml^{-1} was incubated with 25 mM EMPO, 40 mM phosphate buffer (pH 6.5), 20 µM DCMU and 50 µM Desferal. Formation of light-induced EMPO-OOH adduct EPR spectra was measured in PSII membranes after illumination of PSII membranes in a glass capillary tube with continuous white light (1000 µmol photons m^{-2} s^{-1}). For $HO^\bullet$ detection, thylakoid membranes (250 µg Chl ml^{-1}) were incubated in the presence of 50mM POBN, 170mM ethanol and 40mM MES buffer (pH 6.5) in the dark or in high white light (1500 µmol photons m^{-2} s^{-1}) for 30 min and formation of light-induced [POBN-CH(CH$_3$)OH] adduct EPR spectra was measured in thylakoid membranes. For $^1O_2$ detection, thylakoid membranes (250 µg Chl ml^{-1}) were incubated in the presence of 50mM TMPD and 40mM MES buffer (pH 6.5) in dark or high white light (1500 µmol

photons m^{-2} s^{-1}) for 30 min and formation of light-induced TEMPONE EPR signal was measured in thylakoid membranes. Subsequently, the samples were immediately transferred into a glass capillary tube and EPR spectra were collected at room temperature using an EPR spectrometer. EPR conditions used in all the measurements were as follows: microwave power, 10 mW; modulation amplitude, 1 G; modulation frequency, 100 kHz; sweep width, 100 G; and scan rate, 1.62 G s^{-1}.

3.9. Confocal laser scanning microscopy

The visualization of HO$^\bullet$ and $^1O_2$ formation in light stressed leaves was performed by confocal laser scanning microscopy using hydroxyphenyl fluorescein (HPF) and singlet oxygen sensor green (SOSG) fluorescence probes (Molecular Probes Inc., Eugene, OR, USA), respectively. Leaves were sliced into pieces of approximately 5 mm squares after light illumination (1500 µmol photons m^{-2} s^{-1}, 13 h, 8 °C) and then incubated in 2 ml Eppendorf tube either with 10 µM HPF or 50 µM SOSG in presence of HEPES buffer (pH 7.5) for 30 min either in the dark or exposed to high red light (λ≥600nm). Leaf pieces were placed on a wetted glass slide followed by covering it with a glass coverslip. Afterward, the samples were visualized by confocal microscope (Fluorview 1000 unit attached to IX80 microscope; Olympus Czech Group, Prague, Czech Republic). The excitation of HPF/SOSG was performed by a 488 nm line of an argon laser and the emission was detected by a 505–525 nm filter. Chloroplasts were visualized by excitation with 543 nm helium-neon laser, and emission was recorded with a 655–755 nm bandpass filter.

3.10.   SDS-PAGE and immuno-spin trapping

To separate the proteins, we used SDS-PAGE and to detect protein radical in thylakoid membranes, immuno-spin trapping technique was used. To detect the protein radicals, thylakoid membranes (2.5-5 µg Chl ml^{-1}) were incubated with 50 mM DMPO in the dark or illuminated with high light (1500 µmol photons m^{-2} s^{-1}). Protein extraction was done using DTT (dithiothreitol) protein extraction buffer followed by heating at 70 °C in a dry bath for 15 min and centrifuged at 16,000×g for 5 min at 4 °C. To detect protein carbonyls,

thylakoid membranes (5-10 µg Chl ml^{-1}) were illuminated for 30 min with high light (1500 µmol photons m^{-2} s^{-1}). Aqueous SDS (12%) was used to extract proteins and 2,4-dinitrophenylhydrazine (DNPH) (10mM) dissolved in 2M HCl was used for derivatization of proteins. Neutralization was done with TRIS, 2M and 30% glycerol (Sigma Aldrich, Missouri, United States). Protein samples were loaded into the wells and SDS-PAGE was done using Mini-PROTEAN Tetra vertical electrophoresis cell (Bio-Rad, California, USA) according to the protocol Tris-Tricine SDS-PAGE described by (Schagger, 2006). Transfer of protein bands from gel to a nitrocellulose (NC) membrane was completed using a semi-dry blotter (Trans-Blot SD, Semi-dry transfer cell, Bio-Rad, USA). Non-specific sites on NC membrane was blocked by incubating the NC membrane overnight with 5% BSA prepared in phosphate-buffered saline-tween 20 (pH 7.4) at 4 °C. All successive steps were performed on a shaker at room temperature. Overnight incubated NC membrane was incubated with rabbit polyclonal anti-DMPO antibody (Abcam, Cambridge, UK) and rabbit polyclonal anti-DNP antibody (Molecular Probes Europe BV, Leiden, Netherlands) followed by 2-3 washing steps and 1 h incubation with HRP conjugated anti-rabbit secondary antibody. Visualization of protein bands was done using luminol as a chemiluminescent probe (Amersham Imager 600, GE Health Care Europe GmbH, Freiburg, Germany). To identify proteins from anti-DMPO blot, antibody stripping and re-probing with new antibodies raised against the PSII proteins was performed and the apparent size of protein bands was determined using a standard protein ladder (PageRuler™ Prestained Protein Ladder, 10–180 kDa, Thermo Scientific, Lithuania).

3.11. Catalytic amperometry

Potentiostat (HA1010mM4S; Hokuto Denke Co. Ltd., Japan) was used for the electrochemical measurements. For the detection of H$_2$O$_2$ generated in the PSII membrane, the PSII membranes of 150 µg Chl ml^{-1} were introduced into a six-well repro plate (IFP, Research unit for the functional peptides, Yamagata, Japan). Ag/AgCl electrode was used as a reference electrode and the Os-HRP modified carbon electrode was used as a working electrode and the platinum plate in the dimension of 5*5*0.1 mm was used

as a counter electrode. The kinetics of the light-induced H_2O_2 formation was measured in PSII membranes after illumination under continuous white light (1000 µmol photons m^{-2} s^{-1}) for 1 h. The sampling time was kept at 500 ms. For the detection of $O_2^{\bullet-}$ generated in response to wounding we used Ag/AgCl as a reference electrode, polymeric iron-porphyrin-based modified carbon electrode as a working electrode (ϕ1 mm), and a platinum wire (ϕ0.25 × 40 mm) as a counter electrode. The kinetics of the of $O_2^{\bullet-}$ formation was measured in non-wounded and wounded spinach leaves and in the chemical system containing no spinach leaves and, in the absence/presence of SOD (400 U ml^{-1}).

3.12. Bio-LSI based real-time imaging of photosynthetic O_2 evolution

For the two-dimensional real-time imaging of photosynthetic O_2 evolution, spinach leaf in the dimension of 5 mm × 2 mm was positioned on the working electrodes covered with PBS buffer. The reference electrode is composed of Ag/AgCl, a counter electrode composed of Pt wire, and the working electrode is composed of 400 platinum electrodes each with a diameter of 40 µm on the Bio-LSI chip. A potential of − 0.5 V vs. Ag/AgCl was applied to the working electrodes until the reduction current of dissolved O_2 was stabilized to ~0 nA followed by two-dimensional imaging of O_2 evolution from the spinach leaf by continuous application of − 0.5 V vs. Ag/AgCl to the working electrodes. To initiate photosynthesis the light exposure was accomplished using a KL300 LED light source (λ = 400–800 nm) connected with a light guide (Schott AG, Hattenbergstrasse 10, Mainz, Germany) with light intensities of 0 klx, 3 klx (40 µmol photons s^{-1} m^{-2}), 20 klx (260 µmol photons s^{-1} m^{-2}) and 30 klx (400 µmol photons s^{-1} m^{-2}). The light intensities used in the study reflect the situation very similar to field conditions. Experiments in the absence of spinach leaf were performed as a negative control. Reduction current data from a single electrode [indicated by a red open square, (Kumar et al., 2019a)] from the electrode sensor array system was chosen for the time course monitoring of the reduction current. The effect of a photosynthetic inhibitor, DCMU was also studied.

4. CONCLUSIONS AND FUTURE PERSPECTIVES:

Based on the results described in this thesis, we conclude that:

- Oxidation of proteins is associated with the formation of protein radicals involving carbon-centered (alkyl) and oxygen-centered (peroxyl and alkoxyl) radicals. The formation of protein radicals was initiated either by $HO^\bullet$ or $^1O_2$.

- Our *in vitro* and *in vivo* results using the immuno-spin trapping technique show that oxidation of PSII proteins is caused by $HO^\bullet$ or $^1O_2$.

- Our confocal laser scanning microscopy results using the anti-DMPO antibody conjugated with FITC shows that protein radicals are formed in the chloroplasts located at the periphery of the mesophyll cells predominantly in the appressed thylakoid membranes containing PSII complexes.

- A standard immunoblotting technique using PSII protein-specific antibodies showed that protein radicals are formed on D1, D2, CP43, CP47, and Lhcb3 proteins.

- Protein oxidation is reflected by the appearance/disappearance of the protein bands revealing that formation of protein radicals is associated with protein fragmentation (cleavage of the D1 peptide bonds) and aggregation (cross-linking with another PSII subunits).

- D1, C-terminal, D-*de* loop, D2 and α-subunit of cyt b_{559} protein contributed in 55 and 68 kDa aggregate formation

- D1, C-terminal, and α-subunit of cyt b_{559} protein contributed in 41 and 18 kDa band.

- Our results provide clear evidence on the involvement of D1, C-terminal, D-*de*-loop, and α-subunit of cyt b_{559} proteins in aggregation and fragmentation and formation of protein radical on the aggregates and fragments.

- Imaging of protein radicals by immuno-spin trapping represents a selective and sensitive technique for the detection and characterization of protein radicals that might help to clarify mechanistic aspects of the role of protein radicals in the retrograde signaling and oxidative damage in the plant cell.

- Our *in vitro* and *in vivo* results provide the evidence on the formation of $^1O_2$, $O_2^{\bullet-}$, H_2O_2, $HO^{\bullet}$ production during stress.

- High light stress in the PSII membrane primarily leads to the production of $O_2^{\bullet-}$ as the stress response.

- Wounding in plants caused by mechanical injury is associated with the formation of $O_2^{\bullet-}$.

- Addition of exogenous SOD, which is known to catalyze the dismutation of $O_2^{\bullet-}$ to H_2O_2 to PSII membranes before illumination, completely diminish $O_2^{\bullet-}$. The simultaneous addition of SOD and CAT was also found to completely suppress the $O_2^{\bullet-}$. These observations indicate that $O_2^{\bullet-}$ produced during high light illumination is involved in H_2O_2 formation in PSII membranes.

- Photosynthetic water oxidation catalyzed by a tetra-manganese penta-oxygen calcium (Mn_4O_5Ca) cluster bound to the proteins of PSII leads to the production of O_2.

- Application of immuno-spin trapping opens new possibilities to characterize the oxidized proteins and study their role in the signal transduction from the chloroplasts to the nucleus and unravel description of the spatial and temporal dynamics of the oxidative damage in the plant cell.

- Catalytic amperometric measurements using polymeric iron-porphyrin based modified carbon electrode is a direct method for real-time monitoring and precise detection of $O_2^{\bullet-}$ in biological samples, with the potential for wide application in plant research for specific and sensitive detection of $O_2^{\bullet-}$.

- The osmium-HRP modified electrode is specific for H_2O_2 and can be widely used in photosynthetic research where the detection of H_2O_2 has always been a challenge.

- Light-induced O_2 evolution can be imaged using the Bio-LSI chip, suggesting that the Bio-LSI is a promising tool for real-time imaging.

5. REFERENCES

Alche, J. D. (2019). A concise appraisal of lipid oxidation and lipoxidation in higher plants. *Redox Biology, 23*, Article Unsp 101136. https://doi.org/10.1016/j.redox.2019.101136

Ananyev, G., Renger, G., Wacker, U., & Klimov, V. (1994). The photoproduction of superoxide radicals and the superoxide dismutase activity of photosystem II. The possible involvement of cytochrome b_{559}. *Photosynthesis Research, 41*(2), 327-338. https://doi.org/10.1007/BF00019410

Anavi, S., Ni, Z., Tirosh, O., & Fedorova, M. (2015). Steatosis-induced proteins adducts with lipid peroxidation products and nuclear electrophilic stress in hepatocytes. In *Redox Biol*ogy (Vol. 4, pp. 158-168). https://doi.org/10.1016/j.redox.2014.12.009

Andersson, B., & Aro, E. M. (2001). Photodamage and D1 protein turnover in photosystem II. *Regulation of Photosynthesis, 11*, 377-393.

Apel, K., & Hirt, H. (2004). Reactive oxygen species: metabolism, oxidative stress, and signal transduction. *Annual Review of Plant Biology, 55*, 373-399. https://doi.org/10.1146/annurev.arplant.55.031903.141701

Arato, A., Bondarava, N., & Krieger-Liszkay, A. (2004). Production of reactive oxygen species in chloride- and calcium-depleted photosystem II and their involvement in photoinhibition. *Biochimica et Biophysica Acta, 1608*(2-3), 171-180. https://doi.org/10.1016/j.bbabio.2003.12.003

Aro, E. M., Hundal, T., Carlberg, I., & Andersson, B. (1990). *In vitro* studies on light-induced inhibition of photosystem-II and D1-protein degradation at low-temperatures. *Biochimica et Biophysica Acta, 1019*(3), 269-275. https://doi.org/Doi 10.1016/0005-2728(90)90204-H

Aro, E. M., Virgin, I., & Andersson, B. (1993). Photoinhibition of photosystem II. Inactivation, protein damage, and turnover. *Biochimica et Biophysica Acta, 1143*(2), 113-134. https://doi.org/10.1016/0005-2728(93)90134-2

Asada, K. (1999). The water-water cycle in chloroplasts: Scavenging of active oxygens and dissipation of excess photons. *Annual Review of Plant Physiology and Plant Molecular Biology, 50*, 601-639. https://doi.org/10.1146/annurev.arplant.50.1.601

Asada, K. (2006). Production and scavenging of reactive oxygen species in chloroplasts and their functions. *Plant Physiology, 141*(2), 391-396. https://doi.org/10.1104/pp.106.082040

Awad, J., Stotz, H. U., Fekete, A., Krischke, M., Engert, C., Havaux, M., Berger, S., & Mueller, M. J. (2015). 2-cysteine peroxiredoxins and thylakoid ascorbate peroxidase create a water-water cycle that is essential to protect the photosynthetic apparatus under high light stress conditions. *Plant Physiology, 167*(4), 1592-1603. https://doi.org/10.1104/pp.114.255356

Awasthi, Y. C., Yang, Y., Tiwari, N. K., Patrick, B., Sharma, A., Li, J., & Awasthi, S. (2004). Regulation of 4-hydroxynonenal-mediated Signaling by Glutathione S-transferases. *Free Radical Biology and Medicine, 37*(5). https://doi.org/10.1016/j.freeradbiomed.2004.05.033

Barbato, R., Friso, G., Rigoni, F., Frizzo, A., & Giacometti, G. M. (1992). Characterization of a 41 kDa photoinhibition adduct in isolated photosystem II reaction centres. *FEBS Letters, 309*(2), 165-169.

Bartel, B., & Citovsky, V. (2012). Focus on ubiquitin in plant biology. *Plant Physiology, 160*(1), 1-1. https://doi.org/10.1104/pp.112.203208

Bauer, G., & Zarkovic, N. (2015). Revealing mechanisms of selective, concentration-dependent potentials of 4-hydroxy-2-nonenal to induce apoptosis in cancer cells through inactivation

of membrane-associated catalase. *Free Radical Biology and Medicine, 81*. https://doi.org/10.1016/j.freeradbiomed.2015.01.010

Baxter, A., Mittler, R., & Suzuki, N. (2014). ROS as key players in plant stress signalling. *Journal of Experimental Botany, 65*(5), 1229-1240. https://doi.org/10.1093/jxb/ert375

Beltrán, B., Orsi, A., Clementi, E., & Moncada, S. (2000). Oxidative stress and S-nitrosylation of proteins in cells. *British Journal of Pharmacology, 129*(5), 953-960. https://doi.org/10.1038/sj.bjp.0703147

Berthold, D. A., Babcock, G. T., & Yocum, C. F. (1981). A highly resolved, oxygen-evolving photosystem-II preparation from spinach thylakoid membranes-EPR and electron-transport properties. *FEBS Letters, 134*(2), 231-234. https://doi.org/Doi 10.1016/0014-5793(81)80608-4

Brett C.M.A., B. A. M. C. F. O. (1984). *Surface Modified Electrodes — Reasons and Advantages | SpringerLink* (Vol. 85). SpringerLink. https://doi.org/10.1007/978-94-009-6216-3_42

Calderón, A., Lázaro-Payo, A., Iglesias-Baena, I., Camejo, D., Lázaro, J. J., Sevilla, F., & Jiménez, A. (2017). Glutathionylation of pea chloroplast 2-cys Prx and mitochondrial Prx IIF affects their structure and peroxidase activity and sulfiredoxin deglutathionylates only the 2-cys Prx. *Frontiers in Plant Science., 8*. https://doi.org/10.3389/fpls.2017.00118

Chen, S., Yin, C., Strasser, R. J., Govindjee, Yang, C., & Qiang, S. (2012). Reactive oxygen species from chloroplasts contribute to 3-acetyl-5-isopropyltetramic acid-induced leaf necrosis of Arabidopsis thaliana. *Plant Physiology and Biochemistry, 52*, 38-51. https://doi.org/10.1016/j.plaphy.2011.11.004

Chen, W., Li, B., Xu, C., & Wang, L. (2009). Chemiluminescence flow biosensor for hydrogen peroxide using DNAzyme immobilized on eggshell membrane as a thermally stable biocatalyst. *Biosensors and Bioelectronics, 24*(8), 2534-2540. https://doi.org/10.1016/j.bios.2009.01.010

Clark, L. C. (1956). Monitor and control of blood and tissue oxygen tensions. *Transactions American Society for Artificial Internal Organs, 2*, 41-&.

Cleland, R. E., & Grace, S. C. (1999). Voltammetric detection of superoxide production by photosystem II. *FEBS Letters, 457*(3), 348-352. https://doi.org/10.1016/s0014-5793(99)01067-4

Dalle-Donne, I., Rossi, R., Giustarini, D., Milzani, A., & Colombo, R. (2003). Protein carbonyl groups as biomarkers of oxidative stress. *Clinica Chimica Acta, 329*(1-2), 23-38. https://doi.org/10.1016/S0009-8981(03)00003-2

Davies, M. J. (2005). The oxidative environment and protein damage. *Biochimica et Biophysica Acta, 1703*(2). https://doi.org/10.1016/j.bbapap.2004.08.007

Davies, M. J. (2016). Protein oxidation and peroxidation. *Biochemical Journal, 473*(7), 805-825. https://doi.org/10.1042/BJ20151227

Delieu, T., & Walker, D. A. (1981). Polarographic measurement of photosynthetic oxygen evolution by leaf-disks. *New Phytologist, 89*(2), 165-178. https://doi.org/DOI 10.1111/j.1469-8137.1981.tb07480.x

Delieu, T. J., & Walker, D. A. (1983). Simultaneous measurement of oxygen evolution and chlorophyll fluorescence from leaf pieces. *Plant Physiology, 73*(3), 534-541.

Demas, J. N., & DeGraff, B. A. (1997). Applications of luminescent transition metal complexes to sensor technology and molecular probes. *Journal of Chemical Education, 74*(6), 690-695. https://doi.org/DOI 10.1021/ed074p690

Demas, J. N., DeGraff, B. A., & Coleman, P. B. (1999). Oxygen sensors based on luminescence quenching. *Analytical Chemistry, 71*(23), 793A-800A. https://doi.org/10.1021/ac9908546

Deshaies, R. J., Koch, B. D., & Schekman, R. (1988). The role of stress proteins in membrane biogenesis. *Trends in biochemical sciences, 13*(10). https://doi.org/10.1016/0968-0004(88)90180-6

Di, J., Bi, S., & Zhang, M. (2004). Third-generation superoxide anion sensor based on superoxide dismutase directly immobilized by sol-gel thin film on gold electrode. *Biosensors and Bioelectronics, 19*(11), 1479-1486. https://doi.org/10.1016/j.bios.2003.12.006

Diaz, J. M., Hansel, C. M., Apprill, A., Brighi, C., Zhang, T., Weber, L., McNally, S., & Xun, L. (2016). Species-specific control of external superoxide levels by the coral holobiont during a natural bleaching event. *Nature Communications, 7.* https://doi.org/10.1038/ncomms13801

Diaz, J. M., & Plummer, S. (2018). Production of extracellular reactive oxygen species by phytoplankton: past and future directions. *Journal of Plankton Research, 40*(6), 655-666. https://doi.org/10.1093/plankt/fby039

Dixon, D. P., Skipsey, M., Grundy, N. M., & Edwards, R. (2005). Stress-induced protein S-glutathionylation in Arabidopsis. *Plant Physiology, 138*(4). https://doi.org/10.1104/pp.104.058917

Dogra, V., & Kim, C. (2019). Singlet oxygen metabolism: From genesis to signaling. *Frontiers in Plant Science, 10*. https://doi.org/10.3389/fpls.2019.01640

Dogra, V., Rochaix, J. D., & Kim, C. (2018). Singlet oxygen-triggered chloroplast-to-nucleus retrograde signalling pathways: An emerging perspective. *Plant Cell Environment, 41*(8), 1727-1738. https://doi.org/10.1111/pce.13332

Domingues, R. M., Domingues, P., Melo, T., Perez-Sala, D., Reis, A., & Spickett, C. M. (2013). Lipoxidation adducts with peptides and proteins: deleterious modifications or signaling mechanisms? *Journal of Proteomics, 92*, 110-131. https://doi.org/10.1016/j.jprot.2013.06.004

Dumont, S., & Rivoal, J. (2019). Consequences of oxidative stress on plant glycolytic and respiratory metabolism. *Frontiers in Plant Science, 10*. https://doi.org/10.3389/fpls.2019.00166

Edelman, M., & Mattoo, A. K. (2008). D1-protein dynamics in photosystem II: the lingering enigma. *Photosynthesis Research, 98*(1-3), 609-620. https://doi.org/10.1007/s11120-008-9342-x

Esterbauer, H., Schaur, R. J., & Zollner, H. (1991). Chemistry and biochemistry of 4-hydroxynonenal, malonaldehyde, and related aldehydes. *Free Radical Biology and Medicine, 11*(1), 81-128.

Fang, J., & Holmgren, A. (2006). Inhibition of thioredoxin and thioredoxin reductase by 4-hydroxy-2-nonenal *in vitro* and *in vivo*. *Journal of the American Chemical Society, 128*(6). https://doi.org/10.1021/ja057358l

Farmer, E. E., & Mueller, M. J. (2013). ROS-mediated lipid peroxidation and RES-activated signaling. *Annual Review of Plant Biology, 64*, 429-450. https://doi.org/10.1146/annurev-arplant-050312-120132

Ferretti, U., Ciura, J., Ksas, B., Rac, M., Sedlarova, M., Kruk, J., Havaux, M., & Pospíšil, P. (2018). Chemical quenching of singlet oxygen by plastoquinols and their oxidation products in Arabidopsis. *Plant Journal, 95*(5), 848-861. https://doi.org/10.1111/tpj.13993

Finley, D., & Chau, V. (1991). Ubiquitination. *Annual Review of Cell Biology, 7*, 25-69. https://doi.org/10.1146/annurev.cb.07.110191.000325

Fischer, B. B., Hideg, E., & Krieger-Liszkay, A. (2013). Production, detection, and signaling of singlet oxygen in photosynthetic organisms [Research Article]. *Antioxidants & Redox Signaling, 18*(16), 2145-2162. https://doi.org/10.1089/ars.2012.5124

Ford, R. C., & Evans, M. C. W. (1983). Isolation of a photosystem-II preparation from higher-plants with highly enriched oxygen evolution activity. *FEBS Letters, 160*(1-2), 159-164. https://doi.org/10.1016/0014-5793(83)80957-0

Foyer, C. H. (2018). Reactive oxygen species, oxidative signaling, and the regulation of photosynthesis [Review]. *Environmental and Experimental Botany, 154*, 134-142. https://doi.org/10.1016/j.envexpbot.2018.05.003

Foyer, C. H., & Noctor, G. (2005). Redox homeostasis and antioxidant signaling: a metabolic interface between stress perception and physiological responses. *Plant Cell, 17*(7), 1866-1875. https://doi.org/10.1105/tpc.105.033589

Foyer, C. H., Ruban, A. V., & Noctor, G. (2017). Viewing oxidative stress through the lens of oxidative signalling rather than damage [Editorial Material]. *Biochemical Journal, 474*(6), 877-883. https://doi.org/10.1042/BCJ20160814

Foyer, C. H., & Shigeoka, S. (2011). Understanding oxidative stress and antioxidant functions to enhance photosynthesis. *Plant Physiology, 155*(1), 93-100. https://doi.org/10.1104/pp.110.166181

Gao, X. H., Bedhomme, M., Veyel, D., Zaffagnini, M., & Lemaire, S. D. (2009). Methods for analysis of protein glutathionylation and their application to photosynthetic organisms. *Molecular Plant, 2*(2). https://doi.org/10.1093/mp/ssn072

Gegotek, A., & Skrzydlewska, E. (2019). Biological effect of protein modifications by lipid peroxidation products. *Chemistry and Physics of Lipids, 221*, 46-52. https://doi.org/10.1016/j.chemphyslip.2019.03.011

Gligorovski, S., Strekowski, R., Barbati, S., & Vione, D. (2015). Environmental implications of hydroxyl radicals. *Chemical Reviews, 115*(24), 13051-13092. https://doi.org/10.1021/cr500310b

Gobi, K., & Mizutani, F. (2001). Amperometric detection of superoxide dismutase at cytochrome c-immobilized electrodes: Xanthine oxidase and ascorbate oxidase incorporated biopolymer membrane for *in vivo* analysis. *Analytical Sciences: the international journal of the Japan Society for Analytical Chemistry, 17*(1). https://doi.org/10.2116/analsci.17.11

Goldberg, A. L., & Dice, J. F. (1974). Intracellular protein degradation in mammalian and bacterial cells. *Annual Review of Biochemistry, 43*(0). https://doi.org/10.1146/annurev.bi.43.070174.004155

Goldberg, A. L., Howell, E. M., Li, J. B., Martel, S. B., & Prouty, W. F. (1974). Physiological significance of protein degradation in animal and bacterial cells. *Federation Proceedings, 33*(4).

Gollan, P. J., Tikkanen, M., & Aro, E. M. (2015). Photosynthetic light reactions: integral to chloroplast retrograde signalling. *Current Opinion in Plant Biology, 27*, 180-191. https://doi.org/10.1016/j.pbi.2015.07.006

Gouterman, M. (1997). Oxygen quenching of luminescence of pressure-sensitive paint for wind tunnel research. *Journal of Chemical Education, 74*(6), 697-702. https://doi.org/DOI 10.1021/ed074p697

Gracanin, M., Hawkins, C. L., Pattison, D. I., & Davies, M. J. (2009). Singlet-oxygen-mediated amino acid and protein oxidation: formation of tryptophan peroxides and decomposition products. *Free Radical Biology and Medicine, 47*(1), 92-102. https://doi.org/10.1016/j.freeradbiomed.2009.04.015

Groenendaal, B. L., Jonas, F., Freitag, D., Pielartzik, H., & Reynolds, J. R. (2000). Poly(3,4-ethylenedioxythiophene) and its derivatives: Past, present, and future. *Advanced Materials, 12*(7), 481-494.

Gupta, K. J., Kolbert, Z., Durner, J., Lindermayr, C., Corpas, F. J., Brouquisse, R., Barroso, J. B., Umbreen, S., Palma, J. M., Hancock, J. T., Petrivalsky, M., Wendehenne, D., & Loake, G. J. (2020). Regulating the regulator: nitric oxide control of post-translational modifications. *New Phytologist*. https://doi.org/10.1111/nph.16622

Góngora-Benítez, M., Tulla-Puche, J., & Albericio, F. (2014). Multifaceted roles of disulfide bonds. Peptides as therapeutics. *Chemical Reviews, 114*(2). https://doi.org/10.1021/cr400031z

Hadacek, F., & Bachmann, G. (2015). Low-molecular-weight metabolite systems chemistry. *Frontiers in Environmental Science, 3*, Article 12. https://doi.org/10.3389/fenvs.2015.00012

Hagglund, P., Mariotti, M., & Davies, M. J. (2018). Identification and characterization of protein cross-links induced by oxidative reactions. *Expert Review of Proteomics, 15*(8), 665-681. https://doi.org/10.1080/14789450.2018.1509710

Halliwell, B. (2006). Reactive species and antioxidants. Redox biology is a fundamental theme of aerobic life [Article]. *Plant Physiology, 141*(2), 312-322. https://doi.org/10.1104/pp.106.077073

Hashiguchi, A., & Komatsu, S. (2016). Impact of post-translational modifications of crop proteins under abiotic stress. *Proteomes, 4*(4), Article 42. https://doi.org/10.3390/proteomes4040042

Hawkins, C. L., & Davies, M. J. (1998). EPR studies on the selectivity of hydroxyl radical attack on amino acids and peptides. *Journal of the Chemical Society-Perkin Transactions 2*(12), 2617-2622. https://doi.org/DOI 10.1039/a806666c

Henmi, T., Yamasaki, H., Sakuma, S., Tomokawa, Y., Tamura, N., Shen, J. R., & Yamamoto, Y. (2003). Dynamic Interaction between the D1 protein, CP43, and OEC33 at the lumenal side of photosystem II in spinach chloroplasts: evidence from light-induced cross-Linking of the proteins in the donor-side photoinhibition. *Plant Cell Physiology, 44*(4), 451-456.

Hoch, G., & Kok, B. (1963). A mass spectrometer inlet system for sampling gases dissolved in liquid phases. *Archives of Biochemistry and Biophysics, 101*(1), 160-&. https://doi.org/10.1016/0003-9861(63)90546-0

Hunter, T. (2009). Tyrosine phosphorylation: Thirty years and counting. *Current Opinion in Cell Biology, 21*(2). https://doi.org/10.1016/j.ceb.2009.01.028

Ichiishi, E., Tada, M., Ohta, Y., Sami, M., Kanda, T., Ikeda, M., & Kohno, M. (2015). Genomic approaches and oxygen radical measurement as biomarker candidates of off-season predictor of pollinosis: A pilot study [Article]. *Current Pharmacogenomics & Personalized Medicine, 13*(1), 41-50. https://doi.org/10.2174/1875692113011151228154727

Inoue, K. Y., Matsudaira, M., Kubo, R., Nakano, M., Yoshida, S., Matsuzaki, S., Suda, A., Kunikata, R., Kimura, T., Tsurumi, R., Shioya, T., Ino, K., Shiku, H., Satoh, S., Esashi, M., & Matsue, T. (2012). LSI-based amperometric sensor for bio-imaging and multi-point biosensing. *Lab Chip, 12*(18), 3481-3490. https://doi.org/10.1039/c2lc40323d

Inoue, K. Y., Matsudaira, M., Nakano, M., Ino, K., Sakamoto, C., Kanno, Y., Kubo, R., Kunikata, R., Kira, A., Suda, A., Tsurumi, R., Shioya, T., Yoshida, S., Muroyama, M., Ishikawa, T., Shiku, H., Satoh, S., Esashi, M., & Matsue, T. (2015). Advanced LSI-based amperometric sensor array with light-shielding structure for effective removal of photocurrent and mode selectable function for individual operation of 400 electrodes. *Lab Chip, 15*(3), 848-856. https://doi.org/10.1039/c4lc01099j

Janik, E., Bednarska, J., Sowinski, K., Luchowski, R., Zubik, M., Grudzinski, W., & Gruszecki, W. I. (2017). Light-induced formation of dimeric LHCII [Article]. *Photosynthesis Research, 132*(3), 265-276. https://doi.org/10.1007/s11120-017-0387-6

Janik, E., Bednarska, J., Zubik, M., Puzio, M., Luchowski, R., Grudzinski, W., Mazur, R., Garstka, M., Maksymiec, W., Kulik, A., Dietler, G., & Gruszecki, W. I. (2013). Molecular architecture of plant thylakoids under physiological and light stress conditions: a study of lipid-light-harvesting complex II model membranes [Article]. *Plant Cell, 25*(6), 2155-2170. https://doi.org/10.1105/tpc.113.113076

Kale, R., Hebert, A. E., Frankel, L. K., Sallans, L., Bricker, T. M., & Pospíšil, P. (2017). Amino acid oxidation of the D1 and D2 proteins by oxygen radicals during photoinhibition of Photosystem II. *Proceedings of the National Academy of Sciences of the United States of America, 114*(11), 2988-2993. https://doi.org/10.1073/pnas.1618922114

Kangasjarvi, S., Tikkanen, M., Durian, G., & Aro, E. M. (2014). Photosynthetic light reactions - An adjustable hub in basic production and plant immunity signaling. *Plant Physiology and Biochemistry, 81*, 128-134. https://doi.org/10.1016/j.plaphy.2013.12.004

Kasai, S., Sugiura, Y., Prasad, A., Inoue, K., Sato, T., Honmo, T., Kumar, A., Pospíšil, P., Ino, K., Hashi, Y., Furubayashi, Y., Matsudaira, M., Suda, A., Kunikata, R., & Matsue, T. (2019). Real-time imaging of photosynthetic oxygen evolution from spinach using LSI-based biosensor. *Scientific Reports, 9*, Article 12234. https://doi.org/10.1038/s41598-019-48561-y

Kneas, K. A., Xu, W. Y., Demas, J. N., & DeGraff, B. A. (1997). Oxygen sensors based on luminescence quenching: Interactions of tris(4,7-diphenyl-1,10-phenanthroline)ruthenium(II) chloride and pyrene with polymer supports. *Applied Spectroscopy, 51*(9), 1346-1351. https://doi.org/Doi 10.1366/0003702971942024

Koh, E., & Fluhr, R. (2016). Singlet oxygen detection in biological systems: Uses and limitations. *Plant Signaling & Behavior, 11*(7), Article UNSP e1192742. https://doi.org/10.1080/15592324.2016.1192742

Kohno, M., Takeda, M., Niwano, Y., Saito, R., Emoto, N., Tada, M., Kanazawa, T., Ohuchi, N., & Yamada, R. (2008). Early diagnosis of cancer by detecting the chemiluminescence of hematoporphyrins in peripheral blood lymphocytes [Article]. *Tohoku Journal of Experimental Medicine, 216*(1), 47-52. https://doi.org/10.1620/tjem.216.47

Koivuniemi, A., Aro, E. M., & Andersson, B. (1995). Degradation of the D1- And D2-proteins of photosystem II in higher plants is regulated by reversible phosphorylation. *Biochemistry, 34*(49). https://doi.org/10.1021/bi00049a016

Komenda, J., Kuviková, S., Lupínková, L., & Masojídek, J. (2006). Biogenesis and Structural Dynamics of the Photosystem II Complex. In *Biotechnological Applications of Photosynthetic Proteins: Biochips, Biosensors, and Biodevices* (pp. 32-45). Springer US. https://doi.org/10.1007/978-0-387-36672-2_4

Krieger-Liszkay, A. (2005). Singlet oxygen production in photosynthesis. *Journal of Experimental Botany, 56*(411), 337-346. https://doi.org/10.1093/jxb/erh237

Krieger-Liszkay, A., Fufezan, C., & Trebst, A. (2008). Singlet oxygen production in photosystem II and related protection mechanism. *Photosynthesis Research, 98*(1-3), 551-564. https://doi.org/10.1007/s11120-008-9349-3

Krynicka, V., Shao, S. X., Nixon, P. J., & Komenda, J. (2015). Accessibility controls selective degradation of photosystem II subunits by FtsH protease. *Nature Plants, 1*(12), Article Unsp 15168. https://doi.org/10.1038/nplants.2015.168

Kumar, A., Prasad, A., Sedlářová, M., Pospíšil, P. (2018). Data on detection of singlet oxygen, hydroxyl radical and organic radical in Arabidopsis thaliana [Article; Data Paper]. *Data in Brief, 21*, 2246-2252. https://doi.org/10.1016/j.dib.2018.11.033

Kumar, A., Prasad, A., Sedlářová, M., Pospíšil, P. (2019a). Characterization of Protein Radicals in Arabidopsis [Article]. *Frontiers in Physiology, 10*, 10, Article 958. https://doi.org/10.3389/fphys.2019.00958

Kumar, A., Prasad, A., Sedlářová, M., Pospíšil, P. (2019b). Organic radical imaging in plants: Focus on protein radicals. *Free Radical Biology and Medicine, 130*, 568-575. https://doi.org/10.1016/j.freeradbiomed.2018.10.428

Ledford, H. K., & Niyogi, K. K. (2005). Singlet oxygen and photo-oxidative stress management in plants and algae. *Plant Cell and Environment, 28*(8), 1037-1045. https://doi.org/DOI 10.1111/j.1365-3040.2005.01374.x

Levine, R. L., Garland, D., Oliver, C. N., Amici, A., Climent, I., Lenz, A. G., Ahn, B. W., Shaltiel, S., & Stadtman, E. R. (1990). Determination of carbonyl content in oxidatively modified proteins. *Methods in Enzymology, 186*, 464-478.

Levine, R. L., Williams, J. A., Stadtman, E. R., & Shacter, E. (1994). Carbonyl assays for determination of oxidatively modified proteins. *Methods in Enzymology, 233*, 346-357. https://doi.org/10.1016/s0076-6879(94)33040-9

Lichtenthaler, H. K. (1987). Chlorophylls and carotenoids: Pigments of photosynthetic biomembranes. In *Methods in Enzymology* (Vol. 148, pp. 350-382). Academic Press: London. https://doi.org/https://doi.org/10.1016/0076-6879(87)48036-1

Liebthal, M., & Dietz, K. J. (2017). The fundamental role of reactive oxygen species in plant stress response. *Methods in Molecular Biology, 1631*, 23-39. https://doi.org/10.1007/978-1-4939-7136-7_2

Liochev, S. I. (1999). The mechanism of "Fenton-like" reactions and their importance for biological systems. A biologist's view. *Metal Ions in Biological Systems, 36*, 1-39.

Liu, H., Guo, K., Duan, C. Y., Chen, X. J., & Zhu, Z. F. (2016). A novel biosensor based on the direct electrochemistry of horseradish peroxidase immobilized in the three-dimensional flower-like Bi2WO6 microspheres. *Materials Science & Engineering C-Materials for Biological Applications, 64*, 243-248. https://doi.org/10.1016/j.msec.2016.03.079

Liu, K. J., Gast, P., Moussavi, M., Norby, S. W., Vahidi, N., Walczak, T., Wu, M., & Swartz, H. M. (1993). Lithium phthalocyanine: A probe for electron paramagnetic resonance oximetry in viable biological systems. *Proceedings of the National Academy of Sciences of the United States of America, 90*(12). https://doi.org/10.1073/pnas.90.12.5438

Liu, X. R., Zhang, M. M., Zhang, B., Rempel, D. L., & Gross, M. L. (2019). Hydroxyl-radical reaction pathways for the fast photochemical oxidation of proteins platform as revealed by 18 O isotopic labeling. *Analytical Chemistry, 91*(14). https://doi.org/10.1021/acs.analchem.9b02134

Lupínková, L., & Komenda, J. (2004). Oxidative modifications of the Photosystem II D1 protein by reactive oxygen species: from isolated protein to cyanobacterial cells. *Photochemistry and Photobiology, 79*(2), 152-162.

Marshall, E., Costa, L. M., & Gutierrez-Marcos, J. (2011). Cysteine-rich peptides (CRPs) mediate diverse aspects of cell-cell communication in plant reproduction and development. *Journal of Experimental Botany, 62*(5). https://doi.org/10.1093/jxb/err002

Matsue, T., Koike, S., Abe, T., Itabashi, T., & Uchida, I. (1992). An ultramicroelectrode for determination of intracellular oxygen - light-irradiation-induced change in oxygen concentration in an algal protoplast. *Biochimica et Biophysica Acta, 1101*(1), 69-72. https://doi.org/Doi 10.1016/0167-4838(92)90468-S

Matsue, T., Koike, S., & Uchida, I. (1993). Microamperometric estimation of photosynthesis inhibition in a single algal protoplast. *Biochemical and Biophysical Research Communications, 197*(3), 1283-1287. https://doi.org/10.1006/bbrc.1993.2616

Mattila, H., Khorobrykh, S., Havurinne, V., & Tyystjarvi, E. (2015). Reactive oxygen species: Reactions and detection from photosynthetic tissues. *Journal of Photochemistry and Photobiology B: Biology, 152*(Pt B), 176-214. https://doi.org/10.1016/j.jphotobiol.2015.10.001 (Recent Progress in the Studies of Structure and Function of Photosystem I and II)

Mauzerall, D. C. (1990). Determination of oxygen emission and uptake in leaves by pulsed, time-resolved photoacoustics. *Plant Physiology, 94*(1), 278-283. https://doi.org/10.1104/pp.94.1.278

Mehler, A. H. (1951). Studies on Reactions of Illuminated Chloroplasts. I. Mechanism of the Reduction of Oxygen and Other Hill Reagents. *Archives of Biochemistry and Biophysics, 33*(1). https://doi.org/10.1016/0003-9861(51)90082-3

Meyer, A. J., & Hell, R. (2005). Glutathione homeostasis and redox-regulation by sulfhydryl groups. *Photosynthesis Research, 86*(3), 435-457. https://doi.org/10.1007/s11120-005-8425-1

Meyer, B., Schlodder, E., Dekker, J. P., & Witt, H. T. (1989). O_2 evolution and Chl a$^+$ II (P-680$^+$) nanosecond reduction kinetics in single flashes as a function of pH. *Biochimica et Biophysica Acta, 974*(1), 36-43. https://doi.org/10.1016/s0005-2728(89)80163-x

Meyer, E. H., Welchen, E., & Carrie, C. (2019). Assembly of the Complexes of the Oxidative Phosphorylation System in Land Plant Mitochondria. *Annual Review of Plant Biology, Vol 70, 70*, 23-50. https://doi.org/10.1146/annurev-arplant-050718-100412

Mills, A., Tommons, C., Bailey, R. T., Tedford, M. C., & Crilly, P. J. (2007). Reversible, fluorescence-based optical sensor for hydrogen peroxide. *Analyst, 132*(6), 566-571. https://doi.org/10.1039/b618506a

Mizusawa, N., Tomo, T., Satoh, K., & Miyao, M. (2003). Degradation of the D1 protein of photosystem II under illumination in vivo: two different pathways involving cleavage or intermolecular cross-linking [Article]. *Biochemistry, 42*(33), 10034-10044. https://doi.org/10.1021/bi0300534

Moller, I. M., Jensen, P. E., & Hansson, A. (2007). Oxidative modifications to cellular components in plants. *Annual Review of Plant Biology, 58*, 459-481. https://doi.org/10.1146/annurev.arplant.58.032806.103946

Moroder, L., Musiol, H. J., Götz, M., & Renner, C. (2005). Synthesis of single and multiple stranded cystine-rich peptides. *Biopolymers, 80*(2-3). https://doi.org/10.1002/bip.20174

Mubarakshina, M. M., & Ivanov, B. N. (2010). The production and scavenging of reactive oxygen species in the plastoquinone pool of chloroplast thylakoid membranes. *Physiologia Plantarum, 140*(2), 103-110. https://doi.org/10.1111/j.1399-3054.2010.01391.x

Mujika, J. I., Uranga, J., & Matxain, J. M. (2013). Computational study on the attack of ·OH Radicals on aromatic amino acids. *Chemistry (Weinheim an der Bergstrasse, Germany), 19*(21). https://doi.org/10.1002/chem.201203862

Nallamilli, B. R. R., Edelmann, M. J., Zhong, X. X., Tan, F., Mujahid, H., Zhang, J., Nanduri, B., & Peng, Z. H. (2014). Global analysis of lysine acetylation suggests the involvement of protein acetylation in diverse biological processes in rice (Oryza sativa). *Plos One, 9*(2), Article e89283. https://doi.org/10.1371/journal.pone.0089283

Nixon, P. J., Barker, M., Boehm, M., de Vries, R., & Komenda, J. (2005). FtsH-mediated repair of the photosystem II complex in response to light stress. *Journal of Experimental Botany, 56*(411), 357-363. https://doi.org/10.1093/jxb/eri021

Noctor, G., & Foyer, C. H. (2016). Intracellular redox compartmentation and ROS-related communication in regulation and signaling [Article]. *Plant Physiology, 171*(3), 1581-1592. https://doi.org/10.1104/pp.16.00346

Noctor, G., Lelarge-Trouverie, C., & Mhamdi, A. (2015). The metabolomics of oxidative stress. *Phytochemistry, 112*, 33-53. https://doi.org/10.1016/j.phytochem.2014.09.002

Nukuna, B. N., Goshe, M. B., & Anderson, V. E. (2001). Sites of hydroxyl radical reaction with amino acids identified by (2)H NMR Detection of Induced (1)H/(2)H exchange. *Journal of the American Chemical Society, 123*(6). https://doi.org/10.1021/ja003342d

Ogawa, K. (2005). Glutathione-associated regulation of plant growth and stress responses. *Antioxidants & Redox Signaling, 7*(7-8), 973-981. https://doi.org/10.1089/ars.2005.7.973

Patil, N. A., Tailhades, J., Hughes, R. A., Separovic, F., Wade, J. D., & Hossain, M. A. (2015). Cellular disulfide bond formation in bioactive peptides and proteins [Review]. *International Journal of Molecular Sciences, 16*(1), 1791-1805. https://doi.org/10.3390/ijms16011791

Pawson, T., & Scott, J. D. (2005). Protein Phosphorylation in signaling--50 Years and Counting. *Trends in Biochemical Sciences, 30*(6). https://doi.org/10.1016/j.tibs.2005.04.013

Pizzimenti, S., Ciamporcero, E., Daga, M., Pettazzoni, P., Arcaro, A., Cetrangolo, G., Minelli, R., Dianzani, C., Lepore, A., Gentile, F., & Barrera, G. (2013). Interaction of aldehydes derived from lipid peroxidation and membrane proteins. *Frontiers in Physiology, 4*. https://doi.org/10.3389/fphys.2013.00242

Plowman, J. E., Deb-Choudhury, S., Grosvenor, A. J., & Dyer, J. M. (2013). Protein oxidation: identification and utilization of molecular markers to differentiate singlet oxygen and hydroxyl radical-mediated oxidative pathways. *Photochemical and Photobiological Sciences, 12*(11), 1960-1967. https://doi.org/10.1039/c3pp50182e

Pospíšil, P. (2009). Production of reactive oxygen species by photosystem II. *Biochimica et Biophysica Acta-Bioenergetics, 1787*(10), 1151-1160. https://doi.org/10.1016/j.bbabio.2009.05.005

Pospíšil, P. (2009). Production of reactive oxygen species by photosystem II. *Biochimica et Biophysica, 1787*(10), 1151-1160. https://doi.org/10.1016/j.bbabio.2009.05.005

Pospíšil, P. (2011). Enzymatic function of cytochrome b559 in photosystem II. *Journal of Photochemistry and Photobiology B: Biology, 104*(1-2), 341-347. https://doi.org/10.1016/j.jphotobiol.2011.02.013

Pospíšil, P. (2012). Molecular mechanisms of production and scavenging of reactive oxygen species by photosystem II. *Biochimica et Biophysica, 1817*(1), 218-231. https://doi.org/10.1016/j.bbabio.2011.05.017

Pospíšil, P. (2016). Production of reactive oxygen species by photosystem II as a response to light and temperature stress [Review]. *Frontiers in Plant Science, 7*(1950), 1950. https://doi.org/10.3389/fpls.2016.01950

Pospíšil, P., Arato, A., Krieger-Liszkay, A., & Rutherford, A. W. (2004). Hydroxyl radical generation by photosystem II. *Biochemistry, 43*(21), 6783-6792. https://doi.org/10.1021/bi036219i

Powles, S. B. (1984). Photoinhibition of photosynthesis induced by visible light. *Annual Review of Plant Physiology and Plant Molecular Biology, 35*, 15-44. https://doi.org/10.1146/annurev.pp.35.060184.000311

Prasad, A., Kumar, A., Matsuoka, R., Takahashi, A., Fujii, R., Sugiura, Y., Kikuchi, H., Aoyagi, S., Aikawa, T., Kondo, T., Yuasa, M., Pospíšil, P., & Kasai, S. (2017). Real-time monitoring of superoxide anion radical generation in response to wounding: electrochemical study. *PeerJ, 5*, e3050, Article e3050. https://doi.org/10.7717/peerj.3050

Prasad, A., Kumar, A., Suzuki, M., Kikuchi, H., Sugai, T., Kobayashi, M., Pospíšil, P., Tada, M., & Kasai, S. (2015). Detection of hydrogen peroxide in Photosystem II (PSII) using catalytic amperometric biosensor. *Frontiers in Plant Science, 6*, 862, Article 862. https://doi.org/10.3389/fpls.2015.00862

Prasad, A., Sedlarova, M., & Pospíšil, P. (2018). Singlet oxygen imaging using fluorescent probe Singlet Oxygen Sensor Green in photosynthetic organisms. *Scientific Reports, 8*(1), 13685. https://doi.org/10.1038/s41598-018-31638-5

Rad, A. S., Jahanshahi, M., Ardjmand, M., & Safekordi, A. A. (2012). A new electrochemical biosensor for hydrogen peroxide using HRP/AgNPs/cysteamine/p-ABSA/GCE self-assembly modified electrode. *Korean Journal of Chemical Engineering, 29*(12), 1766-1770. https://doi.org/10.1007/s11814-012-0078-0

Refsgaard, H. H. F., Tsai, L., & Stadtman, E. R. (2000). Modifications of proteins by polyunsaturated fatty acid peroxidation products. *Proceedings of the National Academy of Sciences of the United States of America, 97*(2), 611-616. https://doi.org/10.1073/pnas.97.2.611

Riahi, Y., Cohen, G., Shamni, O., & Sasson, S. (2010). Signaling and cytotoxic functions of 4-hydroxyalkenals. *American Journal of Physiology-Endocrinology and Metabolism, 299*(6), E879-E886. https://doi.org/10.1152/ajpendo.00508.2010

Romero-Puertas, M. C., Laxa, M., Mattè, A., Zaninotto, F., Finkemeier, I., Jones, A. M., Perazzolli, M., Vandelle, E., Dietz, K. J., & Delledonne, M. (2007). S-nitrosylation of peroxiredoxin II E promotes peroxynitrite-mediated tyrosine nitration. *The Plant cell, 19*(12). https://doi.org/10.1105/tpc.107.055061

Rothman, J. E. (1989). Polypeptide chain binding proteins: catalysts of protein folding and related processes in cells. *Cell, 59*(4). https://doi.org/10.1016/0092-8674(89)90005-6

Rouhier, N., Lemaire, S. D., & Jacquot, J. P. (2008). The role of glutathione in photosynthetic organisms: Emerging functions for glutaredoxins and glutathionylation. *Annual Review of Plant Biology, 59*, 143-166. https://doi.org/10.1146/annurev.arplant.59.032607.092811

Salikhov, K. M., Doctorov, A. B., Molin, Y. N., & Zamaraev, K. I. (1971). Exchange broadening of ESR lines for solutions of free radicals and transition metal complexes. *Journal of Magnetic Resonance, 5*(2), 189-&. https://doi.org/10.1016/0022-2364(71)90005-9

Schagger, H. (2006). Tricine-SDS-PAGE. *Nat Protoc, 1*(1), 16-22. https://doi.org/10.1038/nprot.2006.4

Schumpe, A., Adler, I., & Deckwer, W. D. (1978). Solubility of oxygen in electrolyte-solutions. *Biotechnology and Bioengineering, 20*(1), 145-150. https://doi.org/10.1002/bit.260200114

Seigneurin-Berny, D., Salvi, D., Joyard, J., & Rolland, N. (2008). Purification of intact chloroplasts from Arabidopsis and spinach leaves by isopycnic centrifugation. *Current Protocols in Cell Biology, Chapter 3*, Unit 3 30. https://doi.org/10.1002/0471143030.cb0330s40

Shacter, E. (2000). Quantification and significance of protein oxidation in biological samples. *Drug Metabolism Reviews, 32*(3-4), 307-326. https://doi.org/10.1081/dmr-100102336

Shao, N., Krieger-Liszkay, A., Schroda, M., & Beck, C. F. (2007). A reporter system for the individual detection of hydrogen peroxide and singlet oxygen: its use for the assay of reactive oxygen species produced in vivo. *Plant Journal, 50*(3), 475-487. https://doi.org/10.1111/j.1365-313X.2007.03065.x

Shipton, C. A., & Barber, J. (1991). Photoinduced degradation of the D1 polypeptide in isolated reaction centers of photosystem II: evidence for an autoproteolytic process triggered by the oxidizing side of the photosystem. *Proceedings of the National Academy of Sciences of the United States of America, 88*(15), 6691-6695.

Shipton, C. A., & Barber, J. (1994). *In-vivo* and *in-vitro* photoinhibition reactions generate similar degradation fragments of D1 and D2 photosystem-II reaction-center proteins [Article]. *European Journal of Biochemistry, 220*(3), 801-808. https://doi.org/DOI 10.1111/j.1432-1033.1994.tb18682.x

Stadtman, E. R. (1993). Oxidation of free amino acids and amino acid residues in proteins by radiolysis and by metal-catalyzed reactions. *Annual Review of Biochemistry, 62*, 797-821. https://doi.org/10.1146/annurev.bi.62.070193.004053

Stadtman, E. R. (2006). Protein oxidation and aging. *Free Radical Research, 40*(12), 1250-1258. https://doi.org/10.1080/10715760600918142

Stengel, E., & Reckermann, J. (1978). Methods for quantitation of photosynthetic oxygen production in open mass-cultures of algae. *Archiv für Hydrobiologie, 82*(1-4), 263-294.

Stomberski, C. T., Hess, D. T., & Stamler, J. S. (2019). Protein S-Nitrosylation: Determinants of Specificity and Enzymatic Regulation of S-Nitrosothiol-Based Signaling. *Antioxidants & Redox Signaling, 30*(10). https://doi.org/10.1089/ars.2017.7403

Stone, S. L. (2014). The role of ubiquitin and the 26S proteasome in plant abiotic stress signaling. *Frontiers in Plant Science, 5*, Article 135. https://doi.org/10.3389/fpls.2014.00135

Stone, S. L. (2019). Role of the ubiquitin-proteasome system in plant response to abiotic stress. *International Review of Cell and Molecular Biology, Vol 343, 343*, 65-110. https://doi.org/10.1016/bs.ircmb.2018.05.012

Subczynski, W. K., & Swartz, H. M. (2005). EPR oximetry in biological and model samples. *Biological Magnetic Resonance, 23*, 229-282. https://doi.org/10.1007/0-387-26741-7_10

Suzuki, N., Koussevitzky, S., Mittler, R., & Miller, G. (2012). ROS and redox signalling in the response of plants to abiotic stress [Review]. *Plant Cell Environment, 35*(2), 259-270. https://doi.org/10.1111/j.1365-3040.2011.02336.x

Tada, M., Ichiishi, E., Saito, R., Emoto, N., Niwano, Y., & Kohno, M. (2009). Myristic acid, a side chain of phorbol myristate acetate (PMA), can activate human polymorphonuclear leukocytes to produce oxygen radicals more potently than PMA [Article]. *Journal of Clinical Biochemistry and Nutrition, 45*(3), 309-314. https://doi.org/10.3164/jcbn.09-30

Tikhonov, A. N., & Subczynski, W. K. (2019). Oxygenic photosynthesis: EPR study of photosynthetic electron transport and oxygen-exchange, an overview. *Cell Biochemistry and Biophysics, 77*(1), 47-59. https://doi.org/10.1007/s12013-018-0861-6

Triantaphylides, C., & Havaux, M. (2009). Singlet oxygen in plants: production, detoxification and signaling [Research Article]. *Trends in Plant Science, 14*(4), 219-228. https://doi.org/10.1016/j.tplants.2009.01.008

Triantaphylides, C., Krischke, M., Hoeberichts, F. A., Ksas, B., Gresser, G., Havaux, M., Van Breusegem, F., & Mueller, M. J. (2008). Singlet oxygen is the major reactive oxygen species involved in photooxidative damage to plants. *Plant Physiology, 148*(2), 960-968. https://doi.org/10.1104/pp.108.125690

Tripathy, B. C., & Oelmuller, R. (2012). Reactive oxygen species generation and signaling in plants. *Plant Signaling & Behavior, 7*(12), 1621-1633. https://doi.org/10.4161/psb.22455

Tyystjarvi, E., Karunen, J., & Lemmetyinen, H. (1998). Measurement of photosynthetic oxygen evolution with a new type of oxygen sensor. *Photosynthesis Research, 56*(2), 223-227. https://doi.org/Doi 10.1023/A:1005994311121

Vongonner, M., Schlosser, E., & Neubacher, H. (1993). Evidence from electron-spin-resonance for the formation of free-radicals during infection of avena-sativa by drechslera spp. *Physiological and Molecular Plant Pathology, 42*(6), 405-412. https://doi.org/10.1006/pmpp.1993.1030

Vylegzhanina, N. N., Gordon, L. K., Minibayeva, F. V., & Kolesnikov, O. P. (2001). Superoxide production as a stress response of wounded root cells: ESR spin-trap and acceptor methods. *Applied Magnetic Resonance, 21*(1), 63-70. https://doi.org/10.1007/bf03162440

Wagner, D., Przybyla, D., Op den Camp, R., Kim, C., Landgraf, F., Lee, K. P., Wursch, M., Laloi, C., Nater, M., Hideg, E., & Apel, K. (2004). The genetic basis of singlet oxygen-induced stress responses of Arabidopsis thaliana. *Science, 306*(5699), 1183-1185. https://doi.org/10.1126/science.1103178

Wei, Y., Jiao, Y., An, D., Li, D., Li, W., & Wei, Q. (2019). Review of Dissolved Oxygen Detection Technology: From Laboratory Analysis to Online Intelligent Detection. *Sensors, 19*(18), Article 3995. https://doi.org/10.3390/s19183995

Williams, D. B. (2006). Beyond lectins: the calnexin/calreticulin chaperone system of the endoplasmic reticulum. *Journal of Cell Science, 119*(4), 615-623. https://doi.org/10.1242/jcs.02856

Wohlgemuth, H., Mittelstrass, K., Kschieschan, S., Bender, J., Weigel, H. J., Overmyer, K., Kangasjarvi, J., Sandermann, H., & Langebartels, C. (2002). Activation of an oxidative burst is a general feature of sensitive plants exposed to the air pollutant ozone. *Plant Cell and Environment, 25*(6), 717-726. https://doi.org/DOI 10.1046/j.1365-3040.2002.00859.x

Wolff, S. P., & Dean, R. T. (1986). Fragmentation of proteins by free-radicals and its effect on their susceptibility to enzymatic-hydrolysis. *Biochemical Journal, 234*(2), 399-403. https://doi.org/10.1042/bj2340399

Xu, G. H., & Chance, M. R. (2007). Hydroxyl radical-mediated modification of proteins as probes for structural proteomics. *Chemical Reviews, 107*(8), 3514-3543. https://doi.org/10.1021/cr0682047

Yadav, D. K., & Pospíšil, P. (2012). Role of chloride ion in hydroxyl radical production in photosystem II under heat stress: electron paramagnetic resonance spin-trapping study. *Journal of Bioenergetics and Biomembranes, 44*(3), 365-372. https://doi.org/10.1007/s10863-012-9433-4

Yamamoto, Y. (2001). Quality control of photosystem II [Review]. *Plant and Cell Physiology, 42*(2), 121-128. https://doi.org/10.1093/pcp/pce022

Yamamoto, Y., Aminaka, R., Yoshioka, M., Khatoon, M., Komayama, K., Takenaka, D., Yamashita, A., Nijo, N., Inagawa, K., Morita, N., Sasaki, T., & Yamamoto, Y. (2008). Quality control of photosystem II: impact of light and heat stresses. *Photosynthesis Research, 98*(1-3), 589-608. https://doi.org/10.1007/s11120-008-9372-4

Yamashita, A., Nijo, N., Pospíšil, P., Morita, N., Takenaka, D., Aminaka, R., Yamamoto, Y., & Yamamoto, Y. (2008). Quality control of photosystem II: reactive oxygen species are responsible for the damage to photosystem II under moderate heat stress. *Journal of Biological Chemistry, 283*(42), 28380-28391. https://doi.org/10.1074/jbc.M710465200

Yang, H., Mu, J., Chen, L., Feng, J., Hu, J., Li, L., Zhou, J. M., & Zuo, J. (2015). S-nitrosylation positively regulates ascorbate peroxidase activity during plant stress responses. *Plant Physiology, 167*(4). https://doi.org/10.1104/pp.114.255216

You, J., & Chan, Z. (2015). ROS regulation during abiotic stress responses in crop plants. *Frontiers in Plant Science, 6*. https://doi.org/10.3389/fpls.2015.01092

You, Y. (2018). Chemical tools for the generation and detection of singlet oxygen. *Organic & Biomolecular Chemistry, 16*(22), 4044-4060. https://doi.org/10.1039/c8ob00504d

Yuasa, M., Oyaizu, K., Yamaguchi, A., Ishikawa, M., Eguchi, K., Kobayashi, T., Toyoda, Y., & Tsutsui, S. (2005). Electrochemical sensor for superoxide anion radical using polymeric iron porphyrin complexes containing axial 1-methylimidazole ligand as cytochrome c mimics. *Polymers for Advanced Technologies, 16*(4), 287-292. https://doi.org/10.1002/pat.590

Yun, B. W., Feechan, A., Yin, M., Saidi, N. B., Le, B. T., Yu, M., Moore, J. W., Kang, J. G., Kwon, E., Spoel, S. H., Pallas, J. A., & Loake, G. J. (2011). S-nitrosylation of NADPH oxidase regulates cell death in plant immunity. *Nature, 478*(7368). https://doi.org/10.1038/nature10427

Zaffagnini, M., Bedhomme, M., Marchand, C. H., Morisse, S., Trost, P., & Lemaire, S. D. (2012). Redox regulation in photosynthetic organisms: Focus on glutathionylation. *Antioxidants & Redox Signaling, 16*(6), 567-586. https://doi.org/10.1089/ars.2011.4255

Zhang, S., Weng, J., Pan, J., Tu, T., Yao, S., & Xu, C. (2003). Study on the photo-generation of superoxide radicals in Photosystem II with EPR spin trapping techniques. *Photosynthesis Research, 75*(1), 41-48. https://doi.org/10.1023/a:1022439009587

Zhao, L., Wang, P., Yan, S., Gao, F., Li, H., Hou, H., Zhang, Q., Tan, J., & Li, L. (2014). Promoter-associated histone acetylation is involved in the osmotic stress-induced transcriptional regulation of the maize ZmDREB2A gene. *Physiologia Plantarum, 151*(4). https://doi.org/10.1111/ppl.12136

Łuczaj, W., Gęgotek, A., & Skrzydlewska, E. (2017). Antioxidants and HNE in redox homeostasis. *Free Radical Biology and Medicine, 111*. https://doi.org/10.1016/j.freeradbiomed.2016.11.033

Šnyrychová, I., Ayaydin, F., & Hideg, E. (2009). Detecting hydrogen peroxide in leaves in vivo - a comparison of methods. *Physiologia Plantarum, 135*(1), 1-18. https://doi.org/10.1111/j.1399-3054.2008.01176.x

APPENDIX

I. **<u>Kumar, A.</u>**, Prasad, A., Sedláˇrová, M., Pospíšil, P. (2019). Organic radical imaging in plants: focus on protein radicals. Free Radical Biology and Medicine, 130, 568–575.

II. **<u>Kumar, A.</u>**, Prasad, A., Sedlářová, M., Pospíšil, P. (2018). Data on detection of singlet oxygen, hydroxyl radical and organic radical in Arabidopsis thaliana. Data in Brief, 21, 2246–2252.

III. **<u>Kumar, A.</u>**, Prasad, A., Sedlářová, M., Pospíšil, P. (2019). Characterization of Protein Radicals in Arabidopsis. Frontiers in Physiology, 10, 958.

IV. Prasad, A., **<u>Kumar, A.</u>**, Suzuki, M., Kikuchi, H., Sugai, T., Kobayashi, M., Pospíšil, P., Tada, M., & Kasai, S. (2015). Detection of hydrogen peroxide in Photosystem II (PSII) using catalytic amperometric biosensor. Frontiers in Plant Science, 6, 862.

V. Prasad, A., **<u>Kumar, A.</u>**, Matsuoka, R., Takahashi, A., Fujii, R., Sugiura, Y., Kikuchi, H., Aoyagi, S., Aikawa, T., Kondo, T., Yuasa, M., Pospíšil, P., Kasai, S. (2017). Real-time monitoring of superoxide anion radical generation in response to wounding: electrochemical study. PeerJ, 5, e3050.

VI. Kasai, S., Sugiura, Y., Prasad, A., Inoue, K., Sato, T., Honmo, T., **<u>Kumar, A.</u>**, Pospíšil, P., Ino, K., Hashi, Y., Furubayashi, Y., Matsudaira, M., Suda, A., Kunikata, R., Matsue, T. (2019). Real-time imaging of photosynthetic oxygen evolution from spinach using LSI-based biosensor. Scientific Reports, 9, 12234 (2019).

Organic radical imaging in plants: Focus on protein radicals

Aditya Kumar[a], Ankush Prasad[a], Michaela Sedlářová[b], Pavel Pospíšil[a],*

[a] Department of Biophysics, Centre of the Region Haná for Biotechnological and Agricultural Research, Faculty of Science, Palacký University, Šlechtitelů 27, 783 71 Olomouc, Czech Republic
[b] Department of Botany, Faculty of Science, Palacký University, Šlechtitelů 27, 783 71 Olomouc, Czech Republic

ABSTRACT

Biomolecule (lipid and protein) oxidation products formed in plant cells exposed to photooxidative stress play a crucial role in the retrograde signaling and oxidative damage. The oxidation of biomolecules initiated by reactive oxygen species is associated with formation of organic (alkyl, peroxyl and alkoxyl) radicals. Currently, there is no selective and sensitive technique available for the detection of organic radicals in plant cells. Here, based on the analogy with animal cells, immuno-spin trapping using spin trap, 5,5-dimethyl-1-pyrroline N-oxide (DMPO) was used to image organic radicals in Arabidopsis leaves exposed to high light. Using antibody raised against the DMPO nitrone adduct conjugated with the fluorescein isothiocyanate, organic radicals were imaged by confocal laser scanning microscopy. Organic radicals are formed predominantly in the chloroplasts located at the periphery of the cells and distributed uniformly throughout the grana stack. Characterization of protein radicals by standard immunological techniques using anti-DMPO antibody shows protein bands with apparent molecular weights of 32 and 34 kDa assigned to D1 and D2 proteins and two protein bands below the D1/D2 band with apparent molecular weights of 23 and 18 kDa and four protein bands above the D1/D2 band with apparent molecular weights of 41, 43, 55 and 68 kDa. In summary, imaging of organic radicals by immuno-spin trapping represents selective and sensitive technique for the detection of organic radicals that might help to clarify mechanistic aspects on the role of organic radicals in the retrograde signaling and oxidative damage in plant cell.

1. Introduction

Under natural conditions, photosynthetic light reactions in higher plants are associated with the formation of reactive oxygen species (ROS) known to play an important role in the retrograde signaling and oxidative damage [1–3]. The retrograde signaling linked with the acclimation response and programmed cell death leads to changes in the expression of nuclear-encoded genes [4]. In the acclimation response, the retrograde signaling supports the plants to defend themselves against the diverse conditions, whereas the activation of programmed cell death in the plants tends to remove damaged cells. As diffusion of ROS out of the chloroplasts is limited due to their high reactivity to the proteins, the signal transduction from the chloroplasts to the nucleus is expected to involve the oxidation products of proteins. It seems to be more feasible that the oxidation products may cross the thylakoid, inner and outer chloroplast membranes to reach the nucleus. The oxidation products of proteins were proposed to serve as a secondary messengers known to maintain the signal transduction from the chloroplast to the nucleus [5]. The oxidative damage is caused by irreversible oxidation of

proteins during the accidental cell death. Protein oxidation is associated with the formation of highly reactive protein radicals comprising carbon-centered (alkyl) and oxygen-centered (peroxyl and alkoxyl) radicals known to form the primary (hydroperoxides) and secondary (reactive carbonyl species and hydroxy amino acid) products. Using mass spectrometry, oxidized amino acids in D1 and D2 proteins in photosystem II (PSII) were shown to be localized close to the site of ROS production on the both lumenal and stromal side of the thylakoid membrane [6–8]. Protein oxidation is accompanied with protein backbone cleavage (fragmentation) and protein aggregation (protein-protein cross-linking) [9–11]. The oxidation of amino acid localized at the lumen exposed AB-loop and the stroma exposed D-de loop of D1 protein produces 24 kDa C-terminal/9 kDa N-terminal and 23-kDa N-terminal/9-kDa C-terminal fragments, respectively [12,13]. Proteolytic degradation of damaged D1 protein and its replacement with a newly-synthetized D1 copy is maintained by repair cycle [14,15].

In view of the progress that has to be made to understand the different biological functions of organic radicals in the initiation of the retrograde transduction and oxidative damage, sensitive and specific
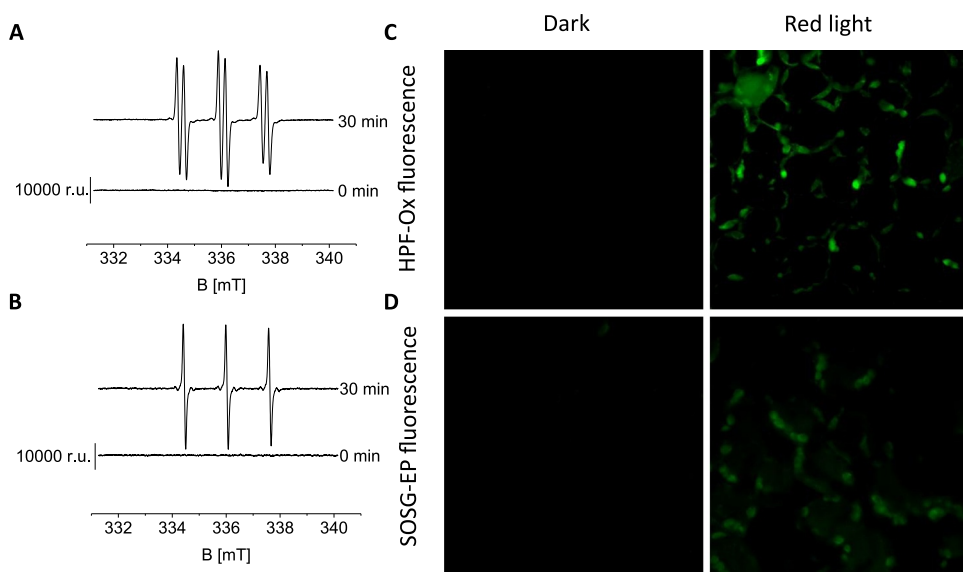

Fig. 1. Hydroxyl radical and singlet oxygen formation in Arabidopsis. (A-B) Hydroxyl radical and singlet oxygen detection in thylakoid membranes by electron paramagnetic resonance spin trapping technique. For hydroxyl radical detection, thylakoid membranes were incubated with 50 mM POBN spin trap in presence of 170 mM ethanol in the dark or exposed to high white light for 30 min and POBN-CH(CH$_3$)OH adduct EPR spectra was measured. For singlet oxygen detection, thylakoid membranes were incubated with TMPD spin probe in the dark or in high white light for 30 min and TEMPONE EPR spectra was measured. **(C-D) Hydroxyl radical and singlet oxygen imaging in Arabidopsis leaves monitored by laser confocal scanning microscopy.** For hydroxyl radical and singlet oxygen detection, Arabidopsis leaves were treated with 10 μM HPF and 50 μM SOSG either in the dark or exposed to high red light for 30 min and HPF-ox and SOSG-EP fluorescence was detected, respectively.

technique for their detection in plant is required. *In vivo* detection of organic radicals has been hindered due to their high reactivity and short lifetime. Electron paramagnetic resonance (EPR) spin trapping technique used for the selective and sensitive detection of organic radicals in vitro does not allow imaging of the organic radicals in tissues and whole organisms. However, recent progress in this field enables the imaging of organic (protein and nucleic acid) radicals by immuno-spin trapping in animal cell, animal tissues and whole animals [16,17]. In this study, imaging of organic radicals by immuno-spin trapping was performed in Arabidopsis leaves exposed to high light. In this technique, organic radicals are trapped by spin trap, 5,5-dimethyl-1-pyrroline N-oxide (DMPO) to form paramagnetic DMPO-organic radical adduct detected by EPR spectroscopy [16]. However, due to the oxidizing conditions, DMPO-R adduct is oxidized within few minutes to diamagnetic DMPO nitrone adducts [18] which might be imaged by confocal laser scanning microscopy using the fluorescein isothiocyanate (FITC) conjugated DMPO antibody specific to DMPO nitrone adducts (anti-DMPO antibody) [19]. The imaging of organic radicals by immuno-spin trapping allows the identification and localization of organic radicals in plant cell, plant tissue and whole plant.

2. Materials and methods

2.1. Plant material, chloroplast and thylakoid membrane isolation

Seeds of *Arabidopsis thaliana*, Columbia-0 (WT) were obtained from Nottingham Arabidopsis Stock Center (NASC), United Kingdom. Plants were grown in the Fytoscope FS-WI-HY (Photon Systems Instruments, Drásov, Czech Republic) under controlled conditions with light intensity of 100 μmol photons m^{-2} s^{-1}, photoperiod of 8/16 h light/dark

and temperature of 22/20 °C, respectively (unless specified otherwise) with a relative air humidity of 60%. Arabidopsis plants (5 or 6 weeks old) were exposed to high white light (1500 μmol photons m^{-2} s^{-1}) at a low air temperature of 8 °C for 13 h in the AlgaeTron AG 230 (Photon Systems Instruments, Drásov 470, Czech Republic). Intact chloroplasts were prepared from Arabidopsis plants previously exposed to high white light using Percoll gradient centrifugation as described by [20] and used immediately for measurements. Thylakoid membranes were prepared from Arabidopsis plants previously exposed to high white light according to Casazza et al. [21] and stored at -80 °C in the dark until use.

2.2. In vitro detection of hydroxyl radical and singlet oxygen by EPR spin trapping spectroscopy

The detection of hydroxyl radical (HO·) and singlet oxygen ($^1O_2$) was performed using EPR spectroscopy. For HO· detection, spin trap α-(4-pyridyl N-oxide)-N-(tert-butylnitrone) (Enzo Life Sciences, Czech Republic) POBN/ethanol system was used. Thylakoid membranes (250 μg Chl ml^{-1}) were incubated in the presence of 50 mM POBN, 170 mM ethanol and 40 mM MES buffer (pH 6.5) in the dark or in high white light (1500 μmol photons m^{-2} s^{-1}) for 30 min. For $^1O_2$ detection, spin probe 2, 2, 6, 6-tetramethyl-4-piperidone (TMPD, Sigma-Aldrich, USA) purified twice by vacuum distillation to reduce impurity from TMPD EPR signal was used. Thylakoid membranes (25 μg Chl ml^{-1}) were incubated in the presence of 50 mM TMPD and 40 mM MES buffer (pH 6.5) in dark or high white light (1500 μmol photons m^{-2} s^{-1}) for 30 min. Subsequently, the samples were immediately transferred into a glass capillary tube (Blaubrand® intraMARK, Brand, Germany) and EPR spectra were collected at room temperature using EPR spectrometer
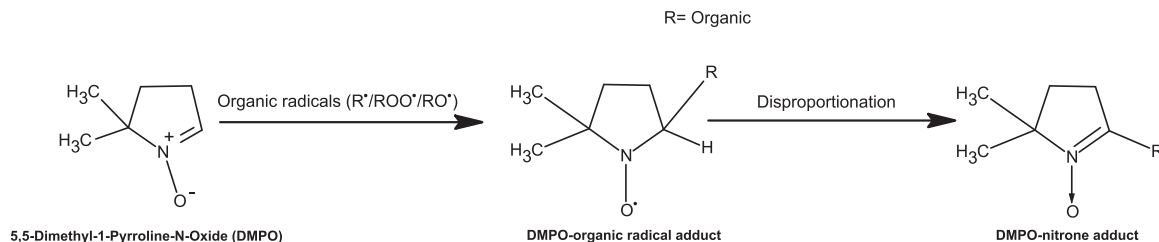
R= Organic

Fig. 2. Schematic representation of immuno-spin trapping of organic radicals. Organic radicals are trapped by DMPO to form DMPO-organic radical adduct. Unstable DMPO-organic radical adduct decays to stable DMPO nitrone adduct. The DMPO motif of DMPO nitrone adduct can be detected with anti-DMPO antibody and visualized either by fluorescence using antibody conjugated FITC fluorescent tag or conventional immunoblot techniques using HRP conjugated secondary antibody and luminol chemiluminescence.

(MiniScope MS400, Magnettech GmbH, Berlin, Germany). EPR conditions were as follows: microwave power, 10 mW; modulation amplitude, 1 G; modulation frequency, 100 kHz; sweep width, 100 G; scan rate, 1.62 G s^{-1}.

2.3. In vivo imaging of hydroxyl radical and singlet oxygen by confocal laser scanning microscopy

The visualization of HO$^{\cdot}$ and $^1O_2$ in leaves was performed by confocal laser scanning microscopy using hydroxyphenyl fluorescein (HPF) and singlet oxygen sensor green (SOSG) fluorescence probes (Molecular Probes Inc., Eugene, OR, USA), respectively. After high white light exposure (1500 μmol photons m^{-2} s^{-1}, 13 h, 8 °C), leaves were sliced into pieces of approximately 5 mm squares and placed on a wetted glass slide followed by covering it with cover glass. The abaxial leaf surface touching the glass slide was wetted with buffer and the adaxial leaf surface was kept exposed to air while cutting into pieces. Leaf pieces were then placed in 2 ml Eppendorf tube and treated with 10 μM HPF or 50 μM SOSG in presence of HEPES buffer (pH 7.5) for 30 min either in the dark or exposed to high red light (λ ≥ 600nm) (Fig. 2) [22]. Subsequently, the samples were visualized by confocal microscope (Fluorview 1000 unit attached to IX80 microscope; Olympus Czech Group, Prague, Czech Republic). The excitation of HPF/SOSG was performed by a 488 nm line of an argon laser and the emission was detected by a 505–525 nm filter. Chloroplasts were visualized by excitation with 543 nm helium–neon laser, and emission recorded with a 655–755 nm band pass filter.

2.4. In vivo imaging of organic radicals by confocal laser scanning microscopy

Organic radicals were visualized in leaves and intact chloroplasts by confocal laser scanning microscopy using mouse monoclonal anti-DMPO antibody conjugated with FITC [17]. The samples were incubated with 50 mM DMPO (Dojindo Molecular Technologies Inc. Rockville, MD, USA) and 5–10 μg ml^{-1} anti-DMPO antibody conjugated with FITC (Abcam, Cambridge, UK) in the presence of MES buffer (pH 6.5) under high red light (1000 μmol photons m^{-2} s^{-1}) for 30 min at 25 °C. To increase the penetration of spin trap and antibody into the cells and chloroplasts, Triton X-100 (0.001%) was added prior to exposure to high red light. Imaging of organic radicals was based on their reaction with DMPO spin trap reagent. The DMPO-organic radical adduct was recognized by anti-DMPO antibody conjugated with FITC and the spatial fluorescence was visualized using confocal laser scanning microscopy. The excitation of fluorochrome was achieved by a 488 nm line of an argon laser and signal was detected by a 505–550 nm emission filter.

Fig. 3. Organic radical imaging in Arabidopsis leaves monitored by laser confocal scanning microscopy. (A) From left to right: Nomarski DIC channel, FITC fluorescence channel, the combination of Nomarski DIC and FITC fluorescence channels and the integral distribution of FITC fluorescence intensity are shown. Prior to FITC fluorescence measurement, Arabidopsis leaves were kept in the dark or illuminated with high red light (1000 μmol photons m^{-2} s^{-1}) for 30 min in the presence of 50 mM DMPO and 10 μg ml^{-1} anti-DMPO antibody. **(B)** Focus on mesophyll cell.
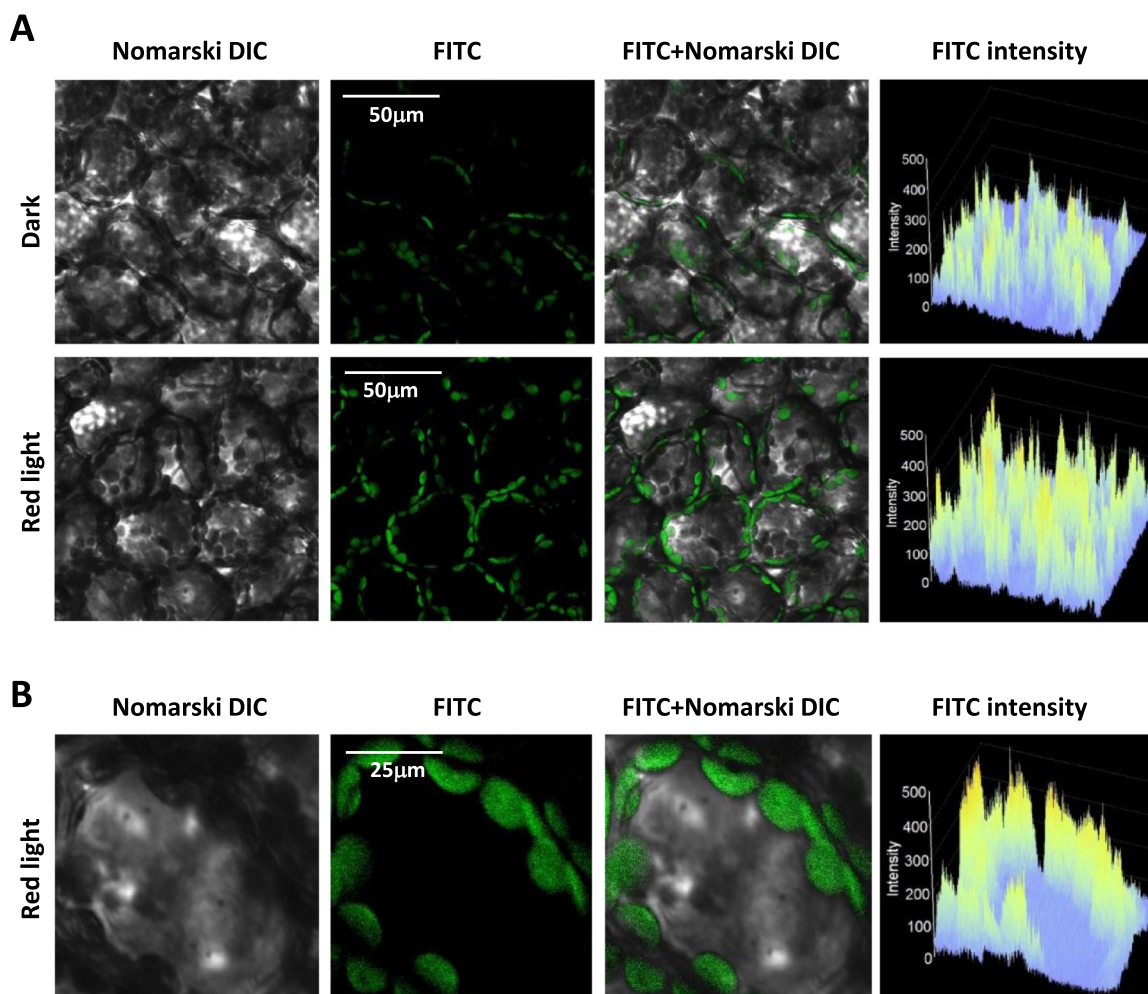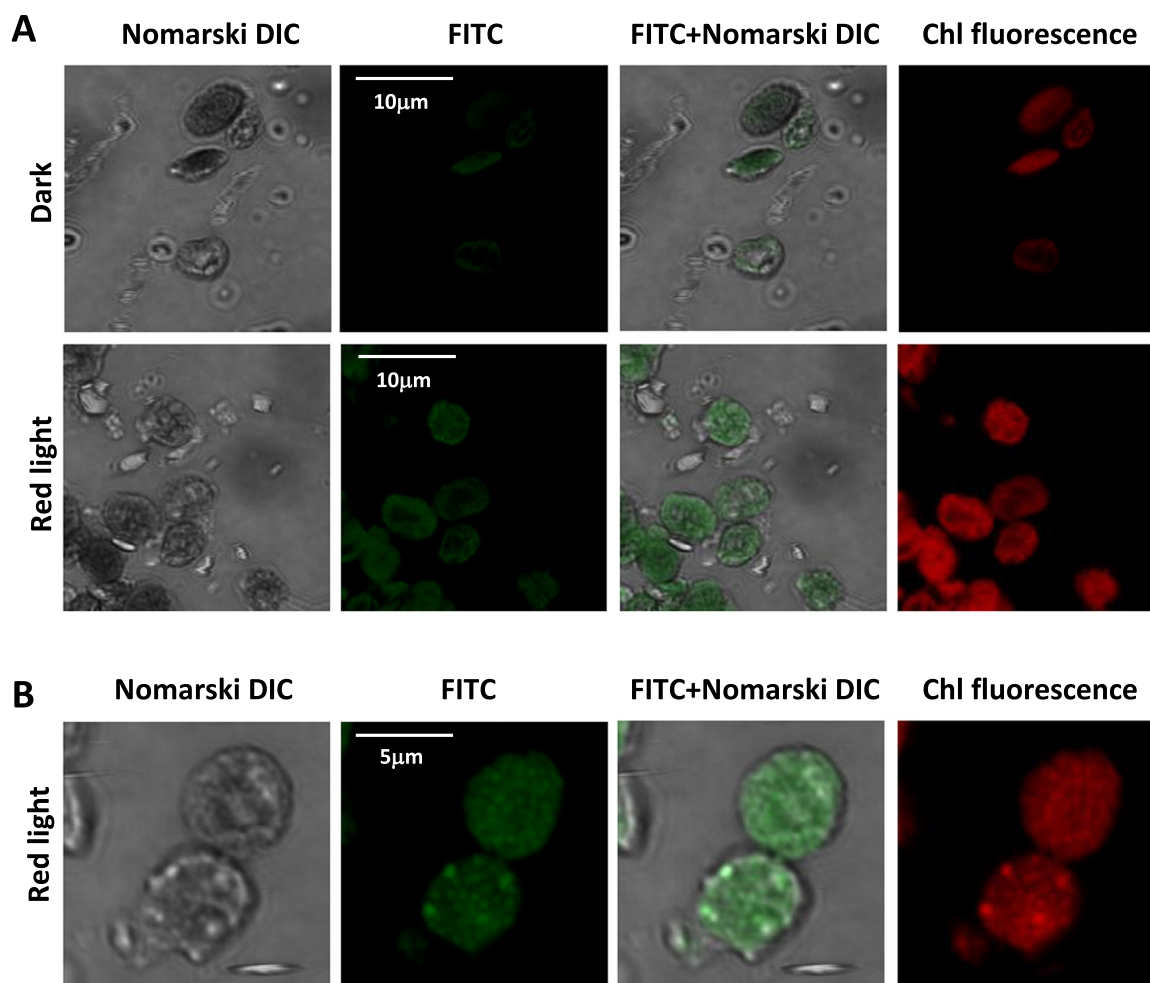
Fig. 4. Organic radical imaging in Arabidopsis chloroplasts monitored by laser confocal scanning microscopy. (A) From left to right: Nomarski DIC, FITC fluorescence, the combination of Nomarski DIC and FITC fluorescence and chlorophyll fluorescence channels are shown. Prior to FITC fluorescence measurement, Arabidopsis chloroplasts were kept in the dark or illuminated with red light (1000 μmol photons m^{-2} s^{-1}) for 30 min in the presence of 50 mM DMPO and 5 μg ml^{-1} anti-DMPO nitrone adduct antibody. **(B)** Focus on two chloroplasts.

2.5. SDS-PAGE and immuno-spin trapping

To detect protein radical in thylakoid membranes, immuno-spin trapping technique was used. In this technique, thylakoid membranes were incubated with 50 mM DMPO in the dark or illuminated for 10, 20 and 30 min with high white light (1500 μmol photons m^{-2} s^{-1}). Afterwards, proteins were extracted using DTT (dithiothreitol) protein extraction buffer followed by heating at 70 °C dry bath for 15 min and centrifuged at $16,000 \times g$ for 5 min at 4 °C. For protein carbonyl detection, thylakoid membranes were illuminated for 30 min with high white light (1500 μmol photons m^{-2} s^{-1}) followed by immediate mixing of 12% aqueous sodium dodecyl sulfate (SDS), derivatization with 10 mM 2,4-dinitrophenylhydrazine (DNPH) dissolved in 2 M HCl for 15 min and neutralization with neutralization buffer containing 2 M TRIS and 30% glycerol (Sigma Aldrich, Missouri, United States). Extracted and neutralized protein sample was loaded into wells and SDS-PAGE was performed using Mini-PROTEAN Tetra vertical electrophoresis cell (Bio-Rad, California, USA) following Tris-Tricine SDS-PAGE protocol described by [23]. Electrophoretic transfer of protein bands from gel to a nitrocellulose (NC) membrane was done using a semi-dry blotter (Trans-Blot SD, Semi-dry transfer cell, Bio-Rad, USA). Blocking step of NC membranes was done at 4 °C overnight with 5% BSA prepared in phosphate buffered saline-tween 20 (pH 7.4). All successive steps were performed on a shaker at room temperature. After blocking, NC membranes were incubated with rabbit polyclonal anti-

DMPO antibody (Abcam, Cambridge, UK) and rabbit polyclonal anti-DNP antibody (Molecular Probes Europe BV, Leiden, Netherlands) followed by washing and 1 h incubation with HRP conjugated anti-rabbit secondary antibody. Protein bands were visualized using luminol as a chemiluminescent probe (Amersham Imager 600, GE Health Care Europe GmbH, Freiburg, Germany). To identify proteins from anti DMPO blot, antibody stripping and re-probing with new antibodies raised against the D1 protein (anti-D1 antibody) and D2 protein (anti-D2 antibody) (Agrisera, Vännäs, Sweden) were performed. The removal of anti-DMPO antibody from NC membrane was accomplished by stripping NC membranes with 200 mM glycine-HCl (pH 2.2), 0.1% SDS and 1% Tween20. Size of protein bands was determined using a standard protein ladder (PageRuler™ Prestained Protein Ladder, 10–180 kDa, Thermo Scientific, Lithuania).

3. Results

3.1. Hydroxyl radical and singlet oxygen formation under high light stress in Arabidopsis

Formation of HO• and $^1O_2$ in the thylakoid membranes exposed to high white light was measured by EPR spectroscopy using POBN/ethanol spin trap system and TMPD spin probe, respectively. The reaction of HO• and ethanol forms 1-hydroxyethyl radical [$CH(CH_3)HO•$] which reacts with POBN yielding paramagnetic POBN-hydroxyethyl

radical [POBN-CH(CH$_3$)OH] adduct [24]. The oxidation of hydrophilic diamagnetic TMPD by ^{1}O$_2$ forms paramagnetic 2, 2, 6, 6-tetramethyl-4-piperidone-1-oxyl (TEMPONE) [25]. No EPR signal was observed in the dark (Fig. 1A and B, trace 0 min), whereas illumination with continuous white light for 30 min results in the formation of the POBN-CH(CH$_3$)OH adduct and TEMPONE EPR signal (Fig. 1A and B, trace 30 min). The six-line and three-line spectra show all the characteristics of the POBN-CH (CH$_3$)OH adduct and TEMPONE EPR spectra, respectively. To image the formation of HO$^\bullet$ and ^{1}O$_2$ in Arabidopsis leaves exposed to high white light, confocal laser scanning microscopy was used using HPF [26] and SOSG [27] fluorescence probes, respectively. Non-fluorescent HPF and SOSG are converted to strongly fluorescent oxidized HPF (HPF-ox) and SOSG endoperoxide (SOSG-EP) after interacting with HO$^\bullet$ and ^{1}O$_2$, respectively (Fig. 1) [22]. No fluorescence was observed in non-illuminated leaves (Fig. 1C and D, left panel and Fig. 3) [22], whereas illumination with continuous high red light for 30 min resulted in the formation of HPF-ox and SOSG-EP fluorescence (Fig. 1C and D, right panel and Fig. 4) [22]. These results indicate that exposure of Arabidopsis to high light results in the formation of HO$^\bullet$ and ^{1}O$_2$ in the chloroplasts located at the periphery of the mesophyll cells.

3.2. Organic radical imaging in Arabidopsis leaves

To image the formation of organic radicals in the high light exposed Arabidopsis leaves, confocal laser scanning microscopy using the anti-DMPO antibody conjugated with FITC was performed. In this technique, short-lived organic radicals (t$_{1/2}$ = μs) are trapped by spin trap DMPO to form a more stable DMPO-organic radical adduct (t$_{1/2}$ = min) (Fig. 2). Due to the unpaired electron localized on oxygen atom coordinated to nitrogen of nitrone spin trap, DMPO-organic radical adduct might be detected by EPR spectroscopy. As a result of the highly reducing and oxidizing conditions, paramagnetic DMPO-organic radical adduct is reduced and oxidized within minutes to diamagnetic hydroxylamine and DMPO nitrone adduct, respectively. Due to the conversion of paramagnetic DMPO-organic radical adduct to diamagnetic DMPO nitrone adduct, the use of EPR spectroscopy for the detection of organic radicals is unfeasible. However, DMPO nitrone adduct might be recognized by anti-DMPO antibody conjugated with FITC and imaged by confocal laser scanning microscopy. FITC fluorescence was measured in Arabidopsis leaves previously treated with DMPO spin trap and anti-DMPO antibody conjugated with FITC in the dark or illuminated with high red light (Fig. 3). Fig. 3A shows the Nomarski DIC channel, the FITC fluorescence channel, the combination of Nomarski DIC and FITC fluorescence channels and the integral distribution of FITC fluorescence intensity. In the dark, low FITC fluorescence was observed due to the presence of organic radicals formed by protein propagation after exposure of Arabidopsis leaves to high white light. When Arabidopsis leaves were exposed to high red light, FITC fluorescence significantly increased due to the formation of organic radicals under high red light. The integral distribution of FITC fluorescence intensity shows that the FITC fluorescence under high red light is more than double compared to dark. Fig. 3B shows that organic radicals are formed predominantly in the chloroplasts located at the periphery of the mesophyll cells.

3.3. Organic radical imaging in Arabidopsis chloroplast

To visualize the formation of organic radical in the chloroplasts, FITC fluorescence was measured in intact chloroplasts isolated from the high white light exposed Arabidopsis leaves using confocal laser scanning microscopy. FITC fluorescence was measured in intact chloroplasts previously treated with DMPO spin trap and anti-DMPO antibody conjugated with FITC in the dark or illuminated with high red light (Fig. 4A). Fig. 4 shows the Nomarski DIC channel, the FITC fluorescence channel, the combination of Nomarski DIC and FITC fluorescence channels and chlorophyll fluorescence channels. The FITC fluorescence
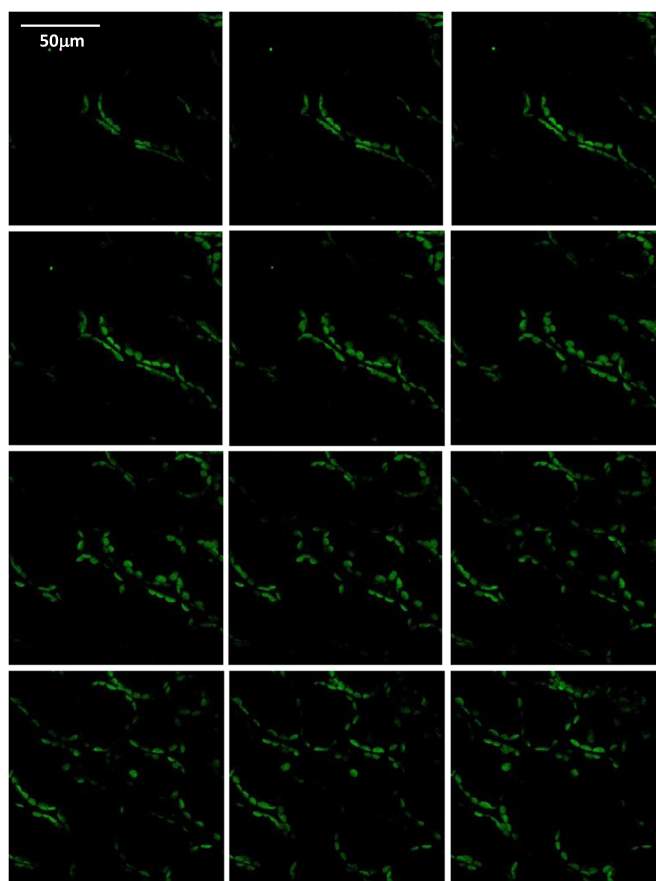

Fig. 5. Series of optical sections through the mesophyll cells of Arabidopsis leaves. FITC fluorescence channels are shown. The step between different pictures is 4 μm. Other experimental conditions as in Fig. 1.

is emitted uniformly from the whole chloroplasts. Comparison of FITC and chlorophyll fluorescence channels shows fluorescent spots of about 0.5 μm separated from one another by dark spaces inside chloroplasts (Fig. 4B). Bright spots reflect the appressed thylakoid membranes containing PSII complexes, whereas less bright spots reflect non-appressed thylakoid membrane containing ATP synthase and PSI complexes. To monitor spatial distribution of FITC fluorescence, z-stack confocal images were measured at optical sections distanced 4 μm (Fig. 5) and the spatial pattern of organic radical formation was visualized in a movie of 12 optical sections (Supplementary data 1A-B). Green circular, oval or elliptical shapes at the periphery of mesophyll cells shows FITC fluorescence in the chloroplasts of the mesophyll cells.

Supplementary material related to this article can be found online at doi:10.1016/j.freeradbiomed.2018.10.428.

3.4. Characterization of proteins radical by immuno-spin trapping

To monitor the formation of protein radicals in the appressed thylakoid membranes containing PSII complexes, immunoblot analysis with anti-DMPO antibody was performed in the thylakoid membranes isolated from the high white light exposed Arabidopsis leaves (Fig. 6A). DMPO nitrone adducts formed on different proteins were separated by SDS-polyacrylamide gel and transferred to NC membrane, identified by anti-DMPO antibody and visualized by luminol as a chemiluminescent probe using horseradish peroxidase conjugated secondary antibody. In dark, several weak protein bands of apparent molecular weights of 32, 34, 41, 43, 55 and 68 kDa were observed. After illumination with high white light, the intensity of these protein bands increased and the additional protein bands of apparent molecular weights of 23 and 18 kDa
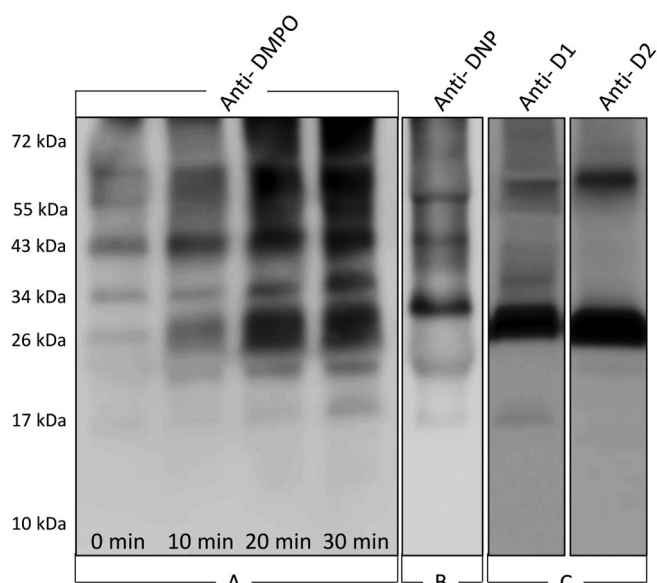
Fig. 6. Protein radical detection in thylakoid membranes using immuno-spin trapping technique. (A) Immunoblot of protein radical. From left to right: formation of protein radicals in thylakoid membranes illuminated with high white light for 0, 10, 20 and 30 min. **(B) Immunoblot of protein carbonyl.** Formation of protein carbonyls in thylakoid membranes was shown in 30 min high white light stress. **(C) Immunoblot of D1 and D2 proteins.** Blot using anti-DMPO presented for 0, 10, 20 and 30 min. Blots using anti-DNP, anti-D1 and anti-D2 antibodies are presented for 30 min. The different antibodies used are labelled above the lanes. Representative blots from three independent experiments are presented.

appeared. To study the formation of protein carbonyls in thylakoid membranes, immunoblotting technique using antibody specific to the DNP (anti-DNP antibody) was performed. The anti-DNP blot shows several protein bands of apparent molecular weights of 18, 23, 32, 34, 43 and 55 kDa (Fig. 6B). These results reveal that the formation of protein radicals and protein carbonyls is accompanied with protein aggregation (protein–protein cross-linking) and protein cleavage (fragmentation), respectively. To identify the bands originated from the D1 and D2 proteins, anti-D1 and anti-D2 antibodies were used. When the anti-DMPO blot was probed with these antibodies, the protein bands with apparent molecular weight of 32 and 34 kDa were detected (Fig. 6 C). These results demonstrate that illumination of thylakoid membranes induced the formation of protein radicals located on D1 and D2 proteins.

4. Discussion

Oxidation of biomolecules is associated with the formation of organic radicals involving carbon-centered (alkyl) and oxygen-centered (peroxyl and alkoxyl) radicals. Formation of organic radicals might be initiated by either HO$^\bullet$ [28] or $^1O_2$ [29]. Hydroxyl radical is formed by the reduction of free hydrogen peroxide (H_2O_2) by free metals (iron or manganese ions) or the reduction of bound peroxide by the non-heme iron [30]. Singlet oxygen is produced by the energy transfer form triplet chlorophyll to O_2 formed either by the intersystem crossing from singlet chlorophyll in the PSII antennae complex or the recombination of the charge separated radical pair in the PSII reaction center [31–33]. A spatial distribution of HO$^\bullet$ and $^1O_2$ achieved by confocal laser scanning microscopy using the HPF and SOSG fluorescence probes reveals the formation of HO$^\bullet$ and $^1O_2$ in the chloroplasts placed at the periphery of the mesophyll cells (Fig. 1C and D).

In this study, we used immuno-spin trapping technique (Fig. 2) for imaging of organic radicals in Arabidopsis leaves exposed to high light. A spatial distribution of organic radicals obtained by confocal laser
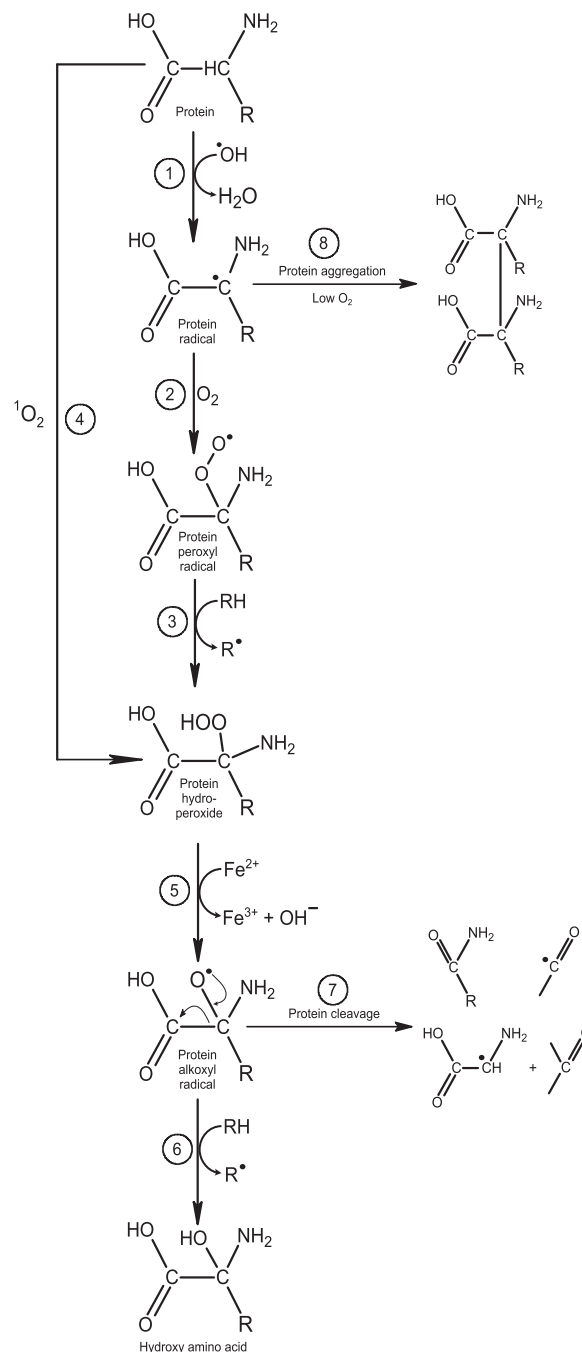
Fig. 7. Schematic representation of protein oxidation. Hydrogen abstraction from protein by hydroxyl radical generates alkyl radical (reaction 1). In the presence of O_2, alkyl radical readily reacts with O_2 and forms peroxyl radical (reaction 2). Peroxyl radical abstracts another hydrogen from an adjacent protein, while hydroperoxide and another alkyl radical are formed (reaction 3). Singlet oxygen addition to double bonds of aromatic amino acids forms hydroperoxide (reaction 4). Hydroperoxide is reduced to alkoxyl radical by ferrous iron (reaction 5). Hydrogen abstraction from an adjacent protein by alkoxyl radical forms hydroxy amino acids (reaction 6). Alkoxyl radical formed on the protein causes cleavage of the protein and creates alkyl radical and protein carbonyl (reaction 7). In the absence or low level of O_2, aggregation of alkyl radicals via covalent bond forms protein aggregates (reaction 8).

scanning microscopy using the anti-DMPO antibody conjugated with FITC shows the formation of organic radicals in the chloroplasts located at the periphery of the mesophyll cells (Fig. 3). More detail focus on the mesophyll chloroplast images reveals that organic radicals are formed predominantly in the appressed thylakoid membranes containing PSII

complexes (Fig. 4). The hydrogen abstraction by HO$^\bullet$ from carbon either at side chain or backbone and the addition of $^1O_2$ to the double bonds of any aromatic amino acid involves the formation of protein radicals either at the side chain or at the backbone sites on amino acids. The hydrogen abstraction from carbon by HO$^\bullet$ forms alkyl radical (Fig. 7, reaction 1) which reacts with O_2 in its abundance to form peroxyl radical (Fig. 7, reaction 2). Peroxyl radical abstracts hydrogen from other protein while hydroperoxide is formed (Fig. 7, reaction 3). Alternatively, the addition of $^1O_2$ to the double bonds of any aromatic amino acid via the ene reaction forms hydroperoxide (Fig. 7, reaction 4). In the presence of ferrous iron (Fe^{2+}), hydroperoxide is reduced to alkoxyl radical (Fig. 7, reaction 5). Both carbon-centered (alkyl) and oxygen-centered (peroxyl and alkoxyl) radicals might abstract another hydrogen from an adjacent amino acid and initiate protein propagation. The hydrogen abstraction from another amino acid by alkoxyl radical forms hydroxy amino acid (Fig. 7, reaction 6).

Re-probing by anti-D1 and anti-D2 antibodies reveals that illumination of thylakoid membranes induced the formation of protein radicals located on D1 and D2 proteins (Fig. 6C). Our previous study confirmed the formation of protein radicals and protein carbonyls on different amino acids of D1 and D2 proteins [8]. It was demonstrated that D1:^{332}H coordinated to the Mn_4O_5Ca cluster and D2:^{244}Y coordinated to non-heme iron via bicarbonate ligand are oxidized after exposure to high light. Apart from D1 and D2 protein, the formation of protein radicals can be seen on two protein bands at 23 and 18 kDa below D1/D2 proteins and on four protein bands at 41, 43, 55 and 68 kDa above D1/D2 proteins.

Formation of protein radicals results in the protein cleavage and protein aggregation [34]. When O_2 is available, protein cleavage occurs via β-scission of protein alkoxyl radical known to form carbon-centered radical and carbonyl located either on the C-terminal or N-terminal fragments (Fig. 7, reaction 7). In agreement with this, our result shows that the protein carbonyls are formed at 18, 23, 32, 34, 43 and 55 kDa proteins. When O_2 is very low or not available, protein radical crosslinked with another protein radical to form protein aggregate (Fig. 7, reaction 8). It was previously reported that the reaction of protein alkyl radical with O_2 is faster at diffusion-controlled rates (10^9–10^{10} dm^3 mol^{-1} s^{-1}) as compared to protein aggregation [35]. However, even when O_2 is low, steric hindrance might prevent protein aggregation and thus promote protein propagation. Such reactions would be anticipated to happen most readily with thiols forming sulfur-centered (thiyl) radicals which react rapidly and therefore maintain the protein propagation [36].

5. Conclusion

In summary, we applied the immuno-spin trapping technique to image organic radicals in plant cells by the laser confocal scanning microscopy. Due to high reactivity and short lifetime of organic radicals, imaging of organic radicals at sub-cellular resolution presents substantial challenges. We focused on protein oxidation under high light stress and tried to characterize the proteins bands where protein radicals and protein carbonyls were detected. Comprehensive description of oxidative modification of all protein bands is required to be performed using mass spectrometry. The application of immuno-spin trapping opens new possibilities to characterize the oxidized proteins and study their role in the signal transduction from the chloroplasts to the nucleus and unravel description of the spatial and temporal dynamics of the oxidative damage in plant cell. Characterization and spatial distribution of organic radicals allows to study an essential role of organic radicals and derived species in the signal transduction in the acclimation response and programmed cell death and oxidative damage in the accidental cell death.

References

[1] E.E. Farmer, M.J. Mueller, ROS-mediated lipid peroxidation and RES-activated signaling, Annu. Rev. Plant Biol. 64 (2013) 429–450.
[2] C. Laloi, M. Havaux, Key players of singlet oxygen-induced cell death in plants, Front. Plant Sci. 6 (2015) 39.
[3] C.H. Foyer, A.V. Ruban, G. Noctor, Viewing oxidative stress through the lens of oxidative signalling rather than damage, Biochem. J. 474 (2017) 877–883.
[4] V. Dogra, J.D. Rochaix, C. Kim, Singlet oxygen-triggered chloroplast-to-nucleus retrograde signalling pathways: an emerging perspective, Plant, Cell Environ. 41 (8) (2018) 1727–1738.
[5] I.M. Moller, L.J. Sweetlove, ROS signalling - specificity is required, Trends Plant Sci. 15 (7) (2010) 370–374.
[6] L.K. Frankel, L. Sallans, P.A. Limbach, T.M. Bricker, Identification of oxidized amino acid residues in the vicinity of the Mn_4CaO_5 cluster of photosystem II: implications for the identification of oxygen channels within the photosystem, Biochemistry 51 (2012) 6371–6377.
[7] L.K. Frankel, L. Sallans, P.A. Limbach, T.M. Bricker, Oxidized amino acid residues in the vicinity of Q(A) and Pheo(D1) of the photosystem II reaction center: putative generation sites of reducing-side reactive oxygen species, Plos One 8 (2) (2013) 7.
[8] R. Kale, A.E. Hebert, L.K. Frankel, L. Sallans, T.M. Bricker, P. Pospíšil, Amino acid oxidation of the D1 and D2 proteins by oxygen radicals during photoinhibition of Photosystem II, Proc. Natl. Acad. Sci. USA 114 (11) (2017) 2988–2993.
[9] B.S. Berlett, E.R. Stadtman, Protein oxidation in aging, disease, and oxidative stress, J. Biol. Chem. 272 (33) (1997) 20313–20316.
[10] M.J. Davies, Protein oxidation and peroxidation, Biochem. J. 473 (7) (2016) 805–825.
[11] B. Halliwell, J.M.C. Gutteridge, Free Radicals in Biology and Medicine, Oxford University Press, New York, 2007.
[12] J. Komenda, S. Kuviková, L. Lupínková, J. Masojídek, Biogenesis and structural dynamics of the photosystem II complex, biotechnological applications of photosynthetic proteins: biochips, biosensors and biodevices, Springer, US, Boston, MA, 2006, pp. 32–45.
[13] M. Edelman, A.K. Mattoo, D1-protein dynamics in photosystem II: the lingering enigma, Photosynth. Res. 98 (1–3) (2008) 609–620.
[14] J. Komenda, R. Sobotka, P.J. Nixon, Assembling and maintaining the photosystem II complex in chloroplasts and cyanobacteria, Curr. Opin. Plant Biol. 15 (3) (2012) 245–251.
[15] S. Jarvi, M. Suorsa, E.M. Aro, Photosystem II repair in plant chloroplasts– Regulation, assisting proteins and shared components with photosystem II biogenesis, Biochim. Biophys. Acta 1847 (9) (2015) 900–909.
[16] S.E. Gomez-Mejiba, Z.L. Zhai, M.C. Della-Vedova, M.D. Munoz, S. Chatterjee, R.A. Towner, K. Hensley, R.A. Floyd, R.P. Mason, D.C. Ramirez, Immuno-spin trapping from biochemistry to medicine: advances, challenges, and pitfalls. Focus on protein-centered radicals, Biochim. Biophys. Acta 1840 (2) (2014) 722–729.
[17] R.P. Mason, Imaging free radicals in organelles, cells, tissue, and in vivo with immuno-spin trapping, Redox Biol. 8 (2016) 422–429.
[18] R.P. Mason, Using anti-5,5-dimethyl-1-pyrroline N-oxide (anti-DMPO) to detect protein radicals in time and space with immuno-spin trapping, Free Radic. Biol. Med. 36 (10) (2004) 1214–1223.
[19] D.C. Ramirez, S.E. Gomez-Mejiba, R.P. Mason, Immuno-spin trapping analyses of DNA radicals, Nat. Protoc. 2 (3) (2007) 512–522.
[20] D. Seigneurin-Berny, D. Salvi, J. Joyard, N. Rolland, Purification of intact chloroplasts from Arabidopsis and spinach leaves by isopycnic centrifugation, Curr. Protoc. Cell Biol. Chapter Chapter 3 (2008) (Unit 3.30).
[21] A.P. Casazza, D. Tarantino, C. Soave, Preparation and functional characterization of thylakoids from Arabidopsis thaliana, Photosynth. Res. 68 (2001) 175–180.
[22] A. Kumar, A. Prasad, M. Sedlářová, P. Pospíšil. Data on detection of singlet oxygen, hydroxyl radical and organic radical in Arabidopsis thaliana. Data in Brief (2018) in press. ⟨https://www.sciencedirect.com/science/article/pii/S2352340918314264⟩.
[23] H. Schagger, Tricine-SDS-PAGE, Nat. Protoc. 1 (1) (2006) 16–22.
[24] S. Pou, C.L. Ramos, T. Gladwell, E. Renks, M. Centra, D. Young, M.S. Cohen, G.M. Rosen, A kinetic approach to the selection of a sensitive spin trapping system for the detection of hydroxyl radical, Anal. Biochem. 217 (1) (1994) 76–83.
[25] J. Moan, E. Wold, Detection of singlet oxygen production by ESR, Nature 279 (5712) (1979) 450–451.
[26] K. Setsukinai, Y. Urano, K. Kakinuma, H.J. Majima, T. Nagano, Development of novel fluorescence probes that can reliably detect reactive oxygen species and distinguish specific species, J. Biol. Chem. 278 (5) (2003) 3170–3175.
[27] A. Prasad, M. Sedlarova, P. Pospíšil, Singlet oxygen imaging using fluorescent probe Singlet Oxygen Sensor Green in photosynthetic organisms, Sci. Rep. 8 (1) (2018) 13685.
[28] C.L. Hawkins, M.J. Davies, EPR studies on the selectivity of hydroxyl radical attack

on amino acids and peptides, J. Chem. Soc.-Perkin Trans. 2 (12) (1998) 2617–2622.

[29] M. Gracanin, C.L. Hawkins, D.I. Pattison, M.J. Davies, Singlet-oxygen-mediated amino acid and protein oxidation: formation of tryptophan peroxides and decomposition products, Free Radic. Biol. Med. 47 (1) (2009) 92–102.

[30] P. Pospíšil, A. Arato, A. Krieger-Liszkay, A.W. Rutherford, Hydroxyl radical generation by photosystem II, Biochemistry 43 (21) (2004) 6783–6792.

[31] C. Triantaphylides, M. Havaux, Singlet oxygen in plants: production, detoxification and signaling, Trends Plant Sci. 14 (4) (2009) 219–228.

[32] P. Pospíšil, Molecular mechanisms of production and scavenging of reactive oxygen species by photosystem II, Biochim. Biophys. Acta 1817 (1) (2012) 218–231.

[33] B.B. Fischer, E. Hideg, A. Krieger-Liszkay, Production, detection, and signaling of singlet oxygen in photosynthetic organisms, Antioxid. Redox Signal. 18 (16) (2013) 2145–2162.

[34] R.T. Dean, S. Fu, R. Stocker, M.J. Davies, Biochemistry and pathology of radical-mediated protein oxidation, Biochem. J. 324 (Pt 1) (1997) 1–18.

[35] P. Neta, R.E. Huie, A.B. Ross, Rate constants for reactions of peroxyl radicals in fluid solutions, J. Phys. Chem. Ref. Data 19 (2) (1990) 413–513.

[36] C.L. Hawkins, M.J. Davies, Generation and propagation of radical reactions on proteins, Biochim Biophys. Acta 1504 (2–3) (2001) 196–219.

Data Article

Data on detection of singlet oxygen, hydroxyl radical and organic radical in *Arabidopsis thaliana*

Aditya Kumar [a], Ankush Prasad [a], Michaela Sedlářová [b], Pavel Pospíšil [a,*]

[a] Department of Biophysics, Centre of the Region Haná for Biotechnological and Agricultural Research, Faculty of Science, Palacký University, Šlechtitelů 27, 783 71 Olomouc, Czech Republic
[b] Department of Botany, Faculty of Science, Palacký University, Šlechtitelů 27, 783 71 Olomouc, Czech Republic

ARTICLE INFO

ABSTRACT

This article contains data related to the research article entitled, "Organic radical imaging in plants: Focus on protein radicals" (Kumar et al., 2018). The data presented herein focus on reactive oxygen species (ROS) and organic radical formed within photosynthetic tissues of *Arabidopsis thaliana* during high light stress and includes (1) Confocal laser scanning microscopic images using 3′-p-(hydroxyphenyl) fluorescein (HPF) as specific probe for the detection of hydroxyl radical (HO$^\bullet$); (2) Confocal laser scanning microscopic images using Singlet Oxygen Sensor Green (SOSG) as a specific probe for the detection of singlet oxygen ($^1O_2$) and; (3) Electron paramagnetic resonance (EPR) spectroscopy using spin traps for the detection of organic radical.

Specifications table

Subject area	Biology
More specific subject area	Redox Biology
Type of data	Images/figures

* Corresponding author. Fax: +420 585225737.
  E-mail address: pavel.pospisil@upol.cz (P. Pospíšil).

How data were acquired	Fluorescence of specific fluorochromes was localized within *Arabidopsis* leaves kept in dark or illuminated with high red light (RL, $\lambda \geq 600$ nm) by confocal laser scanning microscopy (fluorview 1000 unit attached to IX80 microscope; Olympus Czech Group, Prague, Czech Republic) and electron paramagnetic resonance (EPR) spectra were taken in thylakoid membranes isolated from *Arabidopsis* leaves illuminated with high white light (WL) using EPR spectrometer MiniScope MS400 (Magnettech GmbH, Berlin, Germany).
Data format	Analyzed
Experimental factors	Leaves and thylakoid membranes of *Arabidopsis* plant were used.
Experimental features	1. Plants were pre-illuminated with high white light (1500 μmol photons m^{-2} s^{-1}) at low temperature (8 °C) for 13 h to induce oxidative stress.
	2. Leaf tissues were infiltrated with fluorescent probes, 3′-p-(hydroxyphenyl) fluorescein (HPF) or singlet oxygen sensor green (SOSG), and incubated for 30 min at room temperature in dark (control) or illuminated with RL. Fluorescence was visualized subsequently by confocal laser scanning microscopy.
	3. Thylakoid membranes were isolated from pre-illuminated leaves and illuminated by a high white light for 30 min/5 min (as specified). Formation of organic radicals was determined using EPR spin trapping spectroscopy.
Data source location	Department of Biophysics, Centre of the Region Haná for Biotechnological and Agricultural Research and Department of Botany, Palacký University, Olomouc, Czech Republic. Loc: 49°34′33.828″N, 17°16′54.658″E
Data accessibility	The data are available within this article
Related research article	Aditya Kumar, Ankush Prasad, Michaela Sedlářová, Pavel Pospíšil, Organic radical imaging in plants: Focus on protein radicals (in press, Free Radical Biology and Medicine) doi.org/10.1016/j.free radbiomed.2018.10.428 [1].

Value of the data

- We suggest organic radicals and other biomolecules oxidized by $HO^\bullet$ and $^1O_2$ as significant members of the signaling pathways in high-light stressed plants.
- We illustrate the localization of hydroxyl radical ($HO^\bullet$) and singlet oxygen ($^1O_2$) within *Arabidopsis* leaves as well as detection of organic radicals in thylakoid membranes by techniques which might be of interest to the community of plant redox biology and ROS-mediated signaling.
- Apart from malondialdehyde (MDA), organic radicals/ biomolecules oxidized by $HO^\bullet$ and $^1O_2$ have not been reported as major regulators of signaling in stressed plants. However, our current data article can be useful as it deals with the current aspect and hypothesizes the phenomenon.
- We present histochemical staining followed by confocal laser scanning microscopy which can be used as an imaging tool for $HO^\bullet$, $^1O_2$ localization and spin-trap based EPR spectroscopy for qualitative analysis of organic radical.

1. Data

Data presented herein bring together microscopic techniques used to visualize the formation of ROS ($HO^\bullet$ and $^1O_2$) within *Arabidopsis* leaves in the first stage and detection of organic radical formation in the second stage of stress-induced protein oxidation as suggested in [1]. Plants were

subjected to high white light stress (1500 µmol photons m^{-2} s^{-1}) at low temperature (8 °C) for 13 h, i.e. conditions chosen so as to reach oxidative stress in photosystem II but concurrently to avoid chlorophyll degradation. Immediately after the light-induced stress, the leaves were cut into pieces and incubated with specific fluorescent probes in dark/RL for 30 min to gain confocal images from spongy mesophyll cells, omitting 3 lines of cells along the injured edges. To avoid photosensitization of SOSG [2], an RL source ($\lambda \geq 600$ nm) has been used during histochemical staining, recently with both fluorescent probes. Organic radicals formation were determined using EPR spin trapping spectroscopy in thylakoid membranes isolated from pre-illuminated *Arabidopsis* leaves and illuminated by a high white light (30 min/5 min, as specified).

2. Experimental design, materials and methods

2.1. Plant samples – Arabidopsis thaliana

Seeds of *A. thaliana* wild-type Columbia-0 was purchased from the Nottingham *Arabidopsis* Stock Centre (NASC), U.K. The seeds were soaked for 4 days (at 4 °C) followed by potting with a peat substrate (Klasmann, Potgrond H). The plants were grown for 5–6 weeks in a walk-in type growth chamber Fytoscope FS-WI-HY (Photon Systems Instruments, Drásov, Czech Republic) under following conditions: photoperiod of 8/16 h light/dark (100 µmol photons m^{-2} s^{-1}); temperature of 22/20 °C light/dark and a relative humidity of 60%. For high light treatment, illumination at 1500 µmol photons m^{-2} s^{-1} at low temperature (8 °C) for 13 h was achieved using AlgaeTron AG 230 (Photon Systems Instruments, Drásov, Czech Republic).

2.2. Fluorescent probes and spin traps

3′-p-(hydroxyphenyl) fluorescein (HPF) (ThermoFisher Scientific, Paisley, UK) and SOSG (Molecular Probes Inc., Eugene, OR, USA) were infiltrated to leaf tissues for confocal laser scanning microscopy in order to detect and localize HO$^{\bullet}$ and $^1O_2$, respectively. For EPR spin trapping spectroscopy, α-(4-pyridyl N-oxide)-N-tert-butyl nitrone (POBN) (Sigma Aldrich, GmbH, Germany) and 5,5-dimethyl-1-pyrroline N-oxide (DMPO) (Dojindo Molecular Technologies Inc. Rockville, MD, USA) were used to detect organic radicals in thylakoids.

2.3. Histochemical staining for microscopy

Leaf pieces of size 5 × 5 mm were excised from *Arabidopsis* leaf blade on a glass slide wetted with HEPES buffer (pH 7.5) and infiltrated with fluorescent probes (either 10 µM HPF or 50 µM SOSG) in a syringe. Subsequently, the leaf pieces together with probe solution were transferred into 1.5 ml Eppendorf tube and incubated for 30 min either in dark or exposed to high red light. The illumination was performed utilizing a LED source with a light guide CL6000 LED Zeiss (Carl Zeiss Microscopy GmbH, Jena, Germany). The exposure was achieved using a long-pass edge interference filter ($\lambda \geq 600$ nm) (Andover Corporation, Salem, NH, USA). Fig. 2A shows a schematic representation of the experimental procedure for details refer to references [2,3].

2.4. Confocal laser scanning microscopy

Following the staining procedure, the leaf pieces were transferred into a fresh HEPES buffer (pH 7.5) on a slide and visualized by confocal laser scanning microscopy (Fluorview 1000 unit attached to IX80 microscope; Olympus Czech Group, Prague, Czech Republic). The excitation of HPF and SOSG was performed by a 488 nm line of an argon laser and the emission was detected by a 505–525 nm filter, respectively. The excitation/emission parameters utilized is slightly different as compared to excitation/emission maxima mentioned in datasheet (please refer to legend to Fig. 1) due to variation of the instrument used in our study. The laser intensities for Figs. 2–4 were set as described in our previous study [2].
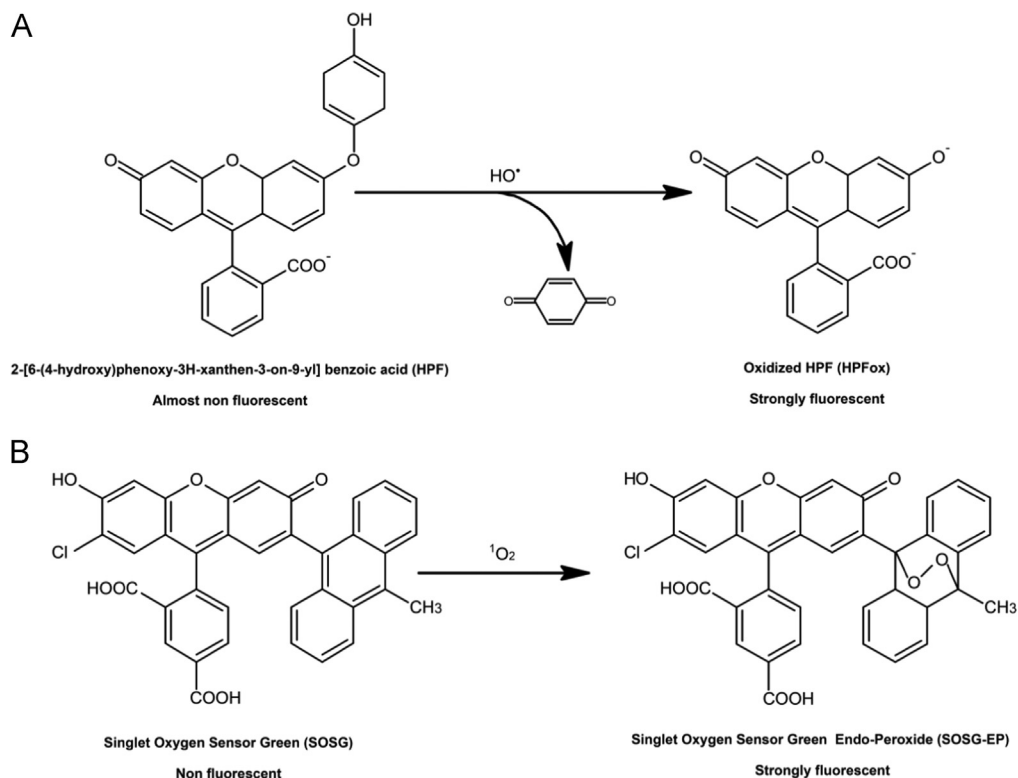
A

2-[6-(4-hydroxy)phenoxy-3H-xanthen-3-on-9-yl] benzoic acid (HPF)

Almost non fluorescent

Oxidized HPF (HPFox)

Strongly fluorescent

B

Singlet Oxygen Sensor Green (SOSG)

Non fluorescent

Singlet Oxygen Sensor Green Endo-Peroxide (SOSG-EP)

Strongly fluorescent

Fig. 1. (A) Non-fluorescent hydroxyphenyl fluorescein (HPF) oxidized by hydroxyl radical (HO$^\bullet$) form a highly fluorescent compound HPF-ox which exhibits bright green fluorescence (excitation/ emission maxima $\sim$490/515 nm). (B) Singlet oxygen sensor green (SOSG) oxidized by singlet oxygen ($^1O_2$) forms SOSG endoperoxide (SOSG-EP) providing bright green fluorescence (excitation/emission maxima $\sim$504/525 nm) (as per datasheet, ThermoFisher Scientific, Paisley, UK and Molecular Probes Inc., Eugene, OR, USA).

2.5. Thylakoid membrane isolation

Thylakoid membranes were prepared according to the protocol of Casazza and co-workers [4] as briefly described below.

- Leaves were harvested from 5–6 weeks old *Arabidopsis* plants.
- The leaves (5–10 g) were floated in dark on ice cold water for 5–10 min and then blotted. All glassware's were pre-cooled before use and all further steps were performed at 4 °C under dark condition.
- Leaves were promptly homogenized in grinding buffer (100–200 ml) containing EDTA (5 mM), EGTA (5 mM), MgCl$_2$ (5 mM), sorbitol (0.4 M), NaHCO$_3$ (10 mM), Tricine/NaOH (20 mM, pH 8.4), 0.5% (w/v) fatty acid-free BSA.
- The homogenate was then filtered through 2 layers of cheesecloth (moderate hand pressure) to increase the final yield of thylakoid membranes.
- The filtrate was centrifuged at 2600*g* (3 min).
- The pellet was re-dissolved in re-suspension buffer [sorbitol (0.3 M), EDTA (2.5 mM), MgCl$_2$ (5 mM), NaHCO$_3$ (10 mM), HEPES (20 mM, pH 7.6), 0.5% (w/v) fatty acid-free BSA].
- Suspension was centrifuged at 2600*g* (3 min, 4 °C); the pellet was washed again in re-suspension buffer and then was suspended in 50–100 ml of hypotonic buffer [EDTA (2.5 mM), MgCl$_2$ (5 mM),
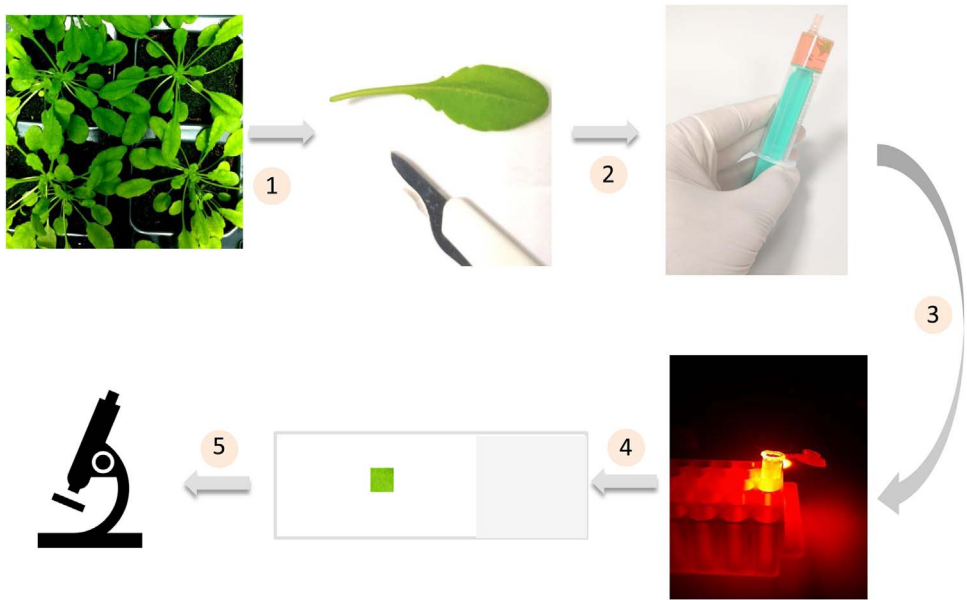
Fig. 2. A schematic representation showing the different steps involved in the preparation of samples for confocal laser scanning microscopy.
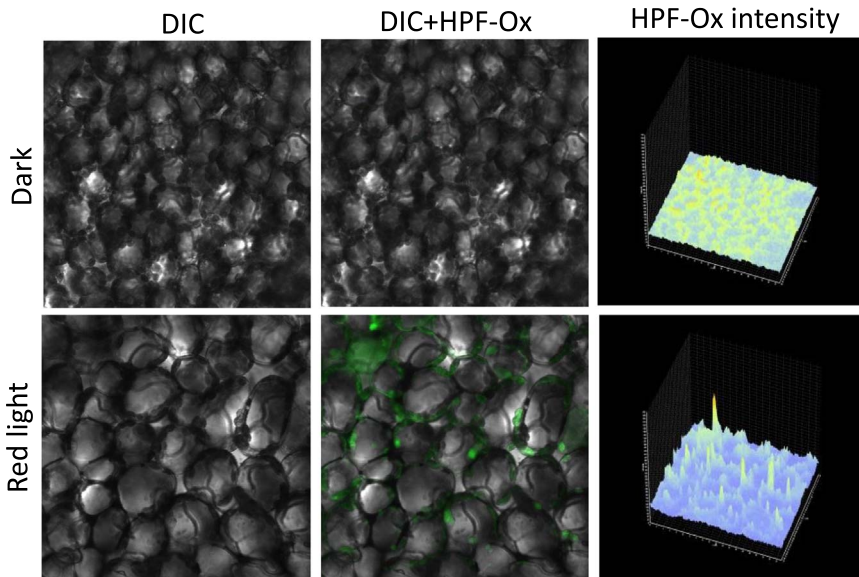
Fig. 3. Hydroxyl radical imaging in *Arabidopsis* leaves. *Arabidopsis* leaves were infiltrated with 10 μM HPF in dark (upper panel) or exposed to high red light (lower panel) for 30 min. From left to right is Nomarski DIC channel, combination of Nomarski DIC channel+HPF-ox fluorescence and integral distribution of the HPF-ox fluorescence signal intensity within the sample.

DIC   DIC+SOSG-EP   SOSG-EP intensity
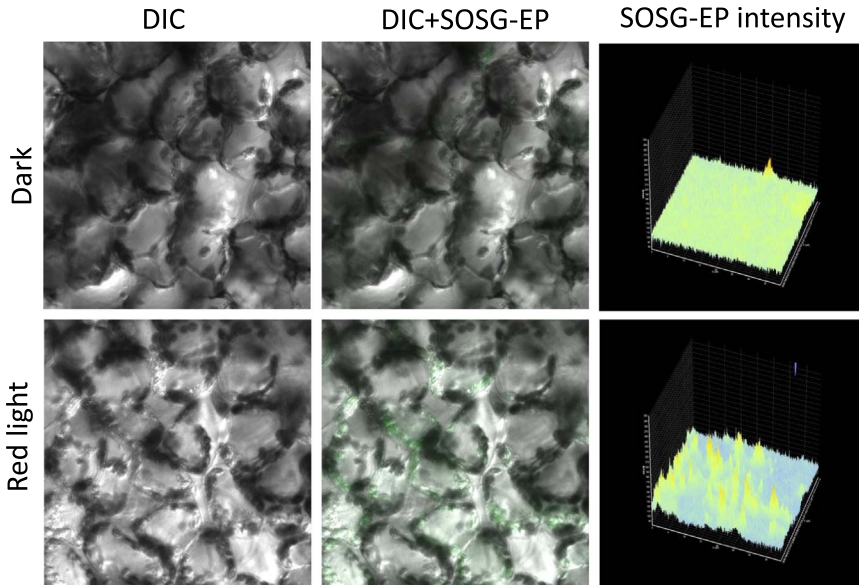
Fig. 4. Singlet oxygen imaging in *Arabidopsis* leaves. *Arabidopsis* leaf tissues were infiltrated with 50 μM SOSG in dark (upper panel) or exposed to high red light (lower panel) for 30 min. From left to right are Nomarski DIC channel, combination of DIC+ SOSG-EP fluorescence channels and integral distribution of the SOSG-EP fluorescence signal intensity within the sample.
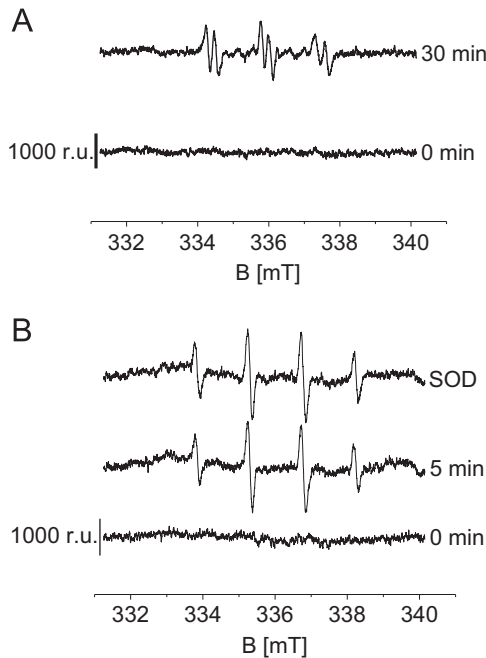
Fig. 5. Detection of organic radical by using EPR spin trapping spectroscopy thylakoid membranes. (A) Thylakoid membranes (200 μg Chl ml^{-1}) were illuminated with high white light in the presence of 50 mM POBN at 0 min and 30 min. (B) Thylakoid membranes (200 μg Chl ml^{-1}) were illuminated with high white light in the presence of 50 mM DMPO at 0 min (lower trace) and 5 min [in absence (middle trace) and presence (upper trace) of superoxide dismutase (SOD) (400 U/ml)].

NaHCO$_3$ (10 mM), HEPES (20 mM, pH 7.6), 0.5% (w/v) fatty acid-free BSA] followed by a last-step centrifugation (2600g, 3 min at 4 °C).

- The pellet was dissolved in a small volume (0.5–1 ml) of the re-suspension buffer; chlorophyll concentration was calculated from the absorbance of an 80% (v/v) acetone extract measured at 645 and 663 nm [5].

2.6. EPR spin-trapping spectroscopy

Organic radicals including alkyl (R$^\bullet$) and peroxyl/alkoxyl (ROO$^\bullet$/RO$^\bullet$) radicals formed in thylakoid membranes (200 μg Chl ml^{-1}) were detected using EPR spin trapping spectroscopy (Fig. 5). Detection of R$^\bullet$ was performed using spin trap POBN (50 mM) while ROO$^\bullet$/RO$^\bullet$ was detected using spin trap DMPO (50 mM). High white light illumination (1500 μmol photons m^{-2} s^{-1}, 30 min) was achieved using a LED source with a light guide CL6000 LED Zeiss (Carl Zeiss Microscopy GmbH, Jena, Germany). POBN-R and DMPO-OOR/DMPO-OR adduct EPR signal spectra were recorded under EPR conditions as follows: microwave power (10 mW), modulation amplitude (1 G), modulation frequency (100 kHz), sweep width (100 G), scan rate (1.62 G s^{-1}).

Acknowledgements

Transparency document.   Supporting information

Transparency document associated with this article can be found in the online version at https://doi.org/10.1016/j.dib.2018.11.033.

References

[1] A. Kumar, A. Prasad, M. Sedlářová, P. Pospíšil, Organic radical imaging in plants: focus on protein radicals, Free Radic. Biol. Med. (2018), https://doi.org/10.1016/j.freeradbiomed.2018.10.428 (In press).
[2] A. Prasad, M. Sedlářová, P. Pospíšil, Singlet oxygen imaging using fluorescent probe Singlet Oxygen Sensor Green in photosynthetic organisms, Sci. Rep. 8 (2018) 13685.
[3] M. Sedlářová, L. Luhová, Re-evaluation of imaging methods of reactive oxygen and nitrogen species in plants and fungi: influence of cell wall composition, Front. Physiol. 8 (2017) 826.
[4] A.P. Casazza, D. Tarantino, C. Soave, Preparation and functional characterization of thylakoids from Arabidopsis thaliana, Photosynth. Res. 68 (2) (2001) 175–180.
[5] D.I. Arnon, Copper enzymes in isolated chloroplasts. Polyphenoloxidase in Beta vulgaris, Plant Physiol. 24 (1) (1949) 1–15.

Check for updates

Characterization of Protein Radicals in Arabidopsis

Aditya Kumar[1†], Ankush Prasad[1‡], Michaela Sedlářová[2§] and Pavel Pospíšil[1]*

[1] *Department of Biophysics, Centre of the Region Haná for Biotechnological and Agricultural Research, Faculty of Science, Palacký University Olomouc, Olomouc, Czechia,* [2] *Department of Botany, Faculty of Science, Palacký University Olomouc, Olomouc, Czechia*

Oxidative modification of proteins in photosystem II (PSII) exposed to high light has been studied for a few decades, but the characterization of protein radicals formed by protein oxidation is largely unknown. Protein oxidation is induced by the direct reaction of proteins with reactive oxygen species known to form highly reactive protein radicals comprising carbon-centered (alkyl) and oxygen-centered (peroxyl and alkoxyl) radicals. In this study, protein radicals were monitored in Arabidopsis exposed to high light by immuno-spin trapping technique based on the detection of 5,5-dimethyl-1-pyrroline N-oxide (DMPO) nitrone adducts using the anti-DMPO antibody. Protein radicals were imaged in Arabidopsis leaves and chloroplasts by confocal laser scanning microscopy using fluorescein conjugated with the anti-DMPO antibody. Characterization of protein radicals by standard blotting techniques using PSII protein specific antibodies shows that protein radicals are formed on D1, D2, CP43, CP47, and Lhcb3 proteins. Protein oxidation reflected by the appearance/disappearance of the protein bands reveals that formation of protein radicals was associated with protein fragmentation (cleavage of the D1 peptide bonds) and aggregation (cross-linking with another PSII subunits). Characterization of protein radical formation is important for better understating of the mechanism of oxidative modification of PSII proteins under high light.

Keywords: aggregate, fragment, photosystem II, protein, reactive oxygen species, singlet oxygen, hydroxyl radical, protein radical

INTRODUCTION

Plants are prone to various environmental stresses throughout their life cycle as high light, UV irradiation, heat, cold, drought and salinity (Murata et al., 2007; Choudhury et al., 2017). Plant responses to various types of stress factor by the formation of reactive oxygen species (ROS) are known to play a crucial role in the retrograde signaling and oxidative damage (Schmitt et al., 2014; Laloi and Havaux, 2015; Dietz et al., 2016; Mittler, 2017). Under high light, ROS are produced when absorption of light energy by chlorophylls surpasses the capacity for its use in the photosynthetic reactions. It is evidenced that photosystem II (PSII) produces various types of ROS at different sites (Pospíšil, 2012; Fischer et al., 2013; Telfer, 2014). Singlet oxygen ($^1O_2$) is formed by energy transfer from triplet chlorophyll to molecular oxygen at the site of coordination of weakly-coupled or uncoupled chlorophylls

in the PSII antenna (CP43, CP47, and Lhcb proteins) and PSII reaction center (D1, D2) proteins. Hydroxyl radical (HO$^\bullet$) is formed by metal-mediated reduction of hydrogen peroxide at the site of metal coordination to PSII reaction center proteins (Pospíšil, 2014). It is well accepted that both $^1O_2$ and HO$^\bullet$ oxidize PSII proteins and thus alter subsequently the structure of the PSII proteins. The oxidation of protein by ROS forms carbon-centered (alkyl) and oxygen-centered (peroxyl and alkoxyl) protein radicals (Davies, 2016). In spite of the fact that oxidative modification of PSII proteins has been intensively studied in past decades, the formation of protein radicals by oxidation of PSII proteins was not explored in detail. It was predominantly due to a limitation in the detection of protein radicals caused by high reactivity of protein radicals toward other proteins and short lifetime of protein radicals (Mattila et al., 2015).

It has been previously established that immuno-spin trapping technique which combines the specificity and sensitivity of spin trapping with various immunoassays is suitable method for the detection of protein radicals in animal cells (Gomez-Mejiba et al., 2014). In this technique, the reaction of spin trap 5,5-dimethyl-1-pyrroline N-oxide (DMPO) with an organic (proteins, lipids, and nucleic acids) radical forms a stable nitrone adduct (DMPO-P adduct), which is identified by an anti-DMPO antibody raised against nitrone moiety of the adduct (Mason, 2016). Recently, protein radicals have been visualized for the first time in Arabidopsis plants using the immuno-spin trapping technique (Kumar et al., 2019). The authors showed by confocal laser scanning microscopy using fluorescein conjugated with anti-DMPO antibody that protein radicals are formed predominantly in the chloroplasts located at the periphery of the cells and distributed uniformly throughout the grana stack. To understand the mechanism of oxidative reactions, it is very important to analyze which PSII proteins are oxidized by ROS. Using tandem mass spectroscopy, natively oxidized amino acid residues in PSII membranes isolated from field-grown spinach showed that oxidized amino acids are localized in the vicinity of the Mn_4O_5Ca cluster, PheoD1 (D1 residues 130E, 133L and 135F) and Q_A (D1 residues 214Q, 239F, and 242E) (Frankel et al., 2012, 2013). Detail analysis of amino acid oxidized in spinach PSII membranes under high light showed that amino acids located in the close proximity to the metal coordinated to D1 and D2 proteins are oxidized (Kale et al., 2017). The authors showed that D1:332H coordinated to the Mn_4O_5Ca cluster and D2:244Y coordinated to the non-heme iron via bicarbonate are oxidized by HO$^\bullet$. Similarly, identification of oxidized residues on the luminal side of PSII in the cyanobacterium *Synechocystis* sp. PCC 6803 showed that D1:332H is oxidized under high light (Weisz et al., 2017). The authors proposed that oxidized amino acid forms wall of the water channel through which ROS formed at the Mn_4O_5Ca cluster are driven away from the catalytic center to the lumen.

In this study, we used immuno-spin trapping to monitor the formation of protein radicals in Arabidopsis. Standard blotting techniques using various antibodies to PSII proteins provided a complete characterization of protein radical formed on various PSII proteins involved in oxidative processes.

MATERIALS AND METHODS

Plant Material, Leaf, Chloroplast and Thylakoid Membrane Isolation

Seeds of wild-type Arabidopsis (*Arabidopsis thaliana*, cv. Columbia-0; WT) obtained from the Nottingham Arabidopsis Stock Center (NASC), University of Nottingham (Loughborough, United Kingdom) were soaked in distilled water and then potted in growing pots with a peat substrate (Klasmann, Potgrond H). Plants were grown in a growing chamber (Photon Systems Instruments, Drásov, Czechia) under controlled conditions with a light intensity of 100 µmol photons $m^{-2} s^{-1}$, photoperiod of 8/16 h and temperature of 25°C (unless specified otherwise) with a relative air humidity of 60%. Arabidopsis plants (5 or 6 weeks old) were exposed to high light stress (1500 µmol photons $m^{-2} s^{-1}$) at a low air temperature of 8°C for 13 h using AlgaeTron AG 230 (Photon Systems Instruments, Drásov 470, Czechia). Leaves were cut into 3–5 mm small square pieces using surgical knife. Intact chloroplasts were prepared using Percoll gradient centrifugation as described by Seigneurin-Berny et al. (2008). Both sliced leaf pieces and isolated chloroplasts were used immediately for confocal measurements. Thylakoid membranes were prepared according to Casazza et al. (2001) and stored at −80°C in the dark until use.

In vitro Detection of Reactive Oxygen Species by Electron Paramagnetic Resonance Spectroscopy

Detection of $^1O_2$ and HO$^\bullet$ was performed by electron paramagnetic resonance (EPR) spectroscopy using an EPR spectrometer (MiniScope MS400, Magnettech GmbH, Berlin, Germany). For $^1O_2$ detection, a hydrophilic diamagnetic compound TMPD (2, 2, 6, 6-tetramethyl-4-piperidone) was used (Moan and Wold, 1979) while for HO$^\bullet$, POBN (4-pyridyl-1-oxide-N-tert-butylnitrone)/ethanol system was used (Pou et al., 1994). For validation of spin trap-compounds, chemically generated $^1O_2$ and HO$^\bullet$ were utilized (**Supplementary Datasheet S1**) and data simulation were performed (for details, refer to **Supplementary Datasheet S2**). EPR spectra were collected using following conditions: microwave power (10 mW), modulation amplitude (0.1 mT), modulation frequency (100 kHz), sweep width (8 mT) and sweep time (60 s). EPR signal intensity was evaluated from the relative height of the central peak of TEMPONE EPR spectrum or central doublet peak of POBN-$CH(CH_3)OH$ adduct EPR spectrum. Simulation of EPR spectra was performed by WinSim software (National Institute of Environmental Health Sciences, Research Triangle Park, NC, United States).

In vivo Imaging of Reactive Oxygen Species by Confocal Laser Scanning Microscopy

Formation of $^1O_2$ and HO$^\bullet$ in leaves was visualized by confocal laser scanning microscopy (Fluorview 1000 unit attached to IX80 microscope; Olympus Czech

Group, Prague, Czechia) (Kumar et al., 2018; Prasad et al., 2018). Leaf pieces were incubated either in dark or red light (1000 µmol photons m^{-2} s^{-1}) at room temperature with 50 µM Singlet Oxygen Sensor Green (SOSG) for the detection of $^1O_2$ and 5 µM Hydroxy Phenyl Fluorescein (HPF) for the detection of HO$^•$ in the presence of HEPES buffer (pH 7.5). Singlet oxygen imaging was based on its interaction with SOSG forming SOSG endoperoxide (SOSG-EP) while HO$^•$ imaging was based on its interaction with HPF forming HPF-ox; both products provide bright green fluorescence. The excitation of SOSG and HPF was achieved by 488 nm line of an argon laser and emission was detected at 505–525 nm using BA505-525 filter (Olympus).

In vivo Imaging of Protein Radicals by Confocal Laser Scanning Microscopy

Formation of protein radicals in leaves and chloroplasts was visualized by confocal laser scanning microscopy (Kumar et al., 2019). Sliced leaf pieces and chloroplasts were incubated either in dark or red light (1000 µmol photons m^{-2} s^{-1}) for 30 min at room temperature, in the presence of MES-NaOH buffer (40 mM, pH 6.5), spin trap DMPO (50 mM), anti-DMPO antibody (5 µg ml^{-1}) conjugated with fluorescein isothiocyanate (FITC) and Triton X-100 (0.001%). Triton X-100 was used in order to increase the penetration of spin trap and antibody through the cell wall and membrane. Protein radicals were imaged based on their interaction with DMPO forming DMPO-protein radical adduct known to disproportionate to stable DMPO-nitrone adduct which is recognized by anti-DMPO antibody conjugated with FITC. Anti-DMPO is claimed by the manufacturer (Abcam, Cambridge, United Kingdom) for its non-cross reactivity with non-adducted proteins or DNA; however, it can recognize free DMPO and thus should be taken into account. FITC fluorescence in leaf and chloroplast was visualized by confocal laser scanning microscopy. The excitation of FITC was achieved by 488 nm line of an argon laser and emission was detected at 505–525 nm using BA505–525 filter (Olympus).

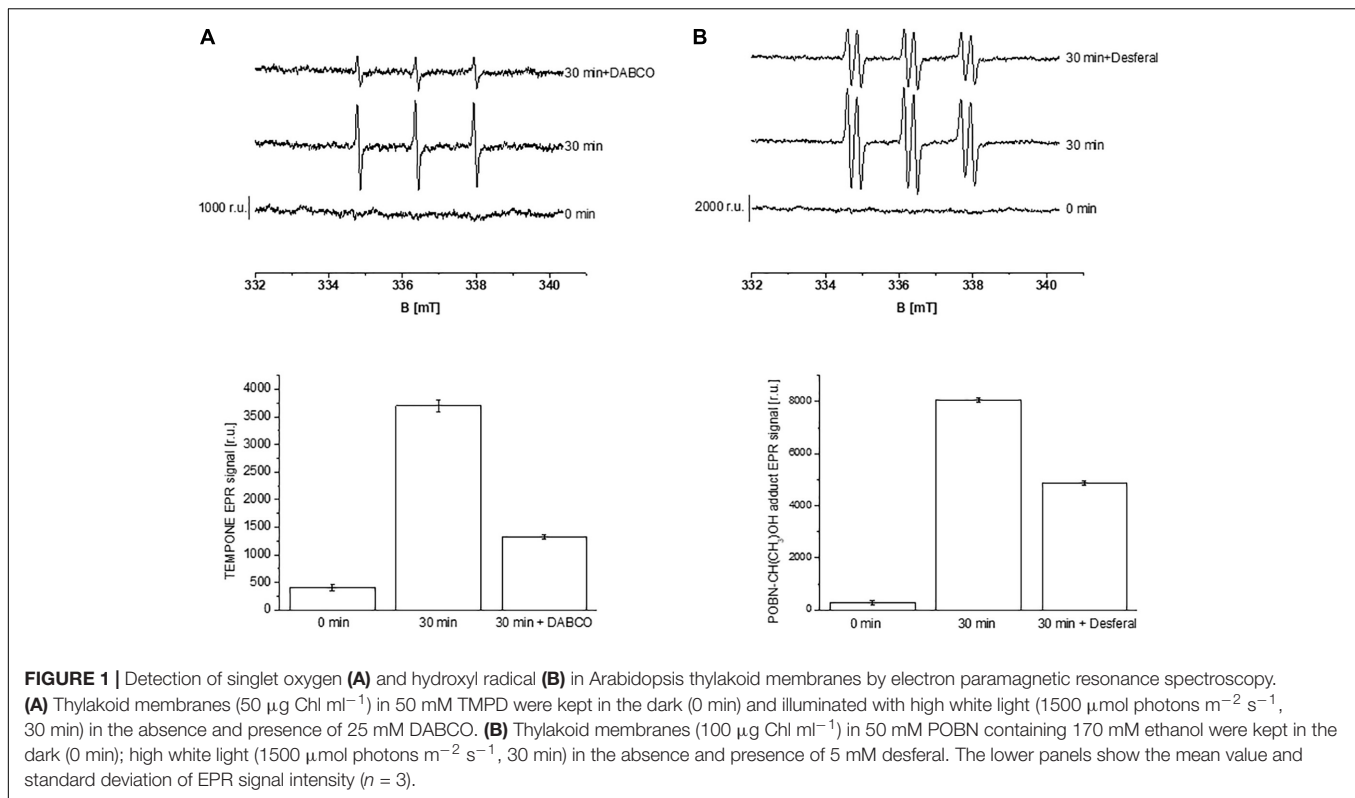## SDS-PAGE and Immuno-Spin Trapping

To visualize the protein degradation/loss during high light illumination, thylakoid membranes (5 µg Chl) isolated from long term high light exposed plants at low air temperature (13 h, 1500 µmol photons m^{-2} s^{-1}, 8°C) was incubated either in dark or in high white light (1500 µmol photons m^{-2} s^{-1}) for 10, 20, and 30 min in the presence of DMPO (50 mM) spin trap at room temperature. After dark/light incubation, protein extraction using DTT (dithiothreitol) protein extraction buffer followed by heating at 70°C in the dry bath for 15 min and centrifugation at 16,000 × *g* for 5 min at 4°C was performed. The supernatant was loaded into wells and SDS-PAGE was completed using a Tris-Tricine SDS-PAGE protocol described by Schagger (2006) using Mini-PROTEAN Tetra vertical electrophoresis cell (Bio-Rad, CA, United States). Proteins resolved in SDS gels were either stained with Coomassie Brilliant Blue (CBB) R-250 in a methanol/acetic acid solution followed by de-staining to remove the high blue background (Brunelle and Green, 2014) or transferred to a nitrocellulose

(NC) membrane using a semi-dry blotter (*Trans*-Blot SD, Semi-dry transfer cell, Bio-Rad, United States). To detect protein radicals formed on the PSII proteins (reaction center proteins and/or antenna complex proteins) or on their aggregate/cleaved peptide, blocking step of NC membrane was done with 5% BSA prepared in phosphate buffered saline-tween 20 (PBST; pH- 7.4) at 4°C overnight to prevents antibodies from binding to the membrane non-specifically. All successive steps were performed on a shaker at room temperature. After blocking, the NC membrane was incubated with rabbit polyclonal anti-DMPO nitrone adduct primary antibody (1:5000, Abcam) raised against DMPO followed by 10 min, three to five washes with PBST and 1 h incubation with horseradish peroxidase (HRP) conjugated goat anti-rabbit secondary antibody (1:10000, Bio-Rad) and protein bands were visualized using luminol as a chemiluminescent probe and images were captured by AI600 (Amersham Imager 600, GE Health Care Europe GmbH, Freiburg, Germany). For the identification of the origin of protein bands, we used specific antibodies from Agrisera raised against PSII proteins. Antibodies used are anti-D1, anti-C-terminal, anti-D-*de* loop, anti-cyt b_{559} α-subunit, anti-D2, anti-CP43, anti-CP47 and anti-Lhcb3. Size of protein bands was determined using a standard protein ladder (PageRuler^{TM} Pre-stained Protein Ladder, 10 to 180 kDa, Thermo Fisher Scientific, Lithuania). Densitometry of western blots was performed with ImageJ (National Institute of Mental Health, Bethesda, MD, United States) and the quantification of protein band intensities was shown as peaks in densitogram. The area under the peak was evaluated to determine the increase or decrease of protein band intensities in the SDS-gel and blots probed with different PSII protein antibodies.

RESULTS

Reactive Oxygen Species Formation Under High Light Stress in Arabidopsis

Formation of ROS ($^1O_2$ and HO$^•$) in the thylakoid membranes exposed to high white light was measured by EPR spectroscopy using TMPD spin probe and POBN/ethanol spin trap system, respectively. No EPR signal was observed in dark (**Figures 1A,B**, trace 0 min), whereas illumination with continuous white light for 30 min resulted in the formation of the 2,2,6,6-tetramethyl-4-piperidone-1-oxyl (TEMPONE) EPR and α-hydroxyethyl radical adduct of POBN [POBN-CH(CH$_3$)OH adduct] EPR signals (**Figures 1A,B**, trace 30 min). Significant suppression in $^1O_2$ and HO$^•$ were observed in the presence of $^1O_2$ quencher, diazabicyclo [2.2.2] octane (DABCO) and iron chelator, deferoxamine (desferal) known to prevent HO$^•$ formation. The formation of $^1O_2$ and HO$^•$ in Arabidopsis leaves exposed to high white light was validated by confocal laser scanning microscopy using SOSG and HPF fluorescent probes, respectively. Negligible fluorescence was observed in non-illuminated leaves (**Figures 2Ab,Bb**), whereas illumination with continuous high red light for 30 min resulted in the formation of SOSG-EP and HPF-ox fluorescence (**Figures 2Ae,Be**). These results indicate that

FIGURE 1 | Detection of singlet oxygen **(A)** and hydroxyl radical **(B)** in Arabidopsis thylakoid membranes by electron paramagnetic resonance spectroscopy. **(A)** Thylakoid membranes (50 μg Chl ml^{-1}) in 50 mM TMPD were kept in the dark (0 min) and illuminated with high white light (1500 μmol photons m^{-2} s^{-1}, 30 min) in the absence and presence of 25 mM DABCO. **(B)** Thylakoid membranes (100 μg Chl ml^{-1}) in 50 mM POBN containing 170 mM ethanol were kept in the dark (0 min); high white light (1500 μmol photons m^{-2} s^{-1}, 30 min) in the absence and presence of 5 mM desferal. The lower panels show the mean value and standard deviation of EPR signal intensity ($n = 3$).

exposure of Arabidopsis to high light results in the formation of $^1O_2$ and HO$^•$.

Imaging of Protein Radicals by Confocal Laser Scanning Microscopy

Imaging of protein radicals in Arabidopsis was performed by confocal laser scanning microscopy using the immuno-spin trapping technique. **Figures 3A,B** show imaging of protein radicals in Arabidopsis leaves previously exposed to high white light at low temperature (1500 μmol photons m^{-2} s^{-1}, 13 h, 8°C) and chloroplasts isolated from high light exposed Arabidopsis leaves, respectively. In immuno-spin trapping technique, short-lived protein radicals ($t_{1/2} \sim$ μs) are trapped by spin trap DMPO to form a more stable DMPO-protein radical adduct ($t_{1/2} \sim$ min). The DMPO-protein radical adduct is reduced to diamagnetic DMPO nitrone adduct in the reducing environment which is detected by anti-DMPO antibody conjugated with FITC and imaged by confocal laser scanning microscopy. FITC fluorescence was measured in Arabidopsis leaves and chloroplasts treated with DMPO spin trap and anti-DMPO antibody conjugated with FITC either in the dark or high red light (**Figure 3**). **Figure 3** shows the FITC fluorescence channel (left panel) and the combination of FITC fluorescence and Nomarski DIC channels (right panel). Arabidopsis leaves and chloroplasts treated in dark showed low FITC fluorescence, whereas leaves and chloroplasts exposed to high red light showed a significant increase in FITC fluorescence due to the formation of protein radicals under high red light. It is noticeable that protein

radicals are formed in chloroplasts located at the periphery of mesophyll cells.

Separation of PSII Proteins by SDS-PAGE

Separation of PSII proteins was performed using SDS-PAGE of thylakoid membranes isolated from high light exposed Arabidopsis leaves and visualization of protein bands was achieved by CBB staining (**Figure 4A**). According to band size based on the use of a standard protein ladder, it was found that protein bands appeared at 9 kDa (α-subunit of cyt b_{559}), 13 kDa (α- and β-subunit heterodimer of cyt b_{559}), 23 kDa (Lhcb), 30–32 kDa (D1/D2), 33 kDa (PsbO), 43 kDa (CP43) and 47 kDa (CP47). Apart from these bands, low-molecular weight bands at 18 kDa and high-molecular weight bands at 41, 58, and 68 kDa were observed. The protein band at 18 kDa is assigned to fragments formed by the cleavage of PSII proteins, whereas the protein bands at 41 and 68 kDa represent aggregates formed by the cross-linking of PSII proteins. The protein band at 58 kDa might be assigned to ATPase and/or PsaA. The band density increased after exposure of the thylakoid membranes to high red light for 10 min and subsequently decreased. These results reveal the formation of protein fragments and aggregates after exposure of Arabidopsis plant to high light and degradation of proteins, their fragments and aggregates due to continuous oxidation.

Formation of Protein Radical Detected by Immuno-Spin Trapping

To explore the formation of protein radicals on the PSII proteins, immunoblot analysis of the thylakoid membranes

FIGURE 2 | Imaging of singlet oxygen **(A)** and hydroxyl radical **(B)** in Arabidopsis leaves monitored by laser confocal scanning microscopy. **(A)** Singlet oxygen imaging was achieved by infiltration with 50 μM SOSG in dark (upper panel) or exposed to high red light (1000 μmol photons m^{-2} s^{-1}) (lower panel) for 30 min. From left to right is chlorophyll fluorescence channel **(a,d)**; SOSG-EP fluorescence channel **(b,e)** and combination of 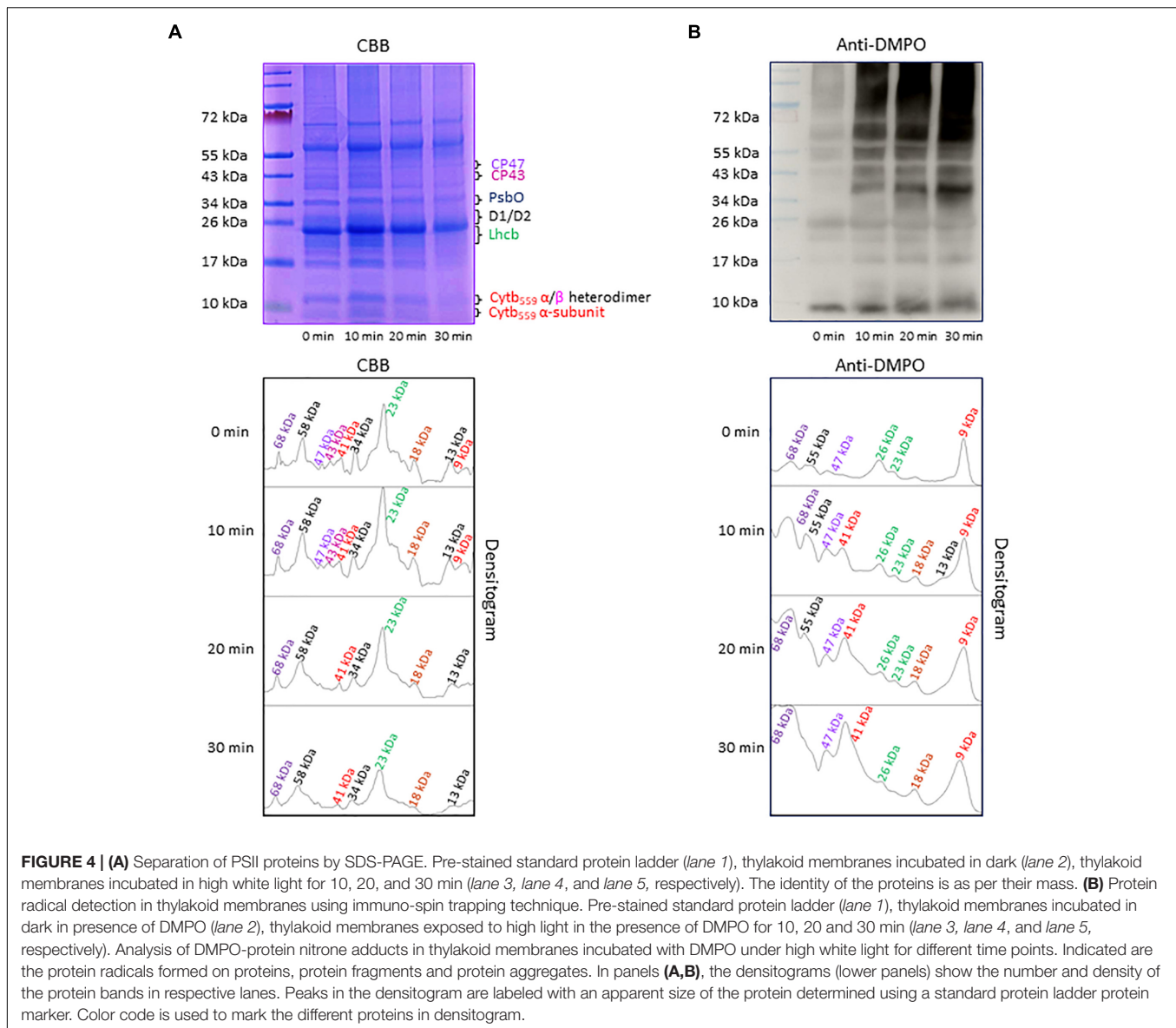chlorophyll fluorescence + SOSG-EP fluorescence channel **(c,f)**. **(B)** Hydroxyl radical imaging was achieved by infiltration with 5 μM HPF in dark (upper panel) or exposed to high red light (lower panel) for 30 min. From left to right is chlorophyll fluorescence channel **(a,d)**; HPF-ox fluorescence channel **(b,e)** and combination of chlorophyll fluorescence + HPF-ox fluorescence channel **(c,f)**.

FIGURE 3 | Protein radical imaging in Arabidopsis leaves **(A)** and chloroplasts **(B)** monitored by laser confocal scanning microscopy. From left to right: FITC fluorescence channel, the combination of FITC fluorescence and Nomarski DIC channels are shown. Prior to FITC fluorescence measurement, Arabidopsis leaves and chloroplasts were kept in the dark or illuminated with red light (1000 μmol photons m^{-2} s^{-1}) for 30 min in the presence of 50 mM DMPO and 5 μg ml^{-1} anti-DMPO nitrone adduct antibody conjugated with FITC.

isolated from high white light exposed plants was accomplished (**Figure 4B**). DMPO protein nitrone adducts formed on different proteins separated by SDS-PAGE were transferred to the NC membrane, identified by anti-DMPO nitrone adduct antibody and visualized by luminol as a chemiluminescent probe using HRP conjugated secondary antibody. In dark, weak protein bands at 9, 23, 26, 47, 55, and 68 kDa were observed which can be due to binding of DMPO to some proteins other than protein radicals as reported recently (Munoz et al., 2019). After exposure to high white light, the intensity of 9, 47, 55, and 68 kDa protein bands increased and two new protein bands appeared at 18 and 41 kDa. Quantification of protein bands in each lane of the blot by densitogram showed four times increase in 41 and 68 kDa protein band density and two times increase in 18 kDa protein band density. These results
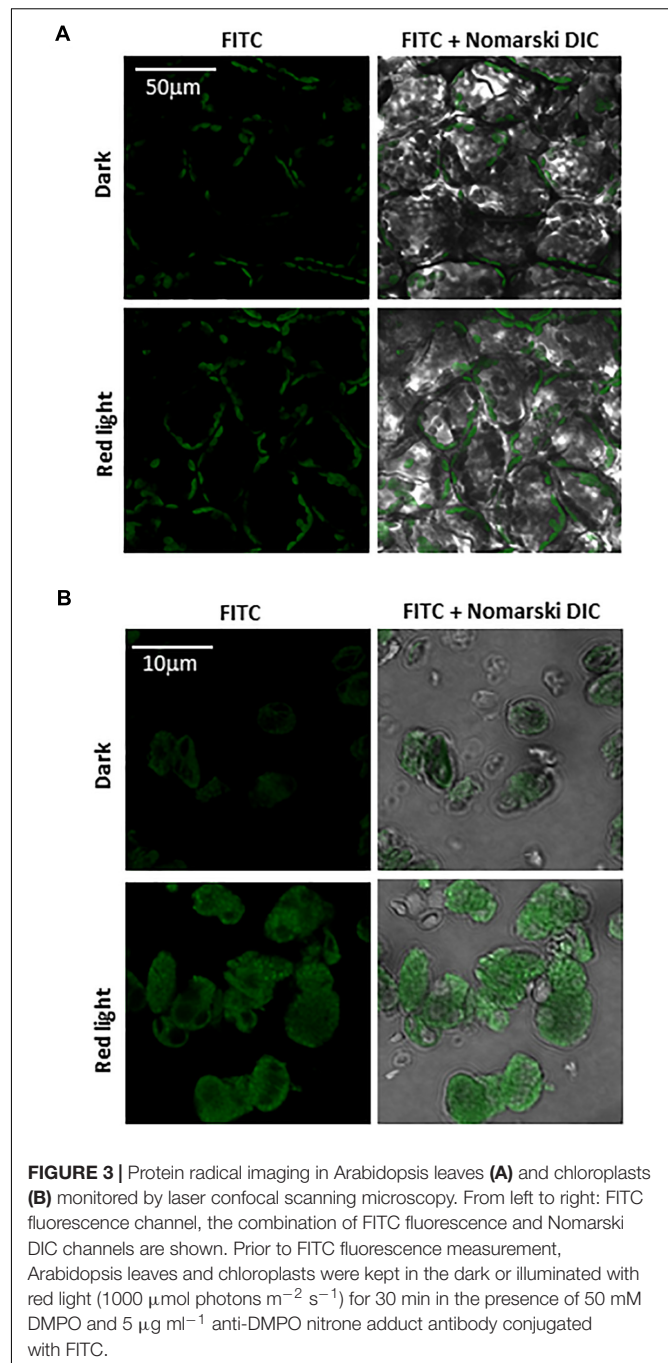
reveal the formation of protein radicals on protein aggregates and fragments.
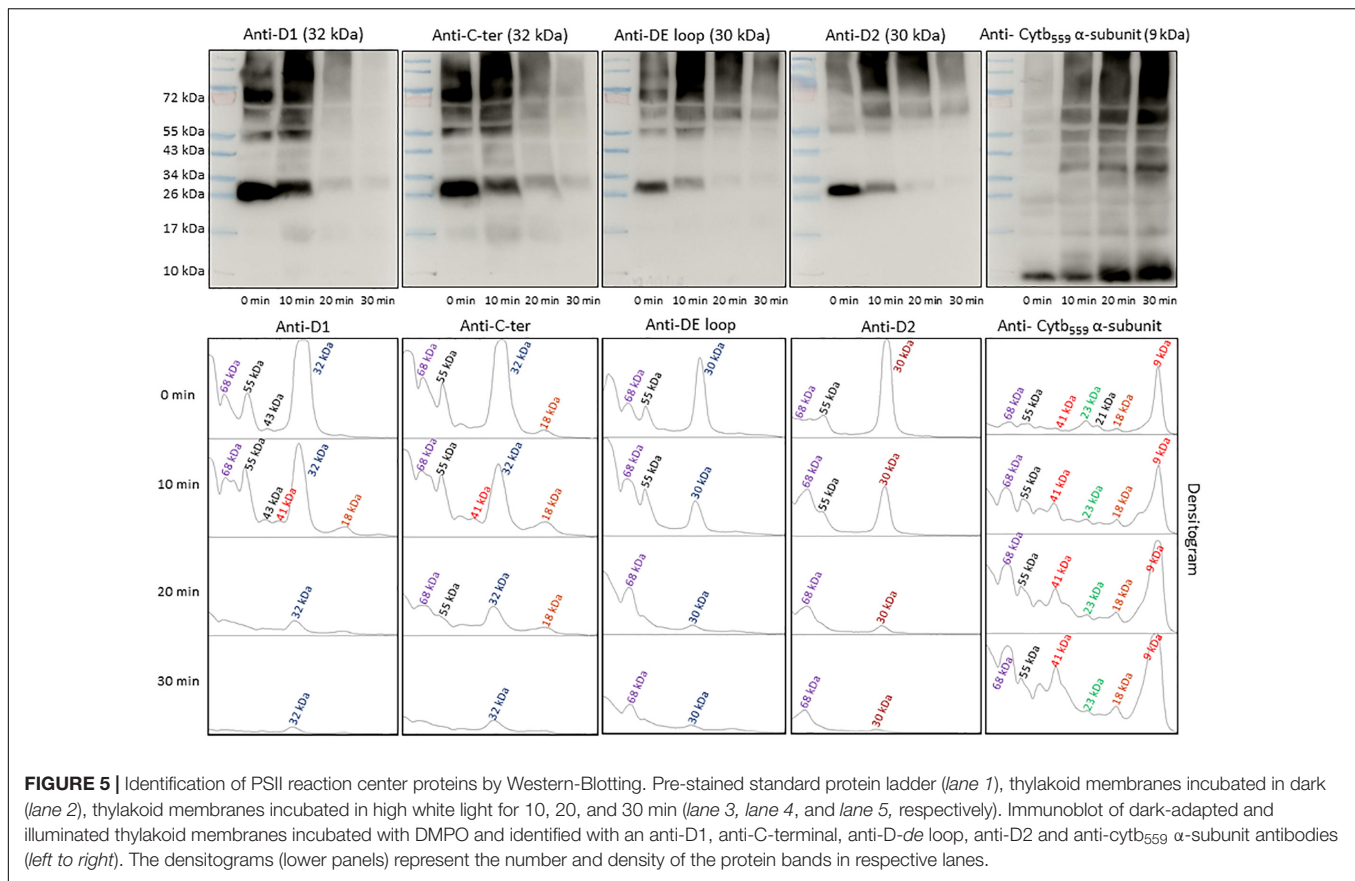
Characterization of PSII Reaction Center Proteins by Western-Blotting

To identify the origin of protein bands in anti-DMPO blot, the NC membranes were probed with different PSII protein antibodies (**Figure 5**). To detect the protein bands originated from the D1, D2 and α-subunit of cyt b_{559} protein, antibodies raised against the D1 protein (anti-D1 antibody), the C-terminal

FIGURE 4 | (A) Separation of PSII proteins by SDS-PAGE. Pre-stained standard protein ladder (*lane 1*), thylakoid membranes incubated in dark (*lane 2*), thylakoid membranes incubated in high white light for 10, 20, and 30 min (*lane 3, lane 4,* and *lane 5,* respectively). The identity of the proteins is as per their mass. **(B)** Protein radical detection in thylakoid membranes using immuno-spin trapping technique. Pre-stained standard protein ladder (*lane 1*), thylakoid membranes incubated in dark in presence of DMPO (*lane 2*), thylakoid membranes exposed to high light in the presence of DMPO for 10, 20 and 30 min (*lane 3, lane 4,* and *lane 5,* respectively). Analysis of DMPO-protein nitrone adducts in thylakoid membranes incubated with DMPO under high white light for different time points. Indicated are the protein radicals formed on proteins, protein fragments and protein aggregates. In panels **(A,B)**, the densitograms (lower panels) show the number and density of the protein bands in respective lanes. Peaks in the densitogram are labeled with an apparent size of the protein determined using a standard protein ladder protein marker. Color code is used to mark the different proteins in densitogram.

of the D1 protein (anti-C-terminal antibody), the D-*de* loop of the D1 protein (anti-D-*de* loop antibody), the D2 protein (anti-D2 antibody) and the α-subunit of cyt b_{559} protein (anti-cyt b_{559} α-subunit antibody) were used. When the blot was probed with an anti-D1 antibody, anti-C-terminal antibody, anti-D-*de* loop antibody and anti-D2 antibody, protein bands with an apparent molecular weight of 32 and 30 kDa were detected. In addition, one protein band below 32 kDa D1 protein band with apparent molecular weight of 18 kDa and two protein bands above 32 kDa D1 protein band with apparent molecular weights of 55 and 68 kDa were observed. When the blot was probed with an anti-cyt b_{559} α-subunit antibody, 9 and 41 kDa protein bands were observed. After exposure to high red light, a significant decrease in the protein band densities of D1 and D2 proteins was observed. Interestingly, the band densities of 9 and 41 kDa proteins

increased under high red light. Quantification of protein bands in each lane of anti-D1 antibody, anti-C-terminal antibody, anti-D-*de* loop antibody, anti-D2 antibody and anti-cyt b_{559} α-subunit antibody blot by densitograms reveals a several fold decrease in D1, C-terminal, D-*de* loop and D2 protein band density and three times increase in α-subunit of cyt b_{559} protein band density. Comparison of these blots with anti-DMPO blot of the same samples performed in parallel suggests the contribution of D1, C-terminal, D-*de* loop, D2 and α-subunit of cyt b_{559} proteins in 55 and 68 kDa aggregate formation, and contribution of D1, C-terminal and α-subunit of cyt b_{559} protein in 41 and 18 kDa aggregate formation. These results provide clear evidence on the involvement of D1, C-terminal, D-*de*-loop and α-subunit of cyt b_{559} proteins in the aggregation and protein radical formation on the aggregates.
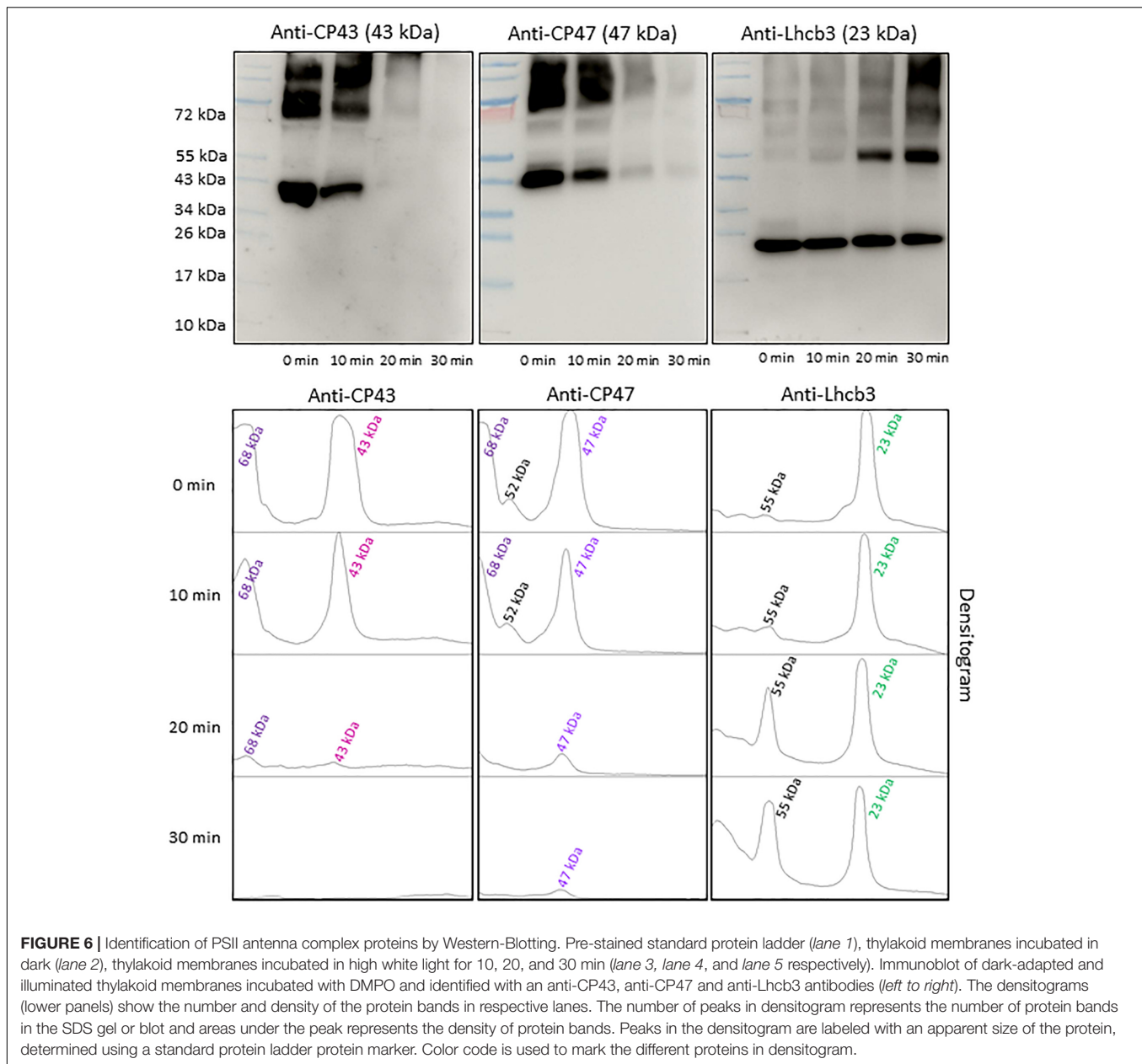
FIGURE 5 | Identification of PSII reaction center proteins by Western-Blotting. Pre-stained standard protein ladder (*lane 1*), thylakoid membranes incubated in dark (*lane 2*), thylakoid membranes incubated in high white light for 10, 20, and 30 min (*lane 3, lane 4,* and *lane 5,* respectively). Immunoblot of dark-adapted and illuminated thylakoid membranes incubated with DMPO and identified with an anti-D1, anti-C-terminal, anti-D-*de* loop, anti-D2 and anti-cytb$_{559}$ α-subunit antibodies (*left to right*). The densitograms (lower panels) represent the number and density of the protein bands in respective lanes.

Characterization of PSII Antenna Complex Protein Radicals by Western-Blotting

To find the contribution of PSII antenna complex proteins in anti-DMPO blot, the NC membranes were probed with different PSII antenna complex protein antibodies (**Figure 6**). To detect the protein bands originated from CP43 and CP47 PSII antenna proteins, the blots were probed with anti-CP43 and anti-CP47 antibodies raised against the CP43 and CP47 proteins, respectively. One prominent protein band with an apparent molecular weight of 43 kDa (CP43 protein band) and one prominent protein band with an apparent molecular weight of 68 kDa was detected when the blot was probed with the anti-CP43 antibody. When anti-CP47 antibody was used, a band with an apparent molecular weight of 47 kDa (CP47 protein band) and two weak intensity protein bands with an apparent molecular weight of 52 and 68 kDa above 47 kDa were detected. Probing of the blot with an anti-Lhcb3 antibody raised against Lhcb3 protein showed one protein band with an apparent molecular weight of 23 kDa (Lhcb3 protein band) and one with an apparent molecular weight of 55 kDa. After exposure to high red light, a significant decrease in the protein band densities of CP43 and CP47 proteins was observed. Interestingly, the band density of 23 kDa protein had a small decrease, whereas the band density of 55 kDa protein band significantly increased under high red light. Quantification of protein bands in each lane of blots probed with

anti-CP43, anti-CP47 and anti-Lhcb3 antibodies by densitogram showed almost complete loss of CP43 and CP47 protein band and less than half decrease in Lhcb3 protein band density. The decrease in Lhcb3 protein band density was accompanied by several folds increase in the 55 kDa protein band density. Based on the comparison of these blots with anti-DMPO blot of the same samples performed in parallel, it was concluded that protein radicals are formed on the aggregates involving CP43, CP47 and Lhcb3 proteins. These results provide clear evidence that similarly to PSII reaction center proteins, PSII antenna complex proteins are also involved in aggregation and radical formation on the aggregates.

DISCUSSION

Under the natural environment, plants are exposed to high light associated with the formation of ROS known to cause oxidative damage to biomolecules (**Figures 1**, **2**). Proteins cover approximately 68% of the dry weight of cells and tissues and are therefore potentially the major targets for oxidative damage. Using the immuno-spin trapping technique, we presented here that exposure of Arabidopsis leaf and chloroplasts to high light results in the formation of protein radicals in leaf and chloroplasts (**Figures 3A,B**). In this study, we provided a characterization of protein radicals in the thylakoid membranes exposed to high light. Our results show the formation of protein

FIGURE 6 | Identification of PSII antenna complex proteins by Western-Blotting. Pre-stained standard protein ladder (*lane 1*), thylakoid membranes incubated in dark (*lane 2*), thylakoid membranes incubated in high white light for 10, 20, and 30 min (*lane 3, lane 4,* and *lane 5* respectively). Immunoblot of dark-adapted and illuminated thylakoid membranes incubated with DMPO and identified with an anti-CP43, anti-CP47 and anti-Lhcb3 antibodies (*left to right*). The densitograms (lower panels) show the number and density of the protein bands in respective lanes. The number of peaks in densitogram represents the number of protein bands in the SDS gel or blot and areas under the peak represents the density of protein bands. Peaks in the densitogram are labeled with an apparent size of the protein, determined using a standard protein ladder protein marker. Color code is used to mark the different proteins in densitogram.

radicals on two fragments at approximately 18 and 23 kDa and three aggregates at approximately 41, 55 and 68 kDa (**Figure 5**). Protein cleavage occurs via β-scission of protein alkoxyl radical known to form carbon-centered radical on the C-terminal and N-terminal fragments. Our results show that the 18 kDa protein band might represent aggregate which arises from two 9 kDa fragments of the C-terminus of D1 protein, two α-subunits of cyt b_{559} protein or C-terminus of the D1 and α-subunit of cyt b_{559} protein. In agreement with this, it was shown that 18 kDa protein may arise from the C-terminus of the D1 protein (Kale et al., 2017). The 18 kDa protein band might arise from the degradation of D1 protein which may be due to the cleavage in the lumenal loop joining helices C and D (Aro et al., 1990; Shipton and Barber, 1991;

Barbato et al., 1992b). The cross-linking of a protein radical with another protein radical results in the formation of protein aggregate. Based on the observation that 41 kDa band was observed when blot was probed with anti-D1 antibody and anti-cyt b_{559} α-subunit antibody, it is very likely that protein radical is formed on an aggregate of the D1 protein and the α-subunit of cyt b_{559} (Barbato et al., 1992a, 1995; Yamamoto, 2001; Lupínková and Komenda, 2004; Yamamoto et al., 2008). The observation that 55 kDa band appeared when blot was probed with anti-D1, anti- C-terminal, anti-D-*de* loop and anti-Lhcb3 antibodies suggests that protein radical is formed on: (i) the aggregates of 23 kDa fragment of D1 protein and D1 protein, (ii) the aggregates of three 18 kDa fragments of D1 protein, (iii) the aggregates of Lhcb3 protein and C-terminal of D1 protein, (iv) the aggregates

of two Lhcb3 proteins. It has been recently reported that light-driven trimer to monomer transition is associated with the appearance of LHCII dimers (Janik et al., 2013, 2017). Similarly, the finding that 68 kDa band was observed when the blot was probed using anti-D1, anti-D2 and anti-CP43 antibodies, reveals that protein radical is formed either on D1/D2 or 23 kDa fragment D1/CP43 protein aggregates as reported in the previous reports (Ishikawa et al., 1999; Henmi et al., 2003). The appearance of 68 kDa band when the blot was probed using an anti-cyt b_{559} α-subunit, anti-D-de loop and anti-D2 antibodies suggests the formation of an aggregate of these peptides. Our results are in agreement with published literature in past, that under high light illumination the D1 protein cross-links covalently or aggregates non-covalently with the nearby polypeptides in PS II complexes (Aro et al., 1993; Barber, 1998; Komenda et al., 2006; Edelman and Mattoo, 2008; Yamamoto et al., 2008).

CONCLUSION

In conclusion, we used the immuno-spin trapping technique to visualize the formation of protein radicals in plant cells by using laser confocal scanning microscopy and characterized the PSII protein oxidized during high light illumination. Formation of protein radicals leads to formation of protein fragments and aggregates and subsequently to formation of protein radicals on these fragments and aggregates. The use of immuno-spin trapping opens new opportunities to study the role of protein radicals in the overall understanding of plant behavior for its survival during the oxidative stress.

DATA AVAILABILITY

All datasets generated for this study are included in the manuscript and/or the **Supplementary Files**.

AUTHOR CONTRIBUTIONS

PP and AK contributed to the conception and design of the work and drafted the manuscript. AK measured and analyzed the data on immunoblots. AP and MS performed the confocal measurements. AK, AP, and PP performed the data interpretation. All authors approved the final version of the manuscript.

FUNDING

SUPPLEMENTARY MATERIAL

The Supplementary Material for this article can be found online at: https://www.frontiersin.org/articles/10.3389/fphys.2019.00958/full#supplementary-material

REFERENCES

Aro, E. M., Hundal, T., Carlberg, I., and Andersson, B. (1990). Invitro studies on light-induced inhibition of photosystem-ii and d1-protein degradation at low-temperatures. *Biochimica Et Biophysica Acta* 1019, 269–275. doi: 10.1016/0005-2728(90)90204-h

Aro, E. M., Virgin, I., and Andersson, B. (1993). Photoinhibition of Photosystem Iinactivation, I., protein damage and turnover. *Biochim. Biophys. Acta.* 1143, 113–134. doi: 10.1016/0005-2728(93)90134-2

Barbato, R., Friso, G., Ponticos, M., and Barber, J. (1995). Characterization of the light-induced cross-linking of the α-subunit of cytochrome b_{559} and the D1 protein in isolated photosystem-ii reaction centers. *J. Biol. Chem.* 270, 24032–24037. doi: 10.1074/jbc.270.41.24032

Barbato, R., Frizzo, A., Friso, G., Rigoni, F., and Giacometti, G. M. (1992a). Photoinduced degradation of the d1 protein in isolated thylakoids and various photosystem-ii particles after donor-site inactivations - detection of a C-terminal 16 Kda fragment. *FEBS Lett.* 304, 136–140. doi: 10.1016/0014-5793(92)80604-f

Barbato, R., Friso, G., Rigoni, F., Frizzo, A., and Giacometti, G. M. (1992b). Characterization of a 41 kDa photoinhibition adduct in isolated photosystem II reaction centres. *FEBS Lett.* 309, 165–169. doi: 10.1016/0014-5793(92)81087-3

Barber, J. (1998). Photosystem two. *Biochim. Biophys. Acta.* 1365, 269–277.

Brunelle, J. L., and Green, R. (2014). Chapter thirteen - coomassie blue staining. *Methods Enzymol.* 541, 161–167.

Casazza, A. P., Tarantino, D., and Soave, C. (2001). Preparation and functional characterization of thylakoids from *Arabidopsis thaliana*. *Photosynth. Res.* 68, 175–180.

Choudhury, F. K., Rivero, R. M., Blumwald, E., and Mittler, R. (2017). Reactive oxygen species, abiotic stress and stress combination. *Plant J.* 90, 856–867. doi: 10.1111/tpj.13299

Davies, M. J. (2016). Protein oxidation and peroxidation. *Biochem. J.* 473, 805–825. doi: 10.1042/bj20151227

Dietz, K. J., Turkan, I., and Krieger-Liszkay, A. (2016). Redox- and reactive oxygen species-dependent signaling into and out of the photosynthesizing chloroplast. *Plant Physiol.* 171, 1541–1550. doi: 10.1104/pp.16.00375

Edelman, M., and Mattoo, A. K. (2008). D1-protein dynamics in photosystem II: the lingering enigma. *Photosynth. Res.* 98, 609–620. doi: 10.1007/s11120-008-9342-x

Fischer, B. B., Hideg, E., and Krieger-Liszkay, A. (2013). Production, detection, and signaling of singlet oxygen in photosynthetic organisms. *Anti. Redox Signal* 18, 2145–2162. doi: 10.1089/ars.2012.5124

Frankel, L. K., Sallans, L., Limbach, P. A., and Bricker, T. M. (2012). Identification of oxidized amino acid residues in the vicinity of the Mn4CaO5 cluster of photosystem II: implications for the identification of oxygen channels within the photosystem. *Biochemistry* 51, 6371–6377. doi: 10.1021/bi300650n

Frankel, L. K., Sallans, L., Limbach, P. A., and Bricker, T. M. (2013). Oxidized amino acid residues in the vicinity of Q(A) and Pheo(D1) of the photosystem II reaction center: putative generation sites of reducing-side reactive oxygen species. *Plos One* 8:7. doi: 10.1371/journal.pone.0058042

Gomez-Mejiba, S. E., Zhai, Z. L., Della-Vedova, M. C., Munoz, M. D., Chatterjee, S., Towner, R. A., et al. (2014). Immuno-spin trapping from biochemistry to medicine: advances, challenges, and pitfalls. Focus on protein-centered radicals. *Biochim. Biophys. Acta Gen. Subj.* 1840, 722–729. doi: 10.1016/j.bbagen.2013.04.039

Henmi, T., Yamasaki, H., Sakuma, S., Tomokawa, Y., Tamura, N., and Shen, J. R. (2003). Dynamic interaction between the D1 protein, CP43 and OEC33 at the lumenal side of photosystem II in spinach chloroplasts: evidence from light-induced cross-linking of the proteins in the donor-side photoinhibition. *Plant Cell Physiol.* 44, 451–456. doi: 10.1093/pcp/pcg049

Ishikawa, Y., Nakatani, E., Henmi, T., Ferjani, A., Harada, Y., Tamura, N., et al. (1999). Turnover of the aggregates and cross-linked products of the D1 protein generated by acceptor-side photoinhibition of photosystem II. *Biochim. Biophys. Acta.* 1413, 147–158. doi: 10.1016/s0005-2728(99)00093-6

Janik, E., Bednarska, J., Sowinski, K., Luchowski, R., Zubik, M., and Grudzinski, W. (2017). Light-induced formation of dimeric LHCII. *Photosynth Res.* 132, 265–276. doi: 10.1007/s11120-017-0387-6

Janik, E., Bednarska, J., Zubik, M., Puzio, M., Luchowski, R., Grudzinski, W., et al. (2013). Molecular architecture of plant thylakoids under physiological and light stress conditions: a study of lipid-light-harvesting complex II model membranes. *Plant Cell* 25, 2155–2170. doi: 10.1105/tpc.113.113076

Kale, R., Hebert, A. E., Frankel, L. K., Sallans, L., Bricker, T. M., and Pospíšil, P. (2017). Amino acid oxidation of the D1 and D2 proteins by oxygen radicals during photoinhibition of Photosystem II. *Proc. Natl. Acad. Sci. U. S. A.* 114, 2988–2993. doi: 10.1073/pnas.1618922114

Komenda, J., Kuviková, S., Lupínková, L., and Masojídek, J. (2006). *Biogenesis and Structural Dynamics of the Photosystem II Complex.* Berlin: Springer.

Kumar, A., Prasad, A., Sedlářová, M., and Pospíšil, P. (2018). Data on detection of singlet oxygen, hydroxyl radical and organic radical in Arabidopsis thaliana. *Data Brief* 21, 2246–2252. doi: 10.1016/j.dib.2018.11.033

Kumar, A., Prasad, A., Sedlářová, M., and Pospíšil, P. (2019). Organic radical imaging in plants: focus on protein radicals. *Free Radic. Biol. Med.* 130, 568–575. doi: 10.1016/j.freeradbiomed.2018.10.428

Laloi, C., and Havaux, M. (2015). Key players of singlet oxygen-induced cell death in plants. *Front. Plant Sci.* 6:39. doi: 10.3389/fpls.2015.00039

Lupínková, L., and Komenda, J. (2004). Oxidative modifications of the photosystem II D1 protein by reactive oxygen species: from isolated protein to cyanobacterial cells. *Photochem. Photobiol.* 79, 152–162. doi: 10.1111/j.1751-1097.2004.tb00005.x

Mason, R. P. (2016). Imaging free radicals in organelles, cells, tissue, and in vivo with immuno-spin trapping. *Redox. Biol.* 8, 422–429. doi: 10.1016/j.redox.2016.04.003

Mattila, H., Khorobrykh, S., Havurinne, V., and Tyystjarvi, E. (2015). Reactive oxygen species: reactions and detection from photosynthetic tissues. *J. photochem. Photobiol. B Biol.* 152(Pt B), 176–214. doi: 10.1016/j.jphotobiol.2015.10.001

Mittler, R. (2017). ROS are good. *Trends Plant Sci.* 22, 11–19. doi: 10.1016/j.tplants.2016.08.002

Moan, J., and Wold, E. (1979). Detection of singlet oxygen production by ESR. *Nature* 279, 450–451. doi: 10.1038/279450a0

Munoz, M. D., Gutierrez, L. J., Delignat, S., Russick, J., Mejiba, S. E. G., Lacroix-Desmazes, S., et al. (2019). The nitrone spin trap 5,5-dimethyl-1-pyrroline N -oxide binds to toll -like receptor-2-TIR-BB-loop domain and dampens downstream inflammatory signaling. *Biochimica Et Biophysica Acta Molecular Basis of Disease* 1865, 1152–1159. doi: 10.1016/j.bbadis.2019.01.005

Murata, N., Takahashi, S., Nishiyama, Y., and Allakhverdiev, S. I. (2007). Photoinhibition of photosystem II under environmental stress. *Biochim. Biophys. Acta.* 1767, 414–421. doi: 10.1016/j.bbabio.2006.11.019

Pospíšil, P. (2012). Molecular mechanisms of production and scavenging of reactive oxygen species by photosystem II. *Biochim. Biophys. Acta.* 1817, 218–231. doi: 10.1016/j.bbabio.2011.05.017

Pospíšil, P. (2014). The role of metals in production and scavenging of reactive oxygen species in photosystem II. *Plant Cell Physiol.* 55, 1224–1232. doi: 10.1093/pcp/pcu053

Pou, S., Ramos, C. L., Gladwell, T., Renks, E., Centra, M., Young, D., et al. (1994). A kinetic approach to the selection of a sensitive spin trapping system for the detection of hydroxyl radical. *Anal. Biochem.* 217, 76–83. doi: 10.1006/abio.1994.1085

Prasad, A., Sedlářová, M., and Pospíšil, P. (2018). Singlet oxygen imaging using fluorescent probe singlet oxygen sensor green in photosynthetic organisms. *Sci. Rep.* 8:13685. doi: 10.1038/s41598-018-31638-5

Schagger, H. (2006). Tricine-SDS-PAGE. *Nat. Protoc.* 1, 16–22. doi: 10.1038/nprot.2006.4

Schmitt, F. J., Renger, G., Friedrich, T., Kreslavski, V. D., Zharmukhamedov, S. K., Los, D. A., et al. (2014). Reactive oxygen species: re-evaluation of generation, monitoring and role in stress-signaling in phototrophic organisms. *Biochim. Biophys. Acta.* 1837, 835–848. doi: 10.1016/j.bbabio.2014.02.005

Seigneurin-Berny, D., Salvi, D., Joyard, J., and Rolland, N. (2008). Purification of intact chloroplasts from Arabidopsis and spinach leaves by isopycnic centrifugation. *Curr. Protocol. Cell Biol.* 40, 3.30.1–3.30.14. doi: 10.1002/0471143030.cb0330s40

Shipton, C. A., and Barber, J. (1991). Photoinduced degradation of the D1 polypeptide in isolated reaction centers of photosystem II: evidence for an autoproteolytic process triggered by the oxidizing side of the photosystem. *Proc. Natl. Acad. Sci. U. S. A.* 88, 6691–6695. doi: 10.1073/pnas.88.15.6691

Telfer, A. (2014). Singlet oxygen production by PSII under light stress: mechanism, detection and the protective role of beta-carotene. *Plant Cell Physiol.* 55, 1216–1223. doi: 10.1093/pcp/pcu040

Weisz, D. A., Gross, M. L., and Pakrasi, H. B. (2017). Reactive oxygen species leave a damage trail that reveals water channels in photosystem II. *Sci. Adv.* 3:eaao3013. doi: 10.1126/sciadv.aao3013

Yamamoto, Y. (2001). Quality control of photosystem II. *Plant Cell Physiol.* 42, 121–128. doi: 10.1093/pcp/pce022

Yamamoto, Y., Aminaka, R., Yoshioka, M., Khatoon, M., Komayama, K., Takenaka, D., et al. (2008). Quality control of photosystem II: impact of light and heat stresses. *Photosynth Res.* 98, 589–608. doi: 10.1007/s11120-008-9372-4

Detection of hydrogen peroxide in Photosystem II (PSII) using catalytic amperometric biosensor

Ankush Prasad[1]*, Aditya Kumar[2], Makoto Suzuki[3], Hiroyuki Kikuchi[3], Tomoya Sugai[3], Masaki Kobayashi[1,4], Pavel Pospíšil[2], Mika Tada[1,5] and Shigenobu Kasai[1,3†]

[1] Biomedical Engineering Research Center, Tohoku Institute of Technology, Sendai, Japan, [2] Department of Biophysics, Faculty of Science, Centre of the Region Haná for Biotechnological and Agricultural Research, Palacký University, Olomouc, Czech Republic, [3] Graduate Department of Environmental Information Engineering, Tohoku Institute of Technology, Sendai, Japan, [4] Graduate Department of Electronics, Tohoku Institute of Technology, Sendai, Japan, [5] Center for General Education, Tohoku Institute of Technology, Sendai, Japan

Hydrogen peroxide (H_2O_2) is known to be generated in Photosystem II (PSII) via enzymatic and non-enzymatic pathways. Detection of H_2O_2 by different spectroscopic techniques has been explored, however its sensitive detection has always been a challenge in photosynthetic research. During the recent past, fluorescence probes such as Amplex Red (AR) has been used but is known to either lack specificity or limitation with respect to the minimum detection limit of H_2O_2. We have employed an electrochemical biosensor for real time monitoring of H_2O_2 generation at the level of sub-cellular organelles. The electrochemical biosensor comprises of counter electrode and working electrodes. The counter electrode is a platinum plate, while the working electrode is a mediator based catalytic amperometric biosensor device developed by the coating of a carbon electrode with osmium-horseradish peroxidase which acts as H_2O_2 detection sensor. In the current study, generation and kinetic behavior of H_2O_2 in PSII membranes have been studied under light illumination. Electrochemical detection of H_2O_2 using the catalytic amperometric biosensor device is claimed to serve as a promising technique for detection of H_2O_2 in photosynthetic cells and subcellular structures including PSII or thylakoid membranes. It can also provide a precise information on qualitative determination of H_2O_2 and thus can be widely used in photosynthetic research.

Keywords: photosystem II, superoxide anion radical, hydrogen peroxide, reactive oxygen species, amperometric biosensor, EPR-spin trapping

INTRODUCTION

Photosystem II (PSII) is a multi-subunit pigment-protein complex which is located in the thylakoid membrane of chloroplasts of cyanobacteria, algae and higher plants that comprises of more than 25 proteins and the concomitant cofactors (Ferreira et al., 2004; Loll et al., 2005; Guskov et al., 2009; Kawakami et al., 2011). In plants, photosynthesis has been considered as a source of reactive oxygen species (ROS) production which works in close association with regulated mechanism of antioxidant network under normal conditions. The ROS in plants are known

to be involved in cell toxicity, defense and signaling, and have been recently overviewed (Krieger-Liszkay, 2005; Foyer and Shigeoka, 2011; Schmitt et al., 2014).

Chlorophyll pigments of the PSII antenna complex absorb light energy and use it for the oxidation of water molecules and reduction of plastoquinone. Light energy absorbed by chlorophyll pigments converted into the energy of separated charges and consequent water-plastoquinone oxidoreductase activity is involuntarily linked with the production of ROS (Pospíšil, 2009, 2012). In unison, released molecular oxygen serves as a forerunner of ROS, which at low concentration play an important role in cell regulation, whereas if formed in excess, is responsible for oxidation of biomolecules such as lipid, proteins, and nucleic acid (Halliwell and Gutteridge, 2007). In addition, direct oxidation of proteins and lipids by UV irradiation and toxic chemicals following subsequent chemical reactions are also known to be associated with formation of ROS (Halliwell and Gutteridge, 2007; Prasad and Pospíšil, 2012).

Production of ROS arises when excitation energy transfer to the PSII reaction center is inadequate or there is inhibition of electron transport chain in PSII. The redox couples in PSII covers a broad range of redox potential, it ranges from a very high negative value of redox couple, $Pheo/Pheo^-$ ($Em = -610\,mV$) to a very high positive value of redox couple $P680^+/P680$ ($Em = +1250\,mV$) (Rappaport and Diner, 2008; Pospíšil, 2012). PSII is capable of either oxidizing water molecule or reducing molecular oxygen on the electron donor and on the electron acceptor side of the membrane, respectively (Pospíšil, 2012). There is leakage of electrons to molecular oxygen during the electron transport on the electron acceptor side of PSII (Pospíšil, 2009).

Formation of $O_2^{\bullet-}$ results from non-enzymatic and enzymatic one-electron reductions of molecular oxygen. Pheophytin (Pheo$^{\bullet-}$) (Ananyev et al., 1994; Pospíšil et al., 2004), tightly bound plastosemiquinone ($Q_A^{\bullet-}$), (Cleland and Grace, 1999; Pospíšil et al., 2004), loosely bound plastosemiquinone ($Q_B^{\bullet-}$), (Zhang et al., 2003; Yadav et al., 2014), and free plastosemiquinone (PQ$^{\bullet-}$) (Mubarakshina and Ivanov, 2010) maintains non-enzymatic reduction of molecular oxygen to $O_2^{\bullet-}$. Heme iron of low-potential (LP) form of cyt b_{559} reduces molecular oxygen to $O_2^{\bullet-}$ in the enzymatic reaction pathway (Pospíšil et al., 2006; Pospišil, 2011).

One electron reduction of $O_2^{\bullet-}$ either via non-enzymatic or enzymatic reaction pathway results in the formation of H_2O_2. In spontaneous dismutation, $O_2^{\bullet-}$ provides an additional electron to another $O_2^{\bullet-}$, and then with protonation brings about the formation of H_2O_2. In enzymatic dismutation, the ferrous heme iron of HP form of cyt b_{559} drives the catalysis of one-electron reduction of $HO_2^{\bullet}$ to H_2O_2 (Tiwari and Pospíšil, 2009; Pospišil, 2011). Spontaneous dismutation is preferred where there is availability of protons e.g., at the membrane edge while PSII metal centers are chosen to catalyze the dismutation reaction in the interior of the membrane (Pospíšil, 2012). The one-electron reduction of $O_2^{\bullet-}$ to H_2O_2 is catalyzed by superoxide dismutase (SOD) and is known to occur predominantly in the mitochondria, peroxisomes, and cytoplasm. At the physiological pH, the dismutation reaction is preferably catalyzed by SOD.

Several spectroscopic techniques (fluorescence and chemiluminescence) and chromatographic techniques (high performance liquid chromatography coupled with peroxyoxalate chemiluminescence detection) have been used in the past for the determination of H_2O_2 in living cells (Mills et al., 2007; Chen et al., 2009; Ahammad, 2013). Light induced production of H_2O_2 have been measured in PSII membranes by oxidation of thiobenzamide with lactoperoxidase. Thiobenzamide sulfoxide was quantified by its absorbance at 370 nm (Schröder and Åkerlund, 1990; Arató et al., 2004; Pospíšil et al., 2004). Production of H_2O_2 by chloroplasts have been measured by the AmplexRed fluorescence assays (Mubarakshina and Ivanov, 2010; Yadav and Pospíšil, 2012). Hydrogen peroxide (H_2O_2) detecting probes, 3,3 diaminobenzidine (DAB), Amplex Red (AR), Amplex Ultra Red (AUR), and a europium-tetracycline complex (Eu3Tc) have been compared by infiltrating into tobacco leaves and tested for sensitivity to light, toxicity, subcellular localization, and capacity to detect H_2O_2 in vivo (Šnyrychová et al., 2009). The induction of H_2O_2 generation at the leaf level after 3-acetyl-4-hydroxyl-5-isopropylpyrroline-2-dione (3-AIPTA) or bentazon treatment has been detected by performing histochemical analysis with 3, 3 DAB staining (Chen et al., 2012). Apart from several spectroscopic techniques (absorbance, fluorescence, chemiluminescence), cyclic voltammetry and histochemical technique, a reporter system based on HSP70A promoter-luciferase fusions have also been developed in past for the detection of H_2O_2 in vivo (Shao et al., 2007).

In the electrochemical method, mediator and non-mediator based electrode have been used in the past. Among the mediator based modified electrodes, HRP is the most commonly used material for the modification of the electrode in the last decade (Lin et al., 2000; Camacho et al., 2007; Radi et al., 2009; Ahammad, 2013). The sensitivity and selectivity of H_2O_2 biosensor depends on the material used and modifications involved (Lin et al., 2000; Nakabayashi and Yoshikawa, 2000; Yao et al., 2005; Wang and Zhang, 2006; Camacho et al., 2007; Radi et al., 2009; Inoue et al., 2010; Li et al., 2013). The mechanism of detection of H_2O_2 biosensor is described in **Scheme 1**. The enzyme HRP is converted to its oxidized form, which is than reduced at the surface of the carbon electrode by the transfer of the electron via the mediator. Different mediators have been used in the past including methylene blue (Lin et al., 2000; Kafi et al., 2009; Tiwari and Singh, 2011); quinones predominantly hydroquinones (Lei et al., 2004, 2005; Zhang et al., 2008; Yang et al., 2010); ferrocene (Wang et al., 2005; Senel et al., 2010), and ferrocene carboxylic acid (Tian et al., 2001; Tripathi et al., 2006; Liu et al., 2011; Luo et al., 2011). The detection limit in utmost cases were found to be in the concentration range of units of millimolar or micromolar (μM) while a limited reports showed detection limit in tens of nanomolar (nM) concentration (Zhang et al., 2008; Loew et al., 2009; Lu et al., 2010). Recently, Os-HRP was compared with native HRP based coated glassy carbon electrode and it was found to possess high sensitivity for hydroperoxide. The electrodes were tested for H_2O_2 and hydroperoxide in the concentration range of 0.01–1 μM (Loew et al., 2009).
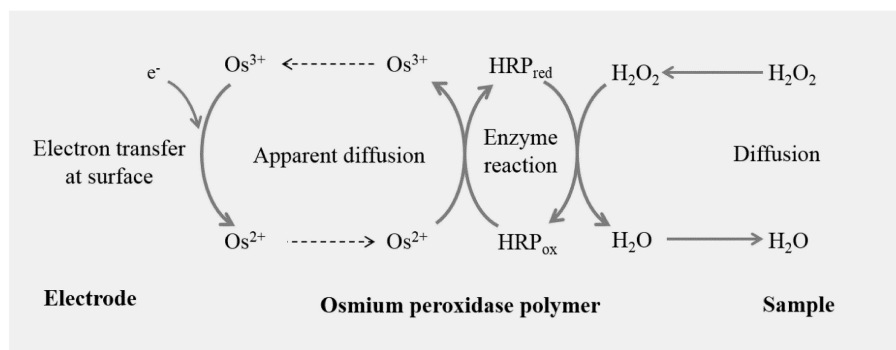
SCHEME 1 | Working principle of catalytic amperometric biosensor device: schematic illustration shows the working principle of Osmium-horseradish peroxidase (Os-HRP) modified carbon electrode depicting the oxidation-reduction cycle leading to generation of reduction current for H_2O_2.

Non-mediator based H_2O_2 biosensor has also been widely used in the past; however, it is known that the electron transfer between HRP and the electrode is difficult due to higher distance between the active site of HRP and the electrode. The voltammetric detection of H_2O_2 at carbon electrodes is challenging due to the slow electron transfer kinetics associated with the irreversible oxidation of peroxide. An anodic scan has been used as an electrochemical pretreatment and a rapid, sensitive and selective voltammetric method has been developed for the detection of physiological concentrations of H_2O_2 at uncoated carbon fiber microelectrodes (Sanford et al., 2011).

In this study, we provide an experimental evidence on the detection of H_2O_2 by using Osmium (Os) as a mediator which promotes shuttling of electrons between the electrode and the enzyme. Detection of H_2O_2 by using highly sensitive and selective Os-HRP modified electrode was tested in PSII membrane under light illumination. The current study introduces the use of catalytic amperometric biosensors in detection of low level of H_2O_2 production in PSII membrane.

MATERIALS AND METHODS

Material and Chemical Reagents
5-(ethoxycarbonyl)-5-methyl-1-pyrroline N-oxide (EMPO) spin trap was obtained from Alexis Biochemicals (Lausen, Switzerland). Capillary tube used for Electron paramagnetic resonance (EPR) measurements was purchased from Blaubrand intraMARK, Brand, Germany. All other chemicals of analytical grade were purchased either from Wako Pure Chemicals Industries, Ltd. (Osaka, Japan), Sigma-Aldrich chemie Gmbh (Munich, Germany), or Sigma-Aldrich Japan K.K (Tokyo, Japan).

Preparation of PSII Membrane
Photosystem II (PSII) membranes were prepared from fresh spinach leaves using the method reported previously by Berthold et al. (1981) with modifications described by Ford and Evans (1983). All steps during the isolation procedure were done at

4°C in green light using green LED strip (Photon Systems Instruments (PSI), Drásov, Czech Republic) or under dark condition using different buffers (A and B). The composition of buffer A (pH 7.5) being 400 mM sucrose, 15 mM NaCl, 5 mM $MgCl_2$, 5 mM $CaCl_2$, 40 mM HEPES (pH 7.5), 5 mM Na-ascorbate, and 2 g/l bovine serum albumin (BSA) while buffer B was composed of 400 mM sucrose, 15 mM NaCl and 5 mM $MgCl_2$, 40 mM MES (pH 6.5). Spinach leaves were washed twice with deionized water. Na-ascorbate and BSA were added immediately before crushing the spinach leaves. Dark adapted leaves (400 g) were homogenized with 500 ml of buffer A. This step was followed by filtering the homogenized mixture through 2 layers of nylon bolting cloth. Filtrate was transferred into ice-chilled centrifugation tubes and was centrifuged for 10 min at 9950 × g at 4°C. The supernatant was thrown out and pellet was mixed properly with paint brush. The pellet was then resuspended in 600 ml of buffer B and again centrifuged at 9950 × g for 10 min at 4°C. After the centrifugation, supernatant was discarded and pellet was again resuspended in buffer B, at this step concentration of chlorophyll was measured. This step was followed by treating the suspension with 5% Triton X-100 on ice bath with continuous stirring for 17 min, and then centrifugation at 7000 × g for 7 min. The pellet was discarded and supernatant was centrifuged again at 48,000 × g for 20 min at 4°C. Pellet was washed for 3 times with buffer B and at the final step, and chlorophyll concentration was measured. PSII membrane were diluted to final chlorophyll concentration (3–6 mg Chl ml^{-1}) and were stored at −80°C until further use.

Chlorophyll concentration was determined in aqueous 80 % (v/v) acetone by absorbance at 646 and 663 nm according to the method described by Lichtenthaler (1987).

Light Illumination
PSII membranes were exposed to continuous white light (1,000 µmol photons $m^{-2}s^{-1}$) for time period as required during the different experimental setups. The illumination was performed using halogen lamps with a light guide (KL1500 Electronic, Schott, Mainz, Germany and PL075, Hoya Candeo

Optonics, Japan). The light intensity was measured by quantum radiometer LI-189 and LI-185B (LI-COR Inc., Lincoln, U.S.A.).

Electron Paramagnetic Resonance (EPR) Spin-trapping Spectroscopy

The detection of $O_2^{\bullet-}$ was performed by EPR spin-trapping spectroscopy. Superoxide anion radical was detected by spin trapping using EMPO, 5-(ethoxycarbonyl)-5-methyl-1-pyrroline N-oxide. The experimental conditions are as follows: PSII membranes (150 μg Chl ml^{-1}); EMPO, 25 mM; phosphate buffer, 40 mM (pH 6.5), DCMU, 20 μM and desferal, 50 μM. Spectra were recorded using EPR spectrometer Mini Scope MS400 (Magnettech GmbH, Berlin, Germany) with EPR conditions as follows: microwave power, 10 mW; modulation amplitude, 1 G; modulation frequency, 100 kHz; sweep width, 100 G; scan rate, 1.62 G s^{-1}. Formation of light-induced EMPO-OOH adduct EPR spectra was measured in PSII membranes after illumination of PSII membranes in glass capillary tube with continuous white light (1000 μmol photons m^{-2} s^{-1}).

Fabrication of Osmium-HRP (Os-HRP) Modified Carbon Electrode

The electrochemical biosensor used in the study was prepared using carbon-electrode (BAS Inc, ALS Co., Ltd., Japan). Prior to each measurement, the carbon electrode was cleaned using PK-3 Electrode Polishing Kit (BAS Inc., ALS Co., Ltd., Japan) with the aim to remove redox reaction products accumulated on the electrode surface. This step was followed by spreading/dropping of 0.5 μL aliquot of Os-HRP polymer solution (Bioanalytical System, USA) on the carbon electrode (φ, 1 mm). The solution was allowed to form a circular thin film after overnight drying at 4°C under dark condition.

Cyclic Voltammetry of Os-HRP Modified Carbon Electrode

For the basic characterization of the Os-HRP modified carbon electrode, a portion of the electrode was soaked in 10 ml of 40 mM Na-phosphate buffer and cyclic voltammetry was performed. Cyclic voltammetry was conducted at a scan rate of 20 mV/s from 0.0 to +0.5 V at room temperature.

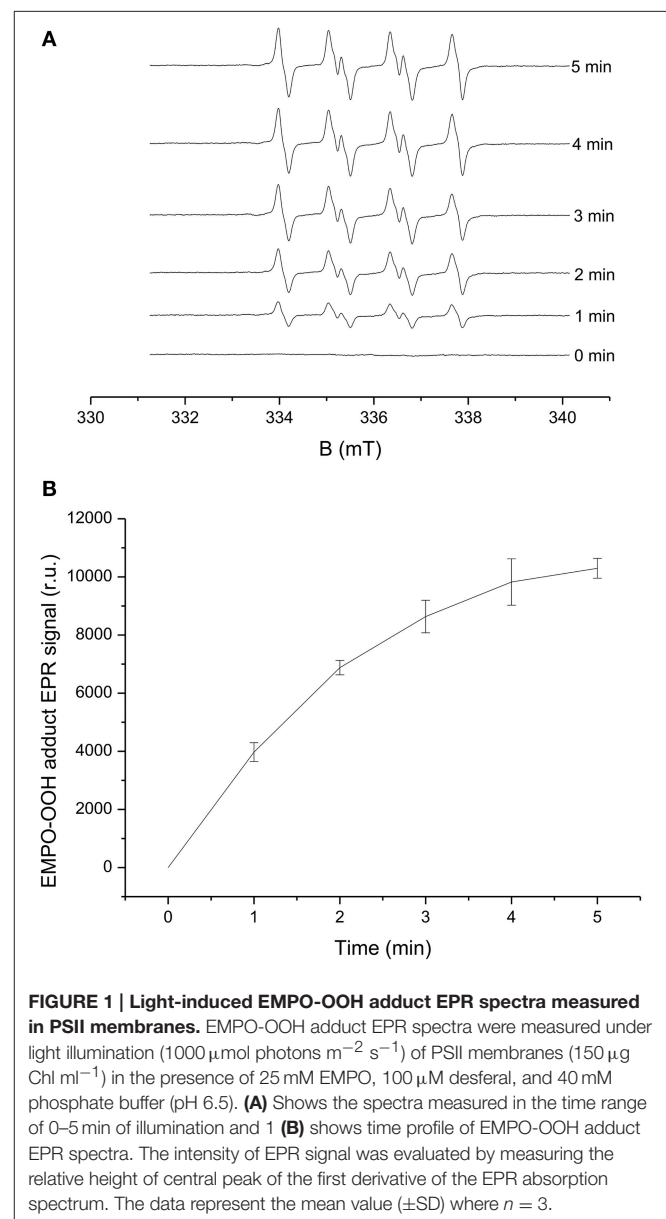## Hydrogen Peroxide Detection using Catalytic Amperometric Biosensor

The electrochemical measurements were performed using a potentiostat (HA1010mM4S; Hokuto Denke Co. Ltd., Japan). For the assay to study H_2O_2 generated in PSII membrane, the PSII membranes at a concentration of 150 μg Chl ml^{-1} was introduced into a six well Repro plate (IFP, Research unit for the functional peptides, Yamagata, Japan). Ag/AgCl electrode was used as a reference electrode and Os-HRP modified carbon electrode was used as working electrode. Platinum plate in the dimension of 5*5*0.1 mm was used as a counter electrode. Kinetics on the formation of light-induced H_2O_2 was measured in PSII membranes after illumination

under continuous white light (1000 μmol photons m^{-2} s^{-1}) for a duration of 1 h. The sampling time was kept at 500 ms.

RESULTS

Superoxide Anion Radical Production in PSII Membranes

The light-induced formation of $O_2^{\bullet-}$ in PSII membranes was measured using EPR spin-trapping spectroscopy. The spin-trapping was accomplished by the spin-trap compound 5-(ethoxycarbonyl)-5-methyl-1-pyrroline N-oxide (EMPO). The EMPO did not induce any EMPO-OOH adduct EPR signal in non-illuminated PSII membranes, whereas illumination with a

FIGURE 1 | Light-induced EMPO-OOH adduct EPR spectra measured in PSII membranes. EMPO-OOH adduct EPR spectra were measured under light illumination (1000 μmol photons m^{-2} s^{-1}) of PSII membranes (150 μg Chl ml^{-1}) in the presence of 25 mM EMPO, 100 μM desferal, and 40 mM phosphate buffer (pH 6.5). **(A)** Shows the spectra measured in the time range of 0–5 min of illumination and 1 **(B)** shows time profile of EMPO-OOH adduct EPR spectra. The intensity of EPR signal was evaluated by measuring the relative height of central peak of the first derivative of the EPR absorption spectrum. The data represent the mean value (±SD) where $n = 3$.

continuous white light (1,000 μmol photons m^{-2} s^{-1}) resulted in the formation of the EMPO-OOH adduct EPR signal (**Figure 1A**). Time dependence of EMPO-OOH adduct EPR signal shows that formation of $O_2^{\bullet-}$ is enhanced linearly for a duration upto 5 min of light illumination (**Figure 1B**). These results suggest that illumination of PSII membranes with a continuous white light (1,000 μmol photons m^{-2} s^{-1}) results in $O_2^{\bullet-}$ production.

Effect of Superoxide Dismutase and Catalase on $O_2^{\bullet-}$ Production in PSII Membranes

To study the contribution of $O_2^{\bullet-}$ leading to H_2O_2 formation in PSII membranes under light illumination, the effect of SOD and catalase (CAT) were studied on $O_2^{\bullet-}$. Upon addition of exogenous SOD, which is known to catalyze the dismutation of $O_2^{\bullet-}$ to H_2O_2 to PSII membranes prior to illumination, EMPO-OOH adduct EPR signal was found to diminish completely. The simultaneous addition of SOD and CAT was also found to suppress the EMPO-OOH EPR signal completely (**Figure 2A**). This observation indicates that $O_2^{\bullet-}$ produced during light illumination is most likely involved in H_2O_2 formation in PSII membranes.

Effect of DCMU on $O_2^{\bullet-}$ Production in PSII Membranes

The effect of herbicides, DCMU [3-(3,4-dichlorophenyl)-1,1-dimethylurea] (Sigma Aldrich, Germany) was tested for its effect on EMPO-OOH adduct EPR signal in PSII membranes. The effect of DCMU which is known to block the electron transfer from Q_A to Q_B was studied on light-induced formation of $O_2^{\bullet-}$. **Figure 2B** shows that the addition of DCMU suppressed EMPO-OOH adduct EPR signal approximately by 50% (**Figure 2B**). These observations indicate that loosely bound plastosemiquinone bound at or after the Q_B site can contribute to the overall production of $O_2^{\bullet-}$ via the reduction of molecular oxygen.

Characterization of Os-HRP Modified Carbon Electrode

The characterization of the Os-HRP modified carbon electrode was performed using cyclic voltammetry (**Figure 3**). Cyclic voltammetry was conducted at a scan rate of 20 mV/s from 0.0 to + 0.5 V at room temperature. The oxidation and reduction current were obtained at 0.3 V vs. Ag/AgCl. Based on the data obtained, the surface concentration of Os-HRP on the carbon electrode was calculated to be 6.78×10^{-9} mol/cm^2. The Calibration curve of Os-HRP modified carbon electrode was also measured using standard H_2O_2 solution (Supplementary Data).
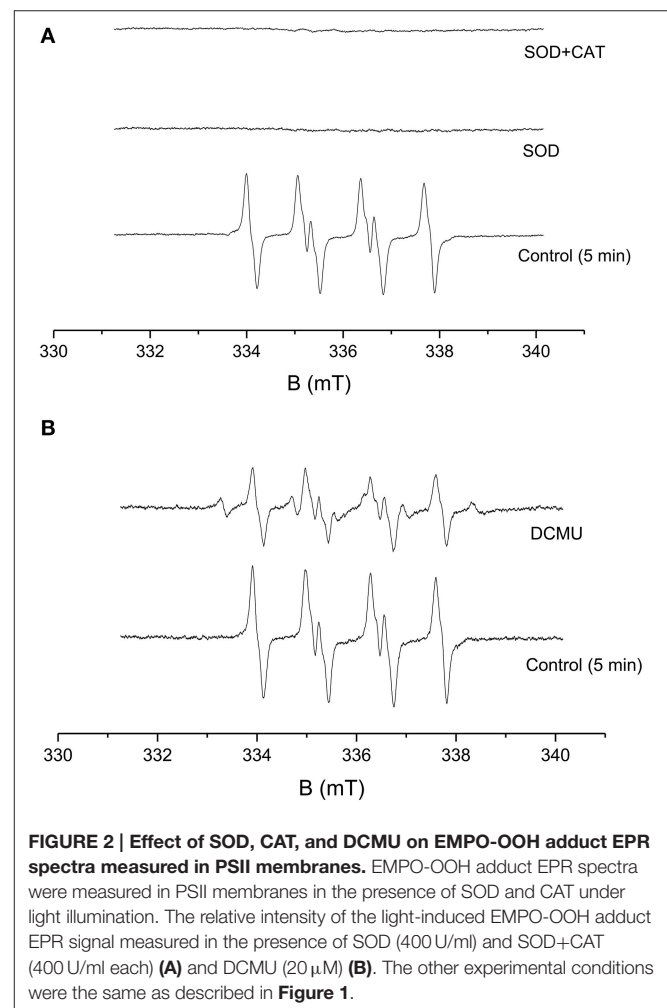
Hydrogen Peroxide Production in PSII Membranes

The light-induced formation of H_2O_2 in PSII membranes was measured using catalytic amperometric biosensor. The study of kinetics of H_2O_2 production was accomplished using Os-HRP modified carbon electrode. The reduction current generated in

the presence of H_2O_2 was monitored. Under dark condition, no change in the reduction current was observed whereas illumination with a continuous white light (1,000 μ mol photons m^{-2} s^{-1}) resulted in change in the reduction current. **Figure 4A** shows typical chronoamperometric responses, the reduction currents gradually increased after light illumination followed by a shoulder which continues for a duration of about 1 h which than rapidly drops at the switching off the light (dark period). The peak value of the reduction current was reached after about 15 min of light illumination with a maximum change in reduction currents of approximately 400 pA. The data presented shows continuous generation of H_2O_2 till the period of light illumination (**Figure 4A**). These results shows that illumination of PSII membranes with continuous white light results in H_2O_2 production.

Effect of SOD and CAT on H_2O_2 Production in PSII Membranes

To monitor the functionality of the sensor, the effect of SOD was measured under light-illumination. Reduction current for $H_2O_2$was measured for first 5 min of light illumination where

FIGURE 2 | Effect of SOD, CAT, and DCMU on EMPO-OOH adduct EPR spectra measured in PSII membranes. EMPO-OOH adduct EPR spectra were measured in PSII membranes in the presence of SOD and CAT under light illumination. The relative intensity of the light-induced EMPO-OOH adduct EPR signal measured in the presence of SOD (400 U/ml) and SOD+CAT (400 U/ml each) **(A)** and DCMU (20 μM) **(B)**. The other experimental conditions were the same as described in **Figure 1**.
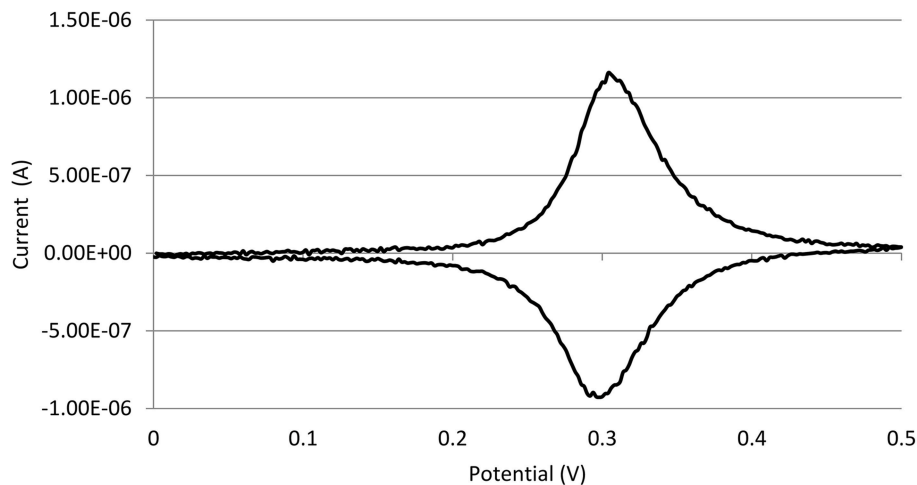
FIGURE 3 | Characterization of Os-HRP modified carbon electrode. Characterization of the Os-HRP modified carbon electrode: cyclic voltammetry was performed for the basic characterization of the modified electrode. Cyclic voltammetry was conducted at a scan rate of 20 mV/s from 0.0 to +0.5 V at room temperature.

a linear increase was observed similar to control (**Figure 4A**). Upon addition of exogenous SOD to PSII membranes during illumination, a fast increase in reduction current was observed bringing a considerable change of about 600 pA. The fast increase was followed by a rapid drop however; the reduction current was still higher as compared to reduction current recorded before the addition of SOD. The addition of CAT completely suppressed the reduction current by about 100% (**Figure 4B**). These results show that under illumination of PSII membranes with a continuous white light, H_2O_2 production in PSII membrane is contributed via dismutation of $O_2^{\bullet-}$.

DISCUSSION

In the current study, we used spectroscopic and amperometric techniques to measure the production of ROS in spinach PSII membrane. Our prime objective was to study the effect of high light stress in PSII membrane reflected by ROS production primarily the generation of H_2O_2 as the stress response formed via the dismutation of $O_2^{\bullet-}$. Superoxide anion radical which is known to be formed by one-electron reduction of molecular oxygen was measured under light illumination (**Figure 1**). EPR spin-trapping data obtained using the urea-type herbicide (DCMU) supports the evidence on the involvement of loosely bound plastosemiquinone in $O_2^{\bullet-}$ production (**Figure 2B**). Suppression of EMPO-OOH adduct EPR signal is in agreement with our previously published results where contribution of loosely bound plastosemiquinone at or after the Q_B site (DCMU-sensitive site) might contribute to the overall $O_2^{\bullet-}$ production (Yadav et al., 2014). The EMPO-OOH adduct EPR signal in the presence of DCMU indicates that molecular oxygen is reduced prior to the Q_B site which is known to occur due to reduction of molecular oxygen by Pheo$^{\bullet-}$ or $Q_A^{\bullet-}$ which serves as electron donors to molecular oxygen due to their low redox potentials

(Pospíšil, 2012). The observation that the EMPO-OOH adduct was completely suppressed in PSII membranes illuminated in presence of SOD indicates that $O_2^{\bullet-}$ formed during the light illumination dismutates to H_2O_2 prior to its interaction with spin trap (**Figure 2A**). It can be concluded here that the H_2O_2 formed in PSII membrane under light illumination is contributed by the dismutation of $O_2^{\bullet-}$.

Amperometric methods for the direct detection of H_2O_2 has been used since last decades in animal cells (Mouithys-Mickalad et al., 2001; Inoue et al., 2010) however, very limited evidences exist on its application in plant cells (Cleland and Grace, 1999). Amperometric measurements have been implemented at the level of protoplast to study the photosynthetic activity under the effect of benzoquinone (Yasukawa et al., 1998, 1999). Redox response of benzoquinone, p-hydroquinone and oxygen was measured by placing a microelectrode close to an algal protoplast to localize concentration of these species (Yasukawa et al., 1999). Direct detection of H_2O_2 using electrochemical methods; however, had never been reported previously in photosynthetic organelles. H_2O_2 detection in subchloroplast oxygen-evolving PSII particles and isolated reaction center complexes of PSII has been studied using luminol-peroxidase chemiluminescence and pulse photoactivation (Zastrizhnaya et al., 1997). Production of H_2O_2 was detected in PSII membranes using AR fluorescent assay (Yadav and Pospíšil, 2012). Levels of H_2O_2 including $O_2^{\bullet-}$ and singlet oxygen has been determined by using both histochemical and fluorescent probes in leaves and thylakoids (Zulfugarov et al., 2014), however, there exist arguments over the selectivity of the molecular probes used.

Two different approaches of the detection of H_2O_2 via electrochemical methods are being used in animal cells. The detection of H_2O_2 is either via a non-mediator or a mediator based biosensor device (Lin et al., 2000; Nakabayashi and

FIGURE 4 | Real-time monitoring of reduction current for hydrogen peroxide in PSII membrane. (A) Kinetics of the production of H_2O_2 was measured using Os-HRP modified carbon electrode during light illumination in PSII membranes. The light illumination was started at 5 min from the start of the measurement and the reduction current was measured for a duration of 1 h. **(B)** Effect of SOD and CAT on reduction current was measured in the presence of SOD (400 U/ml) and SOD + CAT (400 U/ml each).

Yoshikawa, 2000; Yao et al., 2005; Wang and Zhang, 2006; Camacho et al., 2007; Jia, 2008; Radi et al., 2009; Ahammad, 2013). In non-mediator based biosensor, the transfer of electron occurs between the electrode and the enzyme (Ahammad, 2013). The preparation process being very simple, the non-mediator based biosensors have been extensively used in the past. In the mediator based biosensor device, the mediator plays a key role to shuttle electron between the electrode and the enzyme (**Scheme 1**). Most commonly, methylene blue, ferrocene and carboxylic acid are used as mediators (Lin et al., 2000; Tian et al.,

2001; Li et al., 2004; Tripathi et al., 2006; Senel et al., 2010). The mediator in the case of HRP is pointed to be important because the shuttling of electron between electrode and HRP is large as the active site of HRP is located deep in the protein sheath (Ahammad, 2013). In our current device, Os acts as a mediator where Os^{2+} is reduced to Os^{3+} in the process (**Scheme 1**). Different modified electrode has been introduced in the past, the detection limit in most case were in the range of μM concentration with a limited contribution where mediator-based HRP biosensor reached a lower detection limit in the range of

tens-hundreds nm concentration (Chen et al., 2006; Zhang et al., 2008; Lu et al., 2010).

Using Os-HRP modified carbon electrode, we have observed a change in the reduction current during illumination of PSII membranes reflecting the production of H_2O_2 (**Figure 4A**). A change of ~400 pA reflects generation of H_2O_2 which was then found to be stable in the period of 20–60 min of light illumination. The reduction current was found to drop immediately under dark condition. Based on the considerable changes monitored in reduction current, the biosensor device is claimed to be sensitive for its application in photosynthetic samples.

ROS generated in the cell or organelles are eliminated by antioxidant enzymes such as SOD, glutathione peroxidase, CAT or by low molecular antioxidants such as vitamins, glutathione etc. (Halliwell and Gutteridge, 2007). When SOD which dismutates $O_2^{\bullet-}$ to H_2O_2 was added to the illuminated PSII membrane, the reduction current for H_2O_2 was observed to gradually enhance leading to the conclusion that the H_2O_2 generated in the PSII membrane is formed via the formation of $O_2^{\bullet-}$. The addition of SOD (**Figure 4B**) during the light illumination drastically enhanced the reduction current by 600 pA followed by a sudden drop indicate the fast conversion of $O_2^{\bullet-}$ into H_2O_2 available in the PSII pool. This is in agreement with observed result with EPR signal of the EMPO-OOH adduct observed under the effect of SOD (**Figure 2A**). The subsequent addition of CAT which converts H_2O_2 to H_2O and molecular oxygen brings back the reduction current close to the value observed under dark condition.

Electrochemical detection of H_2O_2 is suggested here to be of great importance in addition to other methods that has been used in the recent past. In the detailed study performed by Šnyrychová and co-workers, different H_2O_2 detecting probes were tested. Probes such as amplex red and amplex ultra-red were found to be sensitive to light and thus are not appropriate for the study on the generation of H_2O_2 in plant sample where effect of light stress is frequently studied. Based on the results, the authors also suggested that these probes should be used with caution to avoid artifacts (Šnyrychová et al., 2009). In addition to this, the toxicity caused by the exogenous addition of probes cannot be completely excluded. The method of electrochemical measurements is also preferred because of the simplicity, low-cost, high-sensitivity and selectivity (Ahammad, 2013). The simplicity and low-cost of electrochemical measurements is because of the fact that the electrodes can be used for endless time with easy fabrication with designated mediator and enzyme and overnight incubation at 4°C under dark condition or as per standards. Based on the redox potential of the redox couple, the modified electrode are specific for different species. Os-HRP modified electrode is specific for H_2O_2 and thus can be widely used in photosynthetic research where detection of H_2O_2 has

always been a challenge. The sensitivity of the modified electrode depends on the size and the material used. In our current report, Os-HRP modified carbon electrode has been claimed to be sensitive and highly selective among other H_2O_2 detection techniques available till date. This fact opens the possibility for using Os-HRP modified electrode for H_2O_2 detection in photosystem I (PSI) where H_2O_2 is formed by the transfer of electron from reduced ferredoxin to molecular oxygen via ferredoxin-thioredoxin reductase (Gechev et al., 2006). Plasma membrane NADPH oxidase complex are considered as the major producer of ROS including $O_2^{\bullet-}$ and H_2O_2 in cells (Sagi and Fluhr, 2001, 2006; Halliwell and Gutteridge, 2007). In addition to this, among the enzymatic source of $O_2^{\bullet-}$ and H_2O_2, cell wall bound peroxidases, aminooxidases, flavin containing oxidases, oxalate, and plasma membrane oxidases are known to be involved (Bolwell et al., 2002; Mori and Schroeder, 2004; Svedruzic et al., 2005). In the case of apoplastic oxidative burst, ROS are produced by cell wall bound oxidases, peroxidases and polyamine oxidases (Minibayeva et al., 1998, 2009). Thus, the current electrode also opens the possibility for measuring generation of H_2O_2 from different and localized structures of plants and animals cells.

AUTHOR CONTRIBUTIONS

AP and SK contributed to the conception and design of the work. AP, AK, MS, HK, TS performed the measurements. AP analyzed, interpreted the data and drafted the manuscript. AK, PP participated in drafting the manuscript. SK, MK, and MT revised it critically for important content. All authors approved the final version of the manuscript.

ACKNOWLEDGMENTS

SUPPLEMENTARY MATERIAL

The Supplementary Material for this article can be found online at: http://journal.frontiersin.org/article/10.3389/fpls.2015.00862

REFERENCES

Ahammad, A. J. S. (2013). Hydrogen peroxide biosensors based on horseradish peroxidase and hemoglobin. *J. Biosens. Bioelectron.* S9:001. doi: 10.4172/2155-6210.S9-001

Ananyev, G., Renger, G., Wacker, U., and Klimov, V. (1994). The photoproduction of superoxide radicals and the superoxide-dismutase activity of photosystem II. The possible involvement of cytochrome b559. *Photosynth. Res.* 41, 327–338. doi: 10.1007/BF00019410

Arató, A., Bondarava, N., and Krieger-Liszkay, A. (2004). Production of reactive oxygen species in chloride- and calcium-depleted photosystem II and their involvement in photoinhibition. *Biochim. Biophys. Acta* 1608, 171–180. doi: 10.1016/j.bbabio.2003.12.003

Berthold, D. A., Babcock, G. T., and Yocum, C. F. (1981). A highly resolved oxygen evolving photosystem II preparation from spinach thylakoid membranes. *FEBS Lett.* 134, 231–234. doi: 10.1016/0014-5793(81)80608-4

Bolwell, G. P., Bindschedler, L. V., Blee, K. A., Butt, V. S., Davies, D. R., Gardner, S. L., et al. (2002). The apoplastic oxidative burst in response to biotic stress in plants: a three-component system. *J Exp. Bot.* 53, 1367–1376. doi: 10.1093/jexbot/53.372.1367

Camacho, C., Matías, J. C., Chico, B., Cao, R., Gómez, L., Simpson, B. K., et al. (2007). Amperometric biosensor for hydrogen peroxide, using supramolecularly immobilized horseradish peroxidase on the β-cyclodextrin-coated gold electrode. *Electroanalysis* 19, 2538–2542. doi: 10.1002/elan.200703993

Chen, S., Yin, C., Strasser, R. J., Govindjee, Yang, C., and Qiang, S. (2012). Reactive oxygen species from chloroplasts contribute to 3-acetyl-5-isopropyltetramic acid-induced leaf necrosis of *Arabidopsis thaliana*. *Plant Physiol. Biochem.* 52, 38–51. doi: 10.1016/j.plaphy.2011.11.004

Chen, S., Yuan, R., Chai, Y., Xu, L., Wang, N., Li, X. et al. (2006). Amperometric hydrogen peroxide biosensor based on the immobilization of Horseradish Peroxidase (HRP) on the layer-by-layer assembly films of gold colloidal nanoparticles and toluidine blue. *Electroanalysis* 18, 471–477. doi: 10.1002/elan.200503424

Chen, W., Li, B., Xu, C., and Wang, L. (2009). Chemiluminescence flow biosensor for hydrogen peroxide using DNAzyme immobilized on eggshell membrane as a thermally stable biocatalyst. *Biosens. Bioelectron.* 24, 2534–2540. doi: 10.1016/j.bios.2009.01.010

Cleland, R. E., and Grace, S. C. (1999). Voltammetric detection of superoxide production by photosystem II. *FEBS Lett.* 457, 348–352. doi: 10.1016/S0014-5793(99)01067-4

Ferreira, K. N., Iverson, T. M., Maghlaoui, K., Barber, J., and Iwata, S. (2004). Architecture of the photosynthetic oxygen-evolving center. *Science* 303, 1831–1838. doi: 10.1126/science.1093087

Ford, R. C., and Evans, M. C. W. (1983). Isolation of a photosystem II from higher plants with highly enriched oxygen evolution activity. *FEBS Lett.* 160, 159–164. doi: 10.1016/0014-5793(83)80957-0

Foyer, C. H., and Shigeoka, S. (2011). Understanding oxidative stress and antioxidant functions to enhance photosynthesis. *Plant Physiol.* 155, 93–100. doi: 10.1104/pp.110.166181

Gechev, T. S., Van Breusegem, F., Stone, J. M., Denev, I., and Laloi, C (2006). Reactive oxygen species as signals that modulate plant stress responses and programmed cell death. *Bioessays* 28, 1091–1101. doi: 10.1002/bies.20493

Guskov, A., Kern, J., Gabdulkhakov, A., Broser, M., Zouni, A., and Saenger, W. (2009). Cynobacterial photosystem II at 2.9 Å resolution and the role of quinones, lipids, channels and chloride. *Nat. Struct. Mol. Biol.* 16, 334–342. doi: 10.1038/nsmb.1559

Halliwell, B., and Gutteridge, J. M. C. (2007). *Free Radicals in Biology and Medicine, 4th Edn.* New York, NY: Oxford University Press.

Inoue, K. Y., Ino, K., Shiku, H., Kasai, S., Yasukawa, T., Mizutani, F., et al. (2010). Electrochemical monitoring of hydrogen peroxide released from leucocytes on horseradish peroxidase redox polymer coated electrode chip. *Biosens. Bioelectron.* 25, 1723–1728. doi: 10.1016/j.bios.2009.12.014

Jia, J. (2008). Hydrogen peroxide biosensor based on horseradish peroxidase– Au nanoparticles at a viologen grafted glassy carbon electrode. *Microchim. Acta* 163, 237–241. doi: 10.1007/s00604-008-0002-9

Kafi, A. K., Wu, G., and Chen, A. (2009). A novel hydrogen peroxide biosensor based on the immobilization of horseradish peroxidase onto Au-modified titanium dioxide nanotube arrays. *Biosens. Bioelectron.* 24, 566–571. doi: 10.1016/j.bios.2008.06.004

Kawakami, K., Umena, Y., Kamiya, N., and Shen, J.-R. (2011). Structure of the catalytic, inorganic core of oxygen-evolving photosystem II at 1.9 Å resolution. *J. Photochem. Photobiol. B* 104, 9–18. doi: 10.1016/j.jphotobiol.2011.03.017

Krieger-Liszkay, A. (2005). Singlet oxygen production in photosynthesis. *J. Exp. Bot.* 56, 337–346. doi: 10.1093/jxb/erh237

Lei, C. X., Long, L. P., and Cao, Z. L. (2005). An H_2O_2 biosensor based on immobilization of horseradish peroxidase labeled nano-Au in silica sol-gel/alginate composite film. *Anal. Lett.* 38, 1721–1734. doi: 10.1080/00032710500207762

Lei, C. X., Wang, H., Shen, G. L., and Yu, R. Q. (2004). Immobilization of enzymes on the nano-au film modified glassy carbon electrode for the determination of hydrogen peroxide and glucose. *Electroanalysis* 16, 736–740. doi: 10.1002/elan.200302877

Li, C. X., Deng, K. Q., Shen, G. L., and Yu, R. Q. (2004). Amperometric hydrogen peroxide biosensor based on horseradish peroxidase-labeled nano-Au colloids immobilized on poly(2,6-pyridinedicarboxylic acid) layer by cysteamine. *Anal. Sci.* 20, 1277–1281. doi: 10.2116/analsci.20.1277

Li, Z. H., Guedri, H., Viguier, B., Sun, S. G., and Marty, J. L. (2013). Optimization of hydrogen peroxide detection for a methyl mercaptan biosensor. *Sensors* 13, 5028–5039. doi: 10.3390/s130405028

Lichtenthaler, H. K. (1987). Chlorophylls and carotenoids: pigments of photosynthetic biomembranes. *Methods Enzymol.* 148, 350–382. doi: 10.1016/0076-6879(87)48036-1

Lin, X. Q., Chen, J., and Chen, Z. H. (2000). Amperometric biosensor for hydrogen peroxide based on immobilization of horseradish peroxidase on methylene blue modified graphite electrode. *Electroanalysis* 12, 306–310. doi: 10.1002/(sici)1521-4109(20000301)

Liu, X., Luo, L., Ding, Y., Xu, Y., and Li, F. (2011). Hydrogen peroxide biosensor based on the immobilization of horseradish peroxidase on γ-Al_2O_3 nanoparticles/chitosan film-modified electrode. *J. Solid State Electrochem.* 15, 447–453. doi: 10.1007/s10008-010-1120-y

Loew, N., Wollenberger, U., Scheller, F. W., and Katterle, M. (2009). Direct electrochemistry and spectroelectrochemistry of osmium substituted horseradish peroxidase. *Bioelectrochemistry* 76, 28–33. doi: 10.1016/j.bioelechem.2009.03.015

Loll, B., Kern, J., Saenger, W., Zouni, A., and Biesiadka, J. (2005). Towards complete cofactor arrangement in the 3.0 Å resolution structure of photosystem II. *Nature* 438, 1040–1044. doi: 10.1038/nature04224

Lu, L., Zhang, L., Zhang, X., Wu, Z., Huan, S., Shen, G. et al. (2010). A MgO nanoparticles composite matrix-based electrochemical biosensor for hydrogen peroxide with high sensitivity. *Electroanalysis* 22, 471–477. doi: 10.1002/elan.200900429

Luo, L., Zhu, L., Xu, Y., Shen, L., Wang, X., Ding, Y. et al. (2011). Hydrogen peroxide biosensor based on horseradish peroxidase immobilized on chitosan-wrapped $NiFe_2O_4$ nanoparticles. Microchim. *Acta* 174, 55–61. doi: 10.1007/s00604-011-0591-6

Mills, A., Tommons, C., Bailey, R. T., Tedford, M. C., and Crilly, P. J. (2007). Reversible, fluorescence-based optical sensor for hydrogen peroxide. *Analyst* 132, 566–571. doi: 10.1039/b618506a

Minibayeva, F., Kolesnikov, O., Chasov, A., Beckett, R. P., Lüthje, S., Vylegzhanina, N., et al. (2009). Wound-induced apoplastic peroxidase activities: their roles in the production and detoxification of reactive oxygen species. *Plant Cell. Environ.* 32, 497–508. doi: 10.1111/j.1365-3040.2009.01944.x

Minibayeva, F., Kolesnikov, O. P., and Gordon, L. K. (1998). Contribution of a plasma membrane redox system to the superoxide production by wheat root cells *Protoplasma* 205, 101–106. doi: 10.1007/BF01279299

Mori, I. C., and Schroeder, J. I. (2004). Reactive oxygen species activation of plant Ca2+ channels. A signaling mechanism in polar growth, hormone transduction, stress signaling, and hypothetically mechanotransduction. *Plant Physiol.* 135, 702–708. doi: 10.1104/pp.104.042069

Mouithys-Mickalad, A., Deby-Dupont, G., Nys, M., Lamy, M., and Deby, C. (2001). Oxidative processes in human promonocytic cells (THP-1) after differentiation into macrophages by incubation with *Chlamydia pneumoniae* extracts. *Biochem. Biophys. Res. Commun.* 287, 781–788. doi: 10.1006/bbrc.2001.5643

Mubarakshina, M. M., and Ivanov, B. N. (2010). The production and scavenging of reactive oxygen species in the plastoquinone pool of chloroplast thylakoid membranes. *Physiol. Plant.* 140, 103–110. doi: 10.1111/j.1399-3054.2010.01391.x

Nakabayashi, Y., and Yoshikawa, H. (2000). Amperometric biosensors for sensing of hydrogen peroxide based on electron transfer between horseradish peroxidase and ferrocene as a mediator. *Anal. Sci.* 16, 609–613. doi: 10.2116/analsci.16.609

Pospíšil, P. (2009). Production of reactive oxygen species by photosystem II. *Biochim. Biophys. Acta* 1787, 1151–1160. doi: 10.1016/j.bbabio.2009.05.005

Pospíšil, P. (2011). Enzymatic function of cytochrome b559 in photosystem II. *J Photochem. Photobiol. B* 104, 341–347. doi: 10.1016/j.jphotobiol.2011.02.013

Pospíšil, P. (2012). Molecular mechanisms of production and scavenging of reactive oxygen species by photosystem II. *Biochim. Biophys. Acta* 1817, 218–231. doi: 10.1016/j.bbabio.2011.05.017

Pospíšil, P., Arató, A., Krieger-Liszkay, A., and Rutherford, A. W. (2004). Hydroxyl radical generation by Photosystem II. *Biochemistry* 43, 6783–6792. doi: 10.1021/bi036219i

Pospíšil, P., Šnyrychová, I., Kruk, J., Strzałka, K., and Nauš, J. (2006). Evidence that cytochrome b559 is involved in superoxide production in Photosystem II: effect of synthetic short-chain plastoquinones in a cytochrome b559 tobacco mutant. *Biochem. J.* 397, 321–327. doi: 10.1042/BJ20060068

Prasad, A., and Pospíšil, P. (2012). Ultra-weak photon emission induced by visible light and ultraviolet A radiation via photoactivated skin chromophores: *in-vivo* charge coupled device imaging. *J. Biomed. Opt.* 17:085004. doi: 10.1117/1.JBO.17.8.085004

Radi, A. E., Muñoz-Berbel, X., Cortina-Puig, M., and Marty, J. L. (2009). A third generation hydrogen peroxide biosensor based on horseradish peroxidase covalently immobilized on electrografted organic film on screen-printed carbon electrode. *Electroanalysis* 21, 1624–1629. doi: 10.1002/elan.200904587

Rappaport, F., and Diner, B. A. (2008). Primary photochemistry and energetics leading to the oxidation of the (Mn)4Ca cluster and to the evolution of molecular oxygen in Photosystem II. *Coord. Chem. Rev.* 252, 259–272. doi: 10.1016/j.ccr.2007.07.016

Sagi, M., and Fluhr, R. (2001). Superoxide production by plant homologues of the Gp91phox NADPH oxidase. modulation of activity by calcium and by tobacco mosaic virus infection. *Plant Physiol.* 126, 1281–1290. doi: 10.1104/pp.126.3.1281

Sagi, M., and Fluhr, R. (2006). Production of reactive oxygen species by plant NADPH oxidases. *Plant Physiol.* 141, 336–340. doi: 10.1104/pp.106.078089

Sanford, A. L., Morton, S. W., Whitehouse, K. L., Oara, H. M., Lugo-Morales, L. Z., Roberts, J. G., et al. (2011). Voltammetric detection of hydrogen peroxide at carbon fiber microelectrodes. *Anal Chem.* 82, 5205–5210. doi: 10.1021/ac100536s

Schmitt, F. J., Renger, G., Friedrich, T., Kreslavksi, V. D., Zharmukhadmedov, S. K., Los, D. A., et al. (2014). Reactive oxygen species: re-evaluation of generation, monitoring and role in stress-signaling in phototrophic organisms. *Biochim. Biophys. Acta* 1837, 385–848. doi: 10.1016/j.bbabio.2014.02.005

Schröder, W. P., and Åkerlund, H.-E. (1990). "Hydrogen peroxide production in photosystem II preparations," in *Current Research in Photosynthesis,* Vol. 1, ed M. Baltscheffsky (Dordrecht: Kluwer Academic Publisher), 901–904.

Senel, M. C., Cevik, E., and Abasıyanık, M. F. (2010). Amperometric hydrogen peroxide biosensor based on covalent immobilization of horseradish peroxidase on ferrocene containing polymeric mediator. *Sens. Actuators. B Chem.* 145, 444–450. doi: 10.1016/j.snb.2009.12.055

Shao, N., Krieger-Liszkay, A., Schroda, M., and Beck Christoph, F. (2007). A reporter system for the individual detection of hydrogen peroxide and singlet oxygen: its use for the assay of reactive oxygen species produced *in vivo*. *Plant J.* 50, 475–487. doi: 10.1111/j.1365-313X.2007.03065.x

Šnyrychová, I., Ayaydin, F., and Hideg, É. (2009). Detecting hydrogen peroxide in leaves *in vivo*—a comparison of methods. *Physiol. Plant.* 135, 1–18. doi: 10.1111/j.1399-3054.2008.01176.x

Svedruzic, D., Jónsson, S., Toyota, C. G., Reinhardt, L. A., Ricagno, S, Lindqvist, Y., et al. (2005). The enzymes of oxalate metabolism: unexpected structures and mechanisms. *Arch. Biochem. Biophys.* 433, 176–192. doi: 10.1016/j.abb.2004.08.032

Tian, F., Xu, B., Zhu, L., and Zhu, G. (2001). Hydrogen peroxide biosensor with enzyme entrapped within electrodeposited polypyrrole based on mediated

sol–gel derived composite carbon electrode. *Anal. Chim. Acta* 443, 9–16. doi: 10.1016/S0003-2670(01)01187-4

Tiwari, A., and Pospíšil, P. (2009). Superoxide oxidase and reductase activity of cytochrome b559 in photosystem II. *Biochim. Biophys. Acta* 1787, 985–994. doi: 10.1016/j.bbabio.2009.03.017

Tiwari, I., and Singh, M. (2011). Preparation and characterization of methylene blue-SDS-multiwalled carbon nanotubes nanocomposite for the detection of hydrogen peroxide. *Microchim. Acta* 174, 223–230. doi: 10.1007/s00604-011-0620-5

Tripathi, V. S., Kandimalla, V. B., and Ju, H. (2006). Amperometric biosensor for hydrogen peroxide based on ferrocene-bovine serum albumin and multiwall carbon nanotube modified ormosil composite. *Biosens. Bioelectron.* 21, 1529–1535. doi: 10.1016/j.bios.2005.07.006

Wang, G. H., and Zhang, L. M. (2006). Using novel polysaccharide-silica hybrid material to construct an amperometric biosensor for hydrogen peroxide. *J. Phys. Chem. B* 110, 24864–24868. doi: 10.1021/jp0657078

Wang, H. S., Pan, Q. X., and Wang, G. X. (2005). A biosensor based on immobilization of horseradish peroxidase in chitosan matrix cross-linked with glyoxal for amperometric determination of hydrogen peroxide. *Sensors* 5, 266–276. doi: 10.3390/s5040266

Yadav, D. K., and Pospíšil, P. (2012). Role of chloride ion in hydroxyl radical production in photosystem II under heat stress: electron paramagnetic resonance spin-trapping study. *J. Bioenerg. Biomembr.* 44, 365–372. doi: 10.1007/s10863-012-9433-4

Yadav, D. K., Prasad, A., Kruk, J., and Pospíšil, P. (2014). Evidence for the involvement of loosely bound plastosemiquinones in superoxide anion radical production in photosystem II. *PLoS ONE* 9:e115466. doi: 10.1371/journal.pone.0115466

Yang, Z., Zong, X., Ye, Z., Zhao, B., Wang, Q., and Wang, P. (2010). The application of complex multiple forklike ZnO nanostructures to rapid and ultrahigh sensitive hydrogen peroxide biosensors. *Biomaterials* 31, 7534–7541. doi: 10.1016/j.biomaterials.2010.06.019

Yao, H., Li, N., Wei, Y. L., and Zhu, J. J. (2005). A H_2O_2 biosensor based on immobilization of horseradishperoxidase in a gelatine network matrix. *Sensors* 5, 277–283. doi: 10.3390/s5040277

Yasukawa, T., Uchida, I., and Matsue, T. (1998). Permeation of redox species through a cell membrane of a single, living algal protoplast studied by microamperometry. *Biochim. Biophys. Acta* 1369, 152–158. doi: 10.1016/S0005-2736(97)00220-4

Yasukawa, T., Uchida, I., and Matsue, T. (1999). Microamperometric measurements of photosynthetic activity in a single algal protoplast. *Biophys. J.* 76, 1129–1135. doi: 10.1016/S0006-3495(99)77277-2

Zastrizhnaya, O. M., Khorobrykh, A. A., Khristin, M. S., and Klimov, V. V. (1997). Photoinduced production of hydrogen peroxide at the acceptor side of photosystem II. *Biochemistry* 62, 357–361.

Zhang, H. L., Lai, G. S., Han, D. Y., and Yu, A. M. (2008). An amperometric hydrogen peroxide biosensor based on immobilization of horseradish peroxidase on an electrode modified with magnetic dextran microspheres. *Anal. Bioanal. Chem.* 390, 971–977. doi: 10.1007/s00216-007-1748-3

Zhang, S., Weng, J., Pan, J., Tu, T., Yao, S., and Xu, C. (2003). Study on the photo-generation of superoxide radicals in Photosystem II with EPR spin trapping techniques. *Photosynth. Res.* 75, 41–48. doi: 10.1023/A:1022439009587

Zulfugarov, I. S., Tovuu, A., Eu, Y. J., Dogsom, B., Poudyal, R. S., Nath, K., et al. (2014). Production of superoxide from Photosystem II in a rice (*Oryza sativa* L.) mutant lacking PsbS. *BMC Plant Biol.* 14:242. doi: 10.1186/s12870-014-0242-2

Real-time monitoring of superoxide anion radical generation in response to wounding: electrochemical study

Ankush Prasad[1,2,*], Aditya Kumar[1], Ryo Matsuoka[3], Akemi Takahashi[4], Ryo Fujii[4], Yamato Sugiura[4], Hiroyuki Kikuchi[4], Shigeo Aoyagi[3], Tatsuo Aikawa[5], Takeshi Kondo[5], Makoto Yuasa[5], Pavel Pospíšil[1] and Shigenobu Kasai[2,4,*]

[1] Department of Biophysics, Centre of the Region Haná for Biotechnological and Agricultural Research, Faculty of Science, Palacký University, Olomouc, Czech Republic
[2] Biomedical Engineering Research Center, Tohoku Institute of Technology, Sendai, Japan
[3] Hokuto Denko Corporation, Tokyo, Japan
[4] Graduate Department of Environmental Information Engineering, Tohoku Institute of Technology, Sendai, Japan
[5] Department of Pure and Applied Chemistry, Tokyo University of Science, Noda, Chiba, Japan
[*] These authors contributed equally to this work.

ABSTRACT

Background. The growth and development of plants is deleteriously affected by various biotic and abiotic stress factors. Wounding in plants is caused by exposure to environmental stress, mechanical stress, and via herbivory. Typically, oxidative burst in response to wounding is associated with the formation of reactive oxygen species, such as the superoxide anion radical ($O_2^{\bullet-}$), hydrogen peroxide (H_2O_2) and singlet oxygen; however, few experimental studies have provided direct evidence of their detection in plants. Detection of $O_2^{\bullet-}$ formation in plant tissues have been performed using various techniques including electron paramagnetic resonance spin-trap spectroscopy, epinephrine-adrenochrome acceptor methods, staining with dyes such as tetrazolium dye and nitro blue tetrazolium (NBT); however, kinetic measurements have not been performed. In the current study, we provide evidence of $O_2^{\bullet-}$ generation and its kinetics in the leaves of spinach (*Spinacia oleracea*) subjected to wounding.

Methods. Real-time monitoring of $O_2^{\bullet-}$ generation was performed using catalytic amperometry. Changes in oxidation current for $O_2^{\bullet-}$ was monitored using polymeric iron-porphyrin-based modified carbon electrodes ($\varphi = 1$ mm) as working electrode with Ag/AgCl as the reference electrode.

Result. The results obtained show continuous generation of $O_2^{\bullet-}$ for minutes after wounding, followed by a decline. The exogenous addition of superoxide dismutase, which is known to dismutate $O_2^{\bullet-}$ to H_2O_2, significantly suppressed the oxidation current.

Conclusion. Catalytic amperometric measurements were performed using polymeric iron-porphyrin based modified carbon electrode. We claim it to be a useful tool and a direct method for real-time monitoring and precise detection of $O_2^{\bullet-}$ in biological samples, with the potential for wide application in plant research for specific and sensitive detection of $O_2^{\bullet-}$.

INTRODUCTION

The formation of reactive oxygen species (ROS) in plants is an unavoidable consequence of photosynthesis (*Ledford, Chin & Niyogi, 2007*; *Alessandro et al., 2011*; *Foyer & Shigeoka, 2011*; *Laloi & Havaux, 2015*). The introduction of molecular oxygen into the environment by photosynthetic organisms during the evolution of aerobic life is associated with the formation of ROS (*Tripathy & Oelmüller, 2012*). Plants growing in a fluctuating environment are exposed to various biotic stresses such as bacteria, viruses, fungi, parasites, insects, weeds, etc. and abiotic stresses such as fluctuations in temperature, salinity, water, radiation, toxic chemicals and mechanical stress which are closely linked to higher ROS production. The chloroplasts, mitochondria, and peroxisomes are among the chief organelles involved (*Elstner, 1991*; *Foyer & Harbinson, 1994*; *Asada, 1996*; *Turrens, 2003*; *Liu et al., 2007*; *Murphy, 2009*). As a response, ROS, including the superoxide anion radical ($O_2^{\bullet-}$), hydroperoxyl radical ($HO_2^{\bullet}$), hydrogen peroxide (H_2O_2), hydroxyl radical ($HO^{\bullet}$), singlet oxygen ($^1O_2$), peroxyl radical ($ROO^{\bullet}$), hydroperoxide ($ROOH$) and alkoxyl radical ($RO^{\bullet}$), are produced (*Miller, Shulaev & Mittler, 2008*; *Gill & Tuteja, 2010*; *Foyer & Noctor, 2005*; *Asada, 2006*; *Miller et al., 2009*; *Bhattacharjee, 2010*; *Choudhury et al., 2013*).

The production of ROS by an oxidative burst is an imperative element of the wound response in algae, plants, and animals (*McDowell et al., 2015*). As a response to wounding, plants release oligosaccharide cell wall fragments, which play an important role in the signaling cascade that initiates an intense, localized production of ROS (*Legendre et al., 1993*; *John et al., 1997*; *Stennis et al., 1998*). Wounding stimulates the production of $O_2^{\bullet-}$, H_2O_2 and nitric oxide (NO), which can directly attack encroaching pathogens at the site of the wound (*Murphy, Asard & Cross, 1998*; *Garces, Durzan & Pedroso, 2001*; *Jih, Chen & Jeng, 2003*). In *Arabidopsis thaliana* leaves measured under ambient light conditions, $O_2^{\bullet-}$ and H_2O_2 mainly originate from photosynthetic electron transport, predominantly at the site of wounding (*Morker & Roberts, 2011*). The role of NADPH oxidase in ROS production, however, was not completely ruled out. Therefore, the generation of $O_2^{\bullet-}$ and H_2O_2 can be attributed to the collective effect of wounding and light stress. $O_2^{\bullet-}$ generation in the root cells of plants in response to wounding has been studied by electron paramagnetic resonance (EPR) spin-trap spectroscopy and epinephrine-adrenochrome acceptor methods (*Vylegzhaninat et al., 2001*). Tiron (4, 5-dihydroxy-1, 3-benzene-disulfonic acid disodium salt) was used, and the tiron semiquinone EPR spectra showed $O_2^{\bullet-}$ generation. The level of $O_2^{\bullet-}$ production in the roots was measured with epinephrine which in the presence of $O_2^{\bullet-}$ is converted to adrenochrome and can be monitored at 480 nm by a spectrophotometer (*Misra & Fridovich, 1972*; *Barber & Kay, 1996*). In addition to spectroscopy, staining with dye, such as tetrazolium dye and nitro blue tetrazolium (NBT), has been used to detect the production of $O_2^{\bullet-}$ *in situ*, with visualization of $O_2^{\bullet-}$ generation as a purple formazan deposit within leaflet tissues (*Wohlgemuth et al., 2002*).

Although various methods, such as EPR spin-trapping spectroscopy (*Von, Schlosser & Neubacher, 1993*), chemiluminescence (*Anderson et al., 1991*), the reduction of NBT and the reduction of the redox protein cytochrome c (*Doke, 1983b*; *Doke, 1983a*; *Doke, 1985*) have been used to detect and monitor $O_2^{\bullet-}$, each of these methods has inadequate specificity and sensitivity. EPR spin-trapping spectroscopy is one of the most sensitive and specific method for ROS detection; however, kinetic measurements are not possible at the current stage of development. Chemiluminescence, also known as ultra-weak photon emission, has been widely used recently as a non-invasive method to understand the involvement of ROS in oxidative radical reactions (*Prasad & Pospíšil, 2012*; *Prasad & Pospíšil, 2013*; *Pospíšil, Prasad & Rác, 2014*); however, limitations with respect to the specificity for particular ROS involvement exists (*Halliwell & Gutteridge, 1989*).

Integration of metalloporphyrins into electropolymerized polymer electrodes have been developed rigorously over the last years because these materials are effective electrocatalysts for chemical as well as photochemical applications (*Bedioui et al., 1995*). Numerous authors have recently tested the potential use of electropolymerized metalloporphyrins as new electrode materials for chemical and biological sensors (*Deronzier & Moutet, 1996*; *Yim et al., 1993*; *Bedioui, Trevin & Devynck, 1996*). In our current study, we provide an experimental approach for the detection of $O_2^{\bullet-}$ by polymeric iron-porphyrin-based modified carbon electrode based on the reaction mechanism presented in Fig. 1A (*Yuasa & Oyaizu, 2005*). Detection of $O_2^{\bullet-}$ by highly sensitive and selective polymeric iron-porphyrin-based modified carbon electrodes was tested in *in vivo* leaf sample subjected to wounding. The current study introduces the use of catalytic amperometric biosensors for the real-time detection of $O_2^{\bullet-}$.

MATERIAL AND METHODS

Spinach leaves
Young spinach (*Spinacia oleracea)* leaves were washed twice with deionized water and were dark adapted for 2 h. For each measurement, a fresh spinach leaf of the approximately same age was chosen. All experiments were performed at room temperature under dark conditions to avoid interference from light sources.

Material and chemical reagents
The 5-(ethoxycarbonyl)-5-methyl-1-pyrroline N-oxide (EMPO) spin trap and capillary tubes used for EPR measurements were obtained from Alexis Biochemicals (Lausen, Switzerland) and Blaubrand intraMARK (Brand, Germany), respectively. The carbon electrodes ($\varphi = 1$ mm) were purchased from BAS Inc., ALS Co., Ltd. (Tokyo, Japan). Superoxide dismutase (SOD), xanthine oxidase and xanthine (X/XO) were purchased from Wako Pure Chemicals Industries, Ltd. (Osaka, Japan), Sigma-Aldrich chemie Gmbh (Munich, Germany) or Sigma-Aldrich Japan K.K. (Tokyo, Japan).
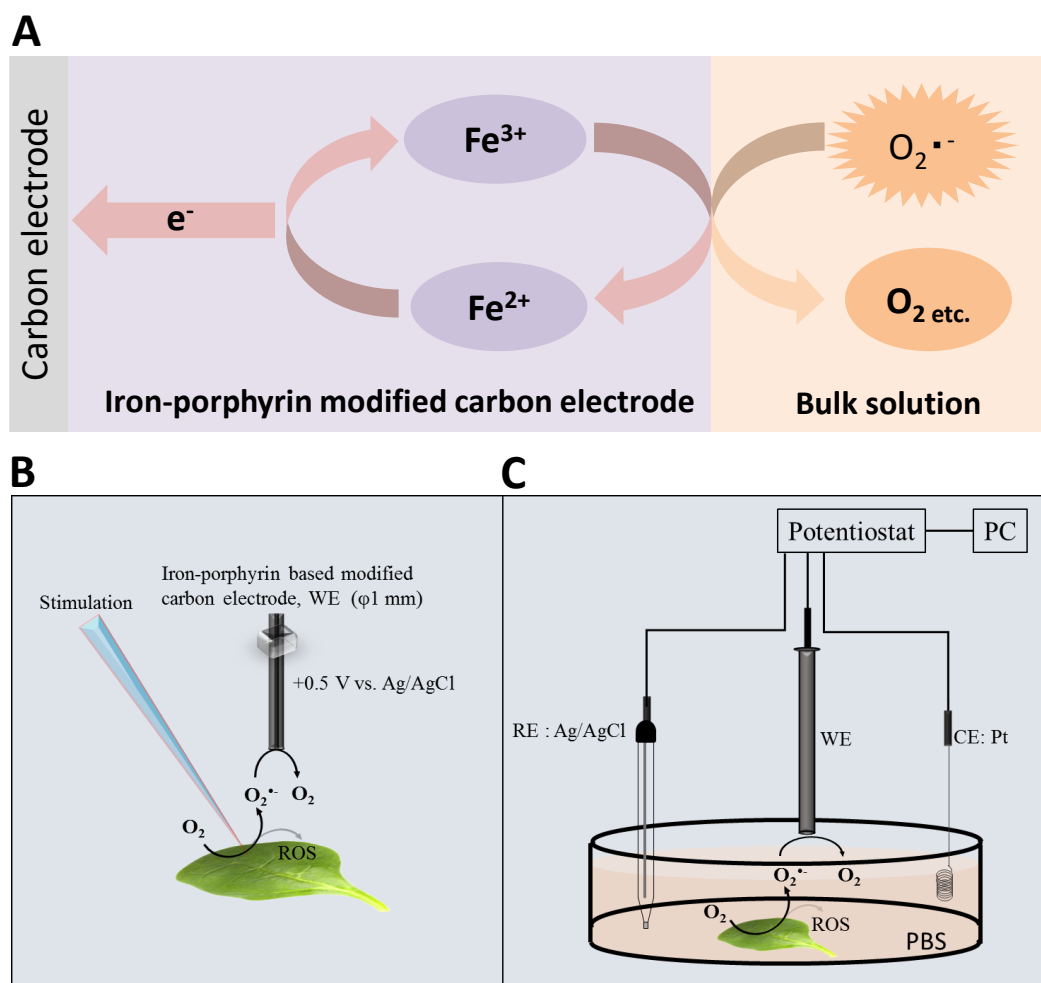
Figure 1 **Reaction mechanism and experimental setup.** (A) Schematic illustration of the reaction mechanism for the amperometric detection of $O_2^{\bullet-}$ using the polymeric iron-porphyrin-based modified carbon electrode depicting the reduction-oxidation cycle leading to generation of the oxidation current. (B and C) Schematic illustration of the experimental setup for the electrochemical measurements. The stimulation was performed using a glass capillary, and the polymeric iron-porphyrin-based modified carbon electron was positioned at a distance of 1 mm using a motor-driven XYZ microscopic stage (B). The *in vivo* generation of $O_2^{\bullet-}$ was measured using a polymeric iron-porphyrin-based modified carbon electron (working electrode, WE), platinum wire (counter electrode, CE) and Ag/AgCl (reference electrode, RE) (C).

Equipment and methods

Simultaneous measurements of the oxidation current of $O_2^{\bullet-}$ were performed using a potentiostat (HA1010mM4S; Hokuto Denko Co., Ltd., Japan). The polymeric iron-porphyrin-based modified carbon electrodes were positioned 1 mm from the site of injury using a motor-driven XYZ-stage (K101-20MS-M; Suruga Seiki Co., Ltd., Japan) (Fig. 1B). The detection of $O_2^{\bullet-}$ in the X/XO system was performed by EPR spin-trapping spectroscopy using 25 mM EMPO in phosphate buffer.
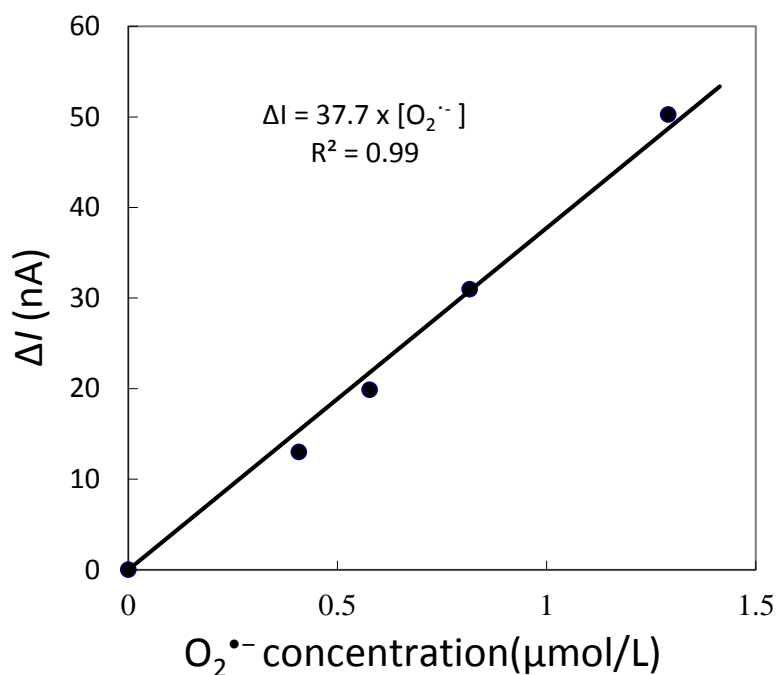
Figure 2 Calibration curve. Changes in oxidation current measured using iron-porphyrin-based modified carbon electrode by exogenous addition of a standard known concentration of $O_2^{\bullet-}$ generated *in situ* using X/XO system in the concentration range of 0.4–1.3 μM.

Experimental conditions for real-time monitoring of the oxidation current of $O_2^{\bullet-}$

The electrochemical detection of $O_2^{\bullet-}$ was measured using the X/XO system based on the method described in our recent study (*Matsuoka et al., 2014*) (Fig. 2). The subsequent oxidation current for $O_2^{\bullet-}$ was monitored using polymeric iron-porphyrin-based modified carbon electrodes ($\varphi = 1$ mm) with Ag/AgCl as the reference electrode.

Spinach leaves were fixed on a petri-dish with a diameter of 60 mm using double-sided adhesive tape. A total of 10 mM phosphate buffer saline (pH 7.2) (PBS) was gradually added to maintain a sufficient volume to submerge the whole spinach leaf in PBS. During the measurement, injury was performed using a glass capillary with an inner diameter of about 1.2 mm and wall thickness of 200 μm as presented in Fig. 1B and Data S1. For data presented in the manuscript, the injury/wounding in spinach leaves were done either one time or multiple times (between 8–10 times) while to visualize the state of leaves, injury/wounding was made one time, five times and 20 times (Data S1). Mechanical injury and mechanical wounding were performed close to the site of the electrode. The oxidation current was measured at +0.5 V vs. Ag/AgCl at room temperature.

Superoxide anion radical detection using polymeric iron-porphyrin-based modified carbon electrodes

The detection of $O_2^{\bullet-}$ was based on catalytic amperometry using a counter electrode and working electrode. The counter electrode was a platinum wire ($\varphi 0.25 \times 40$ mm), and the working electrode ($\varphi 1$ mm) was a polymeric iron-porphyrin-based modified carbon

electrode. Ag/AgCl was used as a reference electrode. The polymeric iron-porphyrin-based modified carbon electrode acted as an $O_2^{\bullet-}$ detection sensor. The polymeric iron-porphyrin-based modified carbon electrode was prepared by the electropolymerization of 1-methylimidazole-coordinated mesotetra (3-thienyl) porphyrin ([Fe(im)$_2$(ttp)]Br) (*Yuasa & Oyaizu, 2005*; *Yuasa et al., 2005*). Electropolymerization was performed in a two-chamber three-electrode electrochemical cell by potential cycling from 0 to +2.0 V vs. Ag/Ag$^+$ with a potential sweep rate of 50 mV s^{-1}. After rinsing with dichloromethane, the polymeric iron-porphyrin-based modified carbon electrode was obtained (*Yuasa & Oyaizu, 2005*; *Yuasa et al., 2005*). For the basic characterization of the polymeric iron-porphyrin-based modified carbon electrode, a differential pulse voltammogram of the electropolymerized [Fe(im)$_2$(ttp)]Br complex was recorded in an aqueous electrolyte solution containing 10 mM PBS (pH 7.2) using a high-performance potentiostat HZ-7000 (Hokuto Denko Co., Ltd., Japan) (Data S2).

RESULTS

Characterization and sensitivity evaluation of an iron-porphyrin-based modified carbon electrode

The characterization of the polymeric iron-porphyrin-based modified carbon electrode was performed using a differential pulse voltammogram (DPV) (Data S2). The polymerized complex was electroactive, with a mean redox potential at −0.25 V for the Fe^{2+}/Fe^{3+} couple.

Generation of $O_2^{\bullet-}$ in the chemical system and sensitivity evaluation of the polymeric iron-porphyrin-based modified carbon electrode

The xanthine/xanthine oxidase system is used for the formation of $O_2^{\bullet-}$ by the reduction of molecular oxygen (*Olson et al., 1974*; *Richter, 1979*; *Porras, Olson & Palmer, 1981*). To confirm the formation of $O_2^{\bullet-}$ in the chemical system used in the later experimental procedures, we measured the EMPO-OOH adduct EPR signal (Data S3: A). The intensity of the EMPO-OOH adduct EPR signal in the control (xanthine) and chemical system (X/XO) was also measured (Data S3: B). In the absence of xanthine oxidase, no EMPO-OOH adduct EPR signal was observed, whereas in the presence of XO, an EMPO-OOH adduct EPR signal was observed (Data S3).

To determine the sensitivity of the polymeric iron-porphyrin-based modified carbon electrode, the response of the exogenous addition of a standard known concentration of $O_2^{\bullet-}$ generated *in situ* was measured using X/XO system. A linear increase in oxidation current was observed with an increase in $O_2^{\bullet-}$ concentration. The calibration curve (Δi vs $O_2^{\bullet-}$) was found to be linear in the concentration range of 0.4 to 1.3 µM (Fig. 2). This indicates that the sensitivity of the electrochemical sensor is in the range of µM concentration, reflecting changes in the oxidation current in the order of tens of nA (Fig. 2).

Real-time monitoring of $O_2^{\bullet-}$ generation during wounding of spinach leaves

To validate that there is no interference in the measurement caused by the suspension of spinach leaf in PBS, the oxidation current was measured in a non-wounded spinach
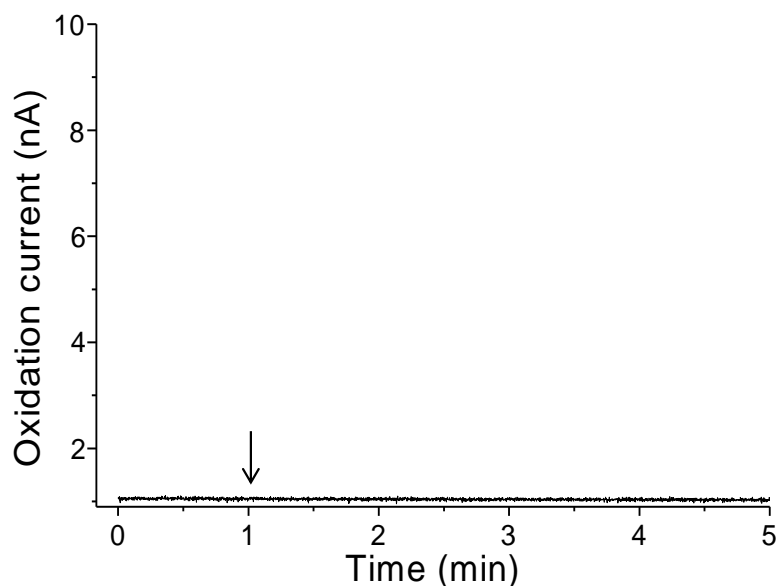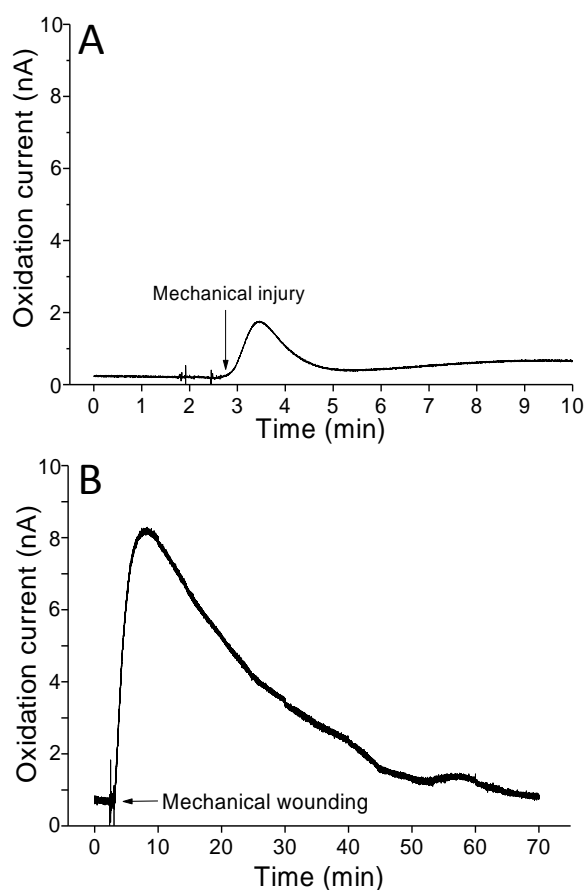
Figure 3 **Real-time monitoring of the oxidation current of $O_2^{\bullet-}$ from spinach leaves.** The kinetics of the production of $O_2^{\bullet-}$ were measured using a polymeric iron-porphyrin-based modified carbon electrode on non-wounded spinach leaves.

leaf suspended in PBS (Fig. 3). No fluctuation in the oxidation current of $O_2^{\bullet-}$ was observed in the non-wounded spinach leaf suspended in PBS, (Fig. 3), whereas a negligible fluctuation was observed with the exogenous addition of SOD (data not shown). These results indicate that these chemical species (PBS and SOD) do not interfere with the measurements. The kinetics of the production of $O_2^{\bullet-}$ were also measured in the chemical system containing no spinach leaves and in the presence of SOD (400 U ml^{-1}) indicating no significant fluctuation in oxidation current (Data S4).

Real-time monitoring of the oxidation current for $O_2^{\bullet-}$ was performed in spinach leaves where mechanical injury was stimulated one time using a glass tube (Fig. 4A) and mechanical wounding was done multiple times (Fig. 4B). The wounding in spinach leaves was done one time (4A) and multiple times (between 8–10 times) (4B) using a glass capillary with an inner diameter of about 1.2 mm and wall thickness of 200 μm. The results indicate that the $O_2^{\bullet-}$ production increased considerably with the dose of mechanical injury (Fig. 4). Furthermore, to visualize the extend of damage to leaf during mechanical injury induced by glass capillary, photograph of leaves showing the physiological state have been presented along with kinetics on real-time monitoring of the oxidation current of $O_2^{\bullet-}$ under experimental condition mentioned in dataset presented (Data S1). To determine the concentration of $O_2^{\bullet-}$ generated in mechanically injured spinach leaves, the calibration curve was established for various concentrations obtained using standard X/XO system (Fig. 2). A maximum oxidation current (Δi) of 1.5 nA (at time span, 60 s) and 7.5 nA (at time span, 300 s) was observed in mechanically injury made at a minimal dose (Fig. 4A) and at multiple sites (Fig. 4B). Based on the data obtained and the maximum
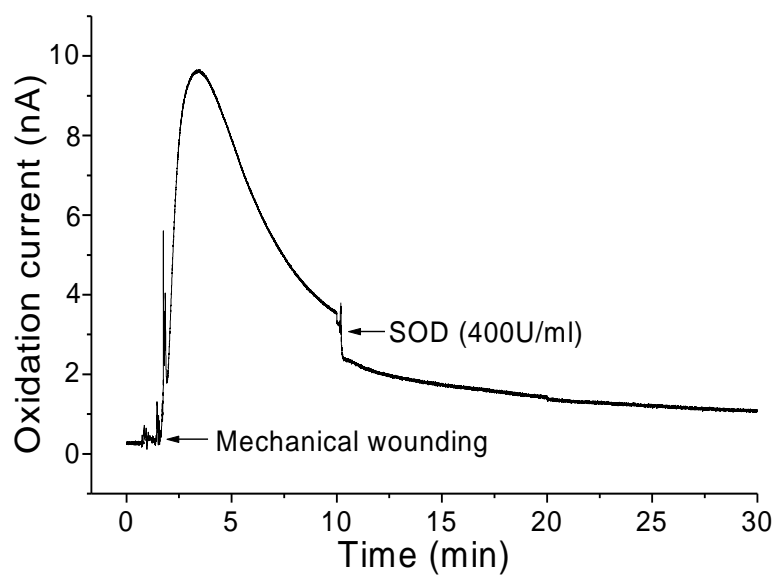
Figure 4 **Real-time monitoring of oxidation current for $O_2^{\bullet-}$ during wounding.** The kinetics of the production of $O_2^{\bullet-}$ were measured using a polymeric iron porphyrin based modified carbon electrode during wounding in spinach leaves. The wounding in spinach leaves was done one time (A) and multiple times (B) close to the site of electrode during the measurement and oxidation current for $O_2^{\bullet-}$ was measured.

Table 1 **Calculation.** Superoxide anion radical ($O_2^{\bullet-}$ concentration calculated using standard calibration curve ($R^2 = 0.9918$) (Fig. 2). The total change in oxidation current was found to be 1.5 nA (Δi) for minimal dose of injury (Fig. 4A) and 7.5 nA (Δi) for injury at multiple sites (Fig. 4B). The total $O_2^{\bullet-}$ concentration was found to be equivalent to 40 nM (Fig. 4A) and 200 nM (Fig. 4B) at 60 s and 300 s, respectively.

	A	B
Δi (nA)	1.5	7.5
Δt (s)	60	300
$O_2^{\bullet-}$ (nM)	**40**	**200**

oxidation current recorded, the $O_2^{\bullet-}$ was calculated and expected production was found to be about 40 nM (4A) and about 200 nM (4B) (Table 1).

In addition, $O_2^{\bullet-}$ generation was also measured in spinach leaves under the effect of wounding at room temperature in presence of exogenous addition of SOD (Fig. 5). In the absence of wounding, as observed during the first minute of real-time monitoring, no considerable change in the oxidation currents of $O_2^{\bullet-}$ was observed. However, wounding
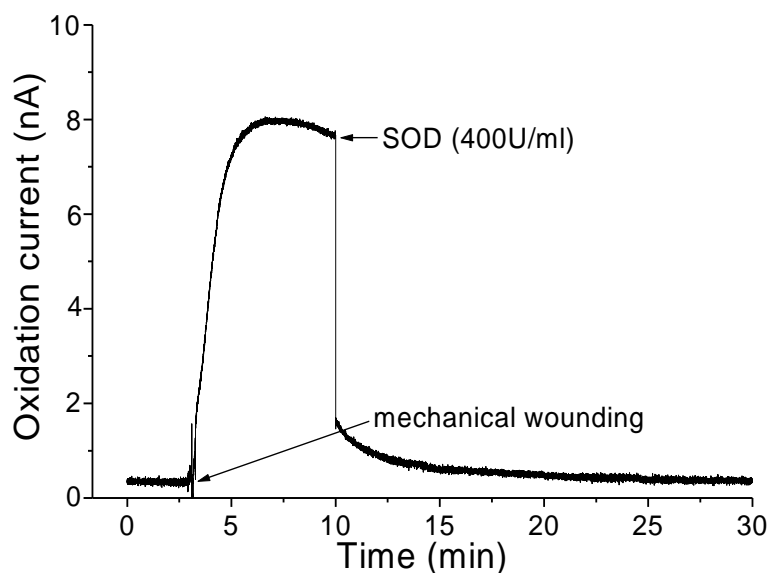
Figure 5 **Real-time monitoring of the oxidation current of $O_2^{\bullet-}$ during wounding.** The kinetics of the production of $O_2^{\bullet-}$ were measured using a polymeric iron-porphyrin-based modified carbon electrode during wounding in spinach leaves. The wounding of spinach leaves was performed during the measurement, and the oxidation current for $O_2^{\bullet-}$ was measured for approximately 30 min. The effect of SOD on the oxidation current was measured in the presence of SOD (400 U ml^{-1}) added exogenously during the measurement.

instantaneously resulted in a fast increase in the oxidation current for $O_2^{\bullet-}$ of approximately 10 nA, followed by a gradual decrease, which continued for more than 10 min. To confirm the production of $O_2^{\bullet-}$, the effect of SOD, which leads to the dismutation of $O_2^{\bullet-}$ to H_2O_2, on the oxidation current in a wounded spinach leaf was analyzed. The addition of 400 U ml^{-1} SOD suppressed the oxidation current for $O_2^{\bullet-}$ from 3.5 nA to 2 nA (Fig. 5). However, complete suppression of the oxidation current was not observed. The oxidation current, which persisted at approximately 1 nA for a few minutes, can be attributed to rapid $O_2^{\bullet-}$ diffusion to the electrode before its conversion to H_2O_2 or to the limited SOD activity at a fixed concentration. The effect of SOD (400 U ml^{-1}) added exogenously was also measured at the point of maximum oxidation current where a comparatively higher suppression was recorded (Fig. 6).

DISCUSSION

In addition to plants, ROS detections have been performed in model system including animals. During recent past, Zuo and coworkers (*2011*, *2013*) presented results on intracellular ROS formation in single isolated frog myofibers during low P_{O2} conditions using dihydrofluorescein (Hfluor), a fluorescein analog of DCFH. Cyt c assay was also used to measure $O_2^{\bullet-}$ in contracting skeletal muscle in pulmonary TNF-α overexpression mice (*Zuo et al., 2014*; *Zuo et al., 2004*). Several mechanisms for the generation of ROS involving $O_2^{\bullet-}$ have been suggested. It has been proposed previously that an NADPH oxidase-like enzyme in the plant plasma membrane is involved in the production of

Figure 6 **Real-time monitoring of oxidation current for $O_2^{\bullet-}$ during wounding.** The kinetics of the production of $O_2^{\bullet-}$ was measured using a polymeric iron porphyrin based modified carbon electrode during wounding in spinach leaves. The wounding in spinach leaves was done during the measurement and oxidation current for $O_2^{\bullet-}$ was measured for a duration of about 30 min. Effect of SOD was measured in the presence of SOD (400 U ml^{-1}) added exogenously during the measurement at the point of maximum oxidation current.

$O_2^{\bullet-}$ which is then converted to the more stable H_2O_2 during the oxidative burst in response to pathogen attack of plant cells (*Murphy & Auh, 1996*; *Doke et al., 1996*). In skeletal muscle, the major source of ROS especially extracellular $O_2^{\bullet-}$ formation is via the arachidonic acid metabolism through lipoxygenase (LOX) activity (*Zuo et al., 2004*). However, in contrast to the view that wound-induced ROS are primarily produced extracellularly by NADPH oxidase enzymes (*Watanabe & Sakai, 1998*; *Flor-Henry et al., 2004*), it has been recently indicated that wound-induced $O_2^{\bullet-}$ and H_2O_2 originate from photosynthetic electron transport measured at wounded sites under ambient light conditions (*Morker & Roberts, 2011*). The $O_2^{\bullet-}$ is produced during the electron transport process by the reduction of molecular oxygen in the chloroplasts and mitochondria. The authors proposed that $O_2^{\bullet-}$ and H_2O_2 production is linked to wounding, which is enhanced significantly under light conditions.

A recent report on *Pisum sativum* seedlings proposes a mechanism responsible for oxidative burst during wounding. During mechanical wounding, polyunsaturated fatty acids (PUFA), polyamines, LOX and peroxidases (Prx) are released in the extracellular matrix. Under these circumstances, LOX is involved in the oxidation of PUFA or polyamines, which induces diamine oxidases (DAO) to produce H_2O_2, further leading to $O_2^{\bullet-}$ production catalyzed by Prx (*Roach et al., 2015*). A diverse range of organisms use Prx to produce $O_2^{\bullet-}$, e.g., *Triticum sativum* roots (*Minibayeva et al., 2009*), *Castanea sativa* and *Trichilia* seeds (*Roach et al., 2009*; *Whitaker et al., 2010*), liverworts (*Li et al., 2010*), and lichens (*Liers et al., 2011*). Another group of redox enzyme involved in the

wound-induced oxidative burst is DAO (*Rea et al., 2002*; *Cona et al., 2006*; *Yoda, Hiroi & Sano, 2006*; *Angelini et al., 2008*), and cooperation between DAO and Prx is considered important in the wound response. In addition to DAO and Prx, LOX not only generates lipid hydroperoxides (LOOH) but can also generate $O_2^{\bullet-}$ via the oxidation of pyridine nucleotides and therefore considerably contributes to oxidative stress in cells (*Roy et al., 1994*). Lipid oxidation by LOX is an important part of the wound-response because oxylipins, the break-down products of lipid peroxides, can act as effective signaling molecules to rapidly induce transcriptional changes during wounding (*Upchurch, 2008*; *Higdon et al., 2012*). Plasma membrane-bound Prx can utilize PUFA such as linoleic acid released at the wound site for the synthesis of $O_2^{\bullet-}$. Even if LOX is not known to be directly involved in $O_2^{\bullet-}$ production, it was suggested that extracellular LOX may play an important role by competing with Prx for fatty acids and producing reactive electrophiles that coordinate signaling responses (*Doke et al., 1996*).

The electrochemical method with the employment of different modified electrodes have been successfully standardized and applied for detection of varied ROS including $O_2^{\bullet-}$ during the recent past (*Groenendaal Jonas et al., 2000*; *Yuasa & Oyaizu, 2005*; *Yuasa et al., 2005*). The polymeric iron-porphyrin-based modified carbon electrode is a useful tool and provides a direct method for real-time monitoring and precise detection of $O_2^{\bullet-}$ in biological samples *in-situ* (*Yuasa et al., 2005*). The kinetic measurement showing the production of $O_2^{\bullet-}$ for a long range of time (minutes) presented in our study (https://ecs.confex.com/ecs/229/webprogram/Paper70675.html) have been demonstrated and thus opens a new area of investigation which have always been difficult to explore using other available methods such as EPR spin trapping spectroscopy, fluorescence microscopy and other biochemical methods etc. Thus, the electrode has strong potential for wide application in plant research for the specific and sensitive detection of $O_2^{\bullet-}$ and the kinetic behavior in real-time. In addition to points mentioned above, using synthetic porphyrin has an additional advantage. To date, $O_2^{\bullet-}$ sensors based on naturally derived enzyme (e.g., SOD, Cyt. c) have been developed (*Di, Bi & Zhang, 2004*). However, enzymes on the sensor are likely to be denatured. In contrast, the porphyrin based sensor can be used without denaturation. At the same time, the current method is cost effective. Certain limitations exist; the current polymeric iron-porphyrin-based modified carbon electrodes are light-sensitive, which might hinder its photo-electrochemical applicability (*Brett & Brett, 1984*).

CONCLUSION

In the current study, we present our polymeric iron-porphyrin based modified carbon electrode for application in real-time monitoring and precise detection of $O_2^{\bullet-}$ in biological system. It has strong potential for wide application in plant research for specific and sensitive detection of $O_2^{\bullet-}$.

ADDITIONAL INFORMATION AND DECLARATIONS

Competing Interests

Ryo Matsuoka and Shigeo Aoyagi are employees of Hokuto Denko Corporation, Tokyo, Japan, and bear no competing interests. In addition, all other authors declare there are no competing interests.

Author Contributions

- Ankush Prasad conceived and designed the experiments, performed the experiments, analyzed the data, wrote the paper, prepared figures and/or tables.
- Aditya Kumar performed the experiments, wrote the paper.
- Ryo Matsuoka performed the experiments, reviewed drafts of the paper.
- Akemi Takahashi, Ryo Fujii and Yamato Sugiura performed the experiments.
- Hiroyuki Kikuchi, Shigeo Aoyagi, Tatsuo Aikawa, Takeshi Kondo and Makoto Yuasa reviewed drafts of the paper.
- Pavel Pospíšil contributed reagents/materials/analysis tools, reviewed drafts of the paper.
- Shigenobu Kasai conceived and designed the experiments, contributed reagents/materials/analysis tools, reviewed drafts of the paper.

Data Availability

The following information was supplied regarding data availability:
The raw data has been supplied as a Supplementary File.

Supplemental Information

Supplemental information for this article can be found online at http://dx.doi.org/10.7717/peerj.3050#supplemental-information.

REFERENCES

Alessandro A, Osto LD, Aprile A, Carillo P, Roncaglia E, Cattivelli L, Bassi R. 2011. Reactive oxygen species and transcript analysis upon excess light treatment in wild-type *Arabidopsis thaliana* vs a photosensitive mutant lacking zeaxanthin and lutein. *BMC Plant Biology* **11**:62 DOI 10.1186/1471-2229-11-62.

Anderson AA, Rogers K, Tepper CS, Blee K, Cardon J. 1991. Timing of molecular events following elicitor treatment of plant cells. *Physiology and Molecular Plant Pathology* **38**:1–13 DOI 10.1016/S0885-5765(05)80139-0.

Angelini R, Tisi A, Rea G, Chen MM, Botta M, Federico R, Cona A. 2008. Involvement of polyamine oxidase in wound healing. *Plant Physiology* **146**:162–177 DOI 10.1104/pp.107.108902.

Asada K. 1996. Radical production and scavenging in the chloroplasts. In: Baker NR, ed. *Photosynthesis and the environment.* Dordrecht: Kluwer, 123–150.

Asada K. 2006. Production and scavenging of reactive oxygen species in chloroplasts and their functions. *Plant Physiology* **141**:391–396 DOI 10.1104/pp.106.082040.

Barber MJ, Kay CJ. 1996. Superoxide production during reduction of molecular oxygen by assimilatory nitrate reductase. *Archives of Biochemistry and Biophysics* **326**:227–232 DOI 10.1006/abbi.1996.0069.

Bedioui F, Devynck J, Charreton CB. 1995. Immobilization of metalloporphyrins in electropolymerized films: design and applications. *Accounts of Chemical Research* **28(1)**:30–36 DOI 10.1021/ar00049a005.

Bedioui F, Trevin S, Devynck J. 1996. Chemically modified microelectrodes designed for the electrochemical determination of nitric oxide in biological systems. *Electroanalysis* **8**:1085–1091 DOI 10.1002/elan.1140081202.

Bhattacharjee S. 2010. Sites of generation and physicochemical basis of formation of reactive oxygen species in plant cell. In: Dutta Gupta S, ed. *Reactive oxygen species and antioxidants in higher plants.* New York: CRC Press, 1–30.

Brett CMA, Brett AMCFO. 1984. Surface modified electrode-reasons and advantages. In: Kossowsky R, Singhal SC, eds. *Surface engineering: surface modification of materials.* Pittsburg: Westinghouse R & D center, 656–664.

Choudhury S, Panda P, Sahoo L, Panda SK. 2013. Reactive oxygen species signalling in plants under abiotic stress. *Plant Signaling & Behaviour* **8**:e23681 DOI 10.4161/psb.23681.

Cona A, Rea G, Botta M, Corelli F, Federico R, Angelini R. 2006. Flavin containing polyamine oxidase is a hydrogen peroxide source in the oxidative response to the protein phosphatase inhibitor cantharidin in Zea mays L. *Journal of Experimental Botany* **57**:2277–2289 DOI 10.1093/jxb/erj195.

Deronzier A, Moutet JC. 1996. Polypyrrole films containing metal complexes: syntheses and applications. *Coordination Chemistry Reviews* **147**:339–371 DOI 10.1016/0010-8545(95)01130-7.

Di J, Bi S, Zhang M. 2004. Third-generation superoxide anion sensor based on superoxide dismutase directly immobilized by sol–gel thin film on gold electrode. *Biosensors and Bioelectronics* **19**:1479–1486 DOI 10.1016/j.bios.2003.12.006.

Doke N. 1983a. Generation of superoxide anion by potato tuber protoplasts during the hypersensitive response to hyphal wall components of Phytophthora infestans and specific inhibition of the reaction by suppressors of hypersensitivity. *Physiological Plant Pathology* **23**:359–367 DOI 10.1016/0048-4059(83)90020-6.

Doke N. 1983b. Involvement of superoxide anion generation in the hypersensitive response of potato tuber tissues to infection with an incompatible race of Phytophthora infestans and to the hyphal wall components. *Physiological Plant Pathology* **23**:345–357 DOI 10.1016/0048-4059(83)90019-X.

Doke N. 1985. NADPH-dependent $O_2^{\bullet-}$ generation in membrane fractions isolated from wounded potato tubers inoculated with Phytophthora infestans. *Physiological Plant Pathology* **27**:311–322 DOI 10.1016/0048-4059(85)90044-X.

Doke N, Miura J, Sanchez LM, Park HJ, Noritake T, Yoshioka H, Kawakita K. 1996. The oxidative burst protects plants against pathogen attack: mechanism and role as an emergency signal for plant bio-defence—a review. *Gene* **179**:45–51 DOI 10.1016/S0378-1119(96)00423-4.

Elstner EF. 1991. Mechanisms of oxygen activation in different compartments of plant cells. In: Pell EJ, Steffen KL, eds. *Active oxygen/oxidative stress and plant metabolism.* Rockville: American Society of Plant Physiologists, 13–25.

Flor-Henry M, McCabe TC, Bruxelles GL de, Roberts MR. 2004. Use of a highly sensitive two-dimensional luminescence imaging system to monitor endogenous bioluminescence in plant leaves. *BMC Plant Biology* **4**:19 DOI 10.1186/1471-2229-4-19.

Foyer CH, Harbinson J. 1994. Oxygen metabolism and the regulation of photosynthetic electron transport. In: Foyer CH, Mullineaux P, eds. *Causes of photooxidative stresses and amelioration of defense systems in plants.* Boca Raton: CRC Press, 1–42.

Foyer CH, Noctor G. 2005. Redox homeostasis and antioxidant signaling: a metabolic interface between stress perception and physiological responses. *The Plant Cell* **17**:1866–1875 DOI 10.1105/tpc.105.033589.

Foyer CH, Shigeoka S. 2011. Understanding oxidative stress and antioxidant functions to enhance photosynthesis. *Plant Physiology* **155**:93–100 DOI 10.1104/pp.110.166181.

Garces H, Durzan D, Pedroso MC. 2001. Mechanical stress elicits nitric oxide formation and DNA fragmentation in *Arabidopsis thaliana*. *Annals of Botany* **87**:567–574 DOI 10.1006/anbo.2000.1356.

Gill SS, Tuteja N. 2010. Reactive oxygen species and antioxidant machinery in abiotic stress tolerance in crop plants. *Plant Physiology and Biochemistry* **48**:909–930 DOI 10.1016/j.plaphy.2010.08.016.

Groenendaal Jonas F, Freitag D, Pielartzik H, Reynolds JR. 2000. Poly(3,4 ethylenedioxythiophene) and its derivatives: past, present, and future. *Advanced Materials* **12**:481–494 DOI 10.1002/(SICI)1521-4095(200004)12:7<481::AID-ADMA481>3.0.CO;2-C.

Halliwell B, Gutteridge JMC. 1989. *Free radicals in biology and medicine.* 2nd edition. Oxford: Clarendon Press.

Higdon A, Diers AR, Oh J, Landar Y, Darley-Usmar VM. 2012. Cell signalling by reactive lipid species: new concepts and molecular mechanisms. *Biochemical Journal* **442**:453–464 DOI 10.1042/BJ20111752.

Jih PJ, Chen YC, Jeng ST. 2003. Involvement of hydrogen peroxide and nitric oxide in expression of the ipomoelin gene from sweet potato. *Plant Physiology* **132**:381–389 DOI 10.1104/pp.102.015701.

John M, Rohrig G, Schmidt J, Walden R, Schell J. 1997. Cell signaling by oligosaccha-rides. *Trends in Plant Science* **2**:111–115 DOI 10.1016/S1360-1385(97)01005-4.

Laloi C, Havaux M. 2015. Key players of singlet oxygen-induced cell death in plants. *Frontiers in Plant Science* **6**:Article 39 DOI 10.3389/fpls.2015.00039.

Ledford HK, Chin BL, Niyogi KK. 2007. Acclimation to singlet oxygen stress in Chlamy-domonas reinhardtii. *Eukaryotic Cell* **6**:919–930 DOI 10.1128/EC.00207-06.

Legendre L, Rueter S, Heinstein PF, Low PS. 1993. Characterization of the oligogalacturonide-induced oxidative cells. *Plant Physiology* **102**:233–240 DOI 10.1104/pp.102.1.233.

Li JLY, Sulaiman M, Beckett RP, Minibayeva FV. 2010. Cell wall peroxidases in the liv-erwort Dumortiera hirsuta are responsible for extracellular superoxide production, and can display tyrosinase activity. *Physiologia Plantarum* **138**:474–484 DOI 10.1111/j.1399-3054.2009.01318.x.

Liers C, Ullrich C, Hofrichter M, Minibayeva FV, Beckett RP. 2011. Oxidoreductases from lichenized ascomycetes: purification and characterization of a heme-peroxidase from Leptogium saturninum that oxidizes high-redox potential substrates. *Fungal Genetics and Biology* **48**:1139–1145 DOI 10.1016/j.fgb.2011.10.004.

Liu Y, Ren D, Pike S, Pallardy S, Gassmann W, Zhang S. 2007. Chloroplast-generated reactive oxygen species are involved in hypersensitive response-like cell death mediated by a mitogen-activated protein kinase cascade. *Plant Journal* **51**:941–954 DOI 10.1111/j.1365-313X.2007.03191.x.

Matsuoka R, Igarashi M, Kondo T, Aikawa T, Yuasa M. 2014. Biomimetic antithrombo-genic electrochemical superoxide anion radical sensor. *Journal of the Electrochemical Society* **161(6)**:B163–B166 DOI 10.1149/2.099403jes.

McDowell RE, Amsler MO, Li Q, Lancaster Jr JR, Amsler CD. 2015. The immediate wound induced oxidative burst of Saccharina latissimi depends on light via photo-synthetic electron transport. *Journal of Phycology* **51**:431–441 DOI 10.1111/jpy.12302.

Miller G, Schlauch K, Tam R, Cortes D, Torres MA, Shulaev V, Dangl JL, Mittler R. 2009. The plant NADPH oxidase RBOHD mediates rapid systemic signaling in response to diverse stimuli. *Science Signaling* **2(84)**:45–49 DOI 10.1126/scisignal.2000448.

Miller G, Shulaev V, Mittler R. 2008. Reactive oxygen signaling and abiotic stress. *Physiologia Plantarum* **133(3)**:481–489 DOI 10.1111/j.1399-3054.2008.01090.x.

Minibayeva F, Kolesnikov O, Chasov A, Beckett RP, Luthje S, Vylegzhanina N, Buck F, Bottger M. 2009. Wound-induced apoplastic peroxidases activities: their roles in the production and detoxification of reactive oxygen species. *Plant Cell Environment* **32**:497–508 DOI 10.1111/j.1365-3040.2009.01944.x.

Misra HR, Fridovich I. 1972. The univalent reduction of oxygen by reduced flavins and quinones. *The Journal of Biological Chemistry* **247**:188–192.

Morker KH, Roberts MR. 2011. Light as both an input and an output of wound-induced reactive oxygen formation in Arabidopsis leaves. *Plant Signaling and Behaviour* **6(8)**:1–3 DOI 10.4161/psb.6.1.13880.

Murphy MP. 2009. How mitochondria produce reactive oxygen species. *Biochemical Journal* **417**:1–13 DOI 10.1042/BJ20081386.

Murphy TM, Asard H, Cross AR. 1998. Possible sources of reactive oxygen during the oxidative burst in plants. In: Asard H, Berczi A, eds. *Plasma membrane redox systems and their role in biological stresses and disease.* Dordrecht: Kluwer Academic Publishers, 215–246.

Murphy TM, Auh CK. 1996. The superoxide synthases of plasma membrane preparations from cultured rose cells. *Plant Physiology* **110**:621–629 DOI 10.1104/pp.110.2.621.

Olson JS, Ballou DP, Palmer GS, Massey V. 1974. The reaction of xanthine oxidase with molecular oxygen. *The Journal of Biological Chemistry* **249**:4350–4362.

Porras AG, Olson JS, Palmer G. 1981. The reaction of reduced xanthine oxidase with oxygen. Kinetics of peroxide and superoxide formation. *The Journal of Biological Chemistry* **256**:9096–9103.

Pospíšil P, Prasad A, Rác M. 2014. Role of reactive oxygen species in ultra-weak photon emission in biological systems. *Journal of Photochemistry and Photobiology B* **139**:11–23 DOI 10.1016/j.jphotobiol.2014.02.008.

Prasad A, Pospíšil P. 2012. Ultraweak photon emission induced by visible light and ultraviolet A radiation via photoactivated skin chromophores: *in vivo* charge coupled device imaging. *Journal of Biomedical Optics* **17(8)**:Article 85004 DOI 10.1117/1.JBO.17.8.085004.

Prasad A, Pospíšil P. 2013. Towards the two-dimensional imaging of spontaneous ultraweak photon emission from microbial, plant and animal cells. *Scientific Reports* **3**:Article 1211 DOI 10.1038/srep01211.

Rea G, Metoui O, Infantino A, Federico R, Angelini R. 2002. Copper amine oxidase expression in defense responses to wounding and Ascochyta rabiei invasion. *Plant Physiology* **128**:865–875 DOI 10.1104/pp.010646.

Richter C. 1979. Redox intermediates between O_2 and H_2O. In: Carafoli E, Semenza G, eds. *Membrane biochemistry. A laboratory manual on transport and bioenergetics.* New York: Springer-Verlag.

Roach T, Beckett RP, Minibayeva FV, Colville L, Whitaker C, Chen H, Bailly C, Kranner I. 2009. Extracellular superoxide production, viability and redox poise in response to desiccation in recalcitrant *Castanea sativa* seeds. *Plant Cell Environment* **33**:59–75.

Roach T, Colville L, Beckett RP, Minibayeva FV, Havaux M, Kranner I. 2015. A proposed interplay between peroxidase, amine oxidase and lipoxygenase in the wounding-induced oxidative burst in *Pisum sativum* seedlings. *Phytochemistry* **112**:130–138 DOI 10.1016/j.phytochem.2014.06.003.

Roy P, Roy SK, Mitra A, Kulkarni AP. 1994. Superoxide generation by lipoxygenase in the presence of NADH and NADPH. *Biochimica et Biophysica Acta* **1214**:171–179 DOI 10.1016/0005-2760(94)90041-8.

Stennis M, Chandra S, Ryan C, Low P. 1998. Systemin potentiates the oxidative burst in cultured tomato cells. *Plant Physiology* **117**:1031–1036 DOI 10.1104/pp.117.3.1031.

Tripathy BC, Oelmüller R. 2012. Reactive oxygen species generation and signaling in plants. *Plant Signaling and Behavior* **7(12)**:1621–1633 DOI 10.4161/psb.22455.

Turrens JF. 2003. Mitochondrial formation of reactive oxygen species. *Journal of Physiology* **552**:335–344 DOI 10.1113/jphysiol.2003.049478.

Upchurch RG. 2008. Fatty acid unsaturation, mobilization, and regulation in the response of plants to stress. *Biotechnology Letters* **30**:967–977 DOI 10.1007/s10529-008-9639-z.

Von GM, Schlosser E, Neubacher H. 1993. Evidence from electron-spin resonance for the formation of free radicals during infection of Avena sativa by Drechslera spp. *Physiology and Molecular Plant Pathology* **42**:405–412 DOI 10.1006/pmpp.1993.1030.

Vylegzhaninat NN, Gordon LK, Minibayeva FV, Kolesnikov OP. 2001. Superoxide production as a stress response of wounded root cells: ESR spin-trap and acceptor methods. *Applied Magnetic Resonance* **21**:63–70 DOI 10.1007/BF03162440.

Watanabe T, Sakai S. 1998. Effects of active oxygen species and methyl jasmonate on expression of the gene for a wound-inducible 1-aminocyclopropane-1-carboxylate synthase in winter squash (C. maxima). *Planta* **206**:570–576 DOI 10.1007/s004250050434.

Whitaker C, Beckett RP, Minibayeva FV, Kranner I. 2010. Production of reactive oxygen species in excised, desiccated and cryopreserved explants of Trichiliadregeana. *South African Journal of Botany* **76**:112–118 DOI 10.1016/j.sajb.2009.09.008.

Wohlgemuth H, Mittelstrass K, Kschieschan S, Bender J, Weigel HJ, Overmyer K, Kangasjärvi J, Sandermann H, Langebartels C. 2002. Activation of an oxidative burst is a general feature of sensitive plants exposed to the air pollutant ozone. *Plant Cell Environment* **25**:717–726 DOI 10.1046/j.1365-3040.2002.00859.x.

Yim HS, Kibbey CE, Ma SC, Kliza DM, Liu D, Park SB, Terre CE, Meyerhoff ME. 1993. Polymer membrane-based ion-, gas- and bio-selective potentiometric sensors. *Biosensors and Bioelectronics* **8**:1–38 DOI 10.1016/0956-5663(93)80041-M.

Yoda H, Hiroi Y, Sano H. 2006. Polyamine oxidase is one of the key elements for oxidative burst to induce programmed cell death in tobacco cultured cells. *Plant Physiology* **142**:193–206 DOI 10.1104/pp.106.080515.

Yuasa M, Oyaizu K. 2005. Electrochemical detection and sensing of reactive oxygen species. *Current Organic Chemistry* **9**:1685–1697 DOI 10.2174/1385272057746110921.

Yuasa M, Oyaizu K, Yamaguchi A, Ishikawa M, Eguchi K, Kobayashi T, Toyoda Y, Tsutsui S. 2005. Electrochemical sensor for superoxide anion radical using polymeric iron porphyrin complexes containing axial 1-methylimidazole ligand as cytochrome c mimics. *Polymers for Advanced Technologies* **16**:287–292 DOI 10.1002/pat.590.

Zuo L, Christofi FL, Wright VP, Bao S, Clanton TL. 2004. Lipoxygenase-dependent superoxide release in skeletal muscle. *Journal of Applied Physiology* **97(2)**:661–668 DOI 10.1152/japplphysiol.00096.2004.

Zuo L, Hallman AH, Roberts WJ, Wagner PD, Hogan MC. 2014. Superoxide release from contracting skeletal muscle in pulmonary TNF-α overexpression mice.

American Journal of Physiology. Regulatory, Integrative and Comparative Physiology **306(1)**:R75–R81 DOI 10.1152/ajpregu.00425.2013.

Zuo L, Nogueira L, Hogan MC. 2011. Reactive oxygen species formation during tetanic contractions in single isolated Xenopus myofibers. *Journal of Applied Physiology* **111**:898–904 DOI 10.1152/japplphysiol.00398.2011.

Zuo L, Shiah A, Roberts WJ, Chien MT, Wagner PD, Hogan MC. 2013. Low P_{O_2} conditions induce reactive oxygen species formation during contractions in single skeletal muscle fibers. *American Journal of Physiology. Regulatory, Integrative and Comparative Physiology* **304(11)**:R1009–R1016 DOI 10.1152/ajpregu.00563.2012.

SCIENTIFIC REPORTS

natureresearch

OPEN

Real-time imaging of photosynthetic oxygen evolution from spinach using LSI-based biosensor

Shigenobu Kasai[1,2], Yamato Sugiura[1], Ankush Prasad[3], Kumi Y. Inoue[4], Teruya Sato[1], Tomohiro Honmo[1], Aditya Kumar[3], Pavel Pospíšil[3], Kosuke Ino[5], Yuka Hashi[4], Yoko Furubayashi[4], Masahki Matsudaira[4], Atsushi Suda[6], Ryota Kunikata[6] & Tomokazu Matsue[4,5]

The light-driven splitting of water to oxygen (O$_2$) is catalyzed by a protein-bound tetra-manganese penta-oxygen calcium (Mn$_4$O$_5$Ca) cluster in Photosystem II. In the current study, we used a large-scale integration (LSI)-based amperometric sensor array system, designated Bio-LSI, to perform two-dimensional imaging of light-induced O$_2$ evolution from spinach leaves. The employed Bio-LSI chip consists of 400 sensor electrodes with a pitch of 250 μm for fast electrochemical imaging. Spinach leaves were illuminated to varying intensities of white light (400–700 nm) which induced oxygen evolution and subsequent electrochemical images were collected using the Bio-LSI chip. Bio-LSI images clearly showed the dose-dependent effects of the light-induced oxygen release from spinach leaves which was then significantly suppressed in the presence of urea-type herbicide 3-(3,4-dichlorophenyl)—1,1-dimethylurea (DCMU). Our results clearly suggest that light-induced oxygen evolution can be monitored using the chip and suggesting that the Bio-LSI is a promising tool for real-time imaging. To the best of our knowledge, this report is the first to describe electrochemical imaging of light-induced O$_2$ evolution using LSI-based amperometric sensors in plants.

Molecular oxygen (O$_2$) during the evolution is known to be introduced into the environment about ~2.7 billion years ago by the O$_2$ evolving photosynthetic organisms[1]. In the photosynthetic organisms, chloroplast and mitochondria are the main organelles responsible for the production and consumption of O$_2$, respectively[2]. Photosynthetic water oxidation to O$_2$ is catalyzed by a tetra-manganese penta-oxygen calcium (Mn$_4$O$_5$Ca) cluster bound to the proteins of photosystem II (PSII)[3–6]. Several techniques have been used in the past to measure O$_2$ evolution in plants[7–11]. Each method utilized for detection and estimation of O$_2$ has some strengths and limitations. The electrochemical method has been used for detection of O$_2$ concentration including the Clark-type and Joloit-type electrode[12–14]. Quenching based O$_2$ sensors which are prepared by embedding the fluorophore in O$_2$ permeable polymer matrix [Polyvinyl chloride (PVC) or silicone] have an advantage as they are generally usable in both liquid and gaseous phase[9]. As quenching-based oxygen sensors, Ru(II) α-diimine complexes (15) and Pt(II)/Pd(II) porphyrin systems are among the most studied[15–18]. In addition to the above techniques, EPR oximetry, mass spectrometry, photoacoustic spectroscopy cannot be easily used in plant systems and therefore not widely employed in photosynthetic research. The electrochemical technique has an advantage of direct detection of O$_2$ without labels and additional reagents. As an example, electrochemical O$_2$ analyzers based on the reduction of O$_2$ at a negatively polarized platinum (Pt; electrode diameter: 25–75 μm) electrode have been demonstrated[19,20]. An ultra-microelectrode (diameter: 1.5 μm) was also introduced and inserted into a single

[1]Graduate Department of Environmental Information Engineering, Tohoku Institute of Technology, Sendai, Japan. [2]Biomedical Engineering Research Center, Tohoku Institute of Technology, Sendai, Japan. [3]Department of Biophysics, Centre of the Region Haná for Biotechnological and Agricultural Research, Faculty of Science, Palacký University, Olomouc, Czech Republic. [4]Graduate School of Environmental Studies, Tohoku University, Sendai, Japan. [5]Graduate School of Engineering, Tohoku University, Aoba-ku, Sendai, Japan. [6]Japan Aviation Electronics Industry, Limited, Tokyo, Japan. Correspondence and requests for materials should be addressed to S.K. (email: kasai@tohtech.ac.jp) or A.P. (email: prasad.ankush@gmail.com)
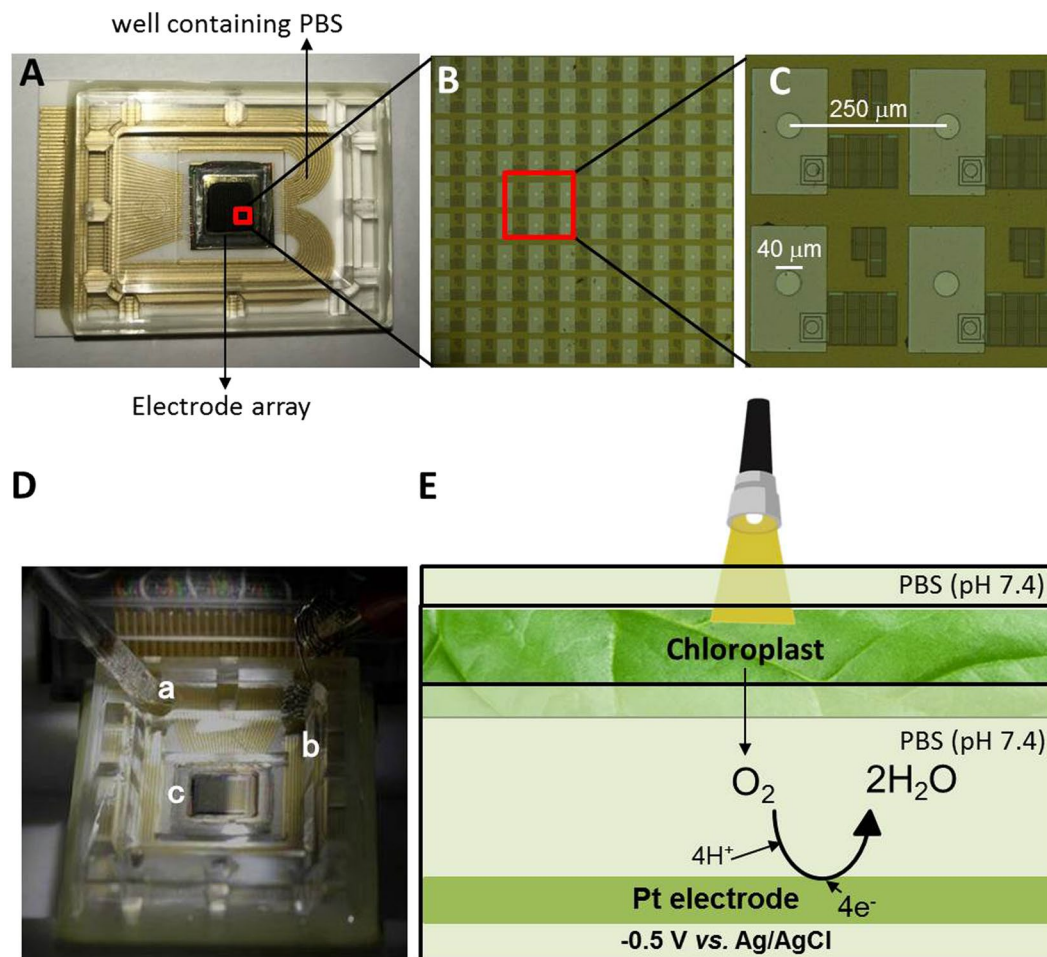
Figure 1. The photograph of the Bio-LSI chip (**A**), magnified images of Bio-LSI chip showing sensor points (**B**) and sensor electrodes (**C**). The diameter of each electrode is 40 μm and the distances between the electrodes are 250 μm. The measurement setup of electrode cell (**D**) with an RE (a) and a CE (b) placed in the same well as WEs (c). Schematic illustration of the measurement system (**E**) for the photosynthetic activity in plant tissues by detecting the O_2 as reduction current on the WEs of Bio-LSI.

cell to determine intercellular reduction current for O_2[19,20]. More recently, scanning electrochemical microscopy (SECM) has been used for the imaging of O_2 evolution during photosynthesis around single living cells[21]. SECM provides in addition to topographic information's, more detailed information (temporal) on the cellular activity such as respiration etc.[22-24].

In the present study, we used our recently developed LSI-based amperometric sensor array system referred to as Bio-LSI[25,26] for two-dimensional imaging of light-induced O_2 evolution from spinach leaves. The Bio-LSI comprised of a 10.4 mm × 10.4 mm complementary metal-oxide semiconductor (CMOS) sensor chip with 20 × 20 unit cells, an external circuit box, a control unit for data acquisition, and a DC power box. Each unit cell of the chip consists of an operational amplifier with a switched-capacitor type I–V converter for in-pixel signal amplification, which realizes a fast acquisition of electrochemical images with high sensitivity. On the Bio-LSI chip, the spinach leaves were illuminated with white light to induce O_2 evolution and simultaneous imaging was performed. To the best of our knowledge, this is the first study to describe real-time electrochemical imaging of light-induced oxygen release from a photosynthetic organism using LSI-based amperometric sensors.

Material and Methods

Sample and chemical reagents. Spinach (*Spinacia oleracea)* leaves were purchased from the local market and washed twice with deionized water. The leaves were stored in dark for two hours before measurement to avoid any kind of light interference during the measurement. For each measurement, a fresh spinach leaf of the approximately same age and size were chosen. The experiments were performed under the dark condition and at room temperature (25 °C). 3-(3, 4-dichlorophenyl)-1, 1-dimethylurea (DCMU) ≥98% was purchased from Wako Pure Chemicals Industries, Ltd. (Osaka, Japan).

Fabrication of Bio-LSI chip and measurement setup. The detailed fabrication process for the sensor chip has been described in our previous study[27]. In summary, it consists of 400 working electrodes arranged in an array of 20 × 20 electrodes as represented in Fig. 1(A–C). The overall measurement setup consists of a reference
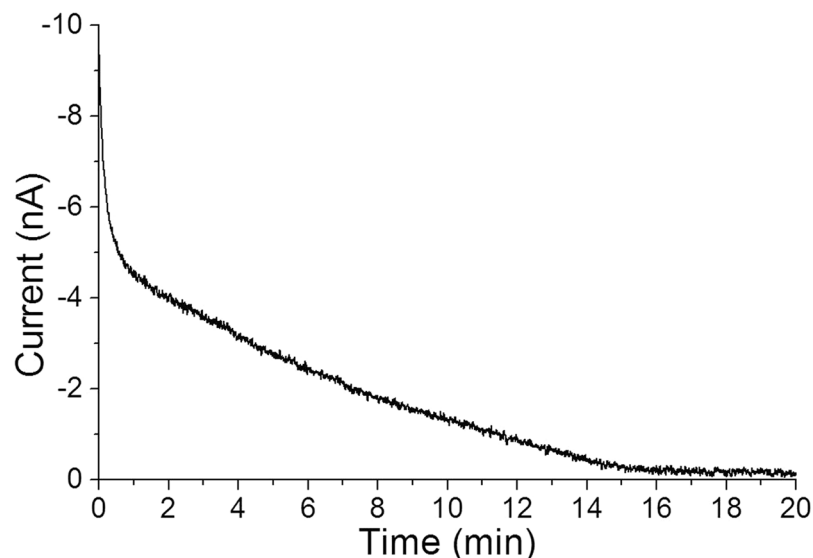
Figure 2. Time course of the deoxygenation. The DO reduction current on a WE of a Bio-LSI chip was monitored during the pretreatment for deoxygenation of the well. A voltage of −0.5 V vs. Ag/AgCl was applied to 400 WEs for 20 min.

electrode (RE): Ag/AgCl; a counter electrode (CE): a platinum (Pt) wire and 400 working electrodes (WEs) on the Bio-LSI chip (Fig. 1D). The WE is a Pt electrode each with a diameter of 40 μm. The RE and CE were inserted from the top as represented in Fig. 1D while the leaf excised sample rests above the WEs. The distance between the leaf sample and the Bio-LSI chip was less than ~1 mm due to the uneven surface area of the leaf. Some parts of the sample contacted to the sensing area. The ventral side of the leaf known to possess the stomata was placed on the electrode part for the purpose of acquiring the image. In the well positioned above the Bio-LSI chip, a phosphate buffer saline (PBS) (40 mM) at pH 7.4 was accommodated. The setup was established precisely using a stereoscopic microscope (Leica S8 APO).

Deoxygenation. To avoid any interference of dissolved oxygen (DO) in the system containing PBS (without leaves), we conducted deoxygenation in the measurement well by applying a potential of −0.5 V *vs*. Ag/AgCl to the WEs before measurements. Reaction on the Pt WEs during the deoxygenation was as follows.

$$O_2 + 4H^+ + 4e^- \rightarrow 2H_2O$$
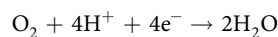
The monitored current generated by the above reaction was gradually decreased from −8 nA to ~−0.2 nA in the time span of 20 min (Fig. 2). The remaining current was derived from diffusion of fresh oxygen from the atmosphere. From this result, we consider that the deoxygenation was completed in about 20 min.

Real-time imaging and current monitoring of oxygen evolution during photosynthesis using Bio-LSI. For the real-time imaging of O_2 evolution during the light-induced photosynthetic process, PBS was filled in the well containing WEs (Fig. 1A). Prior to this, spinach leaf in the dimension 5 mm × 2 mm was positioned on the WEs. A potential of −0.5 V *vs*. Ag/AgCl was applied to the WEs until the reduction current of DO was stabilized to ~0 nA. This was followed by two-dimensional imaging of O_2 evolution from the spinach leaf by continuous application of −0.5 V *vs*. Ag/AgCl to the WEs. The light exposure was achieved using a KL300 LED light source (λ = 400–800 nm) connected with a light guide (Schott AG, Hattenbergstrasse 10, Mainz, Germany) with light intensities of 0 klx, 3 klx (40 μmol photons s⁻¹ m⁻²), 20 klx (260 μmol photons s⁻¹ m⁻²) and 30 klx (400 μmol photons s⁻¹ m⁻²). The intensities of light in the current study were chosen based on the data provided by the Osaka Science Museum, Osaka, Japan. The light intensities used in our study reflect the situation close to field conditions. As a negative control, we performed the same experiments in the absence of spinach leaf. For time course monitoring of the reduction current, current data from a single randomly selected electrode (indicated by a red open square) from the electrode sensor array system was chosen. We also examined the effect of a photosynthetic inhibitor on the oxygen evolution by addition of DCMU prior to start (Supplementary Data 1) and during measurements. All images presented in the manuscript are representative figures of at least 3 measurements.

Results

Real-time imaging of oxygen evolution during photosynthesis with different intensities of illumination. Real-time imaging of O_2 evolution from a spinach leaf was performed under the different illumination intensities (3 klx, 20 klx, and 30 klx). The spatial distribution of O_2 was monitored as O_2 reduction current measured with the Bio-LSI chip applied with −0.5 V *vs*. Ag/AgCl. Figure 3A shows the photograph of 400 WEs on a Bio-LSI and Fig. 3B shows a two-dimensional image of O_2 reduction current measured without any illumination
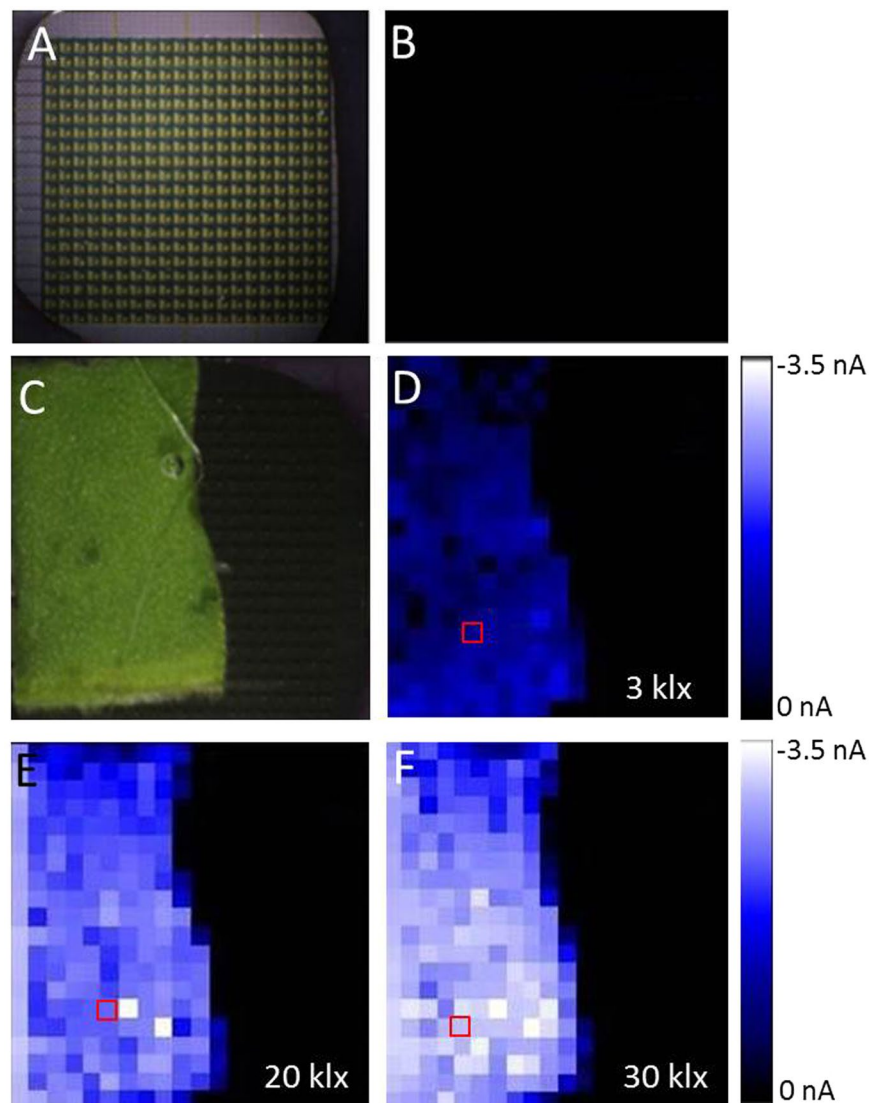
Figure 3. Photograph of 400 WEs on a Bio-LSI (**A**) and an image of O_2 distribution based on the reduction current of O_2 measured in the absence of spinach leaf (**B**). A photograph showing the arrangement of spinach leaf on the electrode surface (**C**) and images of O_2 evolution after 5 min of light exposure from the spinach illuminated with 3 klx (**D**), 20 klx (**E**) and 30 klx (**F**).

in the absence of spinach leaf. Figure 3C shows the arrangement of spinach leaf on the electrode surface of the Bio-LSI chip during the measurements. Figures 3D–F are the two-dimensional images for O_2 reduction current measured at the illumination of 3 klx, 20 klx and 30 klx, respectively. Supplementary Data 2 shows additional set of data on two-dimensional imaging of O_2 reduction current measured at the illumination of 3 klx, 10klx, 20 klx and 30 klx. The electrodes close with the leaf surface showed a change in reduction current in the range of -0.5 nA to ~ -3.5 nA, while the electrodes far from the leaf did not show any significant changes in the reduction current. With the increase of light intensities, the change in O_2 reduction current was increased. Supplementary Data 3 (video 1) shows the change in O_2 reduction current in real-time during the turning on/off the light at 30 klx. As a control experiment, real-time imaging of O_2 evolution from the dorsal side of the spinach leaf bearing no stomata was measured (data not shown). No significant change in O_2 reduction current was observed which is believed to be due to non-feasible long-distance diffusion of oxygen.

Time course of oxygen evolution during photosynthesis at different intensities of illumination.
The time course of O_2 evolution from spinach leaves during illumination with different intensities was compared. The changes in O_2 reduction current monitored at a single electrode of the electrode array system are shown in Fig. 4. Exposure to white light at 3 klx leads to change in O_2 reduction current by -1 nA which was significantly increased to -2.3 nA and -3.0 nA with exposure to light intensities of 20 klx and 30 klx, respectively. The O_2 evolution depending on the illumination intensity was clearly monitored by the Bio-LSI system. With the turning off the light, the oxygen reduction current showed a sharp decrease to a value equivalent to the value observed during
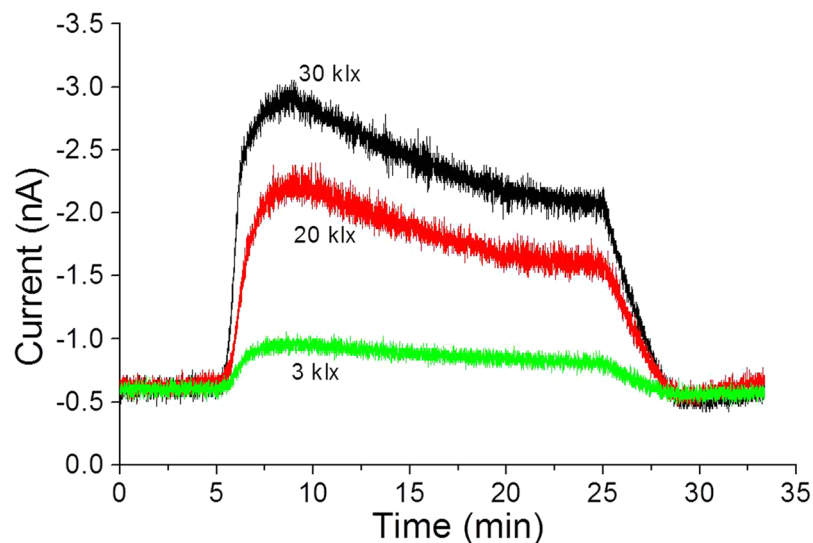
Figure 4. Changes in O_2 reduction current of a single randomly selected electrode (indicated by a red open square in Fig. 3) measured with a spinach leaves illuminated by 3 klx (green trace), 20 klx (red trace) and 30 klx (black trace).
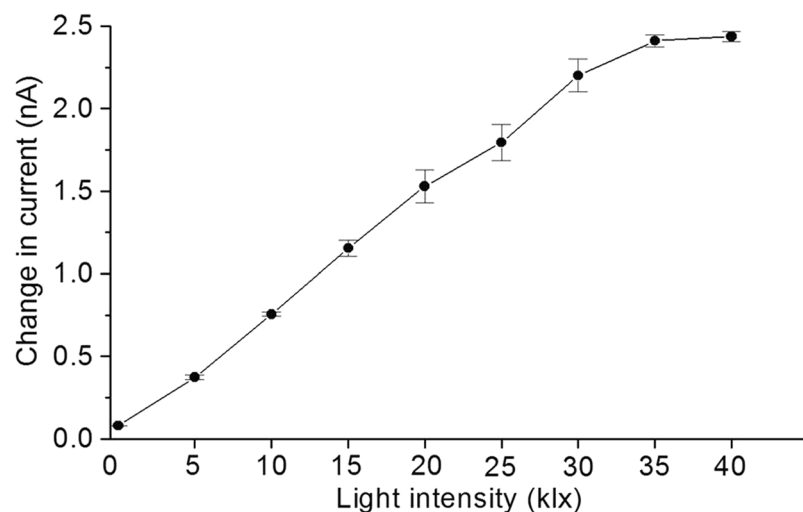

Figure 5. Change in O_2 reduction current (ΔI) showing the difference between the background current and value of oxygen reduction current (moving average) measured using Bio-LSI based on the experimental conditions described in Fig. 4. The change in O_2 reduction current (ΔI, in nA) was measured during the illumination at intensity range of 0–40 klx.

	$\Delta I_{1\,(nA)}$	$\Delta T_{1\,(sec)}$	$V_{1\,(nmol/sec)}$	$\Delta I_{2\,(nA)}$	$\Delta T_{2\,(sec)}$	$V_{2\,(nmol/sec)}$	$\Delta I_{3\,(nA)}$	$\Delta T_{3\,(sec)}$	$V_{3\,(nmol/sec)}$
3klx	0.3	200	47	0.1	880	4	0.2	240	26
20klx	1.6	240	211	0.6	840	23	1.0	240	132
30klx	2.3	240	303	0.8	840	30	1.5	240	198

Table 1. Oxygen evolution (in nmol) calculated using standard bulk dissolved oxygen concentration measured in the case of a Pt electrode (diameter $40\,\mu m$) having a measurement solution (PBS) and temperature of 25 °C. The oxygen evolution (V, in nmol) was calculated during the illumination at the intensity range of 3 klx, 20 klx and 30 klx.

first 5 min (no illumination). It can also be seen that the reduction current value began to gradually decrease after 5 min of illumination (Fig. 4, red and black trace). This may be because of consumption of O_2 due to continuous application of a potential to the electrode, O_2 reduction by PSII and limited O_2 production by the plant tissue.
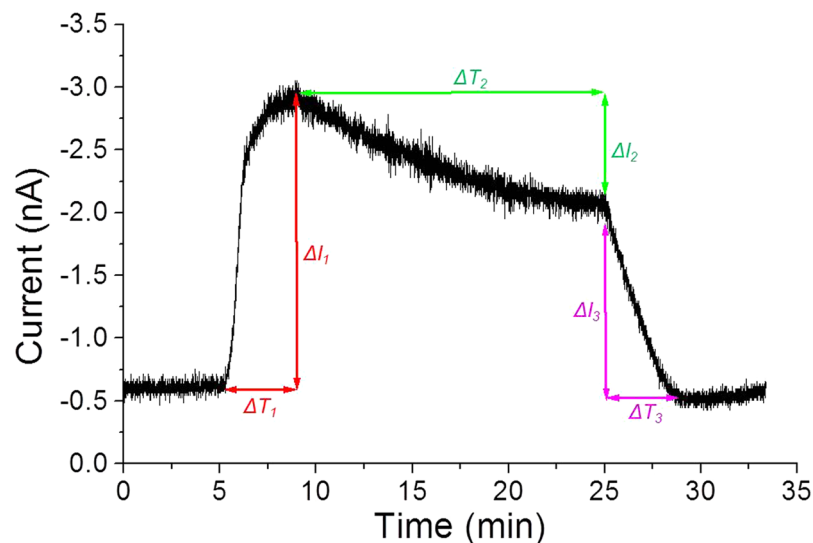
Figure 6. Details showing parameters utilized for calculation of oxygen evolution. Changes in O_2 reduction current of a single randomly selected electrode (indicated by a red open square in Fig. 3) measured with spinach leaves illuminated at 30 klx. V, ΔI and ΔT represents the concentration of evolved O_2, change in O_2 reduction current and time duration, respectively. The parameters were considered for calculations of oxygen evolution as presented in Table 1.

For a further understanding of the behavior of O_2 evolution during illumination, the change in O_2 reduction current (ΔI) from the current just before the turning on of the light at different period of illumination were plotted as averages of 3 randomly selected electrodes under the leaf with error bars indicating standard deviations. Figure 5 shows the ΔI at light intensities in the range of 0–40 klx. The O_2 evolution reflected by a change in reduction current was almost proportional to light intensity up to 30 klx; however, the response was saturated when the light intensity exceeded 35 klx. The saturation intensity and oxygen-evolution rate are important factors describing the photosynthetic capability of plant leaves. The above results indicate that amperometric measurement using Bio-LSI is applicable to screen the photosynthetic capability of the leaves including the oxygen constraining process of carbon fixation.

In order to estimate the molecules of O_2 evolved, the background reduction current value of the measurement solution and the DO concentration (estimated to be about 253 μM in the case of an electrode having a measurement solution temperature of 25 °C and a radius of 40μm) were taken into account. The oxygen concentration was recalculated and has been presented in Table 1 based on parameters shows in Fig. 6.

Real-time imaging of oxygen reduction current with photosynthetic inhibition. Real-time imaging of O_2 reduction current was performed in the presence of photosynthetic inhibitor of electron transport in PSII DCMU (5 μM) to confirm the origin of the reduction current. Figure 7A shows the arrangement of spinach leaf on the Bio-LSI chip (a), an image of O_2 reduction current before illumination (b) and an image during illumination (30 klx) (c). To test the effect of photosynthetic inhibitor, DCMU was exogenously added during the illumination (d) and subsequent images were taken after every 3 min for a time span of 15 min (e-i). At the initial 5 min of DCMU addition, partial inhibition of oxygen evolution was observed and then, the inhibition was increased with time leading to complete inhibition after 15 min (i). Figure 7B shows the time course of the O_2 reduction current changes on one electrode [indicated by a red open square in Fig. 7A(c)]. In addition to the above measurement, light-induced O_2 evolution was also tested after the suppression by DCMU (Fig. 8). Figure 8A shows the arrangement of spinach leaf on the Bio-LSI chip (a), an image of O_2 reduction current without illumination (b), and during illumination (30 klx) (c). After a suppression in O_2 evolution by addition of 5 μM DCMU, illumination was performed again, and subsequent images were taken every 2 min (e-i). Only a slight increase in oxygen reduction current was observed after the illumination which was found to rapidly decrease within 2 min. Figure 8B shows the changes in O_2 reduction current showing similar effects. With the first turning on of light illumination at 5 min in the absence of DCMU, the O_2 reduction current increased to reach to −2.5 nA. With the turning off the light, the current decreased to −0.5 nA within 5 min. With the addition of DCMU at this point and at a lapse of 5 min, the light source was turned on again. The small increase of the O_2 reduction current was observed but the peak of the current was reduced by about 1/2 and quickly decreased due to the inhibitory effect of DCMU on the O_2 evolution activity of the photosynthesis. These results indicate the potential of the Bio-LSI to be used for the monitoring the O_2 evolution activity as well as the impact of the environmental stresses to the tissues.
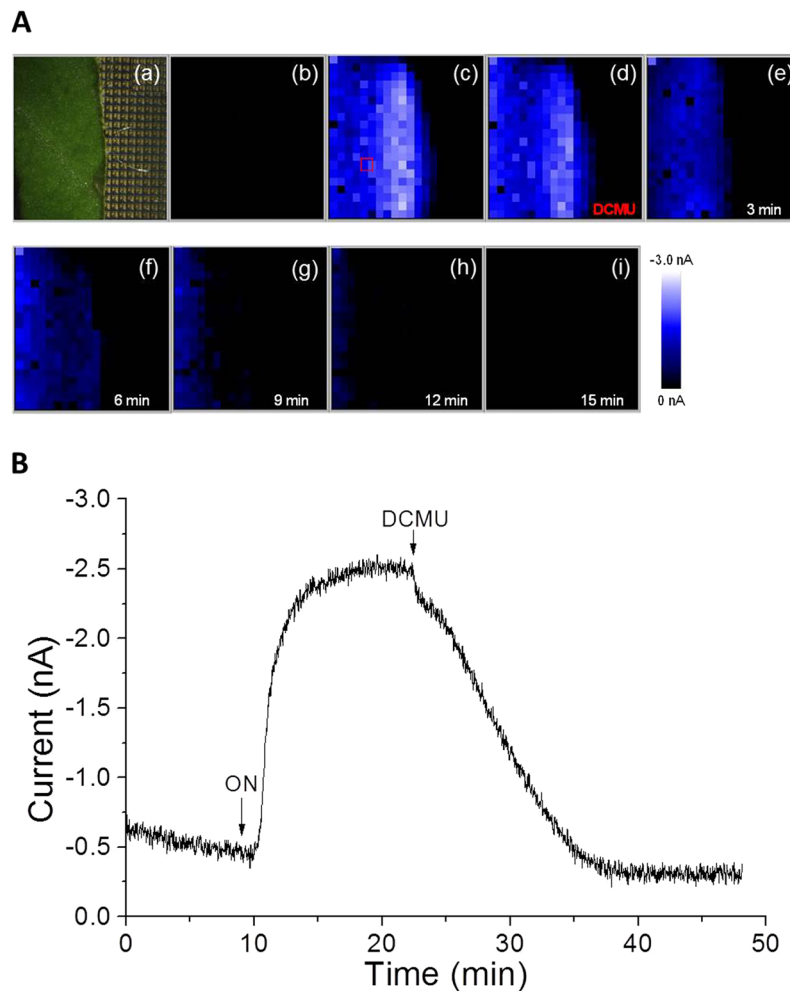
Figure 7. (**A**) Photograph showing the arrangement of spinach leaf on the Bio-LSI chip (a), real-time imaging of O_2 reduction current without illumination (b) and with illumination at 30 klx (c). DCMU ($5\,\mu M$) was added after 13 min from the start of illumination (30 klx) and subsequent images were obtained at 0 min (d), 3 min (e), 6 min (f), 9 min (g), 12 min (h) and 15 min (i). (**B**) The change in reduction current on an electrode indicated by a red open square in Fig. 7A(c). The arrow indicates the time of turning on the light (at 10 min) and subsequent addition of DCMU (at 23 min).

Discussion

In this study, we demonstrated real-time monitoring of O_2 evolution from a spinach leaf with light illumination by a change in O_2 reduction current using an LSI-based amperometric sensor array system called Bio-LSI. With the increase of the light intensities from 0 klx to 30 klx, the reduction current reflecting oxygen evolution from the leaf was increased almost proportional to light intensity while the electrodes far from the leaf did not show any significant changes in the reduction current (Figs 3, 7A, 8A). With the turning off the light, the oxygen reduction current showed a sharp decrease to a value equivalent to first 5 min. In addition, we observed a decrease of O_2 reduction current with applying $5\,\mu M$ of photosynthetic inhibitor DCMU to the illuminated leaf, showing that we detected the photosynthetic activity of plant tissue (Fig. 7B). This technique can be broadly applied to investigate the effect of chemical and physical stimulation on the photosynthetic organism including the impact of the environmental stresses to the plant tissues.

Several conventional methods including polarography, EPR oximetry, mass spectrometry, photoacoustic spectroscopy and galvanic sensors have been used to measure photosynthetic oxygen evolution over the past years; however, most of them can only offer mean values which lack spatial resolution and are therefore blind to any compartmentation within the sample[28]. The imaging methods for oxygen consumption, oxygen evolution and subsequent reactive oxygen species characterization which were used during the past decades in photosynthetic research were mainly the fluorescence-based measurements. Fluorescence measurements offer wide applicability; however undesired fluctuation by quenching/emission from other materials, shielding due to the solution (turbidity of the medium) and need for probe labelling has to be considered. As far as probes labelling is concerned, there are several issues related which includes but not limited to fluorescent probes cross-reactivity, the existence of endogenous fluorochromes, excitation and emission wavelengths overlap, probe uptake, toxicity-either of the fluorescent compounds and/or solvent etc. In the current study, the Bio-LSI chip has been presented for the
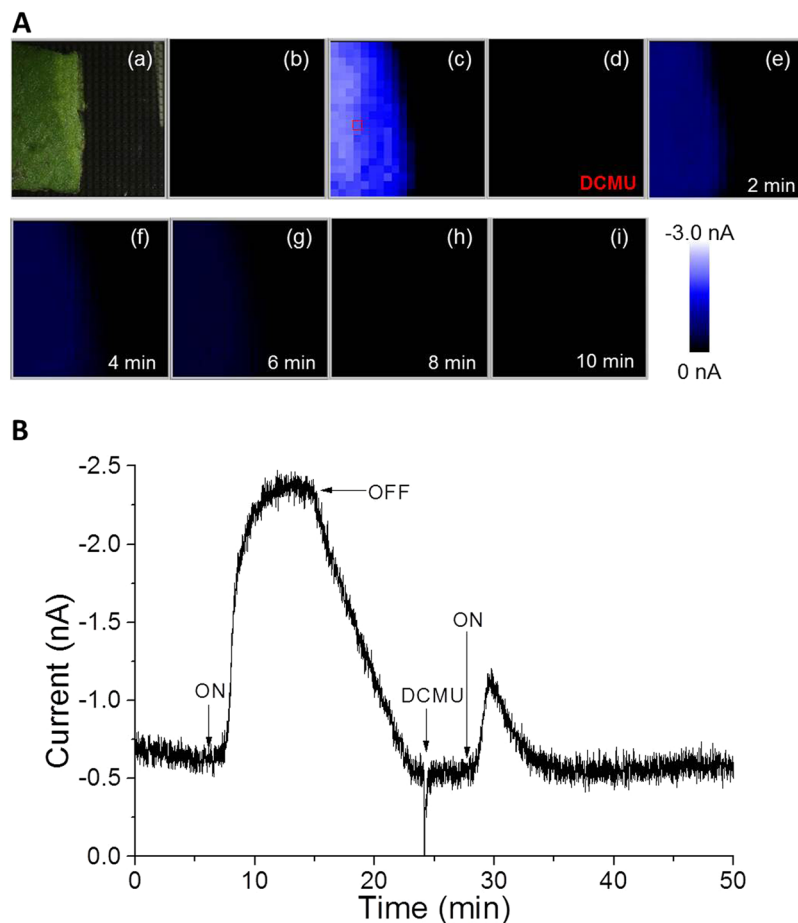
Figure 8. (**A**) Photograph showing the arrangement of spinach leaf on the Bio-LSI chip (a), real-time imaging of O_2 reduction current without (b) and with illumination at 30 klx (c). The illumination was turned off 10 min after the start of illumination and DCMU (5 μM) was added 10 min after turning off the light. Then, the illumination was turned on again after the addition of DCMU and subsequent images were taken at 0 min (d), 2 min (e), 4 min (f), 6 min (g), 8 min (h), 10 min (i) after turning on the light (at 28 min). (**B**) The change in reduction current measured on a single randomly selected electrode (indicated by a red open square in Fig. 8C).

real-time imaging of photosynthetic oxygen evolution from spinach. Through the modification of electrodes, the use of the device can be extended for detection of other chemical species/reactive species. Bio-LSI chip has an advantage considering the simplicity and easy handling of the measurement setup with no interferences from exogenous probes/chemicals and wider applicability. It is possible to detect oxygen production rate with higher sensitivity [in the range of nmol/sec] and from larger surface area. Thus, it offers multi-point biosensing with higher sensitivity. The current system is non-invasive and future development w.r.t sensing points can enhance spatial and temporal resolution considerably. The Bio-LSI being equipped with CMOS sensor chip and operational amplifier within each unit cell not only makes it compactly designed and easy to handle but also offer in-pixel signal amplification, fast acquisition and high sensitivity which makes its a promising tool in photosynthetic research and more broadly in investigating different aspect in plant science research.

Some technical limitations are however associated with Bio-LSI especially in the context of temporal measurements. The data resulting from 400 electrodes at 100ms interval will be enormous and thus choosing to follow 1 electrode/up to few electrodes for plotting the temporal distribution of changes in oxygen reduction current presented as Figs 4, 7B, 8B are more feasible. Spatial resolution can also be affected to some extent since the distance between the leaf sample and the Bio-LSI chip at different electrode positions can slightly vary due to the uneven surface area of the leaf or any other biological sample. Since some part of the sensing area can be closer than other (mostly in case of solid samples), the change of the oxygen concentration can be subject to some errors. Thus, the diffusion of oxygen in the medium has to be taken into account and should not be completely neglected. Although there is a short delay due to the diffusion of molecules from targets to sensors in electrochemical imaging, "real-time" is generally used[29].

References

1. Crowe, S. A. *et al*. Atmospheric oxygenation three billion years ago. *Nature* **501**, 535-+, https://doi.org/10.1038/nature12426 (2013).
2. Ligeza, A., Tikhonov, A. N. & Subczynski, W. K. *In situ* measurements of oxygen production and consumption using paramagnetic fusinite particles injected into a bean leaf. *Biochimica Et Biophysica Acta-Bioenergetics* **1319**, 133–137, https://doi.org/10.1016/s0005-2728(96)00122-3 (1997).
3. Dau, H., Zaharieva, I. & Haumann, M. Recent developments in research on water oxidation by photosystem II. *Current Opinion in Chemical Biology* **16**, 3–10, https://doi.org/10.1016/j.cbpa.2012.02.011 (2012).
4. Yano, J. & Yachandra, V. Mn4Ca Cluster in Photosynthesis: Where and How Water is Oxidized to Dioxygen. *Chemical Reviews* **114**, 4175–4205, https://doi.org/10.1021/cr4004874 (2014).
5. Perez-Navarro, M., Neese, F., Lubitz, W., Pantazis, D. A. & Cox, N. Recent developments in biological water oxidation. *Current Opinion in Chemical Biology* **31**, 113–119, https://doi.org/10.1016/j.cbpa.2016.02.007 (2016).
6. Vinyard, D. J. & Brudvig, G. W. In *Annual Review of Physical Chemistry*, Vol. 68 *Annual Review of Physical Chemistry* (eds Johnson, M. A. & Martinez, T. J.) 101–116 (Annual Reviews, 2017).
7. Clark, L. C. Monitor and Control of Blood and Tissue Oxygen Tensions. *Transactions American Society for Artificial Internal Organs* **2**, 41-& (1956).
8. Delieu, T. & Walker, D. A. Polarographic Measurement of Photosynthetic Oxygen Evolution By Leaf-Disks. *New Phytologist* **89**, 165–178, https://doi.org/10.1111/j.1469-8137.1981.tb07480.x (1981).
9. Tyystjarvi, E., Karunen, J. & Lemmetyinen, H. Measurement of photosynthetic oxygen evolution with a new type of oxygen sensor. *Photosynthesis Research* **56**, 223–227, https://doi.org/10.1023/a:1005994311121 (1998).
10. Kendall, D. N. Berlman,Ib - Handbook of Fluorescence Spectra of Aromatic Molecules. *Applied Spectroscopy* **21**, 203-& (1967).
11. Wolfbeis, O. S. Fiber-optic chemical sensors and biosensors. *Anal Chem* **76**, 3269–3283, https://doi.org/10.1021/ac040049d (2004).
12. Joliot, P. Oxygen evolution in algae illuminated with modulated light. In: Olson, J.M., Hind, G., Siegelman, H.W. (eds) Energy conversion by the photosynthetic apparatus. *Upton, New York*, 418–433 (1967).
13. Joliot, P. & Joliot, A. A polarographic method for detection of oxygen production and reduction of Hill reagent by isolated chloroplasts. *Biochimica et Biophysica Acta (BBA)-Bioenergetics* **153**(3), 625–634 (1968).
14. Clark, L.C. J.R., Wolf, R., Granger, D. & Taylor, Z. Continuous recording of blood oxygen tensions by polarography. *Journal of Applied Physiology* **6**, 189–193 (1953).
15. Demas, J. N. & DeGraff, B. A. Applications of luminescent transition metal complexes to sensor technology and molecular probes. *Journal of Chemical Education* **74**, 690–695, https://doi.org/10.1021/ed074p690 (1997).
16. Demas, J. N., DeGraff, B. A. & Coleman, P. B. Oxygen sensors based on luminescence quenching. *Analytical Chemistry* **71**, 793A–800A, https://doi.org/10.1021/ac9908546 (1999).
17. Kneas, K. A., Xu, W. Y., Demas, J. N. & DeGraff, B. A. Oxygen sensors based on luminescence quenching: Interactions of tris(4,7-diphenyl-1,10-phenanthroline)ruthenium(II) chloride and pyrene with polymer supports. *Applied Spectroscopy* **51**, 1346–1351, https://doi.org/10.1366/0003702971942024 (1997).
18. Gouterman, M. Oxygen quenching of luminescence of pressure sensitive paint for wind tunnel research. *Journal of Chemical Education* **74**, 697–702, https://doi.org/10.1021/ed074p697 (1997).
19. Matsue, T., Koike, S., Abe, T., Itabashi, T. & Uchida, I. An Ultramicroelectrode For Determination of Intracellular Oxygen - Light-Irradiation-Induced Change in Oxygen Concentration in an Algal Protoplast. *Biochimica Et Biophysica Acta* **1101**, 69–72, https://doi.org/10.1016/0167-4838(92)90468-s (1992).
20. Matsue, T., Koike, S. & Uchida, I. Microamperometric Estimation of Photosynthesis Inhibition In A Single Algal Protoplast. *Biochemical and Biophysical Research Communications* **197**, 1283–1287, https://doi.org/10.1006/bbrc.1993.2616 (1993).
21. Yasukawa, T., Kaya, T. & Matsue, T. Dual imaging of topography and photosynthetic activity of a single protoplast by scanning electrochemical microscopy. *Analytical Chemistry* **71**, 4637–4641, https://doi.org/10.1021/ac9903104 (1999).
22. Lee, C. M., Kwak, J. Y. & Bard, A. J. Application of Scanning Electrochemical Microscopy To Biological Samples. *Proceedings of the National Academy of Sciences of the United States of America* **87**, 1740–1743, https://doi.org/10.1073/pnas.87.5.1740 (1990).
23. Tsionsky, M., Cardon, Z. G., Bard, A. J. & Jackson, R. B. Photosynthetic electron transport in single guard cells as measured by scanning electrochemical microscopy. *Plant Physiology* **113**, 895–901, https://doi.org/10.1104/pp.113.3.895 (1997).
24. Yasukawa, T., Kaya, T. & Matsue, T. Characterization and imaging of single cells with scanning electrochemical microscopy. *Electroanalysis* **12**, 653–659, 10.1002/1521-4109(200005)12:9<653::aid-elan653>3.0.co;2-s (2000).
25. Inoue, K. Y. *et al*. LSI-based amperometric sensor for bio-imaging and multi-point biosensing. *Lab on a Chip* **12**, 3481–3490, https://doi.org/10.1039/c2lc40323d (2012).
26. Inoue, K. Y. *et al*. Advanced LSI-based amperometric sensor array with light-shielding structure for effective removal of photocurrent and mode selectable function for individual operation of 400 electrodes. *Lab on a Chip* **15**, 848–856, https://doi.org/10.1039/c4lc01099j (2015).
27. Kanno, Y. *et al*. Electrochemicolor Imaging Using an LSI-Based Device for Multiplexed Cell Assays. *Analytical Chemistry* **89**, 12778–12786, https://doi.org/10.1021/acs.analchem.7b03042 (2017).
28. Tschiersch, H., Liebsch, G., Borisjuk, L., Stangelmayer, A. & Rolletschek, H. An imaging method for oxygen distribution, respiration and photosynthesis at a microscopic level of resolution. *New Phytol* **196**, 926–936, https://doi.org/10.1111/j.1469-8137.2012.04295.x (2012).
29. Kasai, N., Shimada, A., Tobias, N., Torimitsu, K. Fabrication of an electrochemical sensor array for 2D H2O2 imaging. *Electrochemistry* **8**, https://doi.org/10.5796/electrochemistry.74.628 (2006).

Acknowledgements

Author Contributions

S.K. designed the study and wrote the initial draft of the manuscript. Y.S. performed the experiment. A.P. contributed in analysis, interpretation of data and preparation of the manuscript. T.S., T.H. assisted the data collection and its interpretation; A.K., P.P. participated in data interpretation; K.Y.I. assisted in the experiment and the preparation of the manuscript. K.I., Y.H., Y.F. contributed to prepare the Bio-LSI chip and partially assisted in the O$_2$ measurement experiments. M.M., A.S. and R.K. contributed to prepare the Bio-LSI measurement system. T.M. revised the critically important content of the study. All authors approved the final version of the manuscript.

Additional Information

Publisher's note: Springer Nature remains neutral with regard to jurisdictional claims in published maps and institutional affiliations.